

Dissecting the Role of Histone Deacetylases 1, 2, and 6 in Eμ-*myc* Driven B Cell Lymphoma

Inauguraldissertation

zur
Erlangung der Würde eines Doktors der Philosophie
vorgelegt der
Philosophisch-Naturwissenschaftlichen Fakultät
der Universität Basel

von

Vincent Pillonel

aus Lully, Schweiz

Basel, 2016

Genehmigt von der Philosophisch-Naturwissenschaftlichen Fakultät

auf Antrag von:

Prof. Dr. Patrick Matthias
(Dissertationsleiter, und Fakultätsverantwortlicher)

Prof. Dr. Jürg Schwaller
(Korreferent)

Basel, den 20. September 2016

Prof. Dr. Jörg Schibler
(Dekan)

“Il ne saurait exister pour la science des vérités acquises.

**Le savant n'est pas l'homme qui fournit les vraies réponses;
c'est celui qui pose les vraies questions.”**

Claude Lévi-Strauss

“The scientist is not a person who gives the right answers,

he is the one who asks the right questions.”

Claude Lévi-Strauss

Summary

Histone deacetylases (Hdacs) belong to a family of 18 enzymes which removes acetylation marks on lysine residues of histone and non-histone proteins (Reichert et al., 2012). Hdacs were shown to play an important roles in cancer and are attractive pharmacological targets for cancer therapy (Haery et al., 2015). HDAC inhibitors (HDACis) have potent antitumor activity in hematological and solid malignancies, mainly by inducing apoptosis, inhibiting cell cycle progression and cellular differentiation (Falkenberg and Johnstone, 2014; West and Johnstone, 2014). Previous works on classI Hdac1 and Hdac2, as well as classII Hdac6, showed that they play important roles in several cancer settings, including B cell malignancies (Haery et al., 2015; Seidel et al., 2015). However, Hdac1 and Hdac2 (Santoro et al., 2013), but also Hdac6 (Seidel et al., 2015), were shown to have contradicting tumor promoting and tumor suppressive roles in cancer. Despite improved knowledge in Hdac cancer research, the exact role of Hdac1, Hdac2, and Hdac6 in cancer remain largely unexplored. During my PhD thesis I investigated the functional role of Hdac1, Hdac2, and Hdac6 in the E μ -*myc* model of B cell lymphoma.

The first, and main part of my thesis work is the study of the functional role of classII Hdac1 and Hdac2 in the E μ -*myc* mouse model of B cell lymphoma. We found, that Hdac1 and Hdac2 have a pro-oncogenic roles in both, E μ -*myc* tumorigenesis and tumor maintenance. In this study, we reveal for the first time in the E μ -*myc* model, that *Hdac1* and *Hdac2* promote tumorigenesis in a gene dose-dependent manner, with a dominant function of Hdac1. Our findings raise the prospect of using selective HDAC1 (and HDAC2) inhibitors in clinics for the treatment of BL and other B cell lymphomas with Myc deregulation. The results of this work are presented in the

form of a publication manuscript: “Histone deacetylase 1 plays a predominant role in E μ -myc driven B cell lymphoma” (Pillonel *et al.*, *Accepted for publication in Scientific Reports*).

The second part of my thesis addresses the functional role of Hdac1 and Hdac2 in B cell development. This work was done in collaboration with R.M. Heideman. We could confirm our previous findings that *Hdac1* and *Hdac2* regulate B cell development in a gene dose-dependent manner, with a dominant function of *Hdac1*. We show, that *Hdac1*^{*Δ/Δ*};*Hdac2*^{*Δ/+*} mice have abnormal early B cell development. Further preliminary findings provide an insight into the role of Hdac1 and Hdac2 in B cell development, and suggests possible defects in V(D)J recombination.

In the last part of my thesis, I focus on the cytoplasmic classII Hdac6. We dissected the role of Hdac6 in E μ -myc driven B cell lymphoma. We found, that Hdac6 overexpression accelerates lymphomagenesis, whereas Hdac6 knockout in the germ line may delay tumor development in E μ -myc mice.

Table of Contents

Abbreviations	4
Introduction.....	7
1. Lysine acetylation and its enzymes.....	8
1.1. Histone acetyltransferases (HATs).....	9
1.2. Histone deacetylases (HDACs).....	9
2. Regulation of gene expression by HDACs	16
2.1. Chromatin structure and epigenetic gene regulation.....	16
2.2. Epigenetic gene regulation by HDACs.....	19
2.3. Non-epigenetic gene regulation by HDACs.....	20
3. Role of HDAC1 and HDAC2 in B lymphocyte development	21
3.1. B lymphocyte development - overview	21
3.2. Ig recombination and B cell maturation	23
3.3. Epigenetic control of B cell development and Ig recombination.....	24
3.4. HDAC1 and HDAC2 in B cell development	26
4. The biology of HDACs in cancer	27
4.1. B cell lymphomas with <i>c-myc</i> deregulation	27
4.2. Role of acetylation in cancer.....	33
4.3. Impact of HDACs on the hallmarks of cancer	34
4.4. Role of HDACs in B cell malignancies	42
4.5. HDAC inhibitors (HDACis) in treatment of lymphoid malignancies	45
5. Conclusion	52
Aim of this thesis	54
Results.....	58
Results Part1: Histone deacetylase 1 plays a predominant pro-oncogenic role in E μ - <i>myc</i> driven B cell lymphoma (Pillonel <i>et al. Accepted for publication in Scientific Reports</i>)	60
1.1. Manuscript text	62
1.2. Figures.....	85
1.3. Supplementary figures	97
Results Part2: Supplementary findings on the role of Hdac1 and Hdac2 in E μ - <i>myc</i> B cell lymphoma	109
2.1. Supplementary results.....	109
2.2. Supplementary figure legends.....	120

Abbreviations

2.3. Supplementary figures.....	129
Results Part 3: Analysis of the functional role of Hdac1 and Hdac2 in B cell development	140
3.1. Results.....	140
3.2. Figure legends.....	144
3.3. Figures.....	146
3.4. Supplementary figure legends	148
3.5. Supplementary figures.....	150
Results Part 4: Dissecting the role of Hdac6 in E μ -myc B cell lymphoma	153
4.1. Results.....	153
4.2. Figure legends.....	159
4.3. Figures.....	163
4.4. Supplementary figure legends	167
4.5. Supplementary figures.....	171
Discussion	177
1. Hdac1 and Hdac2 in E μ -myc B cell lymphoma.....	178
2. Hdac1 and Hdac2 in B cell development	189
3. Hdac6 in E μ -myc B cell lymphoma.....	192
Material and methods.....	195
Appendix.....	202
<i>Publication</i> : Hematopoietic overexpression of FOG1 does not affect B-cells but reduces the number of circulating eosinophils	203
<i>Manuscript in preparation</i> : HDAC1 and 2 repress lineage inappropriate expression of <i>Flt3</i> and <i>Ptprf</i> in B cells via Pax5 and Grg4	217
Bibliography	219
Acknowledgements.....	245
Curriculum Vitae	249

Abbreviations

APL	<i>Acute Promyelocytic Leukemia</i>
BAC	<i>Bacterial Artificial Chromosome</i>
BC	<i>B Cells</i>
BL	<i>Burkitt's Lymphoma</i>
bp	<i>base pairs</i>
BM	<i>Bone Marrow</i>
BrdU	<i>5-bromo-2-deoxyuridine</i>
CSR	<i>Class Switch Recombination</i>
CTCL	<i>Cutaneous T Cell Lymphoma</i>
DAPI	<i>4',6-Diamidino-2-phenylindole</i>
DLBCL	<i>Diffuse Large B-Cell Lymphoma</i>
FL	<i>Floxed</i>
GL	<i>Germ Line</i>
HAT	<i>Histone Acetyltransferase</i>
HDAC	<i>Histone Deacetylase</i>
HDACi	<i>HDAC inhibitor</i>
HG-NHL	<i>High-Grade Non-Hodgkin Lymphoma</i>
HL	<i>Hodgkin's Lymphoma</i>
HSCs	<i>Hematopoietic Stem Cells</i>
H&E	<i>Hematoxylin and Eosin</i>
Ig	<i>Immunoglobulin</i>
IgH	<i>Immunoglobulin heavy chain</i>
IgL	<i>Immunoglobulin light chain</i>
IHC	<i>Immunohistochemistry</i>
KO	<i>Knock Out</i>
KPLM	<i>Kaplan-Meyer</i>
LN	<i>Lymph Node</i>
Lys	<i>Lysine</i>
Lys-Ac	<i>Lysine Acetylation</i>

Abbreviations

MACS	<i>Magnetic-Activated Cell Sorting</i>
miRNAs	<i>microRNAs</i>
N.S.	<i>Not statistically significant</i>
OE	<i>Overexpression</i>
PBL	<i>Peripheral Blood Lymphocytes</i>
PCR	<i>Polymerase Chain Reaction</i>
PTM	<i>Posttranslational modification</i>
SEM	<i>Standard Error Measurement</i>
SP	<i>Spleen</i>
TF	<i>Transcription Factor</i>
Tg	<i>Transgene</i>
4-OHT	<i>4-hydroxytamoxifen</i>

Introduction

Introduction

1. Lysine acetylation and its enzymes

Lysine acetylation (Lys-Ac) is a reversible posttranslational modification that occurs on the ϵ -amino group of lysine (Lys) residues (Waterborg, 2002). Lys-Ac was discovered on histone proteins almost half a century ago (Allfrey et al., 1964; Gershey et al., 1968). Subsequent research, resulted in the discovery that Lys-Ac residues are conserved in diverse organisms from bacteria to humans, where thousands of eukaryotic proteins, including histones, but also non-histone proteins, were found (Choudhary et al., 2009; Kim et al., 2006; Zhao et al., 2010). By now it is clear that Lys-Ac is a key posttranslational modification (PTM) that potentially rivals phosphorylation and ubiquitination (Kouzarides, 2000; Norris et al., 2009). Acetylation occurs on numerous key Lys residues, including histone H3 (Lys⁹, Lys¹⁴, Lys¹⁸ and Lys²³ and histone H4 (Lys⁵, Lys⁸, Lys¹², and Lys¹⁶) (Kelly and Cowley, 2013; Kouzarides, 2007). Acetylation is a highly dynamic process regulated by the opposing action of two classes of enzymes, histone acetyltransferases (HATs) and histone deacetylases (HDACs) (Inche and La Thangue, 2006). Besides targeting histones in the nucleus, HATs and HDACs also acetylate and deacetylate many nonhistone proteins in the cytoplasm, and thereby regulate their function, localization and stability (Choudhary et al., 2009; Glozak et al., 2005; Kim et al., 2006; Kouzarides, 2000). Hence, these enzymes are also referred as lysine acetyltransferases (KATs) and lysine deacetylases (KDACs). These enzymes play crucial roles in various cellular processes and are intimately linked to human health and diseases. Hence, these proteins are also key drug targets (Aka et al., 2011). I discuss these different enzymes with the emphasis on HDACs and their impact on development and cancer in the following sections.

1.1. Histone acetyltransferases (HATs)

Histone acetyltransferases (HATs) transfer acetyl moiety from acetyl-CoA to the ϵ -amino group of lysine (Lys) residues. HAT proteins are the catalytic core of several large protein coactivator complexes. They function by acetylating Lys residues on core histones of the promoter of genes and thereby activate gene expression (Haery et al., 2015). In addition, HATs also acetylate non-histone proteins, and thereby modulate their protein stability, intracellular localization and DNA binding capacity (Friedmann and Marmorstein, 2013).

1.2. Histone deacetylases (HDACs)

Histone deacetylases (HDACs) have opposing effects to HATs. They remove acetylation marks on Lys residues of target proteins. The first HDAC, HDAC1 was identified in 1990 (Itazaki et al., 1990). Since then, 18 mammalian HDACs enzymes were discovered. HDACs modify the epigenome through regulation of chromatin acetylation by removing acetylation marks on histones. Most HDACs are part of large repressor complexes and generally act as transcriptional corepressors. HDACs regulate gene expression by targeting histone proteins (Dawson and Kouzarides, 2012). However, HDACs also deacetylate non-histone proteins and thereby impact on an increasing number of other cellular processes, including apoptosis, autophagy, and metabolism (Buchwald et al., 2009; Glozak et al., 2005; Xu et al., 2007). Hence, it is not surprising that aberrant deacetylation of histone and nonhistone proteins are implicated in numerous human diseases, including cancer (Hagelkruys et al., 2011; Peng and Seto, 2011).

Classification of HDACs

The family of mammalian *HDACs* comprises 18 genes, which are subdivided into four families (class I-IV) based on sequence similarity, cofactor dependency and their homology to their respective yeast orthologs (Figure 1) (de Ruijter et al., 2003; Gregoretta et al., 2004; Grozinger and Schreiber, 2002; Witt et al., 2009; Yang and Seto, 2007): Class I, II, and IV are “classical” HDACs consisting of 11 family members. These enzymes all have a conserved Zn²⁺-dependent deacetylase domain. Class I HDACs comprises HDAC1, 2, 3, and 8, and which are similar to yeast Rpd3. Class II HDACs are sub grouped in Class IIa containing HDAC4, 5, 7, and 9 and class IIb containing HDAC6 and 10, which are similar to yeast Hda1. Class IV has only HDAC11 as member, which shares characteristics of both class I and class II HDACs (Gao et al., 2002). Class III HDACs comprises seven members called Sirtuins (SIRT1 to SIRT7) by analogy with yeast silent information regulator 2 (SIR2) (Yang and Seto, 2008). These proteins are structurally and mechanistically distinct from “classical” HDACs and have a conserved nicotinamide-adenine dinucleotide (NAD)-dependent deacetylase activity. Sirtuins require for their activity NAD⁺ as coenzyme. (Min et al., 2001; Smith et al., 2008).

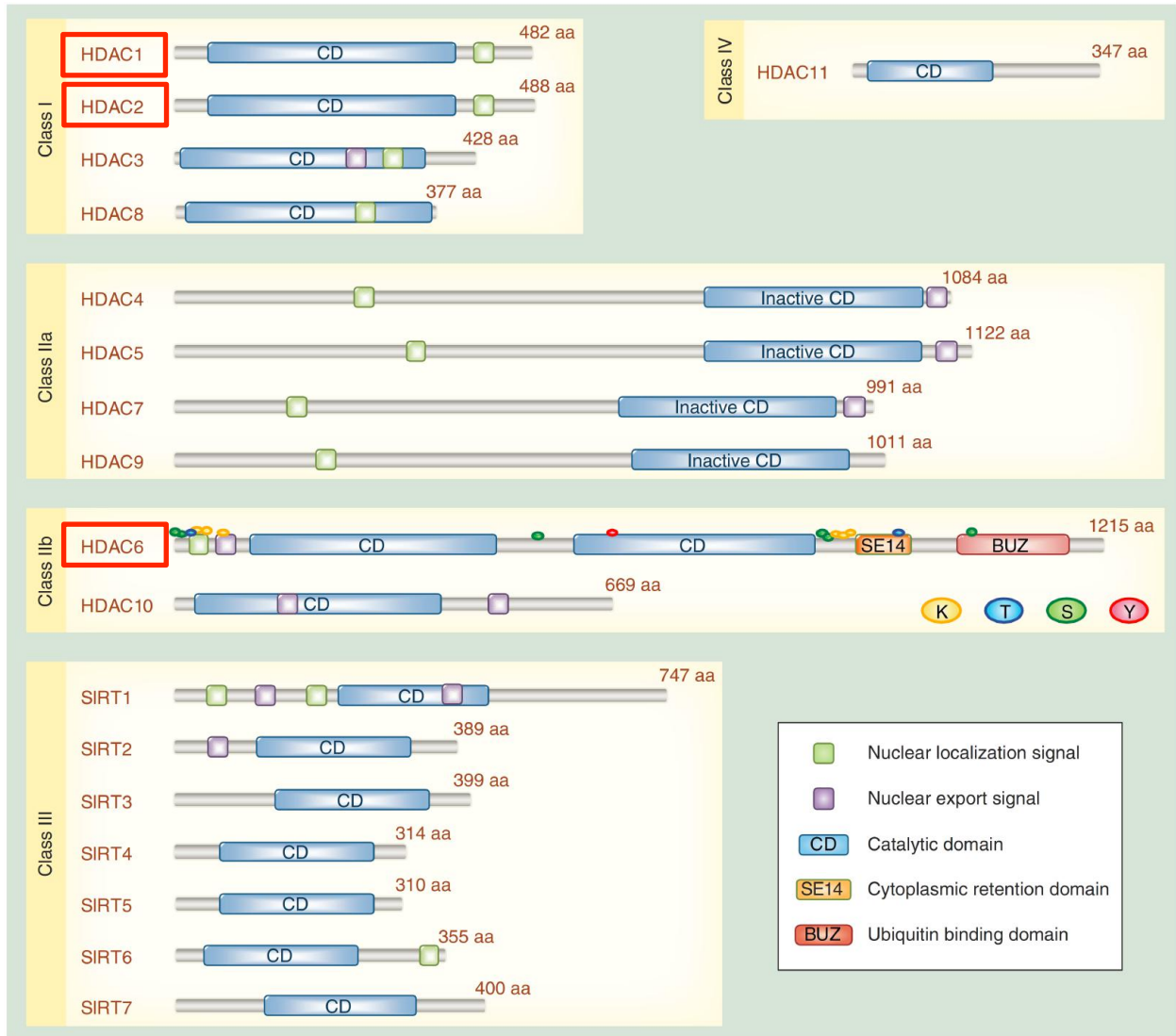


Figure 1: Classification of human HDACs. Class I to class IV. Class I HDAC1 and HDAC2 and class IIb HDAC6 are highlighted. Protein domains of HDAC isoforms are presented. Post-translational modifications on lysine (K), threonine (T), serine (S) or tyrosine (Y) amino acids are shown for HDAC6. The numbers specify the number of amino acids are indicated to the right. (Figure modified from (Seidel et al., 2015)).

HDAC1 and HDAC2

Mammalian class I HDAC1 and HDAC2, are ubiquitously expressed in different tissues. They are almost exclusively localized in the nucleus due to the presence of a nuclear localization

signal (NLS). In the nucleus these enzymes mediate histone deacetylation (Haberland et al., 2009b). HDAC1 and HDAC2 are the biochemically predominant HDACs in the nucleus. Together, they account for approximately 50% of the total HDAC activity level in T cells and embryonic stem (ES) cells (Dovey et al., 2013).

HDAC1 and HDAC2 cannot bind DNA directly and are most likely inactive in the absence of interacting partners (Zhang et al., 1999). HDAC1 and HDAC2, together with HDAC3, are catalytic subunits of large multiprotein transcriptional co-repressor complexes (Grozinger and Schreiber, 2002; Yang and Seto, 2008). For example, HDAC1 and HDAC2 are found in several co-repressor complexes, including Sin3, NuRD (nucleosome remodeling and deacetylation), CoREST (co-repressor for element-1-silencing transcription factor), and SMRT (silencing mediator of retinoid and thyroid repressors)/NCoR (nuclear receptor co-repressor) (Kelly and Cowley, 2013). Through removing acetyl groups on histones, these HDAC1 and HDAC2 containing complexes mediate chromosomal compaction and gene repression (Bannister and Kouzarides, 2011; Yang and Seto, 2008). These complexes mediate HDAC localization, substrate specificity, act as scaffolds to recruit DNA-binding proteins and provide cofactors required for HDAC function (Haery et al., 2015). Currently, the molecular specificities of different isoforms of HDAC1 and HDAC2 containing complexes are still indefinite. Increasing body of evidence indicates a heterogeneity in their composition (Kelly and Cowley, 2013). Some evidence suggests that the composition of these complexes might also be cell-type specific. For instance, in T cells the Sin3A complex contains predominantly HDAC1 (Dovey et al., 2013).

HDAC1 and HDAC2 are two paralogs that originate from a gene duplication. These two genes share 86% identity in amino acid sequence. Hence, it is not surprising, that to a large degree, these two enzymes have redundant functions (Haberland et al., 2009b). Indeed, numerous studies

in different tissues and cell types, including B cells, clearly demonstrate that mouse HDAC1 and HDAC2 have redundant functions (Chen et al., 2011; Dovey et al., 2013; Haberland et al., 2010; Jacob et al., 2011; LeBoeuf et al., 2010; Ma et al., 2012; Montgomery et al., 2007; Montgomery et al., 2009; Wilting et al., 2010; Yamaguchi et al., 2010). Nevertheless, some enzyme specificities have been determined. For example, HDAC1 and HDAC2 are not redundant during mouse embryogenesis, since the two paralogs cannot compensate for each other (Lagger et al., 2002; Trivedi et al., 2007; Zupkovitz et al., 2010).

HDAC6

HDAC6 is a member of class IIb HDAC family. Interestingly, it is the only HDAC family member with two catalytic domains and unique functions among HDACs (Seidel et al., 2015). HDAC6 is an unusual histone deacetylase, which is not known to be part of an HDAC-containing repression complex (Matthias et al., 2008). HDAC6 predominantly localizes in the cytoplasm, where it deacetylates non histone proteins (Boyault et al., 2007). Interestingly, in undifferentiated cells, like embryonic stem cells (ESCs) neural stem cells (NSCs), and some cancer cell lines, HDAC6 is mainly localized in the nucleus. Upon differentiation HDAC6 relocates into the cytoplasm (Chen et al., 2013).

HDAC6 plays important roles in protein trafficking and degradation, cellular shape and polarity, migration, directional movement and angiogenesis (Aldana-Masangkay and Sakamoto, 2011; Seidel et al., 2015). To control these processes, HDAC6 regulates cytoskeleton dynamics by regulating microtubule stability and dynamics. Deacetylation of the α -tubulin subunit by HDAC6 is associated with depolymerisation of microtubules (Hubbert et al., 2002). HDAC6 also

deacetylates cortactin, which then enhances F-actin polymerization to promote cell migration (Zhang et al., 2007; Zhang et al., 2009).

HDAC6 was shown to play a role in the elimination of misfolded proteins. Misfolded proteins are either degraded via the ubiquitin-proteasome pathway or through the aggresome. HDAC6 regulates both processes (Seidel et al., 2015; Simms-Waldrup et al., 2008). HDAC6 acts as an adaptor protein for proteasome-independent degradation. Together with motor proteins like dynein, HDAC6 mediates the transport of misfolded proteins along microtubules to the microtubule organizing center (MTOC). At the MTOC aggresomes are formed around misfolded proteins, which are then transported to the lysosome for degradation (Aldana-Masangkay and Sakamoto, 2011; Hubbert et al., 2002; Lee et al., 2010). In addition, HDAC6 regulates proteasome-dependent protein degradation. HDAC6 has been shown to function as a stress sensor by deacetylating heat shock protein-90 (Hsp90), an abundant cellular chaperone (Bali et al., 2005; Kovacs et al., 2005; Yang et al., 2008). Deacetylation of Hsp90 induces its chaperone activity and prevents degradation of its client proteins (Aldana-Masangkay and Sakamoto, 2011). Under nonstress conditions, protein degradation occurs through the proteasome. Chaperone valosin-containing protein/ATPase (VCP/p97) form a basal complex with heat shock factor (HSF)1 and HSP90 and HDAC6. This leads to disassembly of the ubiquitinated aggregate/HDAC6 complex so that the ubiquitinated proteins can be degraded through the proteasome instead of the aggresome. Under stress, when the number of misfolded proteins increases, HDAC6 binds these ubiquitinated protein aggregates and the basal complex disassembles (Aldana-Masangkay and Sakamoto, 2011; Boyault et al., 2006). Furthermore, HDAC6 together with HSP90 and Rac1 contribute to the regulation of endo- and exocytosis (Gao et al., 2007; Seidel et al., 2015).

HDAC6 is also involved in regulation of apoptosis. HDAC6 inhibits apoptosis by deacetylating Ku70, which then causes sequestration of the proapoptotic BAX (Bcl-2-associated X protein) protein (Subramanian et al., 2011). But HDAC6 was also shown to have other roles. For instance, HDAC6 was shown to impact on the PI3K/AKT and the MAPK/ERK signaling pathways and thereby playing a critical role in oncogenic transformation (Lee et al., 2008). Furthermore, HDAC6 can also contribute to transcriptional repression in some cells where it is located in the nucleus, by interacting with different co-repressors like SUMOylated p300 or HDAC11 (Gao et al., 2002; Girdwood et al., 2003; Seidel et al., 2015).

HDAC6 loss-of-function studies revealed that HDAC6 germline knockout (KO) mice develop normally and remain viable and fertile, despite having hyperacetylated tubulin in most tissues (Zhang et al., 2008). Of note these mice also have normal lymphoid development (Zhang et al., 2008). Hence, HDAC6 seems to be dispensable in normal mouse development to adulthood, suggesting that the main function of HDAC6 could be found under stress or pathologic conditions. Indeed, HDAC6 plays a crucial role in cancer, but also to several other diseases including neurodegeneration (Simoës-Pires et al., 2013), HIV (Valenzuela-Fernandez et al., 2005) and other viral (Banerjee et al., 2014) or bacterial infections (Seidel et al., 2015) and pathological autoimmune response (Seidel et al., 2015).

2. Regulation of gene expression by HDACs

HDACs can regulate transcription in two different ways: First, by altering the pattern of histone acetylation. Thereby, these enzymes modulate chromatin structure and its accessibility to the transcriptional regulatory proteins (Brownell et al., 1996; Taunton et al., 1996). Second, these enzymes mediate deacetylation of nonhistone proteins including TFs that directly regulate transcription (Glozak et al., 2005). I describe the role of HDACs in regulating acetylation on histone and nonhistone proteins and its functional consequences, concentrating mostly on transcription in the following sections.

2.1. Chromatin structure and epigenetic gene regulation

Chromatin modifications and epigenetics

Epigenetics is heritable non-DNA sequence-based gene-expression alterations. Epigenetic was first described in 1942 by C. Waddington (Waddington, 1942). Subsequent studies in the early 1960s demonstrated that histones are post translationally modified (Allfrey et al., 1964). Subsequent studies identified a large number of different histone PTMs (Bannister and Kouzarides, 2011). Histone acetylation, together with other PTMs, including histone methylation, phosphorylation, ubiquitination, and sumoylation, are key epigenetic regulatory mechanism (Bannister and Kouzarides, 2011). The diverse and complex pattern of distinct PTMs on histones act to form a “histone code” (Jenuwein and Allis, 2001; Strahl and Allis, 2000). This histone code is established by “writers” (e.g. HATs) that add, and “erasers” (e.g. HDACs) that remove the respective PTM (Figure 2). Other proteins, called “readers” then recognize these modifications and decipher the code. Such readers are e.g. bromodomain-containing proteins (BRDs) like HATs and chromatin remodeling complexes that can recognize and bind acetylated

marks (Mujtaba et al., 2007; Strahl and Allis, 2000). Alternatively, also tandem plant homeodomain (PHD) finger containing proteins can bind acetylated lysine (Zeng et al., 2010).

The function of these chromatin marks is more complex than initially thought (Berger, 2007). In addition to the important number of histone PTMs, another level of complexity exists due to cross-talk between different modifications (Kouzarides, 2007). For example, cooperation, dependence, or competition among other, may occur between modifications (Bannister and Kouzarides, 2011). Histone PTMs function via two main mechanisms: i) by directly influencing the overall structure of chromatin, either over short or long distances, or ii) by regulating either positively or negatively the binding of effector molecules (Bannister and Kouzarides, 2011). In addition, the epigenetic network has many layers of complexity, including DNA methylation, histone modifications, chromatin remodeling and microRNAs (Bernstein et al., 2007; Esteller, 2006). Hence, histone modifications not only regulate chromatin structure but also recruit chromatin remodeling enzymes (Bannister and Kouzarides, 2011). Thereby, these modifications influence transcription but also many other DNA processes such as repair, replication, and recombination (Bannister and Kouzarides, 2011). Histone PTMs including acetylation play fundamental roles in most biological processes that are involved in the manipulation and expression of DNA (Bannister and Kouzarides, 2011). Aberrations in epigenetic mechanisms underlie several diseases including cancer metabolic and neurodegenerative disorders (Inche and La Thangue, 2006; Portela and Esteller, 2010).

Chromatin structure

Chromatin is composed of nucleosomes consisting of an octamer of core histones (H2A, H2B, H3 and H4) with 147 base pairs (bp) DNA wrapped around (Marino-Ramirez et al., 2005).

Histone proteins have flexible histone tails that are exposed to reversible PTMs, which can both positively and negatively regulate gene transcription (Bannister and Kouzarides, 2011). Chromatin is a highly complex and dynamic structure that acts as scaffold for DNA. It consists of DNA, histone and other proteins. Chromatin can be found in two conformational states: i) heterochromatin, a compacted, transcriptional inactive state and ii) euchromatin, an open, transcriptionally active state (Bannister and Kouzarides, 2011; Ellis et al., 2009a). The remodeling of chromatin underlie gene transcription, DNA replication and repair as well as apoptosis and other regulatory processes acting at the level of DNA (Ellis et al., 2009a; Inche and La Thangue, 2006; Wang et al., 2007).

Impact of histone acetylation on chromatin and nucleosome remodeling

Lys acetylation on histone proteins neutralizes the positive charge of Lys residues and thereby weakens the interactions between positively charged histone proteins and negatively charged DNA, resulting in an open chromatin conformation (Olzscha et al., 2015). Acetylation and deacetylation of histone proteins by HATs and HDACs, respectively, alters the chromatin structure and mediates changes in gene expression (Waterborg, 2002). In general, histone acetylation by HATs leads to an open, less compact chromatin state which is accessible to TFs facilitating gene transcription. Conversely, histone deacetylation by HDACs leads to condensation or closed chromatin state which prevents access to TFs leading to transcriptional repression (Figure 2) (Jenuwein and Allis, 2001; Johnstone, 2002).

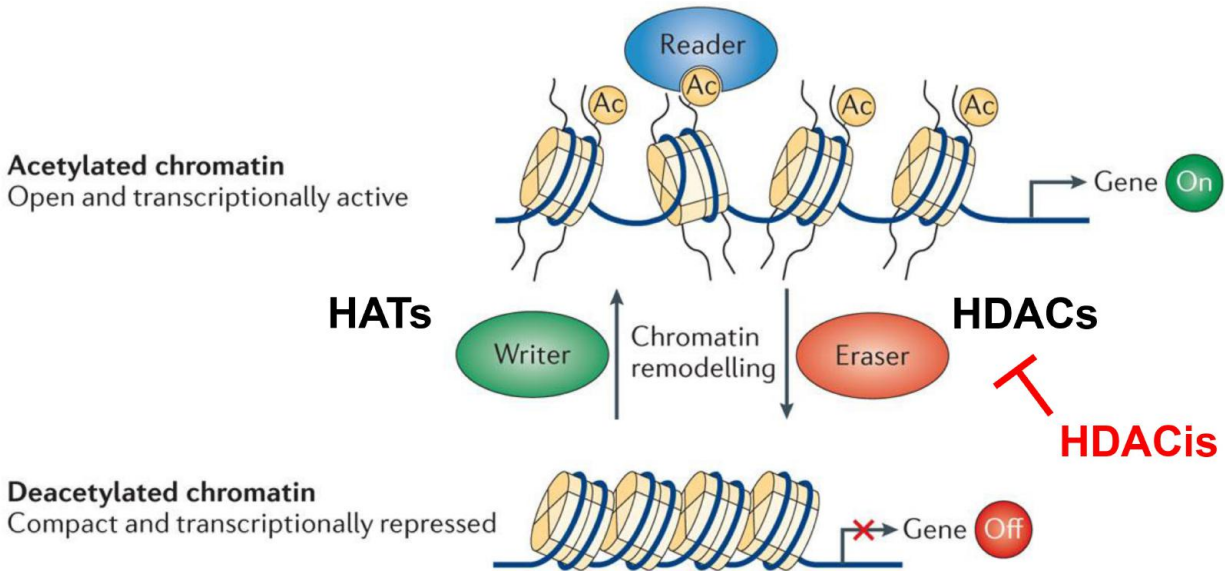


Figure 2: HATs and HDACs in regulation of gene expression. Histone acetylation on Lys residues at amino-terminal tails of core histones proteins is catalyzed by HAT and deacetylation by HDAC. Acetylation of nucleosomes inhibits the folding of nucleosome arrays into secondary and tertiary chromatin structures, and favors gene expression. Hypo-acetylated nucleosomes are condensed, which prevents the gene expression (Figure adapted from (Verdin and Ott, 2015)).

2.2. Epigenetic gene regulation by HDACs

HDACs deacetylate histone proteins and restore the positive charge on lysine residues. This stabilizes the local chromatin architecture and generally represses transcription (Bannister and Kouzarides, 2011). Conversely, hyperacetylation of histones by HATs leads to de-compaction of chromatin and exposes DNA allowing TF binding and initiation of transcription (Figure 2) (Li et al., 2007; Verdin and Ott, 2015).

Class I HDACs (1, 2, 3, and 8) have the most decisive roles in regulating gene expression. They regulate gene expression as catalytic core of multiprotein complexes with transcriptional co-repressors like Sin3 or SMART (Yang and Seto, 2008). These complexes contain multiple

DNA/chromatin recognition motifs. In combination with other DNA-binding proteins like DNA methyltransferases (DMTs), TFs or nuclear receptors recruit HDAC1 and HDAC2 at specific DNA sites (Olzscha et al., 2015).

2.3. Non-epigenetic gene regulation by HDACs

HDACs also regulate gene transcription in a non-epigenetic manner by deacetylating nonhistone proteins including TFs. Acetylation of TFs can affect their function in four different ways: 1) by increasing protein stability by blocking the site of ubiquitination which prevents proteasome degradation; 2) by blocking the DNA-binding domain and decrease the ability of TFs to bind DNA; 3) by increasing or decreasing protein-protein interaction with TF regulators; and 4) by serving as docking domain for bromodomain of HATs, which can increase their transcriptional activity (Haery et al., 2015; Yang and Gregoire, 2005).

Surprisingly, HDAC1 and 2 might also promote gene expression. Numerous KO studies in yeast and mice demonstrated that a significant fraction of genes are down-regulated upon ablation of these enzymes (Bernstein et al., 2000; Montgomery et al., 2007; Yamaguchi et al., 2010; Zupkovitz et al., 2006). This may be explained by indirect effects on increasing expression of transcriptional repressors upon ablation of HDAC1 and HDAC2. Nevertheless, growing evidence indicates that these HDACs might be directly involved in gene activation. Genome wide chromatin immunoprecipitation (ChIP) and ChIP-seq (ChIP combined with high-throughput sequencing) experiments mapped several HDACs, including HDAC1 and 2 to transcriptionally active loci (Kidder and Palmer, 2012; Kurdistani et al., 2002; Wang et al., 2009). Hence, HDAC1 and 2 can mediate both gene repression and gene activation (Kelly and Cowley, 2013).

3. Role of HDAC1 and HDAC2 in B lymphocyte development

Most of the knowledge regarding the function of HDACs in development comes from loss-of-function studies in animal models. Numerous studies using mouse models with tissue-specific conditional deletion were performed to investigate the function of these enzymes in different tissues. These studies demonstrated that ablation of either HDAC1 or HDAC2 had no effect on the development of heart (Montgomery et al., 2007), epidermis (LeBoeuf et al., 2010), adipocytes (Haberland et al., 2010), oocytes (Ma et al., 2012), neuronal precursors (Montgomery et al., 2009), neural crest cells (Montgomery et al., 2007), MEFs (Wilting et al., 2010; Yamaguchi et al., 2010), T cells (Dovey et al., 2013) and B cells (Yamaguchi et al., 2010). Interestingly, ablation of both HDAC1 and HDAC2 results in a strong phenotype in these systems, demonstrating that HDAC1 and HDAC2 have redundant functions. I will discuss in further details the role of HDAC1 and HDAC2 in B cell development in the following sections.

3.1. B lymphocyte development - overview

B lymphocytes, like T lymphocytes and all other blood cell types, are derived from HSCs found in the fetal liver before birth and in the postnatal BM (Kondo et al., 1997; Lai and Kondo, 2008; Mandel and Grosschedl, 2010). These earliest pluripotent progenitor cells have self-renewal potential and are characterized by the absence of lineage markers (Lin⁻) as well as c-kit and Sca-1 expression (Spangrude et al., 1988). HSCs differentiate into multipotent progenitors (MPPs). During the process of differentiation, HSCs gradually lose self-renewing potential. MPPs have lost the ability to self-renew, but retain the capability to differentiate into separate lymphoid and myeloid lineages (Morrison et al., 1997). The first restriction step towards progenitor cell types, concomitant with gradual loss in pluripotency, is made when MPPs differentiate into common

myeloid progenitors (CMPs) and lymphoid multipotent progenitors (LMPPs) containing early lymphoid progenitor (ELPs) (Igarashi et al., 2002; Lai and Kondo, 2008; Medina et al., 2001). CMPs give rise to megakaryocyte/erythrocyte progenitors (MEPs) and granulocyte/macrophage progenitors (GMPs) (Parra, 2009). ELPs give rise to common lymphoid progenitors (CLPs), which in turn branch into B, T, natural killer (NK) lymphocytes, and dendritic cells (DCs) (Cobaleda and Busslinger, 2008; Kondo et al., 1997; Nutt and Kee, 2007). The first clearly identifiable B cell-specific progenitors in the BM that arise from CLPs are variously termed pre-pro B cells, CLP-2 or hereinafter referred as ProB cells (Nutt and Kee, 2007). B cells are then generated by further differentiation steps passing through early B cell precursors proB cells ($B220^+; c\text{-kit}^+; CD19^-; CD25^-; IgM^-$), preBI cells ($B220^+; c\text{-kit}^+; CD19^+; CD25^-; IgM^-$), PreBII cells (large and small) ($B220^+; c\text{-kit}^-; CD19^+; CD25^+; IgM^-$), immature B cells ($B220^+; c\text{-kit}^-; CD19^+; CD25^{+/-}; IgM^+$), expressing the characteristic indicated cell surface markers (Figure 3) (Matthias and Rolink, 2005). Immature B cells are produced in the BM and migrate to the spleen where are they found as transitional B cells (T1-3). Transitional B cells are then negatively selected and develop eventually into naïve B cells. These naïve B cells then differentiate into the terminally differentiated plasma cells and memory B cells (germinal-center B cells) ($B220^+; c\text{-kit}^-; CD19^+; CD25^-; IgM^+; IgD^+$) (Ikawa, 2014; Lopez-Granados, 2011; Matthias and Rolink, 2005).

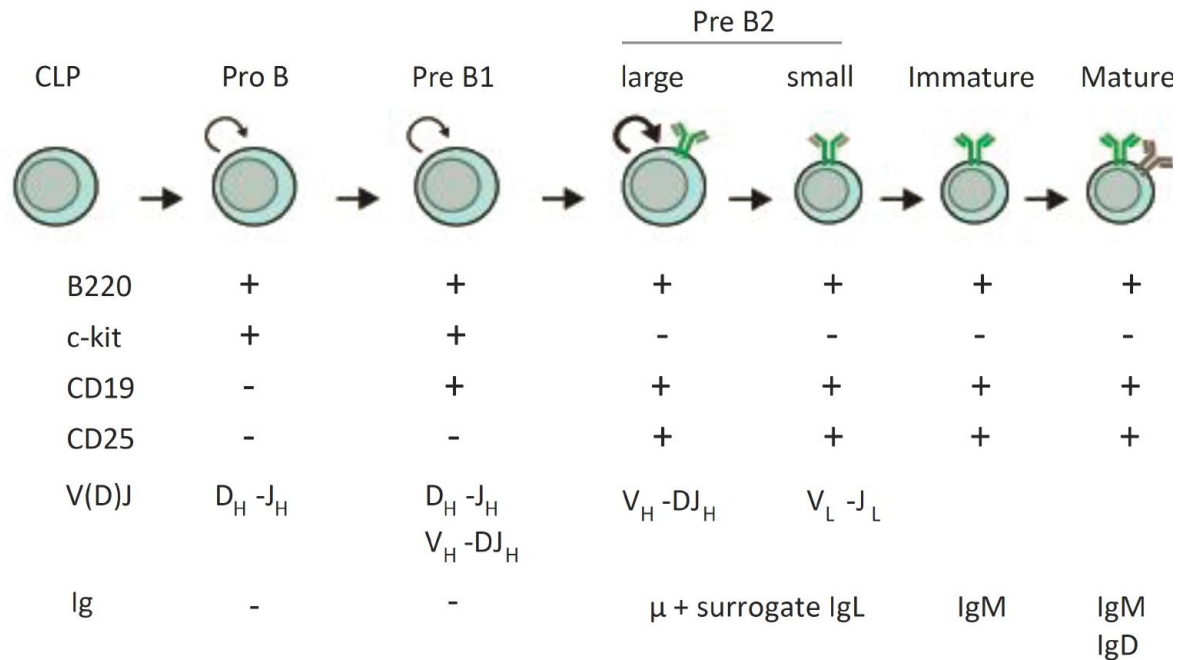


Figure 3: Schematic representation of early B-cell differentiation in the BM. The different developmental stages are shown. Surface cell markers used to discriminate them are indicated below: (+) expressed, (-) not expressed. Curved arrows indicate for proliferation activities: intermediate in pro-BI and pre-BI and high in large pre-BII; small pre-BII and immature and mature B cells are not proliferating. V(D)J rearrangement status of the different Ig gene alleles during B cell differentiation is shown. The kind of membrane bound immunoglobulin is indicated. (Figure adapted from (Yamaguchi et al., 2010)).

3.2. Ig recombination and B cell maturation

A key step during B development is the generation of diverse repertoire of high affinity B cell receptors (BCR) which is needed for adaptive immune response by B cells. The BCRs consist of an *immunoglobulin (Ig) heavy chain (IgH)* and *Ig light chain (IgL)*. The extremely diversified primary BCR repertoire is generated by V(D)J recombination. This process involves recombination activating genes (RAG) 1 and 2 proteins that bind recombination signal sequences (RSS) (Lopez-Granados, 2011). Once the *IgH* chain has been rearranged in large PreBII cells, it assembles at the surface of the cell with the surrogate Ig light chain to form a functional pre-B-

cell receptor (pre-BCR) (Figure 3) (Matthias and Rolink, 2005). Signaling through the pre-BCR mediates allelic exclusion, a mechanism by which only one of the IgH allele undergoes recombination (Mostoslavsky et al., 1999). This stimulates proliferation and clonal expansion of such large preBII cells (Matthias and Rolink, 2005). Efficient signaling through the pre-BCR is required for rearrangement of the IgL locus. Successful rearrangement of the IgL will allow the expression of the BCR. At this immature B cell stage, cells are tested for autoreactivity. Autoreactive B cells undergo a secondary Ig gene rearrangement known as receptor editing otherwise eliminated or inactivated (Nemazee and Weigert, 2000). After having successfully passed this check-point immature B cells exit the BM and circulate to the spleen. There these transitional B cells are negatively selected and then differentiate to mature B cells (Matthias and Rolink, 2005). B cells undergo *Ig* class switch DNA recombination (CSR), resulting in an isotype switch from IgM/IgD to IgG, IgE, or IgA, and also undergo somatic hypermutation (SHM), a mutation process that introduces single nucleotide substitutions into the variable region of Ig genes. Thereby, these antigen specific B cells further improve their affinity to antigens (Zan and Casali, 2015). Finally, these B cells can differentiate to memory B cells or long-lived plasma cells for the immune memory (Zan and Casali, 2015).

3.3. Epigenetic control of B cell development and Ig recombination

B cell development requires appropriate regulation of dynamic TF networks. Lineage commitment requires activation of lineage-specific gene-expression programs and repression of lineage-inappropriate-gene programs (Kioussis and Georgopoulos, 2007; Mandel and Grosschedl, 2010; Nutt and Kee, 2007). Several TFs were shown to induce B cell lineage specification and determination: PU.1, Ikaros, E2A, EBF1, and Pax5 could be considered as the

most important TFs in this process (Busslinger, 2004; Matthias and Rolink, 2005; Nutt and Kee, 2007). Increasing body of evidence demonstrates that B cell development is also regulated by epigenetic mechanisms (Ikawa, 2014; Lopez-Granados, 2011; Parra, 2009). This regulation may act by interplay of transcription factors and epigenetics. Gene expression programs during B cell development are activated by recruitment of lineage-specific TFs, but also by chromatin remodeling upon epigenetic changes. Several changes in histone modifications and DNA methylation have been reported at lineage specific loci in HSCs and MPPs (Attema et al., 2007; Lopez-Granados, 2011). Interestingly, progression through lymphocyte differentiation from HSCs to lymphoid lineages is associated with loss of the well-studied epigenetic marks, histone 3 acetylation (H3Ac) and histone 4 acetylation (H4Ac). This indicates a closed chromatin structure at lineage non-associated genes (Attema et al., 2007; Maes et al., 2008). Hence, this suggests that lymphoid-specific genes are already "primed" for expression before lineage commitment and that this permissive chromatin structure is progressively lost during differentiation (Maes et al., 2008). However, this model was recently challenged by Choukrallah *et al.*, in our lab, demonstrating that enhancer repertoires are reshaped independently of early priming and heterochromatin dynamics during B cell differentiation (Choukrallah et al., 2015).

Another example of epigenetic regulation during B lymphocyte development involves regulation of V(D)J recombination in the Ig gene locus (Li et al., 2013; Schatz and Ji, 2011; Su and Tarakhovsky, 2005). H3Ac and H4Ac were shown to be enriched in the *IgH* locus during V(D)J recombination. This requires an accessible open chromatin conformation allowing RAG1 and RAG2 proteins to access and cleave DNA at the RSS (Busslinger, 2004; Chowdhury and Sen, 2001; Johnson et al., 2003; McMurry and Krangel, 2000; Morshead et al., 2003).

3.4. HDAC1 and HDAC2 in B cell development

Yamaguchi *et al.*, generated in our lab *HDAC1* and *HDAC2* B cell-specific KO mice to dissect the role of individual HDACs in B cell development and showed that in B cells, HDAC1 and HDAC2 have redundant functions. Conditional deletion of either *HDAC1* or *HDAC2* alone in early B cell stages has no obvious effect (Yamaguchi et al., 2010). Conversely, combined loss of HDAC1 and HDAC2 results in a block in B cell development and cell cycle arrest. Hence, HDAC1 and HDAC2 play a key role in B cell development. In resting mature B cells, combined deletion of HDAC1 and 2 has no effect on cell survival or function. However, *HDAC1* and *HDAC2* double KO cells fail to proliferate in response to lipopolysaccharide (LPS) and IL-4 (Yamaguchi et al., 2010).

4. The biology of HDACs in cancer

Initially, cancer has been regarded as consequence of alterations in DNA sequence including mutations, deletions, amplifications and rearrangements affecting oncogenes or tumor suppressor genes. A compelling body of evidence indicates that epigenetic alterations also contribute to cancer initiation and progression. In contrast to genetic alterations, epigenetic changes are reversible, and therefore attractive targets for cancer therapy. Chromatin modification proteins, like HATs and HDACs, were shown to be good targets. One prominent example of such epigenetic drugs with potent anticancer activity are HDACis (Hagelkruys et al., 2011; Rodriguez-Paredes and Esteller, 2011). In the following sections, I briefly introduce B cell malignancies with the focus on lymphomas with *c-myc* deregulation. I will discuss as well the role of HDACs in tumorigenesis, their contribution to the hallmarks of cancer and their involvement in B cell malignancies. Finally, I will discuss the use of HDACis in the treatment of these diseases.

4.1. B cell lymphomas with *c-myc* deregulation

The *c-myc* oncogene is described as one of the most frequently deregulated proteins in cancer and is estimated to be activated in 20% of all human cancers (Nesbit et al., 1999). Deregulated *c-myc* expression in cancer correlates with high proliferation, reprogrammed cellular metabolism and poor prognosis (Dang, 2012; Van Dang and McMahon, 2010).

The c-myc oncogene

c-Myc is the most studied member of the Myc protein family of transcription factors (Dang, 2012; Luscher and Vervoorts, 2012). c-Myc forms a heterodimer with its partners Max (Myc associated x) and Mad (Max dimerization protein). In most cases c-Myc acts by binding E-boxes

(CACGTG) and recruiting transcriptional coactivators to regulatory promoter elements in target genes (Conacci-Sorrell et al., 2014; Dang, 2012). c-Myc also represses genes by recruiting HDACs and by binding and inhibiting Miz-1, a transcriptional activator (Eilers and Eisenman, 2008; Kurland and Tansey, 2008).

c-Myc can activate or repress transcription of numerous genes and thereby regulating multiple cellular processes (Eilers and Eisenman, 2008). The c-Myc protein is important in the regulation of cellular growth and differentiation. *c-myc* is transcriptionally up-regulated during proliferation and repressed during differentiation (Zou et al., 1997). It is involved in many biological functions, including regulation of cell proliferation, differentiation, cell cycle progression and apoptosis (Figure 4) in many cellular types, including B lymphocytes (Meyer and Penn, 2008; Pelengaris et al., 2002). c-Myc promotes during cell cycle the G₀/G₁-S transition by activating genes that encode proteins of the cyclin/cyclin-dependent kinase complexes and by repressing cell cycle inhibitors such as p21 or p27 in numerous cell types (Bernard and Eilers, 2006).

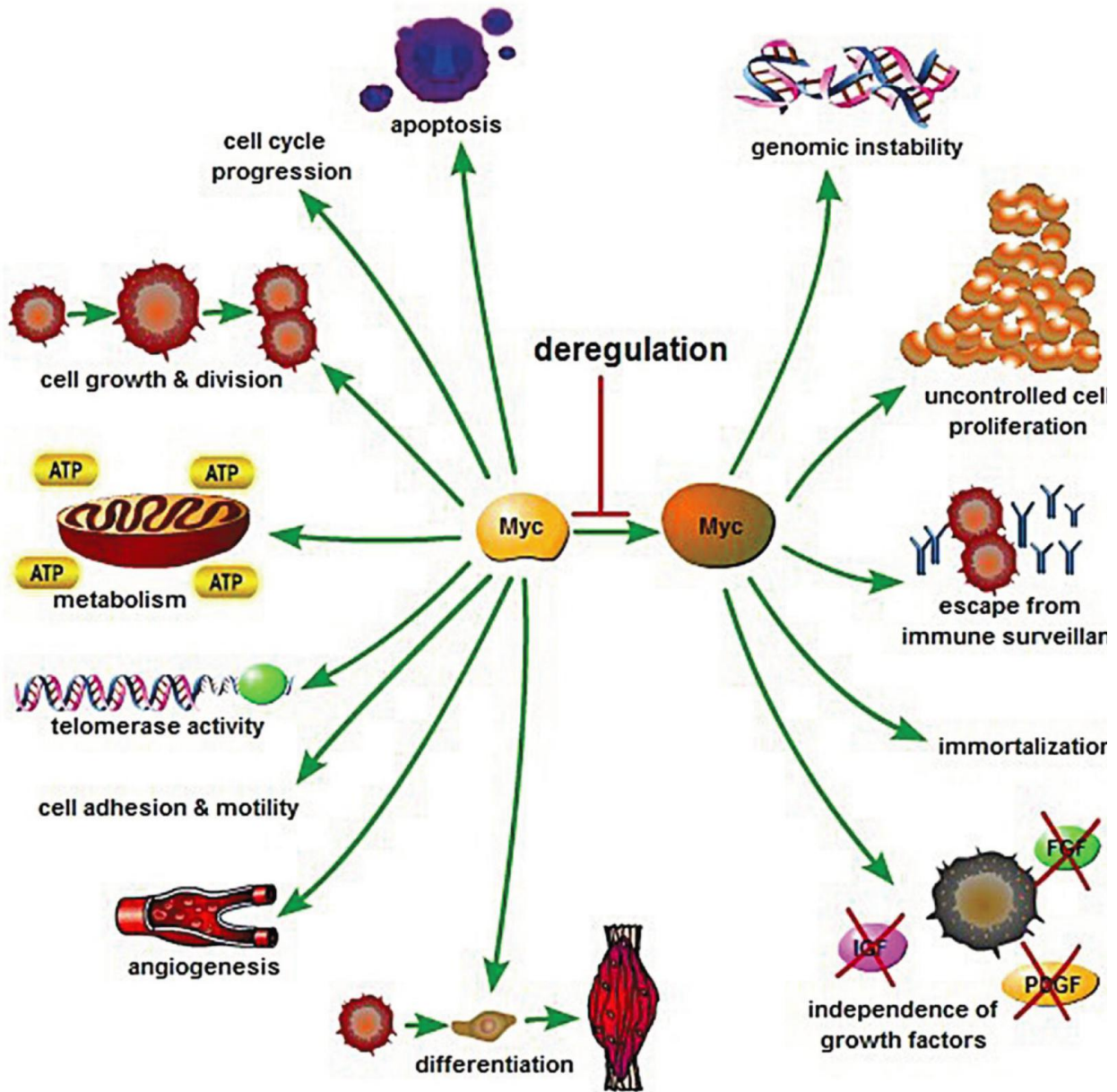


Figure 4: Biological functions of c-Myc in health and disease. c-Myc regulates proliferation, cell-cycle, apoptosis, cell differentiation, cell metabolism, angiogenesis, cell adhesion and motility. Deregulation of Myc may result in apoptosis, uncontrolled cell proliferation, genomic instability, escape from immune surveillance, immortalization and growth factor independence (Cai et al., 2015).

c-Myc was initially described as a general transcription factor that amplifies gene expression without any specificity (Levens, 2013; Lin et al., 2012; Nie et al., 2012). Subsequent studies

reported, that overexpressed c-Myc binds to almost all active promoters within a cell, although with different binding affinities (Guccione et al., 2006; Lin et al., 2012; Sabo et al., 2014), and modulates the expression of distinct subsets of genes (“selective amplification”) (Dang, 2014; Guccione et al., 2006; Sabo et al., 2014; Van Dang and McMahon, 2010; Walz et al., 2014).

The c-Myc transcriptional network also regulates the expression of large number of non-coding RNA, including microRNAs (miRNAs) that bind mRNA, and typically inhibit translation (Bui and Mendell, 2010). These miRNAs regulated by c-Myc were shown to act as oncogenes (Chang et al., 2008) or tumor suppressor genes (Cai et al., 2015). Interestingly, c-Myc represses several miRNAs involved in tumor suppression by recruiting HDACs. These miRNAs regulate important functions in tumorigenesis such as apoptosis, proliferation, or cell differentiation (Cai et al., 2015; Ott et al., 2013). In addition c-Myc was recently shown to act on long-non-coding RNAs (lncRNAs) which typically form functional secondary and higher order structures comprising protein-protein or protein-nucleic acid complexes (Weinberg et al., 2015). Interestingly, c-Myc may also repress transcription by recruiting HDACs to promoter containing E-boxes (Ott et al., 2013; Zhang et al., 2012).

In cancers induced by genetic deregulation of *c-myc* expression, loss of checkpoint components, such as p53, allows c-Myc to drive malignant transformation (Klapproth and Wirth, 2010). Deregulation of c-Myc results in apoptosis, genomic instability, uncontrolled cell proliferation, escape from immune surveillance, immortalization and independence of growth factor (Figure 4) (Cai et al., 2015).

The relevant oncogenic role of c-Myc has encouraged scientist to search for therapeutic strategies. However, targeting c-Myc pharmacologically appears to be difficult due to its lack of a simple enzymatic function that mediates its activity (Vita and Henriksson, 2006). The

breakthrough came in 2011, with the discovery that *c-myc* transcription depends on the regulatory function of BRD4, and the two inhibitors JQ1 and iBET (Delmore et al., 2011; Mertz et al., 2011). This discovery opened the way for new potential therapeutic opportunities. BRD4 is a member of the bromodomain and extraterminal (BET) protein family that can bind specific acetylated lysine residues on histone tails (Albihn et al., 2010; Delmore et al., 2011). Two small molecule inhibitors, JQ1 and iBET, displace BRD4 from acetylated lysine. Thereby, these inhibitors downregulate *c-myc* and modulate its transcriptional program. They were shown to have marked anti-proliferative cell effects and to inhibit tumor growth (Ott et al., 2013).

B lymphocyte malignancies-overview

Lymphomas are solid tumors of the immune system. They represent approximately 5% of all cancers and are the most common hematological malignancy in the United States (Groves et al., 2000). They can be divided in two major groups: 10% of all lymphomas are Hodgkin's lymphoma (HL), and the remaining 90% are referred to as non-Hodgkin lymphomas (NHL) (Shankland et al., 2012; Siegel et al., 2015). NHL is a large heterogeneous group of malignancies that derive from a monoclonal proliferation of B or T lymphocytes and less commonly natural killer (NK) cells. The vast majority of all NHL (85–90 %) derive from B lymphocytes and the rest arise from T lymphocytes or NK lymphocytes. The two most common types are diffuse large B-cell lymphoma (DLBCL) and follicular lymphoma (FL), (Chiu and Hou, 2015). NHL can develop at various stages of differentiation, and can occur in almost any tissue (Chiu and Hou, 2015; Shankland et al., 2012). NHL are distinguished between precursor and mature neoplasms corresponding to stages of differentiation. NHL ranges from the most indolent follicular lymphoma (FL) to the most aggressive DLBCL and Burkitt's lymphomas (BL) (Shankland et al.,

2012). These malignancies are presently classified according to the fourth edition of the World Health Organization (WHO) classification of tumors of hematopoietic and lymphoid tissues (Campo et al., 2011).

The *c-myc* oncogene is dysregulated in most hematopoietic malignancies (Dang, 2012). Almost all lymphomas with deregulated *c-myc* are of B cell origin. The most prominent abnormality are chromosomal translocations involving *c-myc* found in BL and DLBCL.

The E μ -myc mouse model

The transgenic (tg) E μ -*myc* mouse was developed as a preclinical model for studying *c-myc*-induced tumorigenesis (Adams et al., 1985). In these E μ -*myc* mice the *c-myc* gene (from a murine plasmacytoma) was placed under the ectopic control of the lymphoid-specific *IgH* locus enhancer (E μ). Hence, these mice carrying the tg, overexpress the *c-myc* oncogene in the B cell lineage and develop tumors at several stages of B cell development. Tg expression causes hyperproliferation of B-lymphocytes (Harris et al., 1988). These mice rapidly and invariably develop clonal tumors with both pre-B and B cell phenotypes (Adams et al., 1985; Harris et al., 1988), causing massive enlargement of lymph nodes (LN). Blood and lymphoid organs such as spleen (SP), lymph nodes (LNs) and thymus predominantly contain lymphoblastic cells. The pathological diagnosis of these tumors is multicentric lymphosarcoma (disseminated lymphoma) with associated leukemia (Adams et al., 1985).

The E μ -*myc* mouse model has been successfully used to perform genetic manipulation by cross-breeding and retroviral transduction to produce “compound mutant” lymphomas. These are useful tools for *in vitro* and *in vivo* studies to identify molecular pathways important for a given drug, like HDACis, to have an anticancer effect (Lindemann et al., 2007; Schmitt et al., 2000).

4.2. Role of acetylation in cancer

It is now clear that epigenetic changes have important impact on tumor initiation and progression (Bannister and Kouzarides, 2011; Esteller, 2008). Aberrant histone modifications or dysregulated activity of associated enzymes may lead to cancer through at least two different mechanisms: i) by altering gene expression of oncogenes and/or tumor suppressor genes, and ii) by affecting genome integrity and/or chromosome segregation (Bannister and Kouzarides, 2011).

Acetylation has been associated to both hematological and solid malignancies (Esteller, 2008; Wang et al., 2007). Overexpression of *HDACs* or inactivating mutations and gene deletions of HATs are commonly found in B and T cell malignancies. Decreased global histone and TF acetylation appears to correlates with tumor cell proliferation and survival, whereas increased acetylation is associated with tumor growth arrest and cell death (Haery et al., 2015).

HATs and cancer-overview

Altered activity of HATs has been identified in various cancers and can occur due to genetic mutations, chromosomal translocations or aberrant recruitment and localization (Olzscha et al., 2015). One example of HATs involved in chromosomal rearrangement is the MOZ-TIF2 fusion which is associated with acute myeloid leukemia (AML) (Carapeti et al., 1998; Liang et al., 1998). It involves the HAT protein MOZ (Champagne et al., 2001) and the nuclear receptor coactivator TIF2 (Torchia et al., 1997). Deregulation of HATs, including CBP and p300, has been shown to impact on genome integrity and stability during replication in B cell lymphoma (Pasqualucci et al., 2011).

HDACs and cancer-overview

In cancer, several normal cellular functions are deregulated. Several of these processes, including proliferation, apoptosis, autophagy, DNA repair and cell motility have been shown to be regulated at least in part by HDACs (Hagelkruys et al., 2011; Peng and Seto, 2011). In cancer, several HDACs have been shown to be deregulated (usually overexpressed) or misstargeted, but are generally not known to be mutated (Olzscha et al., 2015). For instance HDAC1 and HDAC2 have been reported to be overexpressed in many tumor types, including in B cell lymphomas (Haery et al., 2015). In addition, HDAC function can also become deregulated and ultimately lead to cancer in the context of chromosomal translocations which result in aberrant fusion proteins that bind and misregulate these HDACs. One prominent example is acute promyelocytic leukemia (APL) where the *retinoic acid receptor (RAR)* gene is fused to the *promyelocytic leukemia (PLM)* gene, resulting in the RAR α -PML fusion protein (Ellis et al., 2009a).

4.3. Impact of HDACs on the hallmarks of cancer

The hallmarks of cancer, described by Hanahan and Weinberg (Figure 5) (Hanahan and Weinberg, 2000, 2011), are known to be regulated by epigenetic mechanisms, including histone acetylation (Hagelkruys et al., 2011). In the following sections, I discuss the major impacts of HDACs on some crucial hallmarks for cancer development (Figure 6).

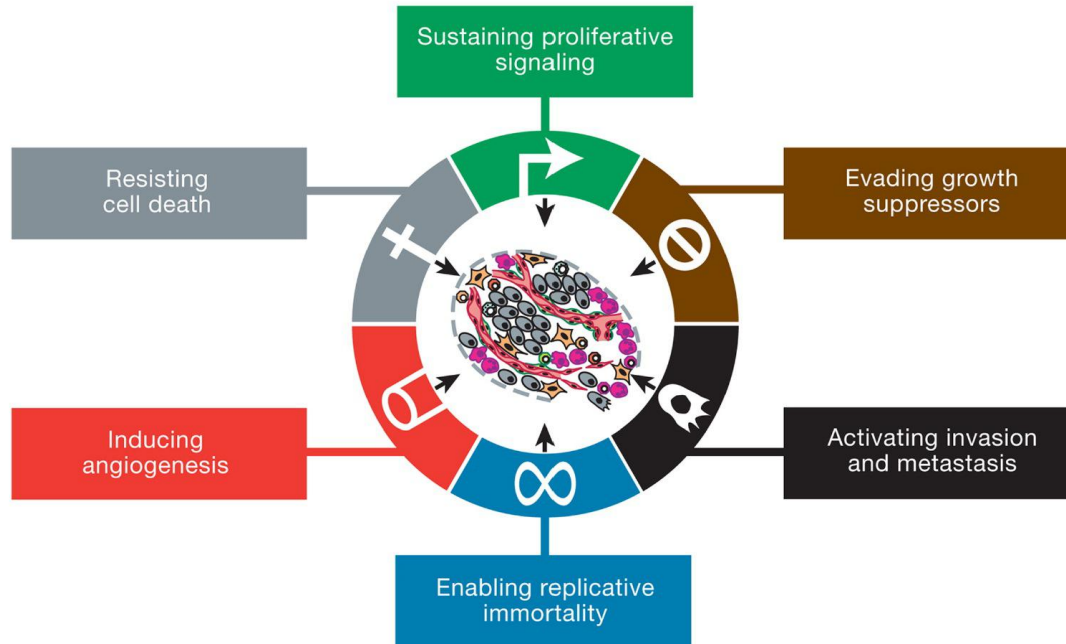


Figure5: The hallmarks of cancer. Illustration of the six hallmark capabilities proposed by Hanahan and Weinberg (Hanahan and Weinberg, 2011).

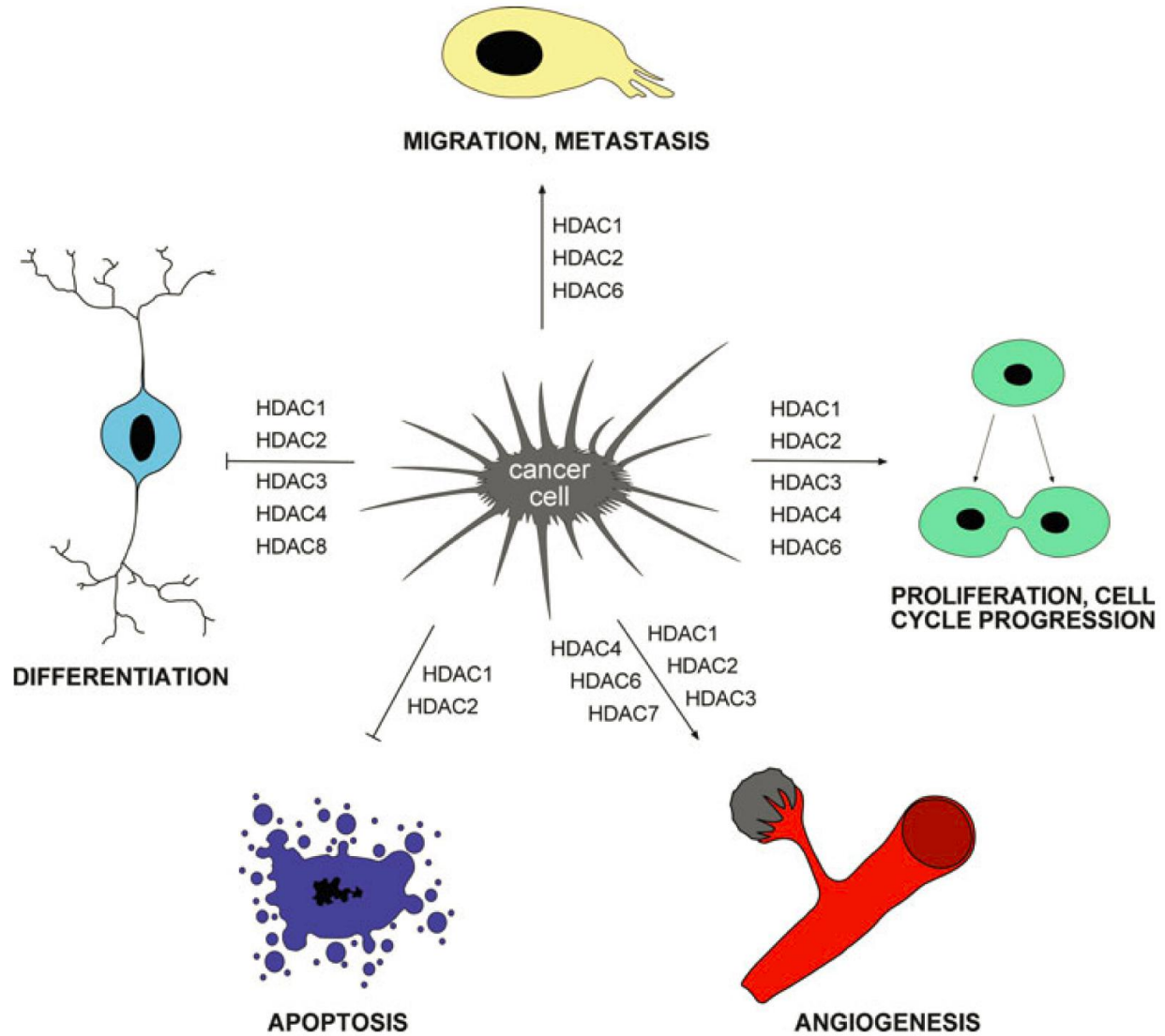


Figure 6: Impact of HDACs on the hallmarks of cancer. HDAC induce proliferation, angiogenesis and metastasis, whereas they block apoptosis and differentiation. The impact of individual HDAC isoforms are indicated (Hagelkruys et al., 2011).

HDACs and proliferation

The ability of cancer cells to sustain chronic proliferation is the most fundamental and the first of the six cancer hallmarks (Hanahan and Weinberg, 2000, 2011). HDAC1, 2, 3, and 4 were shown

to be implicated in proliferation of cancer cells (Glaser et al., 2003; Haberland et al., 2009a; Mottet et al., 2009; Senese et al., 2007; Wilson et al., 2008). These HDACs affect cell cycle, and lead to G1 or G2/M cell cycle arrest and a delay in S-phase progression (Hagelkruys et al., 2011). Ablation of *HDAC1*, 2, 3, or 4 has been shown to have an impact on proliferation by increasing the levels of cyclin-dependent kinase inhibitors (CKI) including p21^{WAF/CIP1}, p27^{KIP1}, and p57^{KIP2} preventing cell cycle progression in different cellular systems including primary and transformed cells (Lagger et al., 2002; Mottet et al., 2009; Senese et al., 2007; Wilson et al., 2008; Wilson et al., 2006; Yamaguchi et al., 2010; Zupkovitz et al., 2010). In addition to the regulation of cell cycle regulatory genes, HDACs also affect cell cycle progression by impacting on histone acetylation and thereby affecting the chromatin structure during mitosis (Krebs et al., 2000).

HDAC1 is mainly considered as positive regulator of proliferation. Mice lacking *HDAC1* have proliferation defects and are embryonically lethal (Lagger et al., 2002). Consistently, ablation of *HDAC1* in embryonic stem (ES) cells also leads to proliferation defects (Zupkovitz et al., 2010). However, the impact of HDAC1 on proliferation depends on the cell type and probably on its corresponding HDAC1 target genes. For example, loss of *HDAC1* was linked to enhanced proliferation of T cells (Grausenburger et al., 2010) and epithelial cells (Lagger et al., 2010).

Ablation of both *HDAC1* and *HDAC2* in tumor cells have been reported to block tumor cell growth, by inducing nuclear bridging and fragmentation and eventually cell death (Haberland et al., 2009a). In fact, combined deletion of both *HDAC1* and *HDAC2*, strongly impacts on proliferation with dramatic defects in cell cycle progression in several systems, including fibroblasts, hematopoietic cells, B and T cells, cardiomyocytes, neural and epidermal cells (Dovey et al., 2013; LeBoeuf et al., 2010; Montgomery et al., 2007; Montgomery et al., 2009;

Wilting et al., 2010; Yamaguchi et al., 2010). HDAC6 as well as Sirtuin 1 (SIRT1) have also been shown to be implicated in proliferation of cancer cells (Hagelkruys et al., 2011; Lee et al., 2008).

Impact of HDACs in resistance to apoptosis

Evasion of apoptotic cell death is a hallmark of most and perhaps all cancer types (Hanahan and Weinberg, 2000, 2011). Apoptosis is a natural barrier to cancer development, and is triggered in response to numerous physiological stresses. Such apoptosis-inducing stresses are among others DNA damage, signaling imbalance resulting from oncogene action of e.g. c-Myc, insufficiency of survival factors, or hypoxia (Evan and Littlewood, 1998; Lowe et al., 2004). Apoptosis is a programmed cell death, which is orchestrated in a precise series of steps leading to the complete degradation of the cell, through selected destruction of subcellular structures and organelles and the genome (Adams and Cory, 2007; Hanahan and Weinberg, 2011).

In tumorigenesis, HDACs act as regulators in the process of apoptosis. (Hagelkruys et al., 2011). The apoptotic machinery is composed of sensor proteins, detecting abnormalities, and effector proteins mediating cell death through two major apoptotic programs, the extrinsic and the intrinsic. Both apoptotic pathways are affected by HDACs. They can both be induced by HDACis treatment (Beumer and Tawbi, 2010; Hagelkruys et al., 2011). In tumor cells, HDACis trigger increased expression of sensor protein receptors and their ligands from the extrinsic apoptotic pathway (Xu et al., 2007). Interestingly, HDAC1 and HDAC2 were shown to be the major targets for this HDACi-mediated extrinsic apoptosis induction (Inoue et al., 2006).

The apoptotic trigger is controlled by pro- and anti-apoptotic members of the Bcl-2 family of regulatory proteins. These proteins are either pro-apoptotic (Bax, Bak, Bid, Bim) or anti-

apoptotic (Bcl-2, Bcl-XL, Bcl-W). Bcl-2 and Bcl-xl inhibit apoptosis largely by suppressing the two pro-apoptotic proteins Bax and Bak (Hanahan and Weinberg, 2000). Inhibition of HDACs by HDACis causes a decrease in expression of such antiapoptotic factors and an increase of proapoptotic Bcl-3 family members (Beumer and Tawbi, 2010). Furthermore, also specific HDAC1 knockdown in some cancer cells can activate such pro-apoptotic genes and thereby increase apoptosis (Senese et al., 2007). These pro- and anti-apoptotic proteins control mitochondrial death signaling through cytochrome C release, which then activates a cascade of caspase proteases that execute the cell death program (Hanahan and Weinberg, 2000). *HDAC1* knockdown was shown to induce the release of Caspase-3 and thereby guide initiation of apoptosis (Senese et al., 2007).

Alterations in components of the apoptotic machinery have dramatic effects on tumor progression. This provides a rationale for the inactivation of apoptosis during tumor development (Hanahan and Weinberg, 2000). The apoptotic program can be circumvented e.g. by overexpression of anti-apoptotic oncogenes like Bcl-2. Differently, OE of oncogenes like *c-myc* triggers apoptosis, unless counterbalanced by anti-apoptotic factors (Junttila and Evan, 2009; Lowe et al., 2004). Furthermore, also tumor suppressors like p53 can cause apoptosis by upregulation of pro-apoptotic Bax in response to DNA damage and need to be counteracted for malignant transformation to occur (Dang et al., 2005). Resistance to apoptosis can be acquired by cancer cells through mutations in p53 that functionally inactivate this tumor suppressor. This was reported to occur in more than 50% of human cancers (Hanahan and Weinberg, 2000; Harris, 1996; Junttila and Evan, 2009). Interestingly, HDAC1 can deacetylate p53, which is destabilized and degraded, and thereby repress p53-dependent transcription (Ito et al., 2002; Luo et al., 2000; Tang et al., 2008).

Angiogenesis and HDACs

Angiogenesis, a process of generation of new blood vessels from preexisting vasculature is another hallmark of cancer (Hanahan and Weinberg, 2000, 2011). Vascularization of all tissues, including tumors is needed to access to oxygen and nutrients, as well as removing carbon dioxide and metabolic waste products. Tumor-associated neovasculature is critical for progression and metastasis of solid tumors. Already early during tumorigenesis, an “angiogenic switch” occurs, which causes normally quiescent vasculature to sprout new blood vessels. This helps to sustain expansion of neoplastic growth (Bergers and Benjamin, 2003; Hanahan and Folkman, 1996; Raica et al., 2009).

Under physiological conditions, angiogenesis is tightly regulated by angiogenic regulators that bind to stimulatory or inhibitory cell surface receptors on vascular endothelial cells (Baeriswyl and Christofori, 2009). The best known angiogenesis inducer is the vasculature endothelial growth factor (VEGF). Such angiogenic factors that promote neovascularization can be upregulated upon hypoxia or in some tumors upon oncogene signaling mediated by e.g. *c-Myc* and *RAS* oncogenes (Carmeliet, 2005; Hanahan and Weinberg, 2011).

The primary trigger of angiogenesis is hypoxia within the tumor microenvironment. This induces hypoxia-inducible factor 1 α (HIF-1 α), a key regulator of angiogenesis (Ellis et al., 2009c). Importantly, the stability of HIF-1 α is regulated partly by acetylation. Under normoxic conditions HIF-1 α undergoes acetylation, and is degraded by the ubiquitin-proteasome pathway. Whereas under hypoxic conditions, HIF-1 α is stabilized and leads to transcriptional induction of its target genes, including VEGF, and thereby mediate angiogenesis (Ke and Costa, 2006).

HDACs were reported to regulate angiogenesis. Several HDACs, including trichostatin A (TSA), were shown to have antiangiogenesis properties by inhibiting HIF-1 α (Kim et al., 2001). Interestingly, expression of *HDAC 1, 2, and 3* has been shown to increase in response to hypoxia. More importantly, *HDAC1* OE leads to increased level of HIF-1 α and VEGF (Kim et al., 2001). HDAC1, 3, 4, and 6 have been shown to interact with HIF-1 α and enhance its stability and activity under hypoxic conditions, suggesting important roles of these enzymes in HIF-1 α mediated neovascularisation in tumors (Kim et al., 2007; Qian et al., 2006). Interestingly, HDAC6 has been shown to repress the expression of the metalloproteinase ADAMTS1 which is responsible for sequestration of VEGF and release of TSP-1/2 (Chou and Chen, 2008). In summary, class I and II HDACs play a crucial role in angiogenesis and are attractive targets for antiangiogenic therapy (Hagelkruys et al., 2011).

Impact of HDACs on invasion and metastasis

In most types of human cancer, some cells acquire the potential to escape the primary tumor mass and colonize new distant sites. This process called invasion and metastasis is associated to higher pathological grades of malignancy and is the main cause of human cancer death (Hanahan and Weinberg, 2011).

Interestingly, HDAC6 has been shown to regulate cell motility and epithelial-mesenchymal transition (EMT) (Shan et al., 2008). EMT is the biological process that allows a stationary epithelial cell to undergo multiple phenotypic changes, including the loss of cell-cell adhesion, to acquire mesenchymal characteristics with enhanced migratory capacity and invasiveness (Polyak and Weinberg, 2009; Thiery et al., 2009).

HDAC6 is a microtubule-associated deacetylase that deacetylates alpha-tubulin and thereby positively impacts on cell migration (Hubbert et al., 2002). In addition to its role in microtubule-dependent cell motility, HDAC6 also modulates cell migration by deacetylation of cortactin (Zhang et al., 2007). In addition, HDAC6 deacetylates HSP90 alpha that regulates client oncoproteins involved in invasion and metastasis (Yang et al., 2008).

Metastatic cells have altered cell shape and lose the attachment to the extracellular matrix. Cancer cells can acquire invasiveness and metastatic ability by activating extracellular proteases, altering the binding specificity of cell adhesion molecules (CAM) and integrins (Hanahan and Weinberg, 2000). The most prominently altered CAM is E-cadherin, a key suppressor of invasion and metastasis (Bex and van Roy, 2009). E-cadherin expression is repressed by SNAIL/SLUG TFs. Interestingly, SNAIL1 interacts with HDAC1 and HDAC2 to repress E-cadherin in tumor cells (Peinado et al., 2007; von Burstin et al., 2009).

Furthermore, several metastasis repressors were shown to be induced in response to HDACis. Hence, HDACs have a promoting role in tumor metastasis (Hagelkruys et al., 2011). Despite considerable advances in this field, the complex process of metastatic dissemination and the role of HDACs in this process is not completely understood yet (Hagelkruys et al., 2011; Hanahan and Weinberg, 2011).

4.4. Role of HDACs in B cell malignancies

HDAC dysregulation in hematological malignancies

Altered expression and function of various HDACs is a common feature of a wide range of human cancers, including in B cell, T cell, and other hematological malignancies but also solid tumors (Haery et al., 2015). HDACs can be deregulated in their expression or abnormally

recruited in tumor cells (Mercurio et al., 2010). However, OE is the most prevalent alteration of HDAC function in tumors (Hagelkruys et al., 2011). Many studies provide compelling evidence that deregulated *HDAC* expression plays a key role in cancer. Elevated levels of different HDACs in cancer cells are often linked to more aggressive disease and poor prognosis (Hagelkruys et al., 2011).

In hematological malignancies, where chromosomal translocations are the main cause, HDACs can be aberrantly recruited to promoters through association with such oncogenic DNA-binding fusion proteins. One prominent example is the fusion protein PML-RAR, which causes APL. In this disease co-repressor complexes containing HDAC3 are recruited and decrease transcription of PML-RAR target genes (Atsumi et al., 2006). Another cause of hematological malignancies is OE of repressive TFs which interacts with HDACs. In DLBCL for example, the TF Bcl6 is overexpressed and recruits HDAC2 causing repression of genes regulating cell growth (Pasqualucci et al., 2003).

HDAC1 and HDAC2 involvement in lymphoma and leukemia

HDAC1 and *HDAC2* have been reported to be overexpressed in several B and T cell lymphomas and leukemias (Haery et al., 2015), including ALL (Gruhn et al., 2013; Moreno et al., 2010; Van Damme et al., 2012); HL (Adams et al., 2010); DLBCL (Marquard et al., 2009). Even though both *HDAC1* and *HDAC2* are highly expressed in classical HL, only *HDAC1* expression correlated with a worse outcome (Adams et al., 2010). However, *HDAC2* expression was found to be higher in aggressive compared to indolent CTCL (Marquard et al., 2008). Hence, the precise role of HDAC1 and HDAC2 in the different cancer types remains elusive. HDAC1 and HDAC2 were shown to have tumor promoting but also tumor suppressive functions. For

example, Santoro et al. performed transient depletion of mammalian *HDAC1* or *HDAC2* using small interfering RNA (Santoro et al., 2013), and demonstrated that HDAC1 has a dual role in APL: oncosuppressor in tumorigenesis, oncogene in tumor maintenance. Similar observations were made in a skin tumor model (Winter et al., 2013). Another study demonstrated that HDAC1 and HDAC2 have a dosage-dependent oncosuppressor role in thymocytes (Heideman et al., 2013). However, more mechanistic studies and genetic based evidences using different cancer models are needed.

HDAC6 in B cell malignancies

HDAC6 expression is also deregulated in several lymphoid malignancies. HDAC6 has been reported to be both overexpressed or underexpressed in different lymphoid malignancies. For example, HDAC6 OE was shown in ALL (Bradbury et al., 2005; Moreno et al., 2010; Van Damme et al., 2012), AML (Bradbury et al., 2005), CLL (Van Damme et al., 2012; Wang et al., 2011) and CTCL (Marquard et al., 2008). Surprisingly, HDAC6 was found to be both, overexpressed (Marquard et al., 2009; Zhang et al., 2004) and underexpressed (Gloghini et al., 2009) in DLBCL.

Furthermore, HDAC6 was shown to have oncogenic or tumor suppressor roles, depending on the cancer type and stage (Seidel et al., 2015). HDAC6 was shown to have oncogenic roles in AML (Bradbury et al., 2005). *HDAC6* was also found to be overexpressed in advanced stage of ALL (Bradbury et al., 2005). However, HDAC6 may also play a role as tumor suppressor. OE of *HDAC6* correlates with a good prognosis in DLBCL (Marquard et al., 2009), CLL (Van Damme et al., 2012) and CTCL (Marquard et al., 2008) and *HDAC6* underexpression was found to be

correlated with a poor prognosis in CLL (Van Damme et al., 2012). Hence, the exact role of HDAC6 in the different cancer types remains elusive.

4.5. HDAC inhibitors (HDACis) in treatment of lymphoid malignancies

Unlike DNA mutations, changes in the epigenome associated with cancer are potentially reversible. This enables the use of “epigenetic drugs” like HDACis in the treatment of several cancers (Sharma et al., 2010). The first indication that HDACis might be useful in cancer treatment came from studies done almost three decades ago showing that the first specific HDACi trichostatin A (TSA) has anti-proliferative activity in transformed cells *in vitro* (Yoshida and Beppu, 1988). Subsequently, various other compounds that inhibit HDAC activity were found. Several studies discovered that *HDACs* are overexpressed in various cancer types and cell lines (Haery et al., 2015). Hence, these enzymes represent an interesting pharmacological target for cancer therapy. Indeed, targeting HDACs using HDACis has demonstrated activity in hematological and solid malignancies (Falkenberg and Johnstone, 2014; West and Johnstone, 2014). HDACis represent now the most extensively studied family of epigenetic modulators (Seidel et al., 2012). In the following sections, I discuss the different types of HDACis and their use in research and clinics in the context of lymphoid cancers.

Mode of action of HDACis

HDACis modulate gene expression and cellular function via various molecular pathways. The major effects of HDAC inhibition by HDACis are 1) induction of apoptosis; 2) inhibition of cell cycle progression; 3) cellular differentiation; 4) suppression of angiogenesis and 5) enhancement

of antitumor immunity (Falkenberg and Johnstone, 2014). Thereby, HDACis impact on almost all hallmarks of cancer to control crucial functions in lymphomagenesis (see above).

The most prominent effect of HDAC inhibition is its effect on cell cycle regulation and control. HDACis block cell proliferation and cause apoptosis in hematologic and solid tumors cells by causing cell cycle arrest. HDACis affect the cell cycle mainly by regulating the expression of several cell cycle proteins including cyclins A and D (Sandor et al., 2000) and cyclin-dependent kinase inhibitors p21^{waf1/cip1}, p27^{Kip1} and p57^{Kip2} (Gui et al., 2004; Ocker and Schneider-Stock, 2007; Peart et al., 2003; Richon et al., 2000; Sambucetti et al., 1999). Thereby, HDACis induce cell cycle arrest at the G1/S or G2/M checkpoints (Bolden et al., 2006).

HDACis impact on survival pathways and induce death in tumor cells. HDACis regulate genome stability and repair, by preventing chromosome compaction and facilitating an accumulation of irreparable DNA breaks. Thereby, HDACis may induce apoptosis and impact on cell survival (Bhaskara et al., 2010; Miller et al., 2010; Robert et al., 2011). HDACis can induce both extrinsic and intrinsic apoptotic pathways. In addition, HDACis also induce tumor cell death through non-apoptotic mechanisms like autophagy (Shao et al., 2010; Zain and O'Connor, 2010). HDACis induce their effect by impacting on gene expression. HDACis induce histone hyperacetylation and mediate chromatin remodeling and thereby increase gene transcription (Figure 2). This is primarily occurring through inhibition of classI HDAC1, 2 and 3. HDACs have pleotropic effects and regulate the expression of numerous genes involved in multiple cellular processes (Falkenberg and Johnstone, 2014).

The therapeutic activity of HDACis is likely based on a combined effect on histone and nonhistone proteins (Johnstone and Licht, 2003). For example, through inhibiting HDAC6, HDACis act through hyperacetylation of nonhistone proteins like Hsp90 or TFs and thereby

increase or decrease their activity. For example, HDACi mediates degradation of HSP90 client oncoproteins, including BCR-ABL and ERBB2. This has been proposed as a major effector of HDACi mechanism of action (Bolden et al., 2006).

Importantly, it is expected that the effects of HDACis vary between different types of tumor cells, but also within a tumor type and even within a given tumor, due to the inter-and intra-tumor heterogeneity (Haery et al., 2015).

Classification of HDACis

Currently, numerous HDACis are used in clinics as therapeutic agents (Table 1). These inhibitors are chemically diverse and inhibit HDAC activity in a wide range of concentrations from low nM to high mM (Batty et al., 2009; Johnstone and Licht, 2003; Zain and O'Connor, 2010). HDACis can be classified into 3 main classes according to their chemical structure and specificity (Bradner et al., 2010): 1) hydroxamic acids, 2) cyclic tetrapeptides, 3) benzamides. The most predominant HDACi family is hydroxamic acids. The currently clinically most successful inhibitor of this family is SAHA (suberoylanilide hydroxamic acid) (Vorinostat, Zolinza; Merck). SAHA inhibits class I HDACs as well as HDAC6 at low nanomolar concentrations (Richon et al., 2009). Two other prominent hydroxamate HDACis are belinostat (PXD101, Beleodaq) that inhibits class I, II and IV HDACs and panobinostat (LBH589, Farydak) that inhibits only class I and II HDACs (Marks, 2010). Another hydroxamate is tubacin, a HDAC6 specific inhibitor (Butler et al., 2010), and trichostatin A (TSA) (Mai and Altucci, 2009). The prominent member of cyclic peptide HDACis is the depsipeptide romidepsin (FK228, Isodax; Celgene). It inhibits with high specificity class I HDACs but almost not HDAC6 (Batty et al., 2009; Furumai et al., 2002). Another group of HDACis are the benzamide

family inhibitors. These HDACis are class I selective and inhibit HDAC1, 2, and 3. It comprises among others entinostat (MS-275) and mocetinostat (MGCD-0103). Entinostat has highest efficacy against HDAC1 and mocetinostat mainly inhibits HDAC1 and HDAC2 (Mottamal et al., 2015).

HDACi	Class	Target of HDACi	Clinical trial stage
Vorinostat, Suberoylanilide hydroxamate (SAHA)	Hydroxamate	Class 1, 2, 4	Phase I, II, III
Belinostat (PDX101)	Hydroxamate	Class 1, 2, 4	Phase I, II, III
Panobinostat (LBH589)	Hydroxamate	Class 1, 2, 4	Phase I, II, III
Tubacin	Hydroxamate	Class 2b	
Tricostatin A (TSA)	Hydroxamate	Class 1, 2, 4	
Romidepsin (FK228)	Cyclic tetrapeptide	Class 1, 2, 4	Phase I, II, III
Valproic Acid (VPA)	Short-chain fatty acid	HDAC1-5, 7, 8, 10	Phase I, II, III
Entinostat (MS- 275)	Benzamide	HDAC1-3	Phase I, II
Mocetinostat (MGCD-0103)	Benzamide	HDAC1-3, 10, 11	Phase I, II

Table 1: Summary of HDACi compounds. Classified according to the HDACi classes. Target of HDACis and clinical trial stage are indicated (modified from ((Haery et al., 2015)

HDACi in clinical settings

HDACis have become promising targets for therapeutic intervention (Table 1). They are particularly active in hematologic malignancies and they gained since 2001 a widespread use in the clinic for the treatment such diseases (Falkenberg and Johnstone, 2014; Mercurio et al., 2010; Rasheed et al., 2008; West and Johnstone, 2014). Currently, four HDACis, varinostat, romidepsin, belinostat, and panobinostat, are Food and Drug Administration (FDA)-approved for

the following hematological malignancies: Cutaneous T cell lymphoma (CTCL), Peripheral T cell lymphoma (PTCL) and multiple myeloma (Ghobrial et al., 2013; Rasheed et al., 2008; Richardson et al., 2013; San-Miguel et al., 2013). Even though these HDACis are relatively well tolerated by patients, in some cases they were shown to have side effects like thrombocytopenia, cardiac toxicity, thrombosis and pulmonary embolism (Zain and O'Connor, 2010).

These FDA approved HDACis, and the majority of available HDACis, are broad-based pan-HDACis that target Zn²⁺-dependent HDACs, including class I and/or II HDACs including HDAC1, 2, 3, and 6 (Bantscheff et al., 2011). Due to the unselectivity of these pan-HDACis it is unclear which HDACs isoforms are crucial for tumor cell growth and/or survival. It still remains unclear whether selective HDAC inhibition might have comparable therapeutic benefit and whether they could limit toxicity observed with broad-spectrum inhibitors (Dawson and Kouzarides, 2012; Ononye et al., 2012). Therefore, isoform-selective HDACis have been developed (Balasubramanian et al., 2009). Currently there are very few HDAC isoform selective inhibitors available. Tubacin, a hydroxamate HDAC6 specific inhibitor, is one of these. Several other HDACis are currently in progress, mostly as oncology agents (Bolden et al., 2006; Khan et al., 2008; Moradei et al., 2008).

However, despite the very promising results in hematological malignancies, the use of HDACis in solid tumors have shown only limited clinical benefit and unfavorable side-effects (Slingerland et al., 2014). Nevertheless, many preclinical data and clinical trials appear promising for the use of HDACis in combination with other chemotherapeutics in the treatment of different types of lymphoma, leukemia and multiple myeloma, but also solid tumors (Dhanak and Jackson, 2014; Haery et al., 2015; Mai and Altucci, 2009; Olzscha et al., 2015; Slingerland et al., 2014). Some of the most promising drug combinations are HDACis with BCL6 inhibitors

or nicotinamide to co-target the *BCL6-p53* pathway, or with proteasome inhibitors like bortezomib (Paoluzzi et al., 2010; Zain and O'Connor, 2010). Hence, development of future therapeutic strategies involves now rational drug combinations to achieve synergistic effects.

HDACi in B cell lymphoma research

Currently, there are no HDACis approved specifically for the treatment of B cell lymphoma. However, increasing amount of pre-clinical data support a beneficial effect of select HDACis for their use in B cell malignancies. One of the first reports of the efficacy of HDACis in the treatment of B cell malignancies was published 10 years ago, demonstrating that the weak HDACi valproic acid induced a complete remission in a patient with refractory DLBCL (Zain et al., 2007). Subsequently, during the last decade, several other more potent HDACis have been tested for the treatment of B cell NHL (Haery et al., 2015). These studies demonstrated that several compounds including vorinostat have therapeutic activity in B cell malignancies. Currently, numerous HDACis are in development for various lymphoid malignancies (reviewed by (Haery et al., 2015)).

Pre-clinical research with the E μ -myc B cell lymphoma model demonstrated the activity of several currently available HDACis: Broad-spectrum HDACis like vorinostat, romidepsin and panobinostat were shown to have therapeutic efficacy in E μ -myc lymphoma (Ellis et al., 2009b; Lindemann et al., 2007; Newbold et al., 2008; Newbold et al., 2013; Newbold et al., 2014). However, it is not known whether single HDAC1 or HDAC2 isoform-selective inhibitors would offer similar or better anti-tumor efficacy. However, there are currently no available HDAC1-specific and only few HDAC2-specific inhibitors (Wagner et al., 2015), but there are several compounds capable of inhibiting both HDAC1 and HDAC2 (Mottamal et al., 2015). One

HDAC1 and HDAC2 isoform selective inhibitor, RGFP233 was shown to induce apoptosis in E μ -myc tumor cells *in vitro* (Matthews et al., 2015). Another, Cpd-60 (“Compound 60”) was shown to inhibit growth of primary B-ALL cells *in vitro* and *in vivo* (Methot et al., 2008; Schroeder et al., 2013; Stubbs et al., 2015), but has not been tested in E μ -myc cells. Although several of HDACis were shown to have an *in vitro* and/or *in vivo* therapeutic efficacy in pre-clinical model like E μ -myc, it is possible that different drugs may have different mechanistic, biological, and therapeutic activities.

5. Conclusion

Huge efforts were made in understanding the relevance of HDACs in health and disease. Particular progress was made in cancer research, where HDAC deregulation was shown to be strongly implicated. HDACs were shown to contribute to the hallmarks of cancer by inducing proliferation, angiogenesis and metastasis, as well as by blocking apoptosis. HDACis were shown to have effective broad-spectrum antitumor effects impacting on these hallmarks of cancer. However, the exact mechanism by which HDACis induce tumor cell death, remains unclear. Furthermore, the knowledge of the relevant HDACs isoforms in the different cancer settings is not comprehensive.

Research focusing on HDAC1, HDAC2 and HDAC6 has shown that these enzymes are implicated in many cancer types, including lymphoid malignancies. Most of these malignancies have dysregulation of the *c-myc* oncogene, which correlates with high proliferation and poor prognosis. The most prominent B cell lymphomas associated with recurrent *c-myc* rearrangement are BL and DLBCL. One prominent preclinical mouse model to study BL is the E μ -*myc* model B cell lymphoma.

Several efforts were made in the last decades to elucidate the role of HDAC1, HDAC2 and HDAC6 isoforms in different cancer settings. However, these isoforms were shown to have contradicting tumor promoting but also tumor suppressive functions, depending on the cancer type and cancer stage. Much more work remains to clarify the role of these HDACs in cancers. Future studies will focus on identifying the relevant HDAC isoforms in the different cancer types and the discovery of selective HDACis.

Aim of this thesis

Aim of this thesis

In the lab of Prof. Dr. Patrick Matthias we focus our research on histone deacetylases (Hdacs) and their role in normal physiology or pathological settings such as cancer. Previous work on classI Hdac1 and Hdac2, as well as classII Hdac6, showed that they play important roles in several cancer settings, including B cell malignancies (Haery et al., 2015; Seidel et al., 2015). However, Hdac1 and Hdac2 (Santoro et al., 2013), but also Hdac6 (Seidel et al., 2015), were shown to have contradicting tumor promoting and tumor suppressive roles in cancer. Despite improved knowledge in Hdac cancer research, the exact role of Hdac1, Hdac2, and Hdac6 in cancer remains largely unexplored. The aim of my PhD thesis is to better understand the functional role of Hdac1, Hdac2, and Hdac6 in the $E\mu$ -*myc* model of B cell lymphoma.

In the first, and main part of my thesis I studied the functional role of classII Hdac1 and Hdac2 in the $E\mu$ -*myc* mouse model of B cell lymphoma. I performed this work in collaboration with Prof. Dr. Alexandar Tzankov, an experienced hematopathologist from the university hospital Basel. The result of this work is presented in the form of a publication manuscript: “Histone deacetylase (Hdac) 1 plays a predominant role in $E\mu$ -*myc* driven B cell lymphoma” (Pillonel *et al.*, *Accepted for publication in Scientific Reports*).

In the second part of my thesis, I started a collaboration with R.M. Heideman, a postdoctoral research fellow in the lab. Together, we started to explore the role of Hdac1 and Hdac2 in B cell development. The work from this side project is presented in the result section of my thesis: “Analysis of the functional role of Hdac1 and Hdac2 in B cell development”.

In the last part of my thesis I investigated the function of the cytoplasmic classII Hdac6 in the $E\mu$ -*myc* model: “Dissecting the role of histone deacetylase 6 in $E\mu$ -*myc* driven B cell lymphoma”. The results from this work are presented in the result section of my thesis.

Aim of this thesis

In parallel, I also participated in the revision work of the manuscript from Camille Du Roure, a previous postdoc in the lab: “Hematopoietic Overexpression of FOG1 Does Not Affect B-Cells but Reduces the Number of Circulating Eosinophils” (Du Roure et al., 2014). This published work is presented in the appendix of my thesis. Furthermore, I also participated in the revision work of the manuscript from another previous lab member, Nina Reichert: “Hdac1 and 2 repress lineage inappropriate expression of *Flt3* and *Ptprf* in B cells via Pax5 and Grg4” (unpublished work). Since this work is not yet submitted, I only show the abstract in the appendix of my thesis.

Results

Results Part 1

(Pillonel *et al.* Accepted for publication in *Sci Rep.*)

Results Part1: Histone deacetylase 1 plays a predominant pro-oncogenic role in Eμ-myc driven B cell lymphoma (Pillonel *et al.* Accepted for publication in *Scientific Reports*)

Vincent Pillonel^{1,2}, Nina Reichert¹, Chun Cao¹, Marinus R. Heideman¹, Teppei Yamaguchi¹, Gabriele Matthias¹, Alexandar Tzankov³ & Patrick Matthias^{1,2,*}

¹*Friedrich Miescher Institute for Biomedical Research, Novartis Research Foundation, 4058 Basel, Switzerland.*

²*Faculty of Sciences, University of Basel, 4031 Basel, Switzerland.*

³*Pathology Institute, University Hospital Basel, 4031 Basel, Switzerland.*

**Correspondence and requests for materials should be addressed to P.M. (email: patrick.matthias@fmi.ch; Tel.: +41 61 697 66 61; Fax.: +41 61 697 39 76)*

Manuscript Text

Abstract

The two histone deacetylases (Hdacs), Hdac1 and Hdac2, are erasers of acetylation marks on histone tails, and are important regulators of gene expression that were shown to play important roles in hematological malignancies. However, several recent studies reported opposing tumor-suppressive or tumor-promoting roles for Hdac1 and Hdac2. Here, we investigated the functional role of Hdac1 and Hdac2 using the E μ -*myc* mouse model of B cell lymphoma. We demonstrate that Hdac1 and Hdac2 have a pro-oncogenic role in both E μ -*myc* tumorigenesis and tumor maintenance. Hdac1 and Hdac2 promote tumorigenesis in a gene dose-dependent manner, with a predominant function of Hdac1. Our data show that Hdac1 and Hdac2 impact on E μ -*myc* B cell proliferation and apoptosis and suggest that a critical level of Hdac activity may be required for E μ -*myc* tumorigenesis and proper B cell development. This provides the rationale for utilization of selective Hdac1 and Hdac2 inhibitors in the treatment of hematological malignancies.

Introduction

Histone deacetylases (Hdacs) belong to a family of 18 enzymes that removes acetylation marks on lysine residues of histone and non-histone proteins [1]. Hdacs modify the epigenome through deacetylation of histone proteins, thereby inducing chromatin condensation leading to transcriptional repression [2, 3]. They also act on an increase number of non-histone substrates, nuclear or cytoplasmic, and therefore impact on multiple cellular functions [4, 5]. Human Hdacs (HDACs) have been reported to have altered function and expression (usually overexpressed) in a wide range of human cancers [6-9] and have been considered attractive pharmacological

targets for cancer therapy. HDAC inhibitors (HDACis) have potent antitumor activity in hematological and solid malignancies, mainly by inducing apoptosis, inhibiting cell cycle progression and cellular differentiation [10, 11]. Currently, four pan-HDACis, (targeting class I and/or class II HDACs [12]) are approved for the treatment of T cell lymphoma and multiple myeloma [13-16] and several others are in clinical trials for various cancers, including B cell malignancies (reviewed by [9]). However, it is unclear which HDAC isoforms are crucial for tumor cell growth and/or survival, and whether selective HDAC inhibition might have comparable therapeutic benefit with less toxicity compared with broad-spectrum HDACis [2, 17].

Although the two class I Hdacs, Hdac1 and Hdac2, have been shown to be implicated in proliferation of cancer cells and to play an important role in hematological malignancies [9, 18-23], their exact functions in the different cancer types remains elusive. Hdac1 has been shown to have opposing tumor-suppressive as well as tumor-promoting functions in tumorigenesis and in tumor maintenance, respectively [24]. Numerous studies in different cell types, including B cells, demonstrated that these two enzymes have largely redundant functions during normal development and malignant transformation [25-32]. Some studies reported a dose-dependent function of Hdac1 and Hdac2 in some cell types, including T cells and epidermal cells [33, 34].

In view of these observations, we assessed the functional role of Hdac1 and Hdac2 in the development and progression of E μ -*myc* driven B cell lymphomas. E μ -*myc* transgenic (tg) mice overexpress the *c-myc* oncogene in B lymphocytes and develop multicentric lymphomas associated with leukemia [35-37]. We investigated the impact of B lymphocyte-specific deletions of combination of *Hdac1* and *Hdac2* alleles using targeted conditional deletion with the *mb1-cre* recombinase [30] in E μ -*myc* mice. Here, we show that Hdac1 and Hdac2 have tumor-promoting

roles in both E μ -*myc* tumorigenesis and tumor maintenance. This study reveals that *Hdac1* and *Hdac2* have a gene dose-dependent pro-oncogenic role in E μ -*myc* tumorigenesis, with a predominant role of *Hdac1*.

Results

Hdac1 and 2 have no tumor suppressor functions in B cells. Previous studies reported that T cell-[32, 33] and epidermal cell-[34] specific ablation of *Hdac1* and *Hdac2* alleles unexpectedly leads to spontaneous tumor formation. Therefore, we first investigated whether ablation of *Hdac1* and *Hdac2* in B cells also induces tumor development. For this we generated B cell-specific deletions of different combinations of *Hdac1* and *Hdac2* alleles *in vivo* (Supplementary Figure 1A) and monitored mice for tumor development over a period of 300 days by the Kaplan-Meier (KPLM) method. Interestingly, in contrast to previous observation in T cells, ablation of *Hdac1* and/or *Hdac2* in B cells did not lead to spontaneous tumor development (Figure 1A). E μ -*myc* tg mice were used as controls and developed tumors as expected (Figure 1A; Supplementary Figure 2D). We then performed histopathological analysis from the mice lacking *Hdac1* and/or *Hdac2* to verify the absence of malignant phenotypes. Consistent with the absence of visible and palpable tumors in the KPLM analysis, we did not detect any pathological signs in *Hdac1* and/or *Hdac2* KO mice at 8, 20, and even 40 weeks in the spleen, lymph nodes, or thymus (Figure 1B). Taken together, our results indicate that *Hdac1* and *Hdac2* do not have a tumor suppressor function in B cells.

E μ -*myc* tumorigenesis is *Hdac1* and *Hdac2* gene dose-dependent. We next investigated the effect of *Hdac1* and *Hdac2* ablation in the E μ -*myc* cancer background, and in particular whether

they have tumor suppressive or tumor promoting functions during E μ -*myc* tumorigenesis. We previously reported that concomitant ablation of *Hdac1* and *Hdac2* in non-transformed B cells induced a cell cycle block and apoptosis [30]. We therefore hypothesized that similar ablation of *Hdac1* and *Hdac2* might also have this effect in malignant E μ -*myc* tg B cells which overexpress the strong *c-myc* oncogene. We crossed mice with B cell-specific deletions of different combinations of *Hdac1* and *Hdac2* alleles with E μ -*myc* mice in order to obtain mice having the E μ -*myc* tg in different backgrounds with respect to *Hdac1* and *Hdac2* (Supplementary Figure 2A). E μ -*myc* mice overexpressed the *c-myc* oncogene in all B lymphocytes, as expected (Supplementary Figure 2B-C), and developed multicentric lymphomas (Supplementary Figure 2D), as previously reported [35-37]. We then monitored tumor-free survival by KPLM analysis in mice having different combinations of *Hdac1* and *Hdac2* alleles. Interestingly, we observed that mono-allelic expression of *Hdac2* in *Hdac1*-deficient E μ -*myc* B cells (*Hdac1*^{Δ/Δ};*Hdac2*^{Δ/+}) resulted in delayed tumor development, whereas complete *Hdac1* and *Hdac2* deletion (*Hdac1*^{Δ/Δ};*Hdac2*^{Δ/Δ}) prevented tumorigenesis altogether (Figure 2A). We observed a gradual decrease in tumor incidence and concomitant gradual increase in mean overall survival upon deletion of combinations of *Hdac1* and *Hdac2* alleles (Figure 2B). Importantly, these findings demonstrate that Hdac1 and Hdac2 have pro-oncogenic roles in tumorigenesis of E μ -*myc* mice, in contrast to other cancer models such as acute promyelocytic leukemia (APL) [24]. These findings further indicate that E μ -*myc* tumorigenesis is *Hdac1* and *Hdac2* gene dose-dependent. We observed that a critical level of Hdac1 and Hdac2 is required for tumorigenesis. Moreover, Hdac1 and Hdac2 are not completely redundant; we observed that Hdac1 functions as the dominant protein (Figure 2 A-B).

Complete *Hdac1* and *Hdac2* ablation prevents E μ -myc tumorigenesis. The foregoing findings demonstrate that complete *Hdac1* and *Hdac2* deletion (*Hdac1*^{Δ/Δ};*Hdac2*^{Δ/Δ}) prevents tumorigenesis (Figure 2). To determine how the lack of Hdac1 and Hdac2 in B cells impacts E μ -myc tumorigenesis, we analysed 8-week old mice by first measuring spleen weight, since E μ -myc mice typically have splenomegaly. We found that only complete ablation of both enzymes (*Hdac1*^{Δ/Δ};*Hdac2*^{Δ/Δ}), but not ablation of either Hdac1 (*Hdac1*^{Δ/Δ};*Hdac2*^{+/+}) or Hdac2 (*Hdac1*^{+/+};*Hdac2*^{Δ/Δ}) alone, prevented spleen enlargement (Figure 3A). We next performed histopathological analysis from spleen (Figure 3B). As expected, some E μ -myc mice displayed high grade non-Hodgkin's lymphomas (HG-NHL, roughly corresponding to Burkitt's lymphoma in humans), as described previously [35, 38]. Importantly, no *Hdac1*^{Δ/Δ};*Hdac2*^{Δ/Δ} E μ -myc mice had HG-NHL in spleen and lymph nodes, whereas ablation of either *Hdac1* or *Hdac2* alone did not prevent HG-NHL development (Figure 3B, table). We next measured circulating peripheral blood lymphocytes (PBL) using an automated blood cell analyzer. E μ -myc mice had significantly elevated PBL compared to control wild-type mice (Figure 3C). Interestingly, we observed that *Hdac1*^{Δ/Δ};*Hdac2*^{Δ/Δ} E μ -myc mice had significantly lower PBL counts, compared to control *Hdac1*^{+/+};*Hdac2*^{+/+} E μ -myc mice, and hence reduced leukemia burdens (Figure 3C). Ablation of *Hdac1* (*Hdac1*^{Δ/Δ};*Hdac2*^{+/+}), but not *Hdac2* (*Hdac1*^{+/+};*Hdac2*^{Δ/Δ}) in E μ -myc mice, significantly reduced PBL counts at 8 weeks (Figure 3C). However, this phenotype is transient, since we did not see any effect in PBL counts in older (10 and 20 week old) *Hdac1*^{Δ/Δ};*Hdac2*^{+/+} E μ -myc mice (Supplementary Figure 4). Hence, we conclude that ablation of *Hdac1* (*Hdac1*^{Δ/Δ};*Hdac2*^{+/+}) alone has no major impact on E μ -myc tumorigenesis. Finally, we performed an analysis of the bone marrow (BM) of E μ -myc mice by flow cytometry. We performed immunofluorescence stainings with B cell-surface-marker-specific antibodies

including B220, IgM, CD19 and CD25 to identify the different B cell populations in the BM (Figure 3D). E μ -myc mice displayed blasts at the Pro/PreB cell stage that dominates the BM, as previously reported [39]. Consistent with the data outlined above, ablation of *Hdac1* (*Hdac1^{Δ/Δ};Hdac2^{+/+}*) or *Hdac2* (*Hdac1^{+/+};Hdac2^{Δ/Δ}*) alone had no effect (Figure 3 E-F). However, ablation of both *Hdac1* and *Hdac2* (*Hdac1^{Δ/Δ};Hdac2^{Δ/Δ}*) prevented the appearance of such E μ -myc-induced B cell blasts at the Pro/PreB stage (B220⁺; IgM⁻; Figure 3E), more specifically at the PreBII cell stage (B220⁺;CD19⁺;CD25⁺; Figure 3F). Altogether, these results indicate that ablation of *Hdac1* and *Hdac2* (*Hdac1^{Δ/Δ};Hdac2^{Δ/Δ}*) prevents E μ -myc tumorigenesis. However, quantification of flow cytometric analysis revealed that *Hdac1^{Δ/Δ};Hdac2^{Δ/Δ}* E μ -myc mice had significantly reduced B cell numbers and almost no PreBII cells (Figure 3G). These findings suggest that the effect of complete *Hdac1* and *Hdac2* ablation on tumorigenesis could be due to a B cell developmental defect at the PreBII cell stage.

Conditional ablation of *Hdac1* and *Hdac2* in E μ -myc tumor cells delays tumor appearance

in vivo. In order to discriminate between indirect B cell developmental defects and direct effects of *Hdac1* and *Hdac2* ablation, we investigated the role of *Hdac1* and *Hdac2* in existing tumor cells. Therefore, we performed conditional targeted deletion of *Hdac1* and *Hdac2* in E μ -myc tumor cells using an *in vivo* transplantation approach (Figure 4A). Briefly, syngeneic recipient mice were injected with E μ -myc lymphoma cells carrying floxed *Hdac1* and *Hdac2* alleles as well as hormone-inducible cre (*Hdac1^{F/F};Hdac2^{F/F}; Actin-cre ER tg; E μ -myc tg*) and subsequently treated with 4-hydroxytamoxifen (4-OHT) to induce deletion of *Hdac1* and *Hdac2* specifically in transplanted tumor cells. We then performed KPLM tumor-free survival analysis and observed that mice treated with 4-OHT had significantly delayed tumor appearance

compared to control mice treated with vehicle (Figure 4B). Thus, Hdac1 and Hdac2 have a pro-oncogenic role in the E μ -myc dependent tumor progression. This transplantation assay clearly demonstrates that conditional ablation of both *Hdac1* and *Hdac2* directly impacts on existing tumor cells and delays tumor appearance.

***Hdac1^{Δ/Δ};Hdac2^{Δ/+}* delays E μ -myc tumorigenesis.** As shown above, E μ -myc tumor development was significantly delayed in mice having a single allele of *Hdac2* and no *Hdac1* (*Hdac1^{Δ/Δ};Hdac2^{Δ/+}*), while this was not the case in mice with a single allele of *Hdac1* and no *Hdac2* (*Hdac1^{Δ/+};Hdac2^{Δ/Δ}*; Figure 2). We analysed 8-week old lymphoma-free E μ -myc mice and first performed flow cytometry analysis of the BM. Interestingly, *Hdac1^{Δ/Δ};Hdac2^{Δ/+}* ;E μ -myc mice had significantly reduced blasts at Pro/PreB cell stages (Figure 5A, upper panels) and displayed a strongly reduced number of B cells and Pro/PreB cells in the BM (Figure 5B, upper panels). Furthermore, we found that these mice had several fold increased PreBI cell numbers and similarly decreased PreBII cell numbers (Figure 5A, lower panels). Quantification revealed significant changes (Figure 5B, lower panels). We next measured circulating PBL, and observed that *Hdac1^{Δ/Δ};Hdac2^{Δ/+}* E μ -myc mice had significantly lowered PBL counts compared to control E μ -myc mice with normal levels of Hdac1 and Hdac2 (Figure 5C). Hence, *Hdac1^{Δ/Δ};Hdac2^{Δ/+}* E μ -myc mice have reduced leukemia. Taken together, these results indicate that reduction of Hdac2 in absence of Hdac1 (*Hdac1^{Δ/Δ};Hdac2^{Δ/+}*) impacts E μ -myc tumorigenesis by reducing the E μ -myc-induced blasts in the BM, resulting in reduced circulating tumor cells and eventually delays E μ -myc tumorigenesis (Figure 2).

Hdac1 has a predominant role in non-malignant B cells. In order to test whether the impact of Hdac1 and Hdac2 on B cells is restricted to the E μ -myc background, we examined mice with B cell-specific deletions of different combinations of *Hdac1* and *Hdac2* alleles but no E μ -myc tg (Supplementary Figure 1A). We first examined the effect of *Hdac1* and *Hdac2* ablation in the BM by flow cytometry. We observed that *Hdac1*^{A/A};*Hdac2*^{A/+} but not *Hdac1*^{A/+};*Hdac2*^{A/A} mice had less B cells, whereas *Hdac1*^{A/A};*Hdac2*^{A/A} mice had a complete block in B cell development (Figure 6A). Quantification of the flow cytometry analysis revealed that *Hdac1*^{A/A};*Hdac2*^{A/+}, but not *Hdac1*^{A/+};*Hdac2*^{A/A} mice, have higher numbers of PreBI cells and reduced PreBII cell numbers compared to control *Hdac1*^{+/+};*Hdac2*^{+/+} mice (Figure 6B). Of note, B cells development was not blocked in *Hdac1*^{A/A};*Hdac2*^{A/+} mice since these mice still had PreBII cells (Figure 6C) that could develop throughout all B cells stages and eventually fill the complete pool of mature B cells in the spleen (Supplementary Figure 6). In comparison, mice lacking both *Hdac1* and *Hdac2* (*Hdac1*^{A/A};*Hdac2*^{A/A}) had almost no PreBII cells (Figure 6C), as shown previously [30].

We next determined the effect of *Hdac1* and *Hdac2* ablation on the global Hdac-activity in BM B cells. Interestingly, we observed that progressive ablation of *Hdac1* and *Hdac2* alleles generated a B cell-specific gradient of Hdac-activity, with *Hdac1* having a greater contribution: *Hdac1*^{+/+};*Hdac2*^{+/+} = *Hdac1*^{+/+};*Hdac2*^{A/A} > *Hdac1*^{A/A};*Hdac2*^{A/A} ≥ *Hdac1*^{A/A};*Hdac2*^{+/+} ≥ *Hdac1*^{A/A};*Hdac2*^{A/A} (Figure 6D). Further assessment by immunoblotting of Hdac1 and Hdac2 protein levels in isolated B cells confirmed that these mice had efficient deletion of Hdac1 and Hdac2 (Figure 6E). Ablation of *Hdac1* resulted in increased Hdac2 protein levels, as shown previously [30], while ablation of *Hdac2* did not result in increased Hdac1 proteins levels. These results suggest compensatory regulation of Hdac1 and Hdac2 protein levels in B cells, with a

predominant compensation of Hdac2 upon loss of the other paralog (Figure 6E). Taken together, these data demonstrate that Hdac1 also has a predominant role in non-malignant B cells.

***Hdac1^{Δ/Δ};Hdac2^{Δ/+}* impact on proliferation and apoptosis.** We previously showed that simultaneous ablation of *Hdac1* and *Hdac2* (*Hdac1^{Δ/Δ};Hdac2^{Δ/Δ}*) in non-transformed B cells induced cell cycle arrest and subsequent apoptosis [30]. These findings prompted us to hypothesize that proliferation and apoptosis might also be affected in Eμ-*myc* B cells lacking Hdac1 and Hdac2. Therefore, we first investigated the impact of *Hdac1* and *Hdac2* ablation on proliferation of Eμ-*myc* B cells, by *in vivo* BrdU labelling experiments. We found that *Hdac1^{Δ/Δ};Hdac2^{Δ/+}* Eμ-*myc* mice had decreased B cell proliferation, as evidenced by reduced BrdU incorporation (Figure 7A). Quantification of B220⁺;BrdU⁺ cells revealed a significant decrease (Figure 7B). We next investigated whether apoptosis was induced in *Hdac1^{Δ/Δ};Hdac2^{Δ/+}* Eμ-*myc* B cells, using AnnexinV apoptosis assay by flow cytometry, and indeed observed that *Hdac1^{Δ/Δ};Hdac2^{Δ/+}* Eμ-*myc* B cells underwent apoptosis at higher frequencies than control *Hdac1^{+/+};Hdac2^{+/+}* Eμ-*myc* B cells (Figure 7C). Quantification of these data revealed a significant decrease in viable cells (AnnV⁻;DAPI⁻), concomitant with a significant increase in apoptotic (AnnV⁺;DAPI⁻) and dead cells (AnnV⁺;DAPI⁺; Figure 7D). In summary, B cells with only one allele of *Hdac2* have decreased proliferation and undergo apoptosis more frequently. Taken together, our data demonstrate that *Hdac1^{Δ/Δ};Hdac2^{Δ/+}* reduces Eμ-*myc* tumorigenesis by decreasing proliferation and inducing apoptosis.

Discussion

In this study, we used targeted conditional deletion of *Hdac1* and *Hdac2*, to investigate the functional role of these enzymes in the *E μ -myc* murine B cell lymphoma model. Our data reveal a predominant role of *Hdac1* in both *E μ -myc* tg B cells and non-malignant B cells. We demonstrate that *Hdac1* and *Hdac2* have a gene dose-dependent pro-oncogenic role in *E μ -myc* tumorigenesis with a predominant role of *Hdac1*. Our results highlight the tumor-promoting role of Hdac1 and Hdac2 in both *E μ -myc* tumorigenesis and tumor maintenance.

In accordance with our previous study with young B cell-specific *Hdac1* and/or *Hdac2* KO mice [30], we show here that Hdac1 and Hdac2 do not have a tumor suppressor function in B lymphocytes of old mice (Figure 1). Indeed, we found that ablation of *Hdac1* and/or *Hdac2* in non-malignant B cells did not lead to spontaneous tumor development, in contrast to T cells [32, 33], and epidermal cells [34], in which Hdac1 and Hdac2 were reported to act as tumor suppressors. One plausible interpretation of this apparent discrepancy between our data and these previous studies could be a cell type-specific role of Hdac1 and Hdac2.

We further investigated the function of Hdac1 and Hdac2 in the *E μ -myc* murine B cell lymphoma model. In accordance with previous reports using HDACis in B lymphoid cancer models [9-11], we demonstrated using genetic ablation that Hdac1 and Hdac2 have pro-oncogenic roles during *E μ -myc* tumorigenesis (Figure 2). Interestingly, these findings differ from previous studies using a skin tumor model [34], or APL [24], in which Hdac1 (but not Hdac2) was reported to act as a tumor suppressor during tumorigenesis. This divergence supports the idea that tumor type- or oncogene-specific effects may be decisive. Moreover, we previously observed that Hdac1 and Hdac2 have partly different target preferences [30], suggesting that they might regulate different set of genes in a cell type-specific manner.

We further show that complete deletion of both *Hdac1* and *Hdac2* (*Hdac1^{Δ/Δ};Hdac2^{Δ/Δ}*) prevents Eμ-*myc* tumorigenesis, whereas ablation of either *Hdac1* (*Hdac1^{Δ/Δ};Hdac2^{+/+}*) or *Hdac2* (*Hdac1^{+/+};Hdac2^{Δ/Δ}*) had no effect (Figure 2). In line with this, we found that absence of these two *Hdacs* prevents Eμ-*myc* splenomegaly, HG-NHL occurrence, reduces leukemia, and stops B cell blasts accumulation, which otherwise dominates the BM of Eμ-*myc* mice (Figure 3). Thus, ablation of *Hdac1* and *Hdac2* prevents tumorigenesis already in the BM by preventing Eμ-*myc*-induced blasts at early B cell stage. This is in agreement with our earlier report in non-transformed B cells, where ablation of *Hdac1* and *Hdac2* (*Hdac1^{Δ/Δ};Hdac2^{Δ/Δ}*) using *Mbl-cre* induced a cell cycle block and apoptosis at the PreBII cell stage [30]. However, the non-inducible *Mbl-Cre* system does not allow proper discrimination between indirect B cell developmental defects and direct effects of *Hdac1* and *Hdac2* ablation in *Hdac1^{Δ/Δ};Hdac2^{Δ/Δ}* Eμ-*myc* mice. We therefore used two different approaches to investigate the direct effect of *Hdac1* and *Hdac2*: *i*) the use of mice with only one allele of *Hdac2* (*Hdac1^{Δ/Δ};Hdac2^{Δ/+}*), which do not have this block in B cell development to study the tumorigenesis and *ii*) a transplantation approach allowing conditional deletion of *Hdac1* and *Hdac2* (using inducible *CreERT*) in existing tumor cells and test the effect of *Hdac1* and *Hdac2* ablation on tumor maintenance. Our transplantation experiment (Figure 4) clearly demonstrates that conditional ablation of both *Hdac1* and *Hdac2* has a direct impact on existing tumor cells, since we observed significantly delayed tumor appearance. Interestingly, we observed that *Hdac1* and *Hdac2* are not deleted in tumors arising in 4-OHT treated transplanted mice (Supplementary Figure 5), suggesting that the delayed tumor growth observed represents cells that have escaped deletion of *Hdac1* and *Hdac2*. From these findings we conclude that the partial effect we observed after 4-OHT treatment of transplanted recipient mice (Figure 4) can be explained by incomplete elimination of *Hdac1* and

Hdac2 using the tamoxifen inducible CreERT system. Our findings demonstrate that loss of *Hdac1* and *Hdac2* has a direct impact on E μ -myc tg B cells and demonstrate a critical pro-oncogenic role of Hdac1 and Hdac2 in E μ -myc tumor progression.

E μ -myc mice with a single allele of *Hdac2* and no *Hdac1* (*Hdac1*^{Δ/Δ};*Hdac2*^{Δ/+}), but not with a single allele of *Hdac1* in absence of *Hdac2* (*Hdac1*^{+Δ};*Hdac2*^{Δ/Δ}), exhibited delayed tumor development (Figure 2). This demonstrates that E μ -myc tumorigenesis is *Hdac1* and *Hdac2* gene dose-dependent, and identifies a predominant role of *Hdac1*. We further observed that Hdac1 has a predominant role also in non-malignant B cells (Figure 6). *Hdac1*^{Δ/Δ};*Hdac2*^{Δ/+} mice, but not *Hdac1*^{+Δ};*Hdac2*^{Δ/Δ} mice, had a reduction in PreBII cell numbers (Figure 6C). Furthermore, ablation of Hdac1 resulted in a strong increase of Hdac2 protein levels, as previously observed [30]. Interestingly, this increase in Hdac2 levels was not sufficient to compensate for the absence of Hdac1, indicating partially redundant functions and highlighting the predominant role of Hdac1. Furthermore, we observed that *Hdac1*^{Δ/Δ};*Hdac2*^{Δ/+} B cells had significantly reduced Hdac activity compared to *Hdac1*^{+Δ};*Hdac2*^{Δ/Δ} B cells. These data demonstrate the predominant role of Hdac1, and suggest that a critical level of Hdac activity may be required for E μ -myc tumorigenesis.

Similar to *Hdac1*^{Δ/Δ};*Hdac2*^{Δ/Δ}, we found that *Hdac1*^{Δ/Δ};*Hdac2*^{Δ/+} impacted E μ -myc tumorigenesis by reducing the E μ -myc-induced blasts at the early preBII cell stage in the BM, resulting in reduced circulating tumor cells (Figure5). We further investigated whether the impact of *Hdac1*^{Δ/Δ};*Hdac2*^{Δ/+} in E μ -myc B cells could be due to proliferation defects and/or apoptosis. Strikingly, we found that *Hdac1*^{Δ/Δ};*Hdac2*^{Δ/+} decreased proliferation and increased apoptosis in E μ -myc B cells (Figure 7). Taken together, these findings demonstrate that *Hdac1*^{Δ/Δ};*Hdac2*^{Δ/+} reduces E μ -myc-induced blasts in the BM and delays tumorigenesis by decreasing proliferation

and inducing apoptosis. Hence, we conclude that Hdac1 and Hdac2 have pro-oncogenic roles in E μ -*myc* tumorigenesis. These findings are consistent with earlier studies reporting that complete loss of Hdac1 and Hdac2 induces cell death in proliferating cells, including B and T cells [30, 32, 33]. In line with this, Hdac1 and Hdac2 were shown to be the major targets for HDACi-mediated apoptosis induction in leukemic cell lines [40]. Furthermore, a recent study also showed that ablation of both Hdac1 and Hdac2 decreases proliferation and induces apoptosis in E μ -*myc* tumor cells [23]. Hence, an effect on proliferation and apoptosis upon Hdac1 and Hdac2 ablation could likely explain the delayed tumor appearance in our transplantation experiment (Figure 4).

Our results describe the pro-oncogenic roles of Hdac1 and Hdac2 in E μ -*myc* tumorigenesis and tumor maintenance and support the clinical use of HDACis. Previous studies clearly demonstrated the therapeutic efficacy of pan-HDACis in E μ -*myc* lymphomas [41-45]. Interestingly, we found that human HDAC1, but not human HDAC2, mRNA expression is increased in some Burkitt's lymphoma (BL) and diffuse large B cell lymphoma (DLBCL) cancer cell lines and human lymphoma samples, when compared to other cancer cell lines or other human cancer samples, respectively (Supplementary Figure 3). Hence, these data are consistent with our findings outlined above, revealing a predominant role of Hdac1. Our findings demonstrate that Hdac1 can be considered an important factor in E μ -*myc* tumorigenesis, and suggest that selective HDAC1 (and HDAC2) inhibitors could be effective for the treatment of BL, as modeled by our preclinical E μ -*myc* system, and possibly other hematological malignancies, including some DLBCL. Accordingly, several HDAC1 and HDAC2 isoform-selective inhibitors were recently shown to have *in vitro* and/or *in vivo* therapeutic efficacy in pre-clinical models such as E μ -*myc* [23, 42].

In conclusion, our results demonstrate that Hdac1 and Hdac2 promote tumor initiation and progression in E μ -myc mice and that they impact on proliferation and apoptosis. To the best of our knowledge, this is the first study showing a gene dose-dependent pro-oncogenic role of *Hdac1* and *Hdac2* in tumorigenesis, with a predominant role of *Hdac1*. Future research will focus on elucidating the underlying molecular mechanisms by which Hdac1 and Hdac2 regulate proliferation and apoptosis in malignant and non-malignant cells. Our study raises the prospect of using selective HDAC1 and HDAC2 inhibitors for the treatment of BL and other B cell lymphomas with Myc deregulation, with possibly less side effects than pan-HDACis currently used.

Material and Methods

Experimental mice. All experiments were performed in accordance with Swiss federal guidelines for animal experimentation (Art.13a TSchG; Art. 60-62 TSchV) and approved by the FMI Animal committee and the local veterinary authorities (Kantonales Veterinäramt of Kanton Basel-Stadt, permit no. 2384-03). All efforts were made to minimize animal suffering and to reduce the number of animal used.

Hdac1^{F/F};Hdac2^{F/F} conditional knockout (KO) mice have been previously described and characterized [30]. B lymphocyte-specific deletion of *Hdac1* and/or *Hdac2* was obtained by crossing *Hdac1^{F/F}* and *Hdac2^{F/F}* mice with heterozygote *Mb1-cre* transgenic (tg) mice [30]. For transplantation, *Actin-Cre* ER mice (The Jackson Laboratory; B6.Cg-Tg(CAG-cre/Esr1)5Amc/J) were used to conditionally delete *Hdac1* and *Hdac2* using tamoxifen. *Hdac1* and *Hdac2* conditional KO mice were interbred to congenic C57BL/6 heterozygote E μ -myc tg mice (The Jackson Laboratory; B6.Cg-Tg (IghMyc)22Bri/J) [35]. All mice were in C57BL/6 genetic backgrounds (backcrossing at least 11 generations). The mice were housed in groups of one to

five at 25°C with a 12:12 h light-dark cycle and received a standard laboratory diet containing 0.8% phosphorus and 1.1% calcium (NAFAG 890, Kliba, Basel, Switzerland) and water *ad libitum*.

Genotyping PCR. Polymerase chain reaction (PCR)-based genotyping was performed on tail-derived DNA. Mice were genotyped for *Hdac1* and *Hdac2* conditional alleles as described previously [30]. The following primer sets were used: *Hdac1* flox or WT (forward; 5'-CCTGTGTCATTAGAATCTACTT, and reverse; 5'-GGTAGTTCACAGCATAGTACTT); *Hdac1* KO (forward; 5'-GTTACGTCAATGACATCGTCCT, and reverse; 5'-GGTAGTTCACAGCATAGTACTT); *Hdac2* flox or WT (forward; 5'-CCCTTTAGGTGTGAGTACAT, and reverse; 5'-rev: AACCTGGAGAGGACAGCAAA); *Hdac2* KO (forward; 5'-CCACAGGGAAAAGGAAACAA, and reverse; 5'-AACCTGGAGAGGACAGCAAA). E μ -*myc* tg (forward; 5'-TCCAGGGTACATGGCGTATT; and reverse; 5'-TCGGCTGAACTGTGTTCTTG), based on previously published insertion site of *c-myc* [46]. *Mbl-cre* tg (forward; 5'-GGGAAGAAAGAGGCCATAGG; and reverse, 5'-TCCCTCACATCCTCAGGTTC). *Actin-Cre* tg (forward; 5'-GCGGTCTGGCAGTAAAACTATC; and reverse, 5'-CAGAGACGGAAATCCATCGCTC). PCRs were performed using the GoTaq Flexi DNA Polymerase Kit (Promega, Cat.M8306) and MJ Mini Thermal Cyclers (BioRad).

RNA isolation and qRT-PCR. Total RNA was isolated using an RNeasy Mini kit (Qiagen) followed by cDNA synthesis using Improm Reverse Transcriptase (RT) Kit (Promega) according to the manufacturer's protocol. 5-10 ng of cDNA were used to perform Semiquantitative real-

time PCR using MESA GREEN qPCR MasterMix Plus for SYBR Assay (Eurogentec) on an ABI PRISM7000 Sequence Detection System (Applied Biosystems). Each reported value is an average of three independent experiments. Relative expression levels were determined by normalizing to *gapdh* expression using the $\Delta\Delta C_t$ method. The following primers were used: for *c-myc* (forward; 5'-TTTGTCTATTTGGGGACAGTGTT; and reverse; 5'-CATCGTCGTGGCTGTCTG); for *Gapdh* (forward; 5'-GCCTCGTCCCGTAGACAAAAT; and reverse; 5'-TTCCCATTTCTCGGCCTTGA).

Kaplan-Meier (KPLM) tumor-free survival analysis. Tumor development was monitored every 2-3 days by palpation of cervical, axillary, and inguinal regions for characteristic “water wing” appearance described for E μ -*myc* tg mice [37]. Typically, moribund mice presented with several of the following visible features: enlarged lymph nodes, hunched posture, dyspnea, weight loss, ruffled coats, paralysis, and immobility. Mice were monitored over a period of 300 days for tumor onset and sacrificed when moribund, or reaching tumor-specific endpoints (lymph nodes > 1cm). For moribund mice without tumors, the date of euthanasia was used as the date of death in survival studies. Tumors were isolated, weighted, and prepared for histopathology or protein and RNA extraction. The survival rate was calculated using the Kaplan-Meier method, using R (R Project for Statistical Computing).

Blood sampling and analysis. Mice were bled at 4 and 8 weeks and blood was collected in EDTA pre-coated tubes. Samples were analyzed utilizing a fully automated hematology analyzer (Sysmex XT-2000i).

Histopathological analysis. Biopsies were formalin-fixed (Shandon Formal-Fixx, Thermo Scientific) for 24h, dehydrated, paraffin-embedded, cut into 3- μ m-thick sections, and stained with hematoxylin and eosin (Merck). Pathological analysis was performed according to the Bethesda proposals for classification of lymphoid neoplasms in mice [38].

Cell preparation. Single cell suspensions were prepared from BMs by flushing tibia and femur with PBS supplemented with 3% fetal bovine serum. Single-cell suspensions from spleen and lymph nodes were prepared by squeezing splenocytes and lymphocytes from their capsule through a 40- μ m nylon mesh of the cell strainer. Peripheral blood was obtained by venous puncture or at autopsy by cardiac puncture. Red blood cells were depleted by lysis in Gey's solution prior to staining.

Immunofluorescent staining and flow cytometric analysis. Flow cytometry was done according to standard procedures [30]. The following directly conjugated antibodies were used: anti-CD45R/B220-FITC (clone RA3-6B2), anti-CD25-PE (clone PC61), anti-IgM-APC (clone II/41), anti-IgD-BV605 (clone 11-26c.2a), were all purchase from BD Biosciences; anti-CD117/c-kit-APC (clone 2B8, eBioscience); and anti-CD19-PE-Cy7 (clone 6D5, Biolegend). All flow cytometry analyses were performed using a multicolor BD LSRII Flow Cytometer (Becton Dickinson). Data were analyzed using Flow-Jo (Tree Star) software.

B cell isolation by magnetic-activated cell sorting (MACS). Separation of B cells was performed using positive selection with CD19 monoclonal antibodies coupled to magnetic

microbeads (anti-CD19 MicroBeads) according to the manufacturer's protocol (MACS, Miltenyi Biotec). Control flow cytometry from MACS separated cells revealed 95% purity.

***In vivo* cell cycle analysis by bromodeoxyuridine (BrdU) incorporation.** For *in vivo* BrdU incorporation, mice were injected intraperitoneally with 1.5 mg of BrdU solution (10 mg/mL; BD Bioscience) and sacrificed 24 hours later. BrdU staining was performed according to the manufacturer's protocol (BD Bioscience). BM cells were analyzed by flow cytometry. Percentages of cells in G₀/G₁-, S-, and G₂/M-phases of the cell cycle were determined by manual gating.

Apoptosis assay. Apoptotic lymphocytes were determined using an antibody against AnnexinV conjugated to FITC (AnnexinV apoptosis detection kit, BD Biosciences) and DAPI (Sigma) counterstain, following the manufacturer's protocol. Percentages of apoptotic cell (FITC⁺, DAPI⁺) were determined by manual gating.

Protein extracts and Western blot analysis. Cells were harvested in cold RIPA buffer containing 50mM Tris, 150 mM sodium chloride, 1% Nonidet P-40, 0.25% sodium deoxycholate, 1mM EDTA, 0.1% SDS and protease inhibitors (Roche). Protein concentrations were determined by Bradford assay, and equal amounts of protein (20 ug) were loaded on 4-12% NuPAGE Bis-Tris Mini Gels (life technologies) separated on SDS-PAGE followed by transfer onto a PVDF transfer membrane (Immobilon-P, Milipore). The following antibodies were used: anti-mouse actin (ab5, Neo Markers), anti-mouse Hdac1 and anti-mouse Hdac2 (provided by Dr. Christian Seiser, Biocenter, Vienna) [47]. Antibodies were diluted 1:1,000.

***In vitro* Hdac-activity assay.** Global Hdac activity was measured with the *Fluor-de-Lys* Hdac assay kit (Enzo; BML-KI104-0050) according to the manufacturer's protocol. Fluorescence intensity was detected with Spectromax Gemini plate reader (Molecular Devices).

E μ -myc lymphoma transplantation. Syngeneic C57BL/6 recipient mice (The Jackson Laboratory; B6.SJL-Ptprca Pepcb/BoyJ) were sub-lethally irradiated (350 cGy whole-body γ -irradiation) using a Rad-source RS2000 irradiator (1.2 Gy/min) and transplanted intra-venously with 2.5×10^5 thawed cryopreserved lymph node-derived tumor cells from *Hdac1^{F/F};Hdac2^{F/F}*, *Actin-creER* tg, E μ -myc tg donor mice, as previously described [36, 48]. Recipient mice were treated with neomycin-supplemented drinking water (2 mg/ml; sigma) 1 week before, and 2 weeks post transplantation. 14 days post transplantation, conditional KO was induced by intraperitoneal injection of 4-hydroxytamoxifen (4-OHT; 5x 2mg). Control mice were injected with vehicle control (ethanol). Mice were monitored for tumor onset and sacrificed when they reached termination criteria as described above.

Oncomine and CCLE database analysis. Human *Hdac1* (*HDAC1*) and human *Hdac2* (*HDAC2*) mRNA expression levels were compared in human tumor samples and human cancer cell lines using the publicly available databases Oncomine (<http://www.oncomine.org>) and Cancer Cell Line Encyclopedia (CCLE), respectively [49, 50] [51].

Statistical analysis. Data are represented as mean \pm s.e.m. (standart error measurement of mean). For all analyses, several independent experiments ($N \geq 3$) were carried out. Student's unpaired 2-

tailed *t*-tests were performed for all analyses using Microsoft Excel. Statistical significance was determined by *p* values: N.S. $p > 0.05$, $*p < 0.05$, $**p < 0.01$. Statistical analysis of the KPLM survival curves was done using the log-rank test in R (www.r-project.org).

Acknowledgements

We thank H. Kohler for help with flow cytometry and cell sorting; S. Bichet for IHC; and C. Seiser for Hdac1 and Hdac2 antibodies. We also thank R.G. Clerc, and M.A. Choukrallah for suggestions on the manuscript. This study was supported by grants from the Swiss National Science Foundation (no. 31003A-122480 to P.M.) and by the Novartis Research Foundation.

Author Contributions

V.P. designed and performed experiments, analyzed data and wrote the manuscript; N.R. designed and performed experiments at the inception of the project; C.C. provided reagents and technical assistance; M.R.H. and T.Y. contributed to flow cytometry with non-E μ -*myc* samples; G.M. contributed technical assistance; A.T. performed histopathological analysis, provided suggestions for experiments and reviewed the manuscript; P.M. supervised the study and reviewed the manuscript.

Additional Information

Supplementary information accompanies this paper.

Competing financial interests: The authors declare no competing financial interests.

References

1. Reichert, N., M.A. Choukrallah, and P. Matthias, *Multiple roles of class I HDACs in proliferation, differentiation, and development*. Cell Mol Life Sci, 2012. **69**(13): p. 2173-87.
2. Dawson, M.A. and T. Kouzarides, *Cancer epigenetics: from mechanism to therapy*. Cell, 2012. **150**(1): p. 12-27.
3. Jenuwein, T. and C.D. Allis, *Translating the histone code*. Science, 2001. **293**(5532): p. 1074-80.
4. Choudhary, C., et al., *Lysine acetylation targets protein complexes and co-regulates major cellular functions*. Science, 2009. **325**(5942): p. 834-40.
5. Glozak, M.A., et al., *Acetylation and deacetylation of non-histone proteins*. Gene, 2005. **363**: p. 15-23.
6. Olzscha, H., S. Sheikh, and N.B. La Thangue, *Deacetylation of chromatin and gene expression regulation: a new target for epigenetic therapy*. Crit Rev Oncog, 2015. **20**(1-2): p. 1-17.
7. Mercurio, C., S. Minucci, and P.G. Pelicci, *Histone deacetylases and epigenetic therapies of hematological malignancies*. Pharmacol Res, 2010. **62**(1): p. 18-34.
8. Hagelkruys, A., et al., *The biology of HDAC in cancer: the nuclear and epigenetic components*. Handb Exp Pharmacol, 2011. **206**: p. 13-37.
9. Haery, L., R.C. Thompson, and T.D. Gilmore, *Histone acetyltransferases and histone deacetylases in B- and T-cell development, physiology and malignancy*. Genes Cancer, 2015. **6**(5-6): p. 184-213.
10. Falkenberg, K.J. and R.W. Johnstone, *Histone deacetylases and their inhibitors in cancer, neurological diseases and immune disorders*. Nat Rev Drug Discov, 2014. **13**(9): p. 673-691.
11. West, A.C. and R.W. Johnstone, *New and emerging HDAC inhibitors for cancer treatment*. J Clin Invest, 2014. **124**(1): p. 30-9.
12. Bantscheff, M., et al., *Chemoproteomics profiling of HDAC inhibitors reveals selective targeting of HDAC complexes*. Nat Biotech, 2011. **29**(3): p. 255-265.
13. Ghobrial, I.M., et al., *Results of a phase 2 trial of the single-agent histone deacetylase inhibitor panobinostat in patients with relapsed/refractory Waldenstrom macroglobulinemia*. Blood, 2013. **121**(8): p. 1296-303.
14. Richardson, P.G., et al., *PANORAMA 2: panobinostat in combination with bortezomib and dexamethasone in patients with relapsed and bortezomib-refractory myeloma*. Blood, 2013. **122**(14): p. 2331-7.
15. San-Miguel, J.F., et al., *Phase Ib study of panobinostat and bortezomib in relapsed or relapsed and refractory multiple myeloma*. J Clin Oncol, 2013. **31**(29): p. 3696-703.
16. Rasheed, W., et al., *Histone deacetylase inhibitors in lymphoma and solid malignancies*. Expert Rev Anticancer Ther, 2008. **8**(3): p. 413-32.
17. Ononye, S.N., et al., *Toward isozyme-selective inhibitors of histone deacetylase as therapeutic agents for the treatment of cancer*. Pharm Pat Anal, 2012. **1**(2): p. 207-21.
18. Glaser, K.B., et al., *Role of class I and class II histone deacetylases in carcinoma cells using siRNA*. Biochem Biophys Res Commun, 2003. **310**(2): p. 529-36.
19. Haberland, M., et al., *Genetic dissection of histone deacetylase requirement in tumor cells*. Proc Natl Acad Sci U S A, 2009. **106**(19): p. 7751-5.

20. Mottet, D., et al., *HDAC4 represses p21(WAF1/Cip1) expression in human cancer cells through a Sp1-dependent, p53-independent mechanism*. *Oncogene*, 2009. **28**(2): p. 243-56.
21. Senese, S., et al., *Role for histone deacetylase 1 in human tumor cell proliferation*. *Mol Cell Biol*, 2007. **27**(13): p. 4784-95.
22. Wilson, A.J., et al., *HDAC4 promotes growth of colon cancer cells via repression of p21*. *Mol Biol Cell*, 2008. **19**(10): p. 4062-75.
23. Matthews, G.M., et al., *Functional-genetic dissection of HDAC dependencies in mouse lymphoid and myeloid malignancies*. *Blood*, 2015. **126**(21): p. 2392-403.
24. Santoro, F., et al., *A dual role for Hdac1: oncosuppressor in tumorigenesis, oncogene in tumor maintenance*. *Blood*, 2013. **121**(17): p. 3459-68.
25. Montgomery, R.L., et al., *Histone deacetylases 1 and 2 redundantly regulate cardiac morphogenesis, growth, and contractility*. *Genes Dev*, 2007. **21**(14): p. 1790-802.
26. LeBoeuf, M., et al., *Hdac1 and Hdac2 act redundantly to control p63 and p53 functions in epidermal progenitor cells*. *Dev Cell*, 2010. **19**(6): p. 807-18.
27. Haberland, M., et al., *Redundant control of adipogenesis by histone deacetylases 1 and 2*. *J Biol Chem*, 2010. **285**(19): p. 14663-70.
28. Ma, P., et al., *Compensatory functions of histone deacetylase 1 (HDAC1) and HDAC2 regulate transcription and apoptosis during mouse oocyte development*. *Proc Natl Acad Sci U S A*, 2012. **109**(8): p. E481-9.
29. Montgomery, R.L., et al., *Histone deacetylases 1 and 2 control the progression of neural precursors to neurons during brain development*. *Proc Natl Acad Sci U S A*, 2009. **106**(19): p. 7876-81.
30. Yamaguchi, T., et al., *Histone deacetylases 1 and 2 act in concert to promote the G1-to-S progression*. *Genes Dev*, 2010. **24**(5): p. 455-69.
31. Wilting, R.H., et al., *Overlapping functions of Hdac1 and Hdac2 in cell cycle regulation and haematopoiesis*. *EMBO J*, 2010. **29**(15): p. 2586-97.
32. Dovey, O.M., et al., *Histone deacetylase 1 and 2 are essential for normal T-cell development and genomic stability in mice*. *Blood*, 2013. **121**(8): p. 1335-44.
33. Heideman, M.R., et al., *Dosage-dependent tumor suppression by histone deacetylases 1 and 2 through regulation of c-Myc collaborating genes and p53 function*. *Blood*, 2013. **121**(11): p. 2038-50.
34. Winter, M., et al., *Divergent roles of HDAC1 and HDAC2 in the regulation of epidermal development and tumorigenesis*. *EMBO J*, 2013. **32**(24): p. 3176-91.
35. Adams, J.M., et al., *The c-myc oncogene driven by immunoglobulin enhancers induces lymphoid malignancy in transgenic mice*. *Nature*, 1985. **318**(6046): p. 533-8.
36. Langdon, W.Y., et al., *The c-myc oncogene perturbs B lymphocyte development in E-mu-myc transgenic mice*. *Cell*, 1986. **47**(1): p. 11-8.
37. Harris, A.W., et al., *The E mu-myc transgenic mouse. A model for high-incidence spontaneous lymphoma and leukemia of early B cells*. *J Exp Med*, 1988. **167**(2): p. 353-71.
38. Morse, H.C., 3rd, et al., *Bethesda proposals for classification of lymphoid neoplasms in mice*. *Blood*, 2002. **100**(1): p. 246-58.
39. Sidman, C.L., et al., *Cell populations during tumorigenesis in Eu-myc transgenic mice*. *Leukemia*, 1993. **7**(6): p. 887-95.

40. Inoue, S., et al., *Inhibition of histone deacetylase class I but not class II is critical for the sensitization of leukemic cells to tumor necrosis factor-related apoptosis-inducing ligand-induced apoptosis*. *Cancer Res*, 2006. **66**(13): p. 6785-92.
41. Lindemann, R.K., et al., *Analysis of the apoptotic and therapeutic activities of histone deacetylase inhibitors by using a mouse model of B cell lymphoma*. *Proc Natl Acad Sci U S A*, 2007. **104**(19): p. 8071-6.
42. Newbold, A., et al., *Molecular and biologic analysis of histone deacetylase inhibitors with diverse specificities*. *Mol Cancer Ther*, 2013. **12**(12): p. 2709-21.
43. Newbold, A., et al., *The role of p21(waf1/cip1) and p27(Kip1) in HDACi-mediated tumor cell death and cell cycle arrest in the Emu-myc model of B-cell lymphoma*. *Oncogene*, 2014. **33**(47): p. 5415-23.
44. Newbold, A., et al., *Characterisation of the novel apoptotic and therapeutic activities of the histone deacetylase inhibitor romidepsin*. *Mol Cancer Ther*, 2008. **7**(5): p. 1066-79.
45. Ellis, L., et al., *The histone deacetylase inhibitors LAQ824 and LBH589 do not require death receptor signaling or a functional apoptosome to mediate tumor cell death or therapeutic efficacy*. *Blood*, 2009. **114**(2): p. 380-93.
46. Corcoran, L.M., S. Cory, and J.M. Adams, *Transposition of the immunoglobulin heavy chain enhancer to the myc oncogene in a murine plasmacytoma*. *Cell*, 1985. **40**(1): p. 71-9.
47. Zupkovitz, G., et al., *Negative and positive regulation of gene expression by mouse histone deacetylase 1*. *Mol Cell Biol*, 2006. **26**(21): p. 7913-28.
48. Wall, M., et al., *The mTORC1 inhibitor everolimus prevents and treats Emu-Myc lymphoma by restoring oncogene-induced senescence*. *Cancer Discov*, 2013. **3**(1): p. 82-95.
49. Rhodes, D.R., et al., *Oncomine 3.0: genes, pathways, and networks in a collection of 18,000 cancer gene expression profiles*. *Neoplasia*, 2007. **9**(2): p. 166-80.
50. Rhodes, D.R., et al., *ONCOMINE: a cancer microarray database and integrated data-mining platform*. *Neoplasia*, 2004. **6**(1): p. 1-6.
51. Barretina, J., et al., *The Cancer Cell Line Encyclopedia enables predictive modelling of anticancer drug sensitivity*. *Nature*, 2012. **483**(7391): p. 603-7.

1.1. Figures

Figure legends

Figure 1: Hdac1 and Hdac2 have no tumor suppressor function in B cells. (A) KPLM tumor-free survival curves for 15 age-matched mice are shown with indicated genotypes. E μ -myc tg mice are shown as control. Mice were monitored over a period of 300 days for tumor onset and sacrificed when they reached termination criteria (see Material and Methods). (B) Table summarizing histopathological analysis from spleen and lymph nodes of Hdac1 and/or Hdac2 KO mice with indicated genotypes at 8, 20, and 40 weeks. n=4-10 as indicated, N.A. for not analyzed.

Figure 2: E μ -myc tumorigenesis is Hdac1 and Hdac2 gene dose-dependent. (A) Kaplan-Meier tumor-free survival curves are shown for 15 age-matched mice with indicated genotypes. The log-rank test was used to determine the level of significance between curves in the KPLM plots. Significant differences between genotypes are indicated, * $p < 0.05$; **, $p < 0.01$. N.S., not statistically significant. (B) Tumor incidence (%; upper panel), and mean overall survival (days; lower panel), according to indicated Hdac1 and Hdac2 genotypes. Bar plots show values extracted from panel A.

Figure 3: Complete Hdac1 and Hdac2 ablation prevents E μ -myc tumorigenesis. All experiments were performed in 8-week-old mice. (A) Boxplot shows relative spleen weight (% of body weight) of mice with indicated genotypes. p -values were generated using Wilcoxon Signed-Rank Test (n=11). (B) Representative pictures from histopathological analysis of

hematoxylin and eosin stained spleen sections of E μ -*myc* mice with indicated genotypes and healthy *Hdac1*^{+/+};*Hdac2*^{+/+} control. Original magnification of 4X and 10X as indicated (left panel). Pathological findings of HG-NHL were scored in spleen and lymph nodes and summarized (table, right panel, n=10). *p*-value was calculated using Student unpaired 2-tailed *t* test. (C) Blood analysis with automated blood analyzer. Percentage (%) of PBL of indicated genotypes (n \geq 10). *p*-value calculated with Wilcoxon Signed-Rank Test. (D-F) E μ -*myc* BM cells from mice with indicated genotypes were stained with B cell surface marker-specific antibodies, including B220, IgM, CD19 and CD25, and analyzed by flow cytometry. (D) Schematic representation of wild-type BM profile: B220/IgM to distinguish between Pro/preB (B220⁺; IgM⁻), immatureB (B220^{low}; IgM⁺), transitional B (B220⁺; IgM⁺) and mature B (B220^{high}; IgM⁺) cells (upper panels). CD19/CD25 to identify PreBII cell subset (B220⁺; CD19⁺; CD25⁺; lower panels). (E) Representative flow cytometry dot plots of B220/IgM staining gated on total BM lymphocytes. Gated regions indicate B cell subsets of interest with frequency in percent. (F) Representative flow cytometry dot plots showing PreBII lymphocytes subsets. (G) Quantification of flow cytometry analysis from (E-F; n=4-6 biological replicates). Average percentage of B cells (B220⁺) and PreBII cells represented with s.e.m. Statistical analysis was performed with Student unpaired 2-tailed *t* test. Significant differences in means between genotypes are indicated, **p* < 0.05; ***p* < 0.01. N.S., not statistically significant.

Figure 4: Conditional ablation of Hdac1 and Hdac2 in E μ -*myc* tumor cells delays tumor appearance *in vivo*. (A) Experimental workflow scheme for transplantation experiments. Wild-type syngeneic recipient mice were sub-lethally irradiated (350 cGy of whole-body γ -irradiation) and transplanted intra-venously with lymph node-derived tumor cells from *Hdac1*^{F/F};*Hdac2*^{F/F};

Actin-creER tg; *Eμ-myc* tg mice after development of overt malignancy. Recipient mice were treated with neomycin-supplemented drinking water 1 week before transplantation and up to 2 weeks post transplantation. At two weeks post transplantation, conditional KO was induced in one group of mice by intraperitoneal injection of 4-hydroxytamoxifen (4-OHT, 5x 2mg). Control mice were injected with vehicle. Mice were monitored for tumor onset and sacrificed when they reached termination criteria (see Material and Methods). **(B)** KPLM tumor-free survival curves of mice transplanted with tumor cells and treated with 4-OHT (n=6) or vehicle (Ctr, n=4) are shown. Survival is plotted as days post transplantation. The log-rank test was used to determine the level of significance between curves in the two groups.

Figure 5: *Hdac1*^{Δ/Δ};*Hdac2*^{Δ/+} *Eμ-myc* mice have delayed tumorigenesis. All experiments were performed in 8-week-old lymphoma-free mice. **(A-B)** BM cells obtained from 8-week old *Eμ-myc* mice with indicated genotypes were stained with B cell surface marker-specific antibodies, including B220, IgM, CD19 and c-kit, and analyzed by flow cytometry (representative dot plots are shown). **(A)** Representative flow cytometry dot plots gated on total BM lymphocytes. Gated regions indicate B cell subsets of interest with frequency in percent. Pro/preB cell subset (B220⁺; IgM⁻) is indicated (red gate, upper panels). Gated PreBI (B220⁺;c-kit⁺; CD19⁺) and PreBII (B220⁺;CD19⁺; c-kit⁻) cell populations are indicated (lower panels). **(B)** Quantification of flow cytometry analysis with s.e.m. (n=3 biological replicates). Average percentage of B cells (B220⁺) and Pro/PreB cells (upper plots), and PreBI and PreBII (lower plots). Statistical analysis was performed with Student unpaired 2-tailed *t* test. **(C)** Blood was analyzed with automated blood analyzer. Shown are box plots with frequency (%) of PBL from indicated genotypes (n=10). *p*-

value calculated with the Wilcoxon Signed-Rank Test. Significant differences are indicated, $*p < 0.05$; $**$, $p < 0.01$. N.S., not statistically significant.

Figure 6: Hdac1 has a predominant role in non-malignant B cells. All experiments were performed in 8-week-old animals. **(A)** Representative flow cytometry dot plots of B220/IgM staining, gated on B220⁺ lymphocytes derived from BM of mice with indicated genotypes. Gated regions in dot plots indicate B cell subsets of interest with frequency in percent: Pro/preB (B220⁺; IgM⁻), ImmatureB (B220^{low}; IgM⁺), Transitional B (B220⁺; IgM⁺) and mature B (B220^{high}; IgM⁺) cells. **(B)** Quantification of flow cytometry analysis shown in (A). Bar plots represent average numbers of cells (gated 50,000 lymphocytes) from the different B lymphocyte subsets in the BM. **(C)** Quantification of flow cytometry analysis shown in (A). Average numbers of absolute PreBII cells. **(D)** Global Hdac-activity assay performed in CD19⁺ MACS sorted B cells from BM of mice with indicated genotypes. Values are shown in Relative Fluorescence Units (RFU) relative to control *Hdac1*^{+/+}; *Hdac2*^{+/+} cells. **(E)** Immunoblot analysis of Hdac1 and Hdac2 expression, and actin as loading control from CD19⁺ MACS sorted splenic B cells derived from mice with indicated genotypes. The cropped blots originate from a single blot for each protein. The full-length blots are presented in Supplementary Figure 7. All graphs represent mean \pm s.e.m. from 3 mice of each genotype. Statistical analysis with Student unpaired 2-tailed *t* test, $*p < 0.05$; $**$, $p < 0.01$. N.S., not statistically significant.

Figure 7: Hdac1^{Δ/Δ};Hdac2^{Δ/+} impact on proliferation and apoptosis. Experiments were performed in 8-week-old lymphoma-free mice. **(A-B)** Proliferation analysis by flow cytometry from BM B cells of mice with indicated genotypes injected with BrdU. **(A)** Representative flow

cytometry dot plots from indicated genotypes. Gated regions indicate B220⁺;BrdU⁺ cycling B cells with frequency in percent. **(B)** Quantification from flow cytometry analysis with mean and s.e.m. of BrdU-positive B cells is shown. **(C-D)** BM cells isolated from *Hdac1*^{+/+};*Hdac2*^{+/+} and *Hdac1*^{Δ/Δ};*Hdac2*^{Δ/Δ} Eμ-*myc* mice and stained with Annexin V, DAPI and B cell surface markers for flow cytometry analysis. **(C)** Representative flow cytometry dot plots from apoptosis assay: viable B cells (P5; annexinV⁻ DAPI⁻), apoptotic B cells (P6; annexinV⁺ DAPI⁻) cells, and dead cells (P7; annexinV⁺ DAPI⁺). **(D)** Quantification of figure (C). Mean percentages and standard deviations are shown. All statistical analysis were performed with the Student unpaired 2-tailed *t* test. Significant differences in means between genotypes are indicated, **p* < 0.05.

Figures

Figure 1

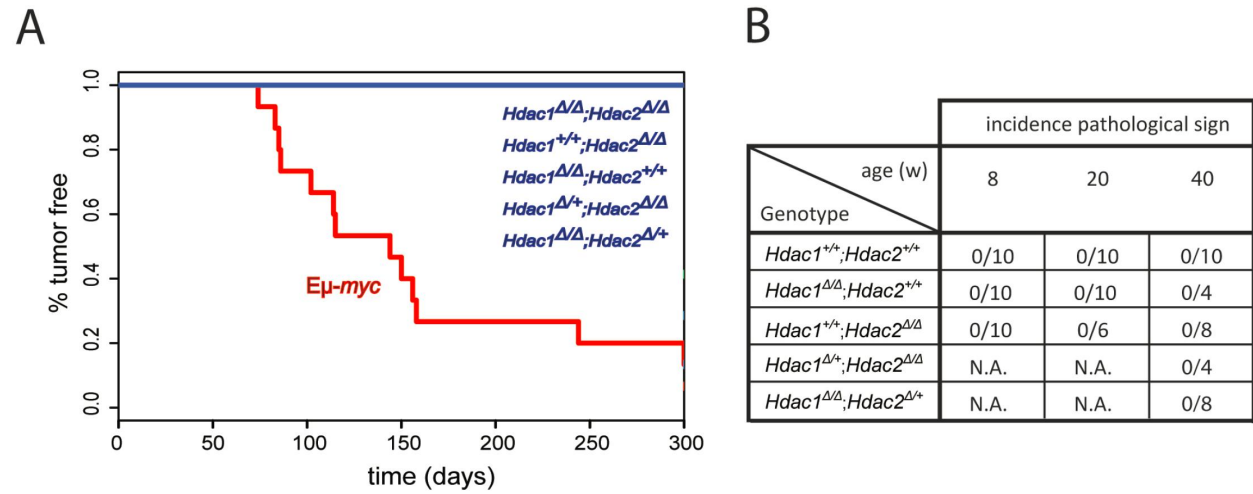
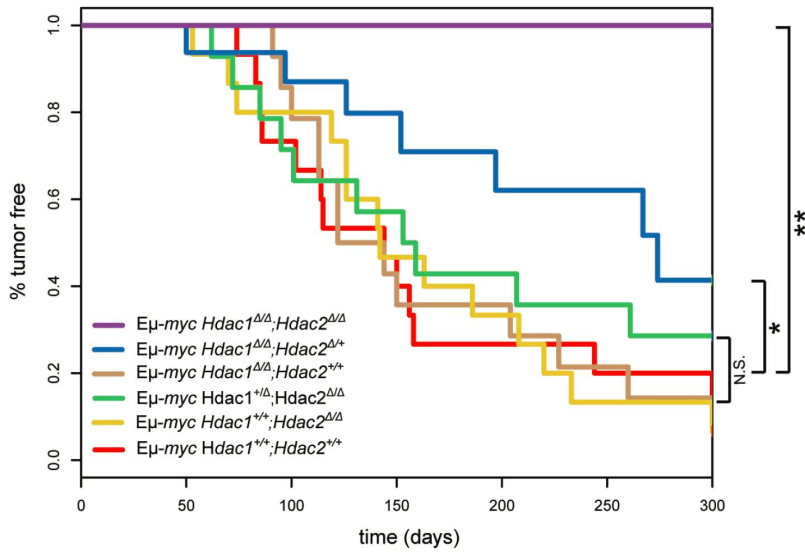


Figure 2

A



B

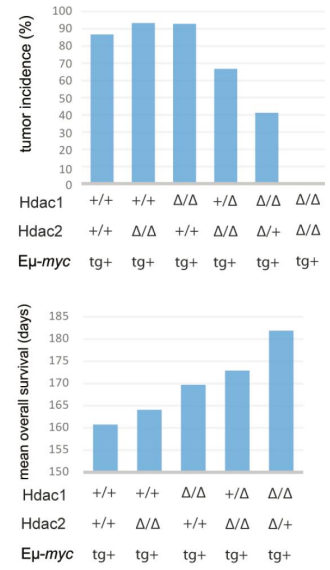


Figure 3

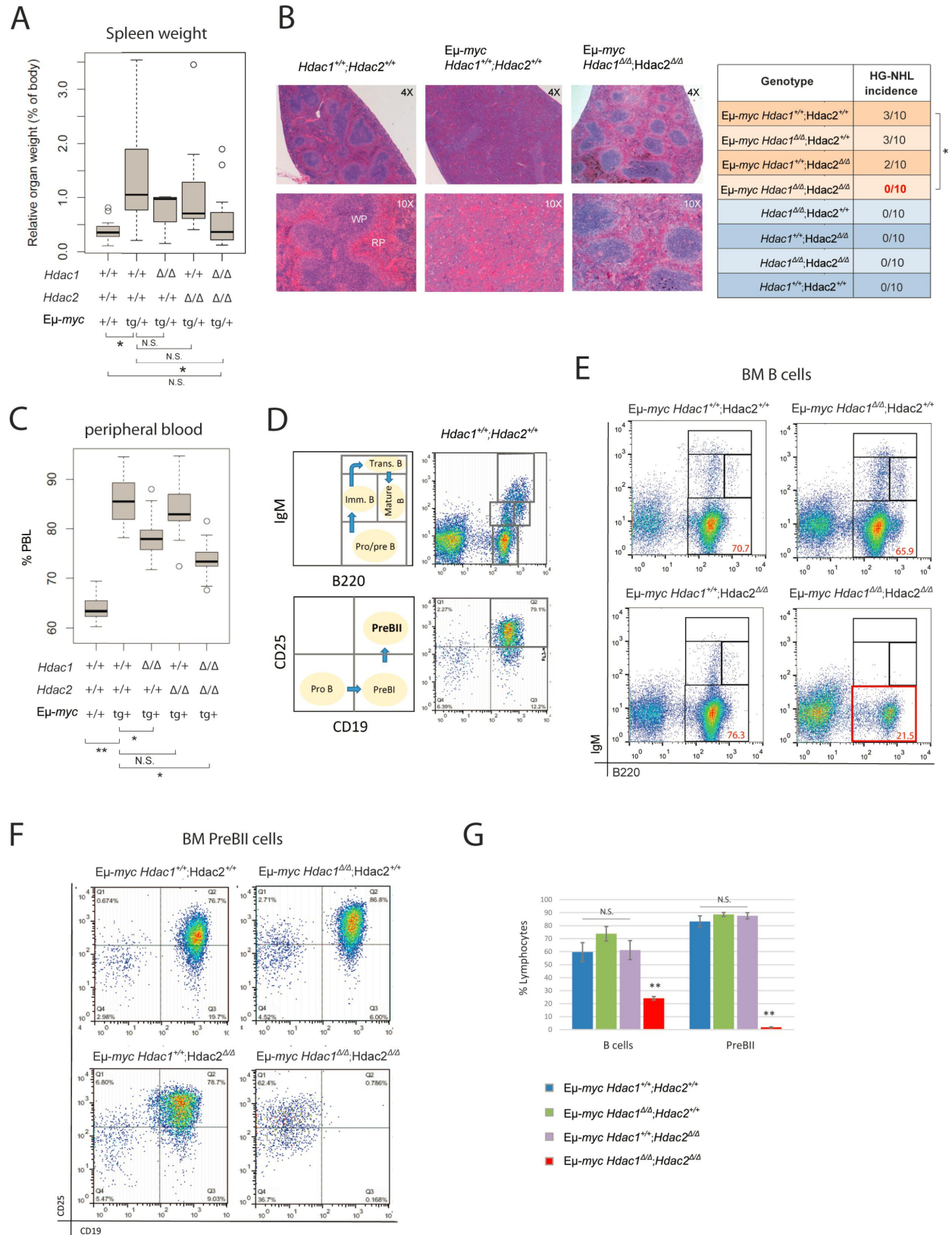


Figure 4

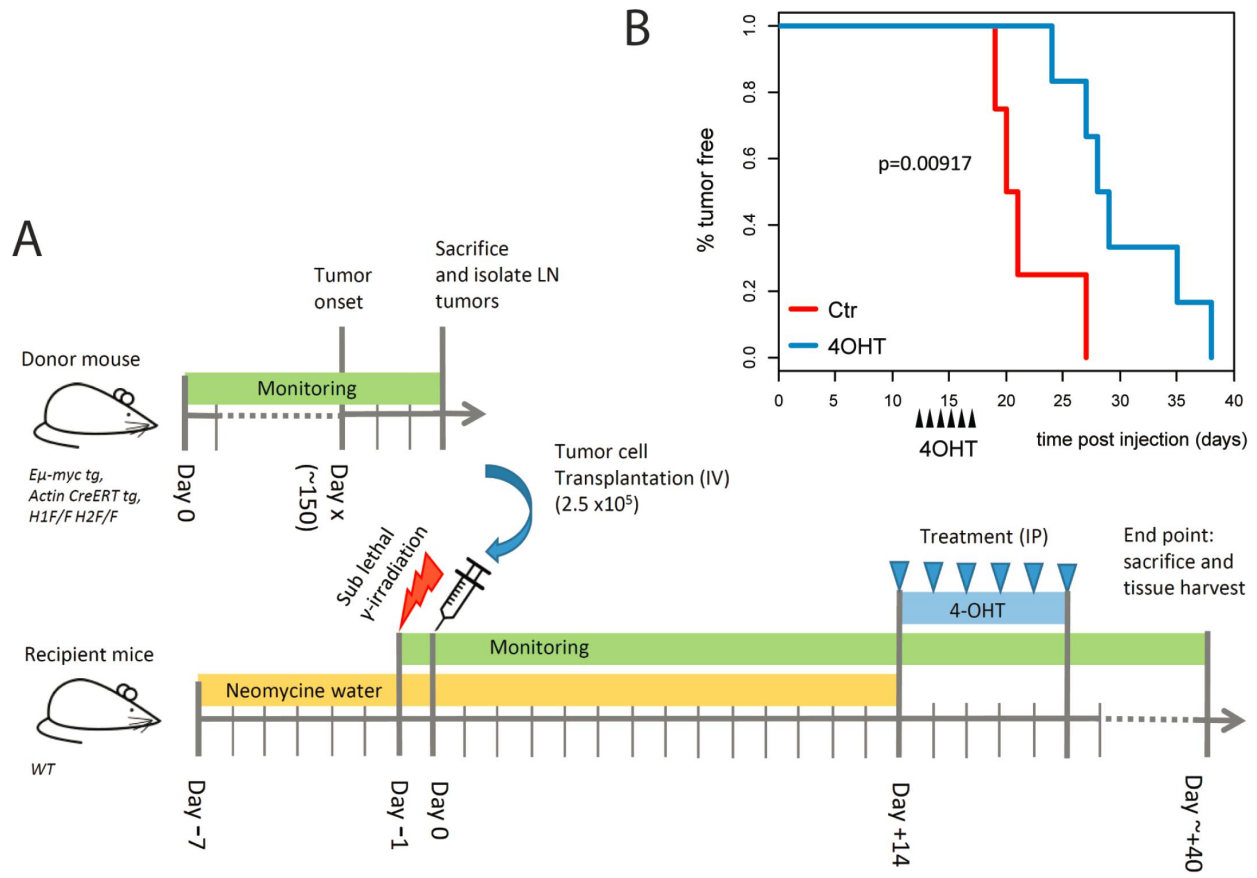


Figure 5

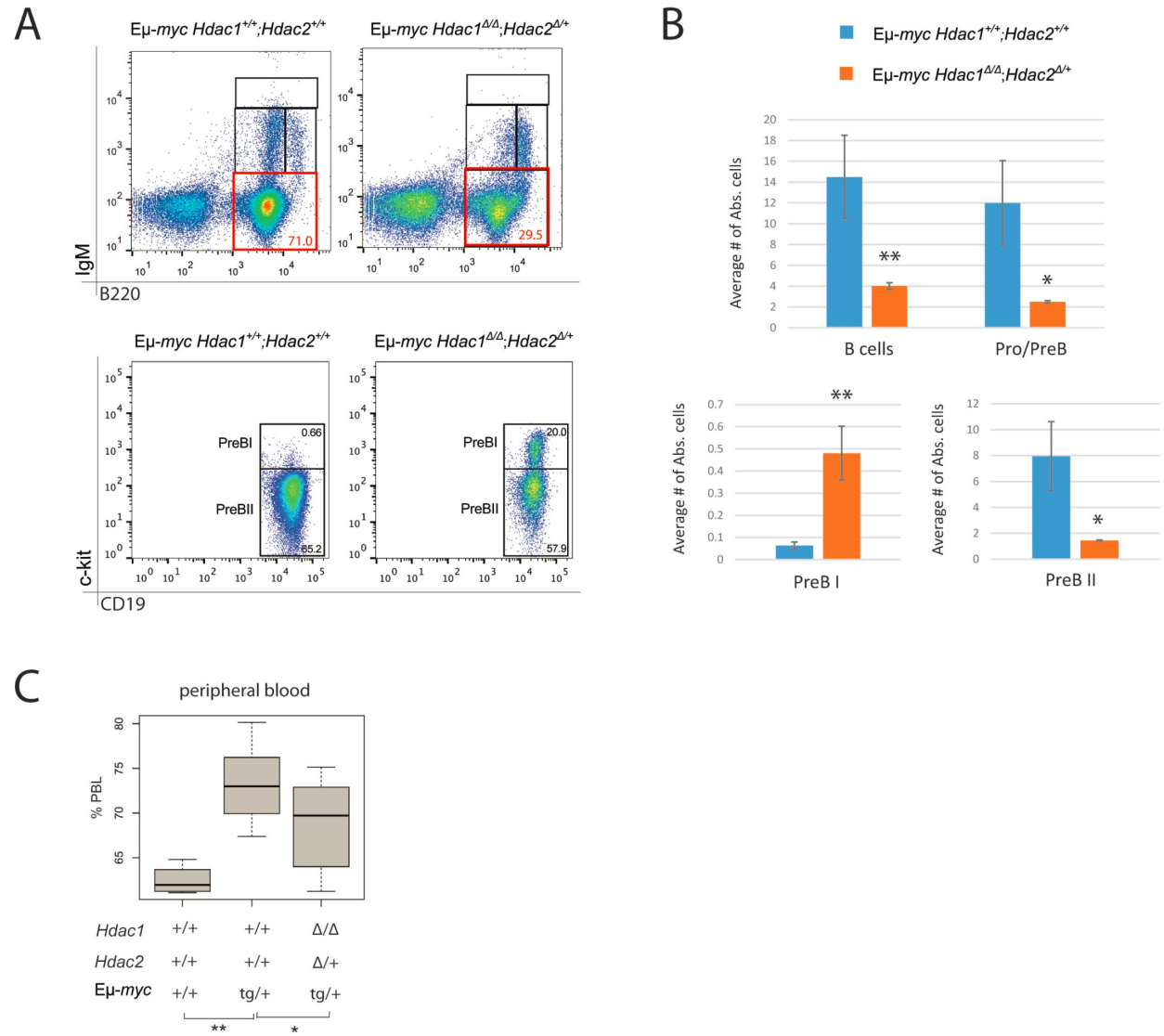


Figure 6

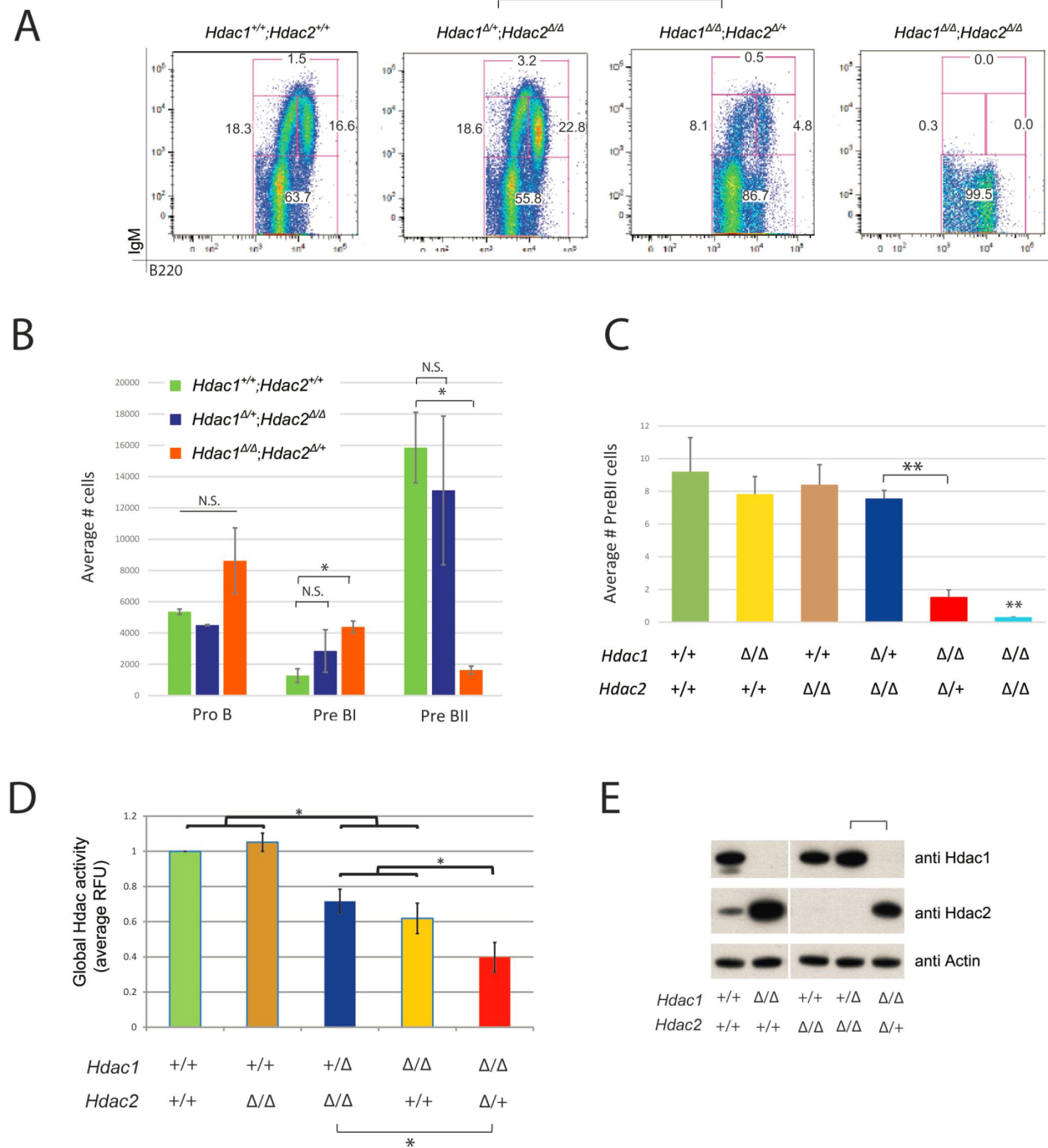
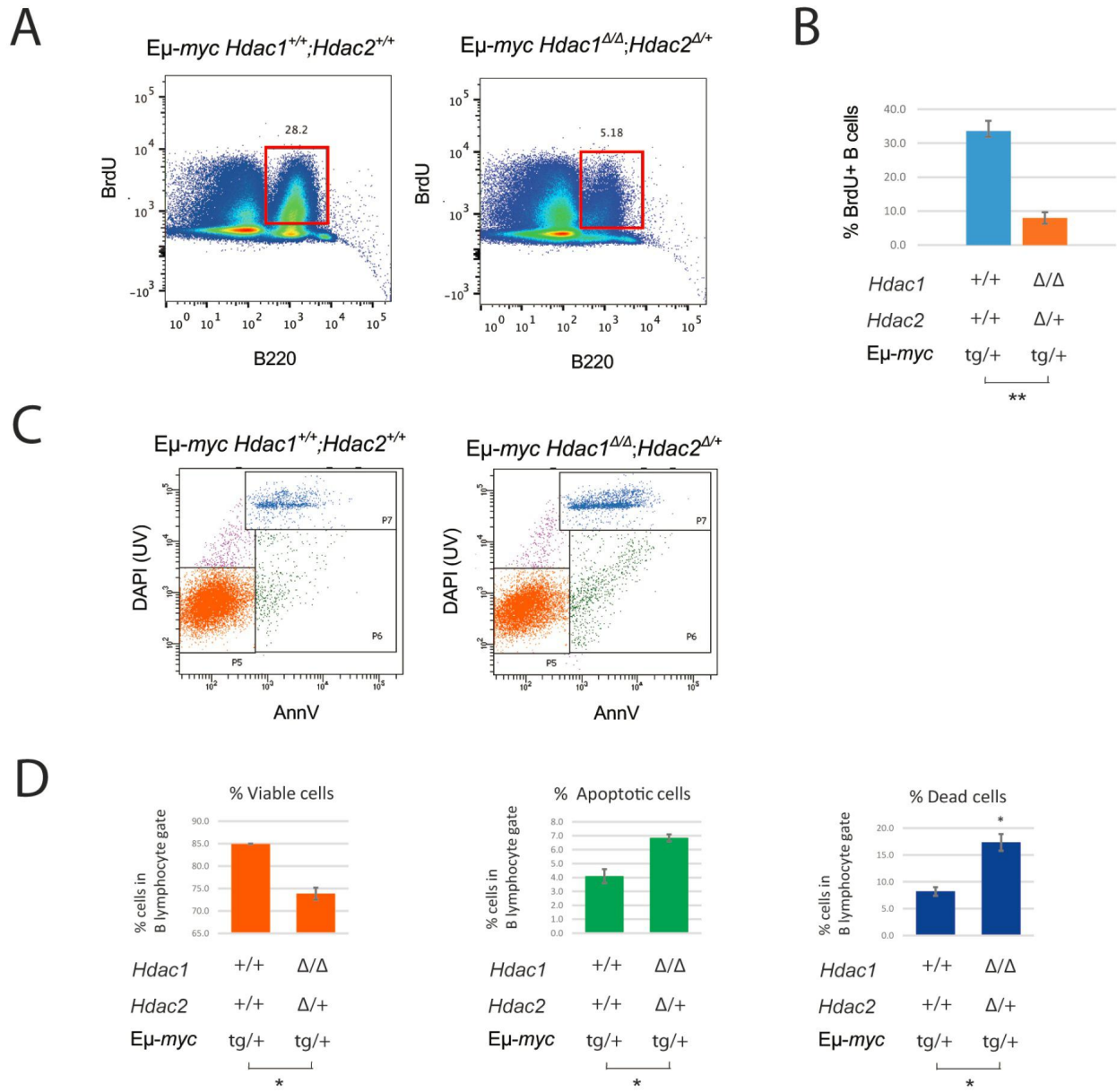


Figure 7



1.2. Supplementary Figures

Supplementary Figure legends

Supplementary Figure 1: B cell specific deletion of *Hdac1* and *Hdac2*. (A) PCR genotyping for *Hdac1* and *Hdac2* wild-type (WT), flox (FL), and knockout (KO) allele and *mb1-cre* transgene (tg). PCR was performed from mouse tails and CD19⁺ MACS sorted splenic B cells from 8-week-old mice with indicated genotypes. Specific allele annotations are to the left of the gel. Size marker (M) is indicated.

Supplementary Figure 2: Analysis of E μ -*myc* tg mice lacking *Hdac1* and/or *Hdac2* in B lymphocytes. (A) Schematic representation of the breeding setup to generate E μ -*myc* tg mice lacking *Hdac1* and/or *Hdac2* in B cells. *Hdac1* and *Hdac2* Floxed (F), WT (+) and knockout (Δ) alleles and transgenes (tg) are indicated. Red circle represents visibly enlarged and palpable lymph nodes scored in the KPLM. (B) Schematic representation illustrating the key steps of B cell development in the bone marrow (BM) with the expression of the different cell surface markers listed below. Curved arrows indicate cells in cell cycle. *c-myc* expression in the E μ -*myc* tg mouse and *mb1* expression in the *Mb1-cre* tg mouse is shown above. (C) B lymphocytes from isolated from 8-week-old WT and E μ -*myc* tg mice were FACS sorted for indicated B cell developmental stages and quantitative real-time PCR (RT-qPCR) was performed for *c-myc*. Data represents means \pm s.e.m. (n=3). (D) Development of pathologic diseased stage in E μ -*myc* tg mice. Representative picture of dissected enlarged inguinal lymph nodes (LN), spleen (S), and thymus (T) of E μ -*myc* tg *Hdac1*^{+/+};*Hdac2*^{+/+}, and control WT (*Hdac1*^{+/+};*Hdac2*^{+/+}) mice at termination criteria of 1cm LN for KPLM analysis.

Supplementary Figure 3: Predominant overexpression of *HDAC1*, but not *HDAC2*, in BL and DLBCL compared to other cancers. Search for HDAC1 and HDAC2 mRNA expression of human lymphomas with the focus on diffuse large B-cell lymphoma (DLBCL) and Burkitt's lymphomas (BL), two *myc*-driven B cell lymphomas. Online, publically available databases were used. Cancer Cell Line Encyclopedia (CCLE) (www.broadinstitute.org) was used to screen for HDAC1 (**A**) and HDAC2 (**B**) mRNA expression in tumor cell lines. Extracted mRNA expression levels (log₂ scale) are shown. Gene expression profiles of *HDAC1* (**C**) and *HDAC2* (**D**), analyzed on Oncomine microarray database. Analysis of HDAC1 and HDAC2 mRNA levels in lymphoma tissues vs. other cancers (Ramaswamy Multi-cancer statistic datasets).

Supplementary Figure 4: Loss of *Hdac1* (*Hdac1*^{ΔΔ};*Hdac2*^{+/+}) has no impact on PBL at 10 weeks and 20 weeks in Eμ-*myc* mice. Mice were bled at 10 and 20 week of age and blood was analyzed in an automated blood analyzer, (Sysmex XT-2000). *Hdac1*^{ΔΔ};*Hdac2*^{+/+} Eμ-*myc* mice had no significant difference in PBL counts at (**A**) 10 and (**B**) 20 weeks compared to control *Hdac1*^{+/+};*Hdac2*^{+/+} Eμ-*myc* mice. Shown are detailed analysis of different *Hdac1* knockout animals with or without Eμ-*myc* at 10 and 20, weeks (n≥10). Frequency (%) of PBL of indicated. p-value calculated with the Wilcoxon Signed-Rank Test. Significant differences in means is indicated, **p < 0.01; N.S. for not statistically significant.

Supplementary Figure 5: *Hdac1* and *Hdac2* are not deleted in tumors arising in 4-OHT treated transplanted mice. (**A**) In vivo conditional ablation of *Hdac1* and *Hdac2* using the CreER-LoxP system inducible with tamoxifen (4-OHT) treatment in *Hdac1*^{F/F};*Hdac2*^{F/F}; ActinCre tg mice. Recombination was not 100%, since *Hdac1* (and *Hdac2*) floxed alleles did not

disappear completely. **(B)** Representative PCR genotyping of tumors from control (Ctr) and tamoxifen (4-OHT) treated transplanted mice. Control Hdac1 and Hdac2 KO PCR from Hdac1^{Δ/Δ};Hdac2^{Δ/Δ} mice is included. PCR genotyping for Hdac1 and Hdac2 wild type (WT), floxed (FL) and knockout (KO) alleles are indicated to the left of each gel. PCR for Hdac1, Hdac2 and Eμ-myc are to the left of each gels. **(C)** Hdac1 and Hdac2 are expressed in tumors from 4-OHT treated transplanted mice. Immunohistochemistry (IHC) of tumors from Ctr and 4-OHT treated transplanted mice (splenic sections). **(D)** Control IHC experiment for Hdac1, Hdac2 and c-Myc antibodies using Hdac1^{Δ/Δ};Hdac2^{+/+} Eμ-myc mice, Hdac1^{+/+};Hdac2^{Δ/Δ} Eμ-myc mice and Hdac1^{+/+};Hdac2^{+/+} Eμ-myc mice from serial splenic sections stained for c-Myc, Hdac1, and Hdac2.

Supplementary Figure 6: Hdac1^{Δ/Δ};Hdac2^{Δ/+} mice have normal numbers of mature B cells in the spleen. **(A)** Spleen cells were obtained from 8-week old mice with indicated genotypes and stained with B cell surface marker-specific antibodies, including B220, IgM and IgD and analyzed by flow cytometry. Quantification of flow cytometry analysis with s.e.m. (n=3 biological replicates). Average number of absolute B cells (B220⁺, IgM⁺, IgD⁺) are shown in bar plots. Statistical analysis was performed with Student unpaired 2-tailed *t* test. N.S., not statistically significant.

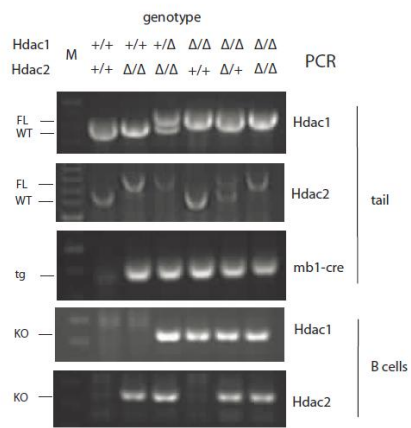
Supplementary Figure 7: Full-length immunoblots of Hdac1 and Hdac2 expression. Immunoblots for **(A)** Hdac1, **(B)** Hdac2, and **(C)** actin are shown. **(C)** Hdac1 blot was stripped and reblotted for actin (see residual Hdac1 bands). Mice genotypes are indicated below.

Molecular size marker is shown in the first row of each gel. Protein of interest is indicated on the right of each gel.

Supplementary Figures

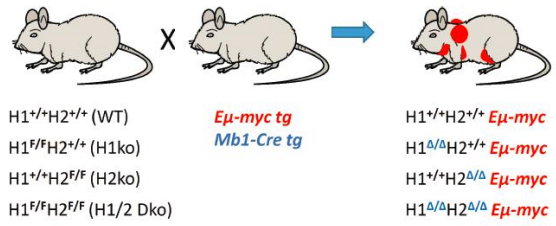
Suppl. Figure 1

A

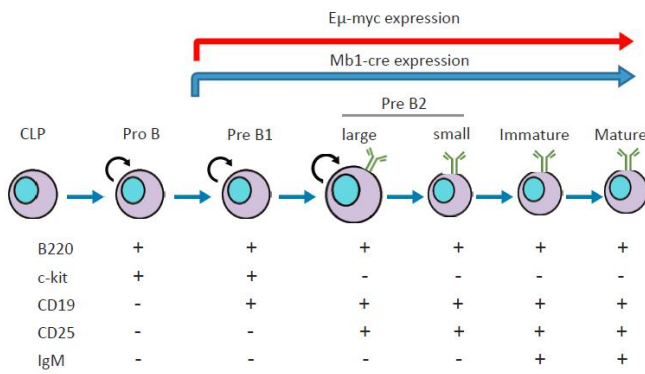


Suppl. Figure 2

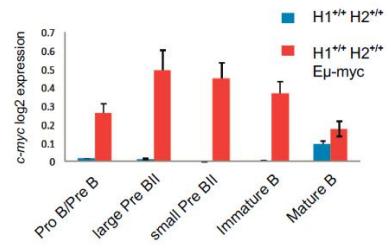
A



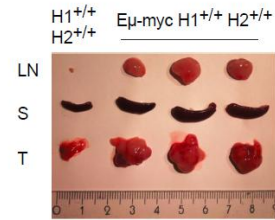
B



C

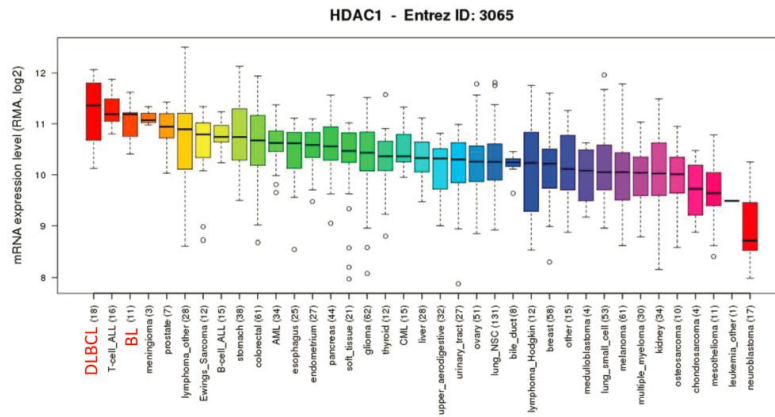


D

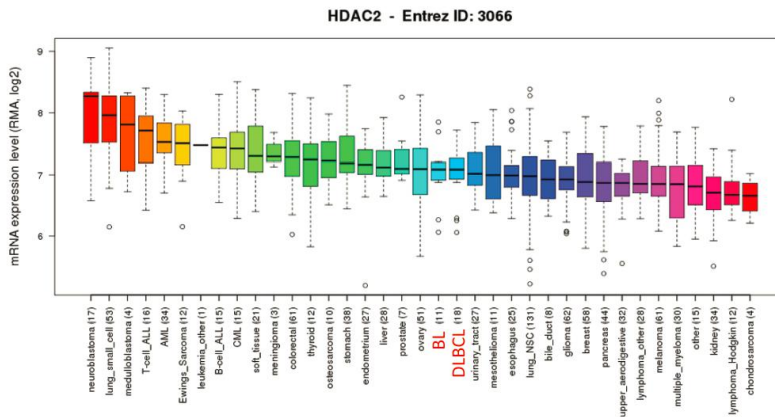


Suppl. Figure 3

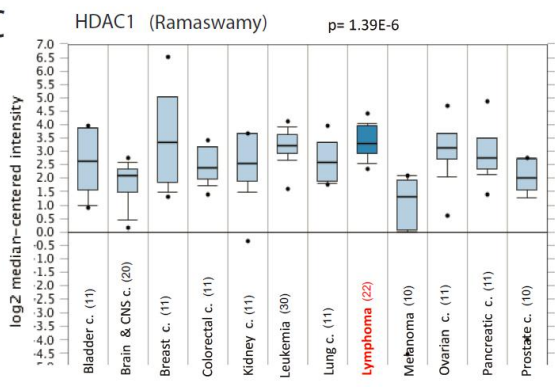
A



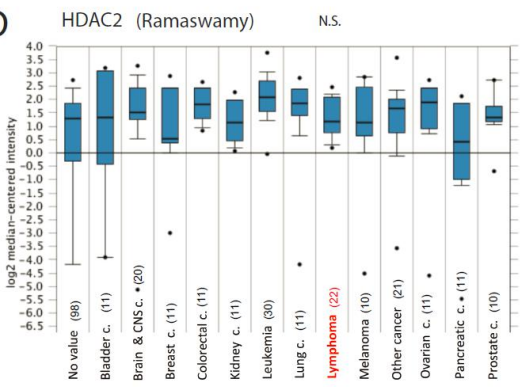
B



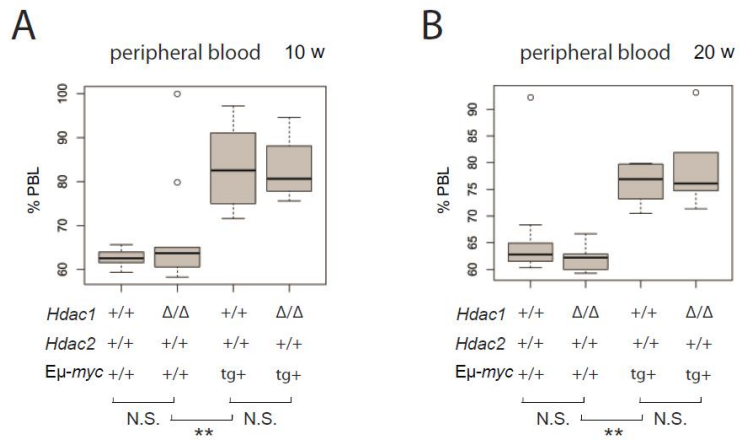
C



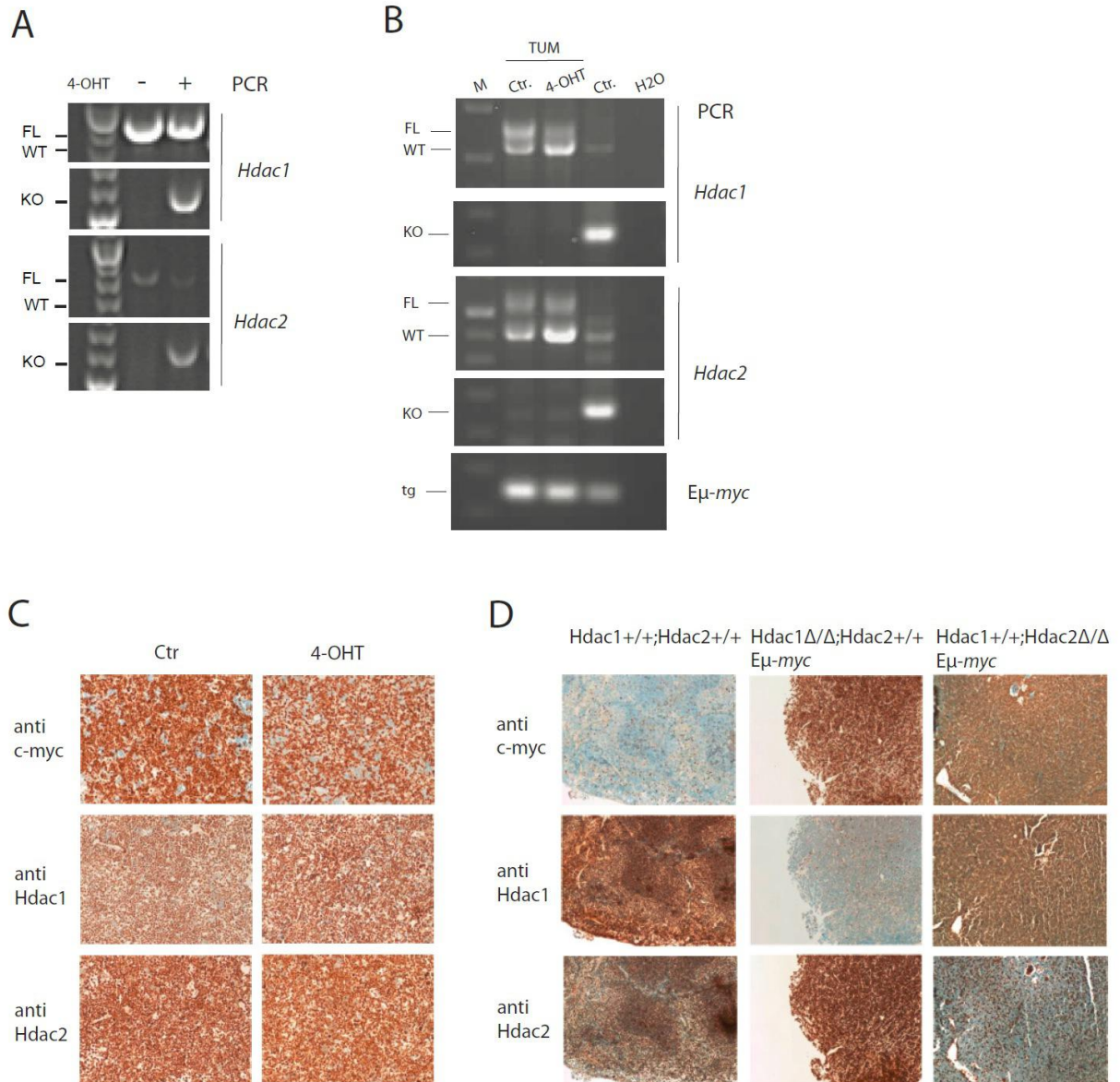
D



Suppl. Figure 4

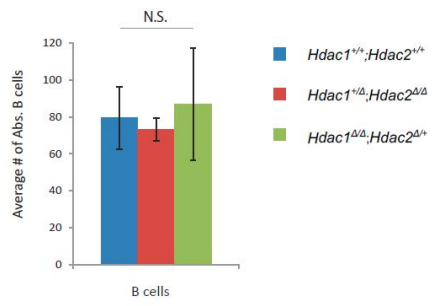


Suppl. Figure 5

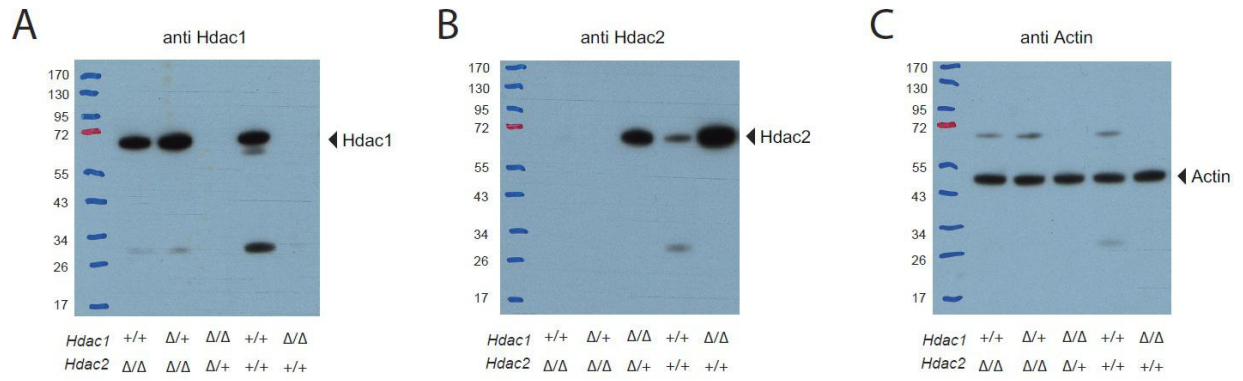


Suppl. Figure 6

A



Suppl. Figure 7



Supplementary methods

Immunohistochemistry (IHC)

Immunohistochemistry experiments were performed on Ventana DiscoveryUltra instrument (Roche Diagnostics, Mannheim) with the procedure RUO Discovery Universal. CC1 (Roche Diagnostics, Mannheim) pre-treatment was used for anti-HDAC1, -HDAC2, and -c-Myc antibodies with the following incubation times: 16, 24, and 72 min respectively. Antibodies were incubated for one hour at 37°C except for anti-c-Myc which was incubated for 16 min. In addition, a blocking step (Innovex Background Buster NB306, Innovex, 12 min incubation) was added for anti-HDAC1 and -HDAC2 antibodies. Detection of bound anti-HDAC1, -HDAC2 and -c-Myc antibodies was achieved by using anti-rabbit HQ followed by anti-HQ horseradish peroxidase (Roche Diagnostics, Mannheim) incubated for 32 min at 37°C. ChromoMap DAB kit (Roche Diagnostics, Mannheim) was used for the detection and slides were counterstained with Hematoxylin II and Bluing Reagent (Roche Diagnostics, Mannheim) for 8 min. Hdac1 and Hdac2 staining were used to confirm the genotype of the lymphoma.

Results Part 2

Results Part2: Supplementary findings on the role of Hdac1 and Hdac2 in Eμ-*myc* B cell lymphoma

2.1. Supplementary results

Old Hdac1^{Δ/Δ};Hdac2^{+/+} mice do not develop spontaneous tumors

As previously shown, Hdac1 and Hdac2 have no tumor suppressor function in B cells (Figure 1). To further validate our observation, we analyzed more extensively old *Hdac1^{Δ/Δ};Hdac2^{+/+}* mice. We first assessed whether 20- and 70 week-old *Hdac1^{Δ/Δ};Hdac2^{+/+}* animals had any enlarged lymphoid organs, including SP, LN and Thymus (Thy) compared to control *Hdac1^{+/+};Hdac2^{+/+}* mice. Consistent with our previous findings (Figure 1), we observed that old *Hdac1^{Δ/Δ};Hdac2^{+/+}* mice had normal SP and LN weights at 20 weeks (Suppl. Figure 4A). Similarly, SP, LN, and thymus weights were normal in 70-week-old *Hdac1^{Δ/Δ};Hdac2^{+/+}* mice. We then determined by flow cytometry the percentage of large B220⁺ subset of cells in the BM, which is massively elevated in Eμ-*myc* mice. We observed, that 20-week-old *Hdac1^{Δ/Δ};Hdac2^{+/+}* mice have normal large B220⁺ cell number in the BM compared to control *Hdac1^{+/+};Hdac2^{+/+}* mice. These results are consistent with our findings described in Figure 1 and confirm that mice with B cell specific *Hdac1^{Δ/Δ};Hdac2^{+/+}* do not develop spontaneous tumors.

Hdac1 and Hdac2 have no tumor suppressor function in B cells

As previously shown (Suppl. Figure 1B), *Jdp2* is not de-repressed in *Hdac1* and/or *Hdac2* B cell KOs in contrast to T cell specific KO (Heideman et al., 2013). We further assessed *Jdp2* expression in mice with only one allele of *Hdac2* (*Hdac1^{Δ/Δ};Hdac2^{Δ/+}*), since these mice were shown to develop spontaneous tumors with the highest frequency in T cell specific KO

Results

(Heideman et al., 2013). To test this, we measured by RT-qPCR analysis the *Jdp2* gene transcripts in 8-week-old *Hdac1^{Δ/Δ};Hdac2^{Δ/+}* and control *Hdac1^{+/+};Hdac2^{+/+}* CD19⁺ MACS sorted B lymphocytes. In contrast to T cell specific KO, but consistent with the previously shown microarray in B cells (Suppl. Figure 1B), we did not observe any change in *Jdp2* expression in B cell specific *Hdac1^{Δ/Δ};Hdac2^{Δ/+}* cells (Suppl. Figure 5A, preliminary results). Taken together, our results shows, that Hdac1 and Hdac2 do not regulate this gene in B cells. This is in contrast to T cells where Hdac1 and Hdac2 regulate p53-dependent barrier to constrain *myc*-overexpressing thymocytes from progressing into lymphomas by regulating Myc-collaborating genes like *Jdp2* (Heideman et al., 2013). It was previously reported, that most tumors found in Eμ-*myc* mice display a disruption of the p19^{ARF}-MDM2-p53 tumor suppressor pathway, and p53 mutations are the most frequent event in this model (Eischen et al., 1999). Inactivation of the p53 pathway can occur through inactivating p53 mutations, which results in high p53 levels and stabilized, but inactive p53 protein (Eischen et al., 1999). In T cells, *Hdac1^{Δ/Δ};Hdac2^{Δ/+}* results in spontaneous lymphomagenesis with tumors having low p53 levels due to de-repression of the p53 repressor *Jdp2* (Heideman et al., 2013). In B cells, *Hdac1^{Δ/Δ};Hdac2^{Δ/+}* does not result in spontaneous lymphomagenesis (Figure 1) and *Jdp2* is not de-repressed (Suppl. Figure 5A). Hence, if *Hdac1^{Δ/Δ};Hdac2^{Δ/+}* does not affect p53 in B cells, we would expect to have similar p53 levels in Eμ-*myc* *Hdac1^{Δ/Δ};Hdac2^{Δ/+}* tumors vs. control Eμ-*myc* *Hdac1^{+/+};Hdac2^{+/+}* tumors. In contrast, if *Hdac1^{Δ/Δ};Hdac2^{Δ/+}* would affect p53 we would expect to see less p53 positive Eμ-*myc* *Hdac1^{Δ/Δ};Hdac2^{Δ/+}* tumors as previously reported in T cell specific *Hdac1^{Δ/Δ};Hdac2^{Δ/+}* (Heideman et al., 2013). We therefore performed Immunohistochemistry (IHC) staining for p53 in Eμ-*myc* *Hdac1^{Δ/Δ};Hdac2^{Δ/+}* tumors and control Eμ-*myc* *Hdac1^{+/+};Hdac2^{+/+}* tumors. We observed, that p53 was strongly expressed in all Eμ-*myc* tumor samples (Suppl. Figure 5C),

suggesting for stabilized/mutant p53 disrupting the p53 tumor suppressor function. Interestingly, E μ -myc *Hdac1*^{A/A};*Hdac2*^{A/+} tumors had also high p53 expression (Suppl. Figure 5C), with similar intensity and frequency compared to control E μ -myc *Hdac1*^{+/+};*Hdac2*^{+/+} tumors (Suppl. Figure 5D). Hence, this suggests, that p53 is mutated in E μ -myc *Hdac1*^{A/A};*Hdac2*^{A/+} tumors to circumvent p53 induced apoptosis, thereby enabling tumorigenesis. This is consistent with our previous findings (Suppl. Figure 1 and Suppl. Figure 5A), and suggest that in B cells Hdac1 and Hdac2 do not impact on p53 via Jdp2 like in T cells (Heideman et al., 2013). Therefore, we propose, that in B cells, Hdac1 and Hdac2 do not impact on p53 tumor suppressor pathway via *Jdp2* (Suppl. Figure 5B). Our data collectively show, that Hdac1 and Hdac2 do not have any tumor-suppressor function in B cells.

Development of pathologic diseased state in E μ -myc tg mice

In complement to Suppl. Figure 2, we further analyzed E μ -myc mice by histopathology from H&E-stained sections taken from a terminally ill E μ -myc *Hdac1*^{+/+};*Hdac2*^{+/+} animal. We observed, that E μ -myc *Hdac1*^{+/+};*Hdac2*^{+/+} mice had marked enlarged spleen (S), thymus (T), lymph nodes (LN) due to infiltration of neoplastic cells. The form and architecture of these organs was also altered (Suppl. Figure 6A). Further analysis demonstrated, that E μ -myc *Hdac1*^{+/+};*Hdac2*^{+/+} mice have infiltration of tumor cells into the peripheral organs which is indicative of disseminated disease (Suppl. Figure 6B). SP and mandibular LN of E μ -myc *Hdac1*^{+/+};*Hdac2*^{+/+} mice were enlarged and had destroyed architecture due to diffuse infiltration by neoplastic lymphocytes. These mice also had neoplastic cell infiltration into: liver, myocardium of the heart, submucosa of the urinary bladder, pelvis of the kidney, all layers of the small intestine, duodenum (mucosa, submucosa, muscular layer and serosa), as well as stomach

mucosa (Suppl. Figure 6B). These data show that our E μ -myc mice develop multicentric lymphosarcomas which is consistent with the previous description of the E μ -myc tg mouse (Adams et al., 1985; Harris et al., 1988; Langdon et al., 1986).

E μ -myc mice have a trend to slightly increased Hdac1 and Hdac2 expression levels

In complement to Figure 2 and Suppl. Figure 2, we analyze by quantitative real-time PCR (RT-qPCR) *Hdac1* and *Hdac2* expression in E μ -myc mice. Interestingly, we found that E μ -myc mice have a trend to slightly increased *Hdac1* and *Hdac2* expression levels in the cells of most B cell developmental stages (Suppl. Figure 7A).

Loss of both, Hdac1 and Hdac2 (*Hdac1* ^{Δ/Δ} ;*Hdac2* ^{Δ/Δ}) reduces leukemia in E μ -myc mice

We showed that *Hdac1* ^{Δ/Δ} ;*Hdac2* ^{Δ/Δ} reduces leukemia in E μ -myc mice (Figure 3C). In complement to these data we further performed a detailed blood analysis in E μ -myc mice lacking Hdac1 and/or Hdac2 at 4 and 10 (Suppl. Figure 8). We found, that E μ -myc *Hdac1* ^{Δ/Δ} ;*Hdac2* ^{Δ/Δ} mice had significantly lower PBL counts at 4 and 10 weeks compared to control E μ -myc *Hdac1* ^{$+/+$} ;*Hdac2* ^{$+/+$} mice (Suppl. Figure 8B). Interestingly, we observed that *Hdac1* ^{Δ/Δ} ;*Hdac2* ^{$+/+$} mice had reduced PBL only at 4 but not at 10 weeks (Suppl. Figure 8B). These results are consistent with our observation that only ablation of both, Hdac1 and Hdac2 prevents tumorigenesis, whereas ablation of either Hdac1 or Hdac2 had no major effects.

Only ablation of both, but not single Hdac1 and Hdac2, prevents B cell blast in BM of Eμ-myc mice

We previously showed, that only complete *Hdac1* and *Hdac2* deletion prevents tumorigenesis by blocking Eμ-*myc* induced blast in the BM (Figure 3E-G). Here, in supplement, we show the impact of *Hdac1^{Δ/Δ};Hdac2^{Δ/Δ}*, *Hdac1^{Δ/Δ};Hdac2^{+/+}*, and *Hdac1^{+/+};Hdac2^{Δ/Δ}* in absence of Eμ-*myc* tg. We further analyzed for comparison Eμ-*myc* mice with lymphadenopathy that had reached endpoint criteria, and with a pathological findings of HG-NHL (indicated by asterisk). We measure by flow cytometry the BM B lymphocytes by B220/IgM (Suppl. Figure 9A) and PreBII lymphocytes subsets (B220⁺;CD19⁺;CD25⁺) (Suppl. Figure 9B). Quantification of these flow cytometry analysis revealed that only ablation of both, Hdac1 and Hdac2 (*Hdac1^{Δ/Δ};Hdac2^{Δ/Δ}*) resulted in a statistically significant decrease in B lymphocytes (B220⁺) (Suppl. Figure 9C) and PreBII (B220⁺;CD19⁺; CD25⁺) subsets (Suppl. Figure 9D). Hence, ablation of both Hdac1 and Hdac2 prevents normal B cell development as we previously reported (Yamaguchi et al., 2010), but prevents also Eμ-*myc* induced blast which dominate the BM of these mice. Some rare *Hdac1^{Δ/Δ};Hdac2^{Δ/Δ}* mice had tumors and showed the typical Eμ-*myc* induced blast (Suppl. Figure 9A-B). In summary, we conclude, that *Hdac1^{Δ/Δ};Hdac2^{Δ/Δ}* prevents tumorigenesis by blocking Eμ-*myc* induced blast at PreBII B cell stage.

Ablation both, Hdac1 and Hdac2 (Hdac1^{Δ/Δ};Hdac2^{Δ/Δ}) is required to reduce tumor cell load

We demonstrated that *Hdac1^{Δ/Δ};Hdac2^{Δ/Δ}* prevents tumorigenesis by blocking Eμ-*myc* induced B cell blasts at PreBII cell stage (Figure 3F). We further assessed the tumor cell load in a different way by quantifying the large lymphocyte subset as well as the B220^{low} population, which are

characteristically highly overrepresented in E μ -*myc* mice (Croxford et al., 2013; Langdon et al., 1986). We first measure by flow cytometry large lymphocyte subsets in BM. Consistently, with the results previously observed, we found that *Hdac1*^{Δ/Δ};*Hdac2*^{Δ/Δ} significantly reduced the percentage of large lymphocyte subset in BM of E μ -*myc* mice (Suppl. Figure 10A). Rare E μ -*myc* *Hdac1*^{Δ/Δ};*Hdac2*^{Δ/Δ} mice, which developed end stage tumors (indicated with red asterisks), had almost only large lymphocytes similar to control E μ -*myc* *Hdac1*^{+/+};*Hdac2*^{+/+} tumor mice. Malignant cells in E μ -*myc* tg mice express B220 at a low level (B220^{low}) (Croxford et al., 2013). Hence, we analyzed by flow cytometry B220^{low} cells populations in in BM, SP, and LN, and blood (BL) of E μ -*myc* *Hdac1*^{+/+};*Hdac2*^{+/+} mice compared to wild type (*Hdac1*^{+/+};*Hdac2*^{+/+}) control animals (Suppl. Figure 10B-D). Consistent with previously published data, we observed, that E μ -*myc* *Hdac1*^{+/+};*Hdac2*^{+/+} mice had massive increase in B220^{low} cells population in all these organs (Suppl. Figure 10B). Quantification revealed a significant increase in B220^{low} cells population in E μ -*myc* *Hdac1*^{+/+};*Hdac2*^{+/+} compared to control *Hdac1*^{+/+};*Hdac2*^{+/+} mice (Suppl. Figure 10B). We next determined the effect of Hdac1 and/or Hdac2 ablation on B220^{low} cells population in BM, SP, and LN. Ablation of Hdac1 (*Hdac1*^{Δ/Δ};*Hdac2*^{+/+}) or Hdac2 (*Hdac1*^{+/+};*Hdac2*^{Δ/Δ}) had no effect, but ablation of both enzymes (*Hdac1*^{Δ/Δ};*Hdac2*^{Δ/Δ}) massively reduced B220^{low} cells population (Suppl. Figure 10D). Quantification revealed no significant changes in B220^{low} cells population comparing E μ -*myc* *Hdac1*^{+/+};*Hdac2*^{+/+} mice to E μ -*myc* mice lacking either Hdac1 (*Hdac1*^{Δ/Δ};*Hdac2*^{+/+}) or Hdac2 (*Hdac1*^{+/+};*Hdac2*^{Δ/Δ}) (Suppl. Figure 10C). Collectively, these data presented here demonstrate, that ablation both, Hdac1 and Hdac2 is required to reduce tumor cell load.

Hdac1^{Δ/Δ};Hdac2^{Δ/Δ} induced a B cell developmental block in the BM that prevents Eμ-myc tumorigenesis

We previously showed, that *Hdac1^{Δ/Δ};Hdac2^{Δ/Δ}* prevents tumorigenesis by blocking Eμ-*myc* induced blast in the BM (Figure 3F-G). Here, in supplement, we analyzed the exact impact of *Hdac1^{Δ/Δ};Hdac2^{Δ/Δ}* not only in Eμ-*myc* mice, but also in non-Eμ-*myc* mice, to rule out the effect of the Eμ-*myc* tg. We first performed B220/IgM flow cytometry analysis in the BM, and observed that *Hdac1^{Δ/Δ};Hdac2^{Δ/Δ}* induced a B cell developmental block in both, Eμ-*myc* and non Eμ-*myc* tg mice (Suppl. Figure 11A). More precisely, CD19/CD25 flow cytometry revealed that this block occurred at PreBII (CD25⁺;CD19⁺) cell stage (Suppl. Figure 11B). We further analyzed SP and LN by B220/IgM flow cytometry and found that *Hdac1^{Δ/Δ};Hdac2^{Δ/Δ}* also prevented or massively reduced mature B cell populations (B220⁺;IgM⁺) in both, Eμ-*myc* mice, but also in non-Eμ-*myc* mice. Quantification of flow cytometry analysis revealed significant reduction of B cells and almost absence of PreBII cells in BM of Eμ-*myc* *Hdac1^{Δ/Δ};Hdac2^{Δ/Δ}* mice, but also in *Hdac1^{Δ/Δ};Hdac2^{Δ/Δ}* mice (Suppl. Figure 11E). Similarly, quantification SP and LN flow cytometry analysis revealed significant reduction and almost absence of mature B cell populations upon *Hdac1^{Δ/Δ};Hdac2^{Δ/Δ}* in both Eμ-*myc* and non Eμ-*myc* mice (Suppl. Figure 11E). Thus we conclude, that B cell specific double KO of Hdac1 and Hdac2 (*Hdac1^{Δ/Δ};Hdac2^{Δ/Δ}*) impairs B cell development in both, non-transgenic and in Eμ-*myc* tg mice. *Hdac1^{Δ/Δ};Hdac2^{Δ/Δ}* induces a B cell developmental block in the BM that prevents Eμ-*myc* tumorigenesis and colonization of SP and LN with mature B cells.

Rare Hdac1^{F/F};Hdac2^{F/F} Mb1-Cre tg; Eμ-myc animals are not KO for Hdac1 and Hdac2 and develop tumors

We observed that rare *Hdac1^{F/F};Hdac2^{F/F} Mb1-Cre tg; Eμ-myc* animals developed tumors. Histopathological analysis from H&E stained tumor sections revealed, a malignant phenotype (granulocytic leukemia) (Suppl. Figure 12A). The SP of these *Hdac1^{F/F};Hdac2^{F/F} Mb1-Cre tg; Eμ-myc* mice had red pulp expanded with neoplastic cells (different than *Hdac1^{+/+};Hdac2^{+/+} Eμ-myc* phenotype, Suppl. Figure 6). In the decalcified sternum of these mice normal BM was replaced by neoplastic cells and the liver was infiltrated with neoplastic cells (Suppl. Figure 12A). Since we demonstrated, that complete ablation of Hdac1 and Hdac2 prevents tumorigenesis (Figure 2 and Figure 3), we hypothesized, that in *Hdac1^{F/F};Hdac2^{F/F} Mb1-Cre tg; Eμ-myc* animal, Hdac1 and Hdac2 are not completely ablated. To test this hypothesis, we performed immunohistochemistry (IHC) analysis from serial splenic sections from *Hdac1^{F/F};Hdac2^{F/F} Mb1-cre tg Eμ-myc* tumors for c-Myc, Hdac1, and Hdac2. Interestingly, we found that these tumors expressed high c-Myc but also Hdac1 and Hdac2 (Suppl. Figure 12B). Interestingly, *Hdac1^{F/F};Hdac2^{F/F} Mb1-Cre tg; Eμ-myc* animals never had any tumors lacking both Hdac1 and Hdac2. Therefore, we speculate, that sporadic deletion due to inefficient cre expression or inefficient loxP recombination might underlie this phenotype. Taken together, our results indicates, that complete ablation of Hdac1 and Hdac2 is not compatible with development and progression of Eμ-myc tg B cells and consequently prevents tumorigenesis. In rare cases, Hdac1 and Hdac2 are not efficiently ablated in *Hdac1^{F/F};Hdac2^{F/F} Mb1-Cre tg; Eμ-myc* mice which then eventually develop tumors.

Rare Hdac1^{Δ/Δ};Hdac2^{Δ/Δ} animals developed interstitial pneumonia

We also observed that rare *Hdac1^{F/F};Hdac2^{F/F} Mbl-Cre tg* mice unexpectedly died. We investigated the reason of this death by extensive histopathological analysis. We stained several organs, including SP, LN, thymus, liver, heart, and lung with H&E. We did not detect any pathological sign in any organ, except for the lung. Histopathological analysis of lung samples from *Hdac1^{Δ/Δ};Hdac2^{Δ/Δ}* and control *Hdac1^{+/+};Hdac2^{+/+}* mice with and without *Eμ-myc tg*, revealed interstitial pneumonia (Suppl. Figure 13). Inflammation sites with infiltration of macrophages were clearly visible (Suppl. Figure 13A lower panels). We observed multifocal enlargement of alveolar septae due to infiltration of macrophages. Multifocally alveoli were filled with foamy exudate mixed with inflammatory cells, including macrophages, lymphocytes and neutrophils (Suppl. Figure 13A lower panels). We observed multifocal alveolar inflammatory exudate (foamy exudate) infiltrated with protein and liquid as well as massive infiltration of inflammatory cells including macrophages mainly (Suppl. Figure 13B). General staining for fungus with Grocott staining revealed fungal elements and abundant fungal cysts present within the alveolar foamy exudate (Suppl. Figure 13C). In summary, we observed, that rare *Hdac1^{Δ/Δ};Hdac2^{Δ/Δ}* mice suffer from interstitial pneumonia due to abundant presence of fungal elements.

In vivo conditional ablation of Hdac1 and Hdac2 using the CreER-LoxP system in Eμ-myc tumor cells

We showed, that Hdac1 and Hdac2 also have pro-oncogenic roles in tumor progression (Figure 4). In supplement, we show a schematic representation of the experimental workflow for the transplantation experiment (Suppl. Figure 14A). We performed conditional targeted deletion of

Hdac1 and *Hdac2* in E μ -*myc* tumor cells using the tamoxifen inducible CreER-LoxP system. To examine whether tamoxifen efficiently induced deletion of both, *Hdac1* and *Hdac2*, we performed PCR genotyping for *Hdac1* and *Hdac2* wild type (WT), floxed (FL) and knockout (KO) alleles. Interestingly, we observed, that recombination was not 100%, since *Hdac1* (and *Hdac2*) FL alleles did not disappear completely (Suppl. Figure 14B). Importantly, these findings are consistent with the data outlined above showing that conditional ablation of *Hdac1* and *Hdac2* in E μ -*myc* tumor cells only delays and do not completely prevent tumor appearance (Figure 4).

E μ -myc tg Hdac1^{A/A};Hdac2^{A/+} mice have less circulating leukemic cells but eventually develop HG-NHL

As previously shown, *Hdac1^{A/A};Hdac2^{A/+}* significantly delayed E μ -*myc* tumor development (Figure 2). We further investigated the impact of *Hdac1^{A/A};Hdac2^{A/+}* on E μ -*myc* induced splenomegaly. We therefore measured SP weights. However, no difference was observed on SP weight between E μ -*myc Hdac1^{A/A};Hdac2^{A/+}* and E μ -*myc Hdac1^{+/+};Hdac2^{+/+}* mice (Suppl. Figure 15A). We further determined the impact of *Hdac1^{A/A};Hdac2^{A/+}* on circulating PBL in E μ -*myc* mice, by analyzing the blood of lymphoma-free E μ -*myc* mice using an automated blood cell counter. We found, that *Hdac1^{A/A};Hdac2^{A/+}* significantly lowered PBL count in E μ -*myc* mice at 8 weeks (Figure 5C). We further examined the impact of *Hdac1^{A/A};Hdac2^{A/+}* on PBL at 4 weeks, and found a similar significant decrease in PBL count (Suppl. Figure 15B). Furthermore, we quantified white blood cells (WBC) counts and observed, that *Hdac1^{A/A};Hdac2^{A/+}* significantly reduced WBC numbers at 4 and 8 weeks (Suppl. Figure 15C). Hence, we conclude, that *Hdac1^{A/A};Hdac2^{A/+}* mice reduces leukemia in E μ -*myc* mice at 4 and 8 week of age. We next

performed histopathological analysis of E μ -myc *Hdac1^{Δ/Δ};Hdac2^{Δ/+}* mice, in order to determine which type of tumors these mice develop. We compared E μ -myc *Hdac1^{Δ/Δ};Hdac2^{Δ/+}* mice with lymphoma to *Hdac1^{+/+};Hdac2^{+/+}* control mice (Suppl. Figure 15D). All depicted peripheral organs, including SP, LN, liver, and thymus (Thy), were enlarged and had destroyed architecture due to diffuse infiltration by neoplastic lymphocytes. This state was pathologically diagnosed as HG-NHL characteristic for E μ -myc tg mice. Hence, as expected, *Hdac1^{Δ/Δ};Hdac2^{Δ/+}* E μ -myc mice develop the characteristic pathological state of E μ -myc mice. Taken together, our results demonstrate, that E μ -myc tg *Hdac1^{Δ/Δ};Hdac2^{Δ/+}* mice have less circulating leukemic cells but eventually develop HG-NHL.

Hdac1^{Δ/Δ};Hdac2^{Δ/+} impacts on E μ -myc proliferation at the G1 phase of the cell cycle

We previously showed, that *Hdac1^{Δ/Δ};Hdac2^{Δ/+}* decreased proliferation of E μ -myc B cells (Figure 7). We performed *in vivo* BrdU assays and found, that E μ -myc *Hdac1^{Δ/Δ};Hdac2^{Δ/+}* B cells had massively less incorporation of BrdU compared to E μ -myc *Hdac1^{+/+};Hdac2^{+/+}* B cells (Suppl. Figure 16A). We next investigated which phases of the cell cycle are affected in E μ -myc *Hdac1^{Δ/Δ};Hdac2^{Δ/+}* B cells. Our preliminary data show, that *Hdac1^{Δ/Δ};Hdac2^{Δ/+}* impairs cell cycle at G1 phase (Suppl. Figure 16B).

2.2. Supplementary figure legends

Suppl. Figure 4: Old *Hdac1^{Δ/Δ};Hdac2^{+/+}* mice do not develop spontaneous tumors

(A) SP and LN organ weight analysis in old *Hdac1^{Δ/Δ};Hdac2^{+/+}* mice. Dot plot showing relative organ weights (in % of body weight) from 20-week-old *Hdac1^{+/+};Hdac2^{+/+}* and *Hdac1^{Δ/Δ};Hdac2^{+/+}* mice (n=4) and Eμ-*myc* mice with or without tumors as control (n=1). Horizontal bars represent median. Statistical analysis with Wilcoxon Signed-Rank Test. N.S. for not statistically significant. (B) SP, LN, and thymus (Thy) weight analysis in 70-week-old *Hdac1^{Δ/Δ};Hdac2^{+/+}* mice. Bar plots show relative organ weights (in % of body weight) from 70-week-old *Hdac1^{+/+};Hdac2^{+/+}* (n=2), *Hdac1^{Δ/Δ};Hdac2^{+/+}* (n=3) and control Eμ-*myc* *Hdac1^{+/+};Hdac2^{+/+}* (n=1) mice. (C) Quantification of flow cytometry analysis from 20-week-old mice with indicated genotypes. The bar plots represents the average percentage of large B220⁺ cell. SEM are indicated for the comparison of *Hdac1^{+/+};Hdac2^{+/+}*, and *Hdac1^{Δ/Δ};Hdac2^{+/+}* mice (n=4). The statistical analysis was performed with the Student unpaired 2-tailed *t* test. N.S. for not statistically significant.

Suppl. Figure 5: *Hdac1* and *Hdac2* have no tumor suppressor function in B cells

(A) *Jdp2* expression is not affected in B cell specific *Hdac1^{Δ/Δ};Hdac2^{Δ/+}*. *Jdp2* gene transcript abundance was measured by quantitative real-time PCR (RT-qPCR) analysis in CD19⁺ MACS sorted B lymphocytes from 8-week-old *Hdac1^{+/+};Hdac2^{+/+}* and *Hdac1^{Δ/Δ};Hdac2^{Δ/+}* mice. Data were normalized to *Gapdh* and log 2 expression values of *Jdp2* mRNA are shown. Data are representative of a single experiment using 3 individuals of each genotype (preliminary results). The statistical analysis was performed with the Student unpaired 2-tailed *t* test. N.S. for not statistically significant. (B) p53 tumor suppressor pathway and the impact of *Hdac1* and *Hdac2*

Results

on p53 regulation in T cells based on previous study by Heideman et al., 2013, showing that Hdac1 and Hdac2 regulate p53-dependent barrier to constrain *myc*-overexpressing thymocytes from progressing into lymphomas by regulating Myc-collaborating genes like Jdp2. (C) *Hdac1^{Δ/Δ};Hdac2^{Δ/+}* Eμ-*myc* tumors have high p53 staining, indicating for stabilized/mutant p53. Representative pictures of immunohistochemistry (IHC) analysis of p53 expression in *Hdac1^{+/+};Hdac2^{+/+}* Eμ-*myc* and *Hdac1^{Δ/Δ};Hdac2^{Δ/+}* Eμ-*myc* tumors from spleen (SP). Healthy tissue from a *Hdac1^{+/+};Hdac2^{+/+}* mouse is shown as control with and without 1st Ab against p53 (SP1 and SP2 respectively). (D) Incidence of p53 staining in *Hdac1^{Δ/Δ};Hdac2^{Δ/+}* Eμ-*myc* tumors and control *Hdac1^{+/+};Hdac2^{+/+}* Eμ-*myc* tumors is comparable. Summary of p53 staining intensity of Figure (C). High (++) and medium (+) staining of p53 is present in all samples (n=7).

Suppl. Figure 6: Development of pathologic diseased state in Eμ-*myc* tg mice

(A) Pathological analysis: representative organs from *Hdac1^{+/+};Hdac2^{+/+}* and Eμ-*myc* *Hdac1^{+/+};Hdac2^{+/+}* mice (H&E staining). Eμ-*myc* mice have marked enlarged spleen (S), thymus (T), lymph nodes (LN) (mesenteric) due to infiltration of neoplastic cells. The form and architecture of these organs is altered. Shown are transversal cut of organs at 3X magnification. (B) Pathological analysis of Eμ-*myc* mice. H&E-stained sections illustrating infiltration of tumor cells into the peripheral organs of the Eμ-*myc* mice indicative of disseminated disease. Depicted are representative sections taken from a terminally ill Eμ-*myc* *Hdac1^{+/+};Hdac2^{+/+}* animal and control *Hdac1^{+/+};Hdac2^{+/+}* mice. Spleen and mandibular LN of Eμ-*myc* *Hdac1^{+/+};Hdac2^{+/+}* mice are enlarged and have destroyed architecture due to diffuse infiltration by neoplastic lymphocytes (tumor cells). White pulp (W), red pulp (R). These mice also have neoplastic cell infiltration into: the liver, the myocardium (arrow) of the heart, the submucosa of the urinary

bladder, the pelvis of the kidney, all layers of the small intestine, the duodenum (mucosa, submucosa, muscular layer and serosa), as well as the stomach mucosa (arrow). Epithelial cell layer (mucosa) (E), and muscle layer (M). Infiltration of tumor cells are indicated (T). Images were taken and processed at Novartis NIBR. Scale bar are indicated.

Suppl. Figure 7: Eμ-myc mice have a trend to slightly increased Hdac1 and Hdac2 expression levels

(A) Eμ-myc mice have a trend to slightly increased *Hdac1* and *Hdac2* expression levels in the cells of most B cell developmental stages. B lymphocytes from isolated from 8-week-old WT (n=2) and Eμ-myc tg (n=4) mice were sorted by flow cytometry for indicated B cell developmental stages and quantitative real-time PCR (RT-qPCR) was performed for *Hdac1* and *Hdac2*. Data represents means ± SEM.

Suppl. Figure 8: Loss of both, Hdac1 and Hdac2 (Hdac1^{Δ/Δ};Hdac2^{Δ/Δ}) reduces leukemia in Eμ-myc mice

Mice were bled at 4 and 10 week of age and blood was analyzed in an automated blood analyzer, (Sysmex XT-2000). (A) Representative plot of the manual gating for peripheral blood lymphocytes (PBL) used for Sysmex blood analysis. (B) *Hdac1^{Δ/Δ};Hdac2^{Δ/Δ}* Eμ-myc mice had significantly lower PBL counts at 4 and 10 weeks than control *Hdac1^{+/+};Hdac2^{+/+}* Eμ-myc mice. *Hdac1^{Δ/Δ};Hdac2^{+/+}* mice had reduced PBL only at 4 but not at 10 weeks. Shown are detailed analysis of different Hdac1 and/or Hdac2 KO animals with or without Eμ-myc tg at 4 and 10, weeks (n≥10). Frequency (%) of PBL of indicated. p-value calculated with the Wilcoxon Signed-

Rank Test. Significant differences in means is indicated, ** $p < 0.01$; N.S. for not statistically significant.

Suppl. Figure 9: Only ablation of both, but not single Hdac1 and Hdac2, prevents B cell blast in BM of E μ -myc tg mice

Immunofluorescence staining with B cell surface marker-specific monoclonal antibodies (B220, IgM, CD19 and CD25) followed by flow cytometry analysis was performed on BM. All experiments were performed with 8-week-old mice and from lymphoma-free E μ -myc mice, unless otherwise indicated. Mice genotypes are indicated. **(A-B)** Representative flow cytometry dot plots from BM lymphocytes derived from mice with indicated genotypes and gated on total lymphocytes for B cells B220/IgM **(A)** and PreBII lymphocytes subsets (B220⁺ lymphocytes gated for CD19⁺ and CD25⁺) **(B)**. BM cells from E μ -myc mice with lymphadenopathy that had reached endpoint criteria were assessed for comparison (indicated by asterisk) (pathological findings: HG-NHL). Gated regions in dot plots indicate the B cell subsets of interest with frequency in percent. **(C)** Quantification of B lymphocytes (B220⁺) and **(D)** PreBII (B220⁺;CD19⁺; CD25⁺) subsets (figure A and B, 4 to 6 mice of each genotype). The graph represents the average percentage of with SEM. The statistical analysis was performed with the Student unpaired 2-tailed t test. Significant differences in means between genotypes are indicated, ** $p < 0.01$. N.S. for not statistically significant.

Suppl. Figure 10: Ablation both, Hdac1 and Hdac2 (Hdac1 Δ/Δ ;Hdac2 Δ/Δ) is required to reduce tumor cell load

Experiments were performed in 8-week-old pre-lymphoma mice (unless mentioned otherwise).

(A) Representative flow cytometry histograms showing the large lymphocyte subset in BM of

Results

mice with indicated genotypes. Asterisks indicates end stage animals. **(B)** Analysis of B220^{low} cells population in E μ -myc *Hdac1*^{+/+};*Hdac2*^{+/+} mice compared to wild type *Hdac1*^{+/+};*Hdac2*^{+/+} control animals. Representative B220 and IgM immunophenotyping flow cytometry plots of lymphomas arising in SP, LN as well as BM and blood (BL) are depicted. **(C)** Quantification of the proportion of B220^{low} flow cytometry analysis in the indicated organs (represented in D). Differences between all E μ -myc tg mice with indicated genotypes were not statistically significant (N.S.). The graph represents the average percentage of B220^{low} cells with SEM (n=4-6 mice per genotype). The statistical analysis was performed with the Student unpaired 2-tailed *t* test. Significant differences in means between genotypes are indicated, **p* < 0.05; **, *P* < 0.01. **(D)** Analysis of B220^{low} cells population in E μ -myc mice lacking Hdac1 (*Hdac1*^{Δ/Δ};*Hdac2*^{+/+}), Hdac2 (*Hdac1*^{+/+};*Hdac2*^{Δ/Δ}) or both enzymes (*Hdac1*^{Δ/Δ};*Hdac2*^{Δ/Δ}) and control (*Hdac1*^{+/+};*Hdac2*^{+/+}) mice. Representative flow cytometry dot plots of B220/IgM staining previously gated on total lymphocytes derived from BM, SP and LN and gated for B220^{low} and B220^{high} populations.

Suppl. Figure 11: Hdac1^{Δ/Δ};*Hdac2*^{Δ/Δ} induces a B cell developmental block in the bone marrow that prevents E μ -myc tumorigenesis in SP and LNs

B cell specific double KO of Hdac1 and Hdac2 (*Hdac1*^{Δ/Δ};*Hdac2*^{Δ/Δ}) impairs B cell development in both, non-transgenic and in E μ -myc tg mice. All experiments were performed in 8-week-old lymphoma-free mice from indicated genotypes. BM, SP and LN cells were isolated and subjected to immunofluorescence staining with B cell surface marker-specific monoclonal antibodies (including B220, IgM, CD19, and CD25) followed by flow cytometry analysis. Representative BM flow cytometry dot pots with B220/IgM staining **(A)** and CD19/CD25

staining (B). Representative flow cytometry dot plots from SP cells (C) and LN cells (D) showing B220/IgM staining characteristic for B cell. All flow cytometry plots are representative of 3 independent experiments. (E) Quantification of flow cytometry analysis (A-D) (n=4 mice of each genotype). The graph represents the average percentage of B220⁺ B lymphocytes and percentage of PreBII cell subsets (B220⁺;CD19⁺; CD25⁺) with SEM. All the statistical analysis were performed with the Student unpaired 2-tailed *t* test. Significant differences in means between genotypes are indicated, **p* < 0.05; **, *P* < 0.01. N.S. for not statistically significant.

Suppl. Figure 12: Rare Hdac1^{F/F};Hdac2^{F/F} Mb1-Cre tg; Eμ-myc animals are not KO for Hdac1 and Hdac2 and develop tumors

(A) Histopathological analysis revealed few *Hdac1^{F/F};Hdac2^{F/F} Mb1-Cre tg; Eμ-myc* animal developed a malignant phenotype (granulocytic leukemia). SP, BM, and liver were stained with H&E. *Hdac1^{F/F};Hdac2^{F/F} Mb1-Cre tg; Eμ-myc* SP have red pulp expanded with neoplastic cells. In the decalcified sternum of these mice the normal BM is replaced by neoplastic cells. Tumor (T), RBC (red blood cells), B (bone). Infiltration of neoplastic cells into the liver (arrow). (B) Rare *Hdac1^{F/F};Hdac2^{F/F} Mb1-cre tg Eμ-myc tg* animals develop tumors but still express *Hdac1* and *Hdac2*. Immunohistochemistry (IHC) from serial splenic sections from *Hdac1* and/or *Hdac2* KO animals with *Eμ-myc tg* stained for c-Myc, *Hdac1*, and *Hdac2*.

Suppl. Figure 13: Rare Hdac1^{Δ/Δ};Hdac2^{Δ/Δ} animals developed interstitial pneumonia

Rare *Hdac1^{Δ/Δ};Hdac2^{Δ/Δ}* mice suffer from interstitial pneumonia due to abundant presence of fungal elements. Histopathological analysis of lung samples from *Hdac1^{Δ/Δ};Hdac2^{Δ/Δ}* and control *Hdac1^{+/+};Hdac2^{+/+}* mice with and without *Eμ-myc tg*. (A) H&E staining revealed interstitial

pneumonia in *Hdac1^{Δ/Δ};Hdac2^{Δ/Δ}* mice. Arrow indicates inflammation site with infiltration of macrophages (1x magnification). At 10x magnification, multifocal enlargement of alveolar septae due to infiltration of macrophages. Multifocally alveoli are filled with foamy exudate mixed with inflammatory cells (macrophages, lymphocytes and neutrophils) (arrow shows foamy exudate). **(B)** 20x magnification clearly shows multifocal alveolar inflammatory exudate (foamy exudate) infiltrated with protein and liquid (arrow) as well as massive infiltration of inflammatory cells including macrophages mainly (asterisk). **(C)** General staining for fungus with Grocott staining at 10X, 40X, and 60X magnification. Grocott staining shows fungal elements (black structures) and abundant fungal cysts present within the alveolar foamy exudate. Arrow indicates exudate, asterisk indicates macrophages. Images were taken and processed at Novartis NIBR. Scale bar are indicated.

Suppl. Figure 14: In vivo conditional ablation of Hdac1 and Hdac2 using the CreER-LoxP system in Eμ-myc tumor cells

(A) Schematic representation of the experimental workflow for the transplantation experiment. (1) Syngeneic recipient mice that were previously sub lethally gamma-irradiated (350 cGy of whole-body γ -irradiation) were (2) injected with lymph node derived Eμ-*myc* tumor cells isolated from (*Hdac1^{F/F};Hdac2^{F/F}*, *Actin-cre* tg, Eμ-*myc* tg) mice after development of overt malignancy (represented by red filled circles). (3) Conditional KO was induced in one group of mice by intraperitoneal (IP) injection of 4-OHT (tamoxifen). Control mice were injected with vehicle. (4) Mice were monitored for tumor onset and sacrificed when they reached termination criteria (see Material and Methods). Tumor weight and flow cytometry analysis were performed. **(B)** Conditional KO of Hdac1 and Hdac2 using the CreER-LoxP system. Recombination was not

100%, since *Hdac1* (and *Hdac2*) floxed alleles did not disappear completely. PCR genotyping for *Hdac1* and *Hdac2* wild type (WT), floxed (FL) and knockout (KO) alleles are indicated to the right. Allele specification and molecular weights in base pairs (bp) of individual fragments are to the left of each gel.

Suppl. Figure 15: Eμ-myc tg Hdac1^{Δ/Δ};Hdac2^{Δ/+} mice have less circulating leukemic cells but eventually develop HG-NHL

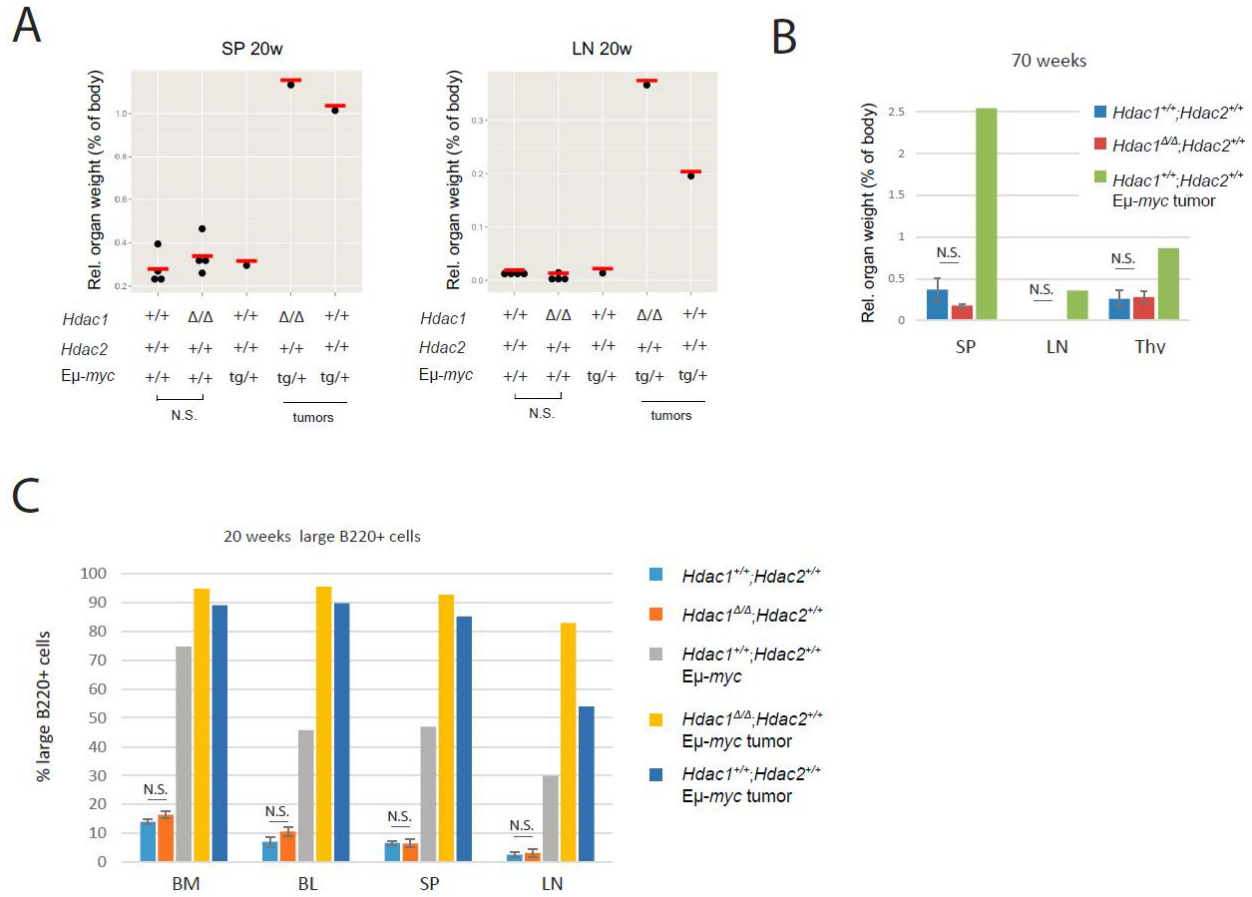
(A) *Hdac1^{Δ/Δ};Hdac2^{Δ/+}* has no significant impact on spleen weight (n=10). Comparison of relative spleen weights (in % of body weight) of 8-week-old mice with indicated genotypes. (B-C) *Hdac1^{Δ/Δ};Hdac2^{Δ/+}* mice reduces leukemia in Eμ-*myc* mice. Mice were bled at 4 and 8 week of age and blood was analyzed in an automated blood analyzer (Sysmex XT-2000). Shown are dot plots of number of total PBL count (B) and white blood cells (WBC) (C) from indicated genotypes (n=10). p-value calculated with the Wilcoxon Signed-Rank Test. **, $P < 0.01$. N.S. for not statistically significant. (D) Histopathological analysis of Eμ-*myc Hdac1^{Δ/Δ};Hdac2^{Δ/+}* mice with lymphoma compared to *Hdac1^{+/+};Hdac2^{+/+}* control mice. Eμ-*myc Hdac1^{Δ/Δ};Hdac2^{Δ/+}* mice develop HG-NHL. Representative sections of spleen, lymph nodes, liver, and thymus by H&E staining. All depicted peripheral organs are enlarged and have destroyed architecture due to diffuse infiltration by neoplastic lymphocytes. Original magnification of 4X and 20X are indicated (Nikon Eclipse E600).

Suppl. Figure 16: Hdac1^{Δ/Δ};Hdac2^{Δ/+} impacts on Eμ-myc proliferation at the G1 phase of the cell cycle (Preliminary data)

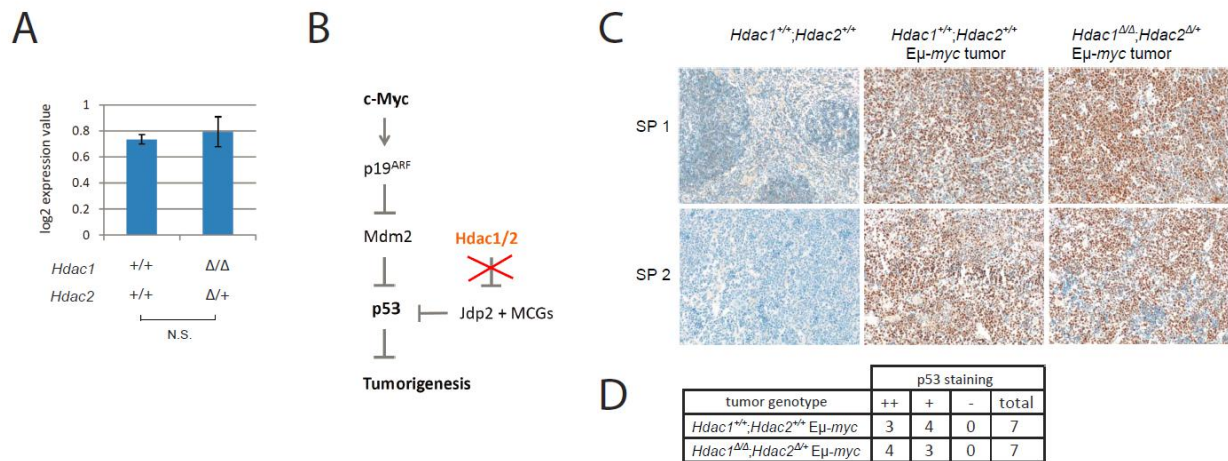
Experiments were performed in 8-week-old mice. Proliferation is decreased in *Hdac1^{Δ/Δ};Hdac2^{Δ/+}* Eμ-myc tg B cells compared to control *Hdac1^{+/+};Hdac2^{+/+}* Eμ-myc tg B cells. Cell cycle analysis, mice of indicated genotype were intraperitoneally injected with 1.5mg of BrdU. 24h after BrdU injection mice were sacrificed and BM cells were isolated and stained with anti-BrdU antibody for flow cytometry analysis. **(A)** Representative flow cytometry histograms showing count (%) of BrdU incorporation representing cells in S-phase from indicated genotypes. **(B)** Cell cycle analysis (n=3). Mean and standard error of BrdU-positive cells is shown. The percentages of cells in the G₀/G₁-, S-, and G₂/M-phase, obtained by manual gating, are indicated in the plots.

2.3. Supplementary figures

Suppl. Figure 4

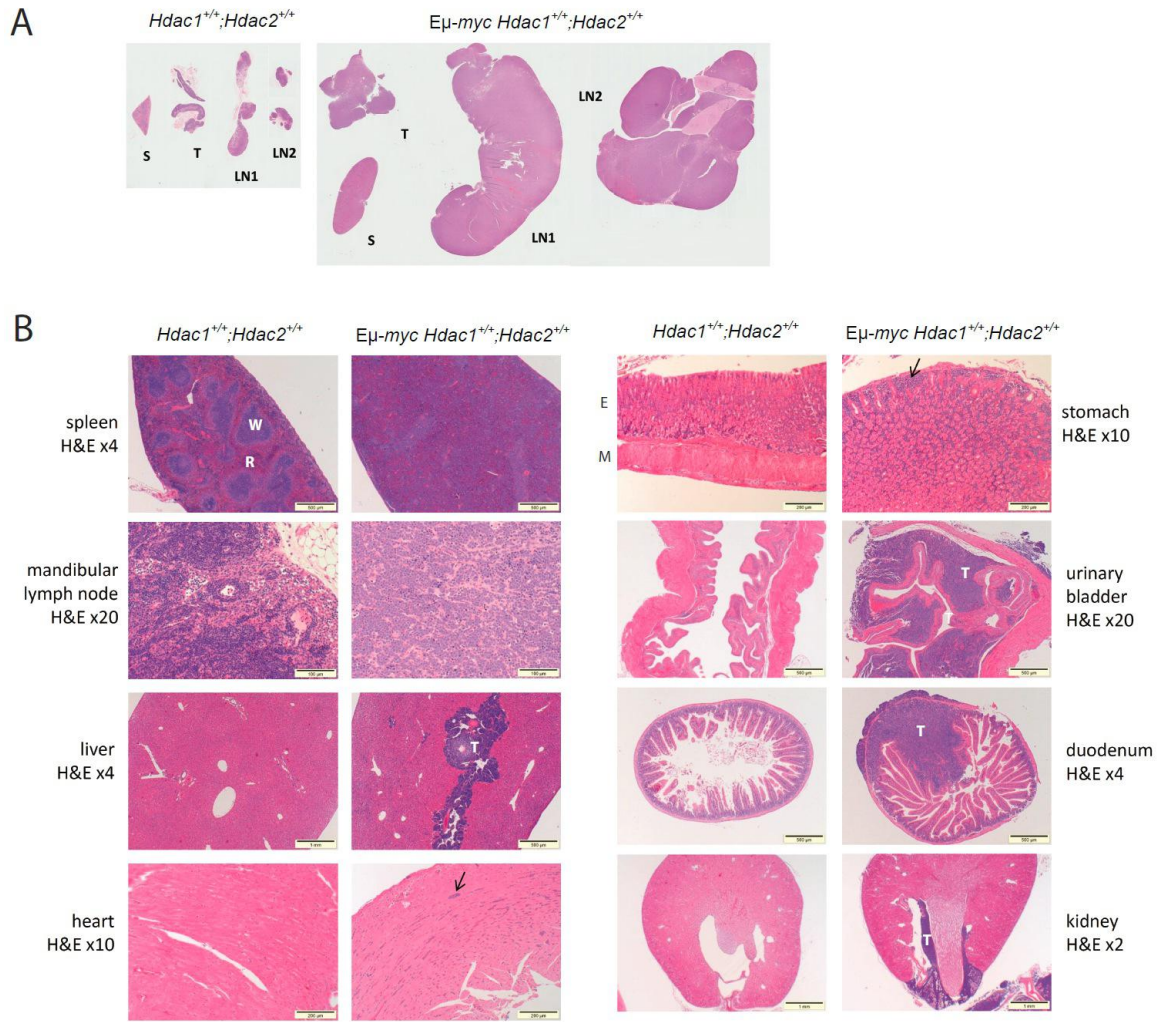


Suppl. Figure 5

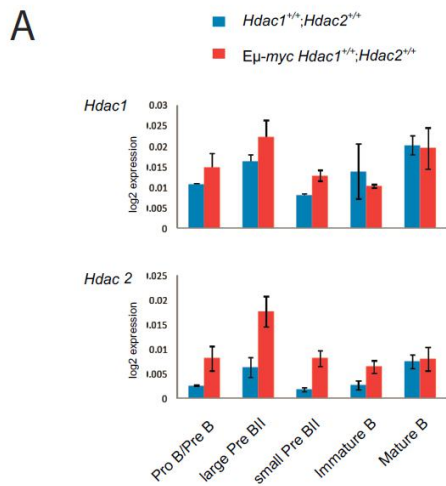


Results

Suppl. Figure 6

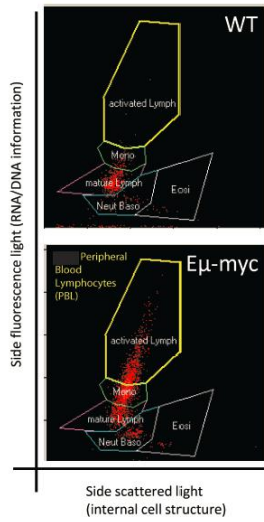


Suppl. Figure 7

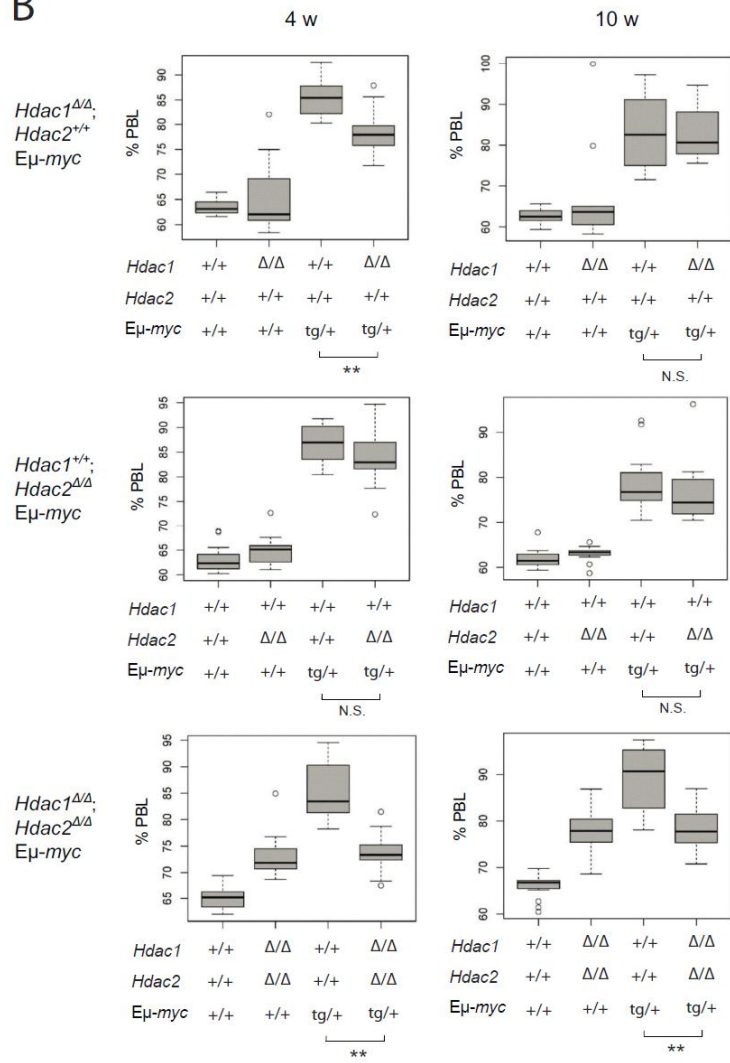


Suppl. Figure 8

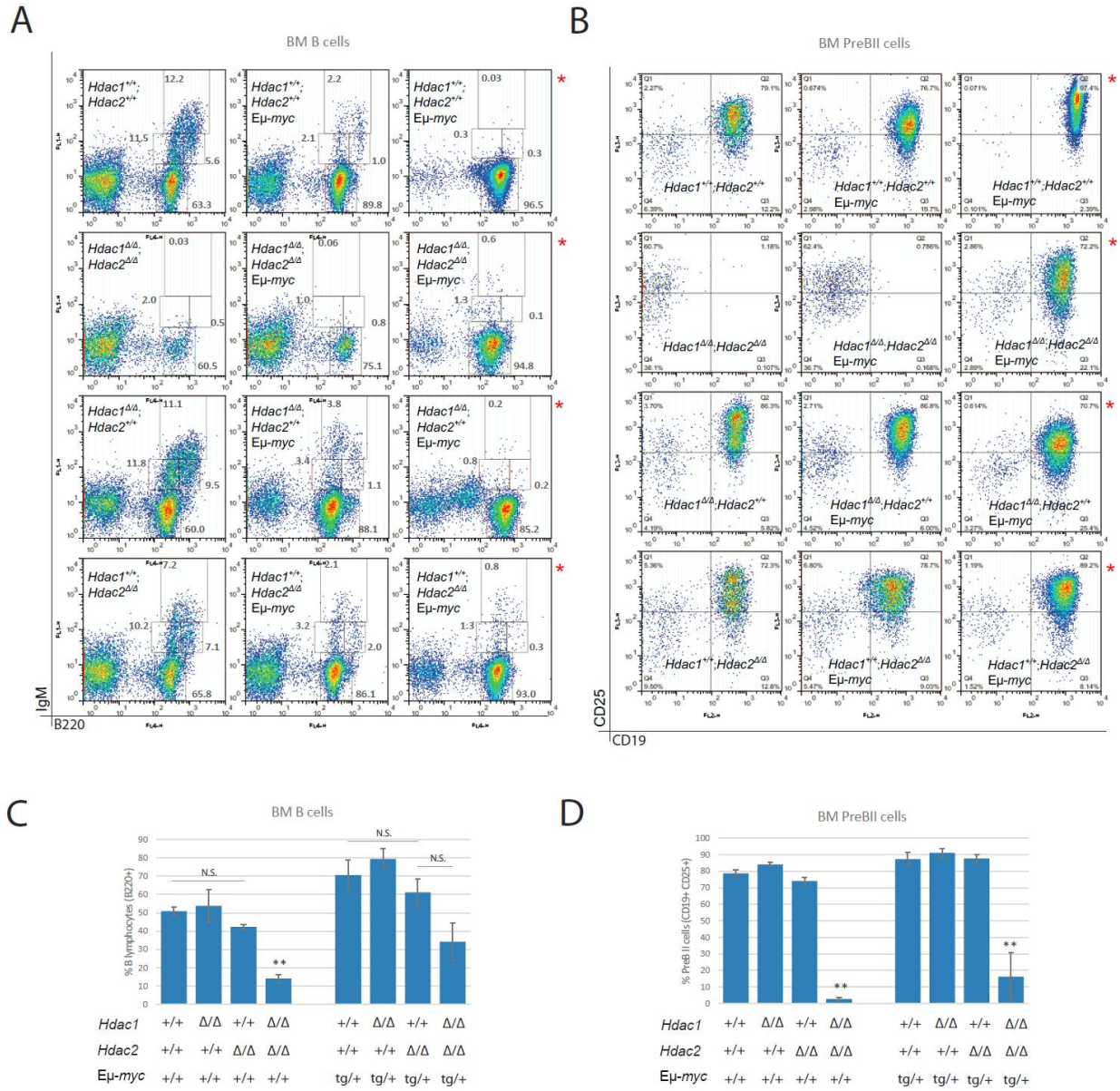
A



B

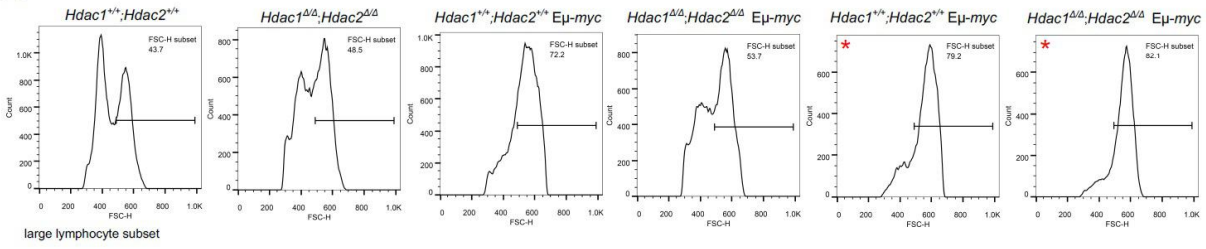


Suppl. Figure 9

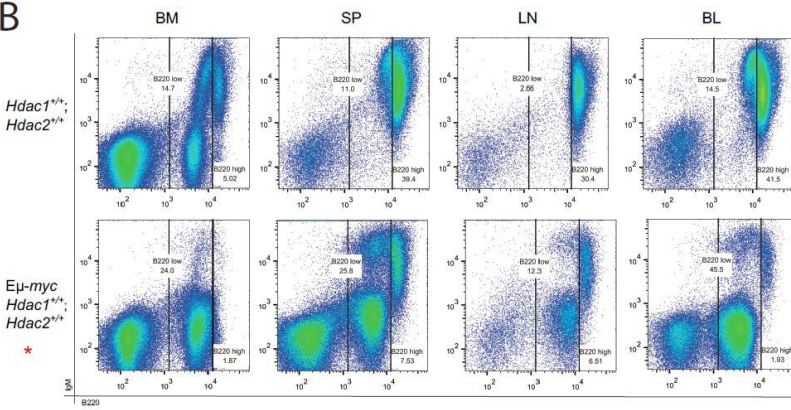


Suppl. Figure 10

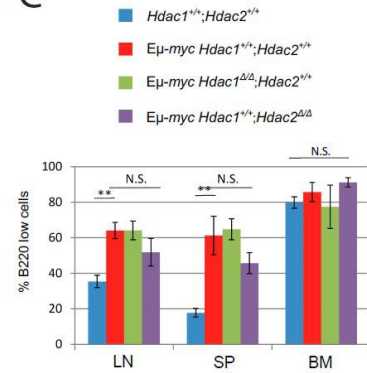
A



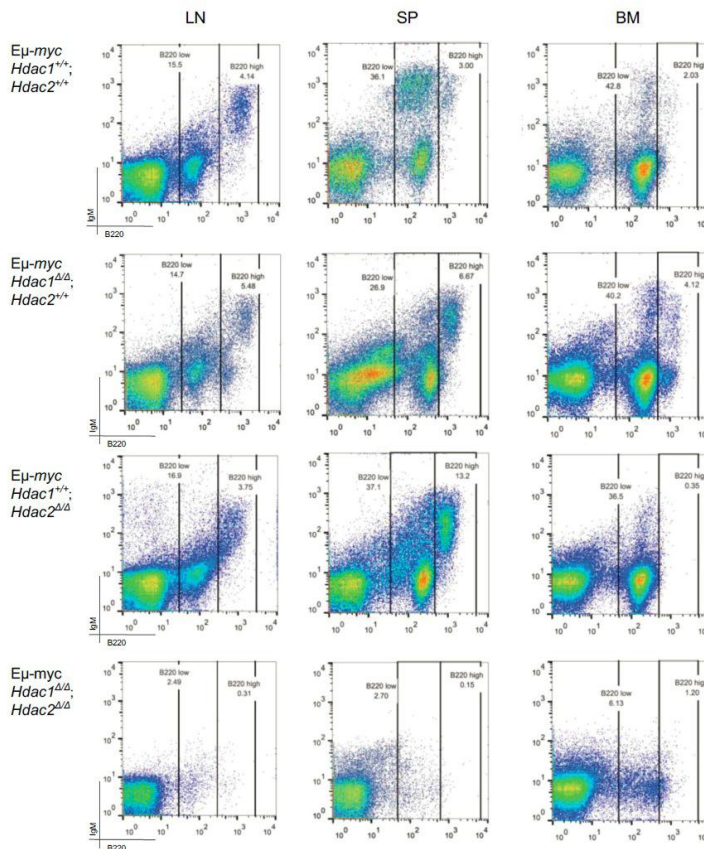
B



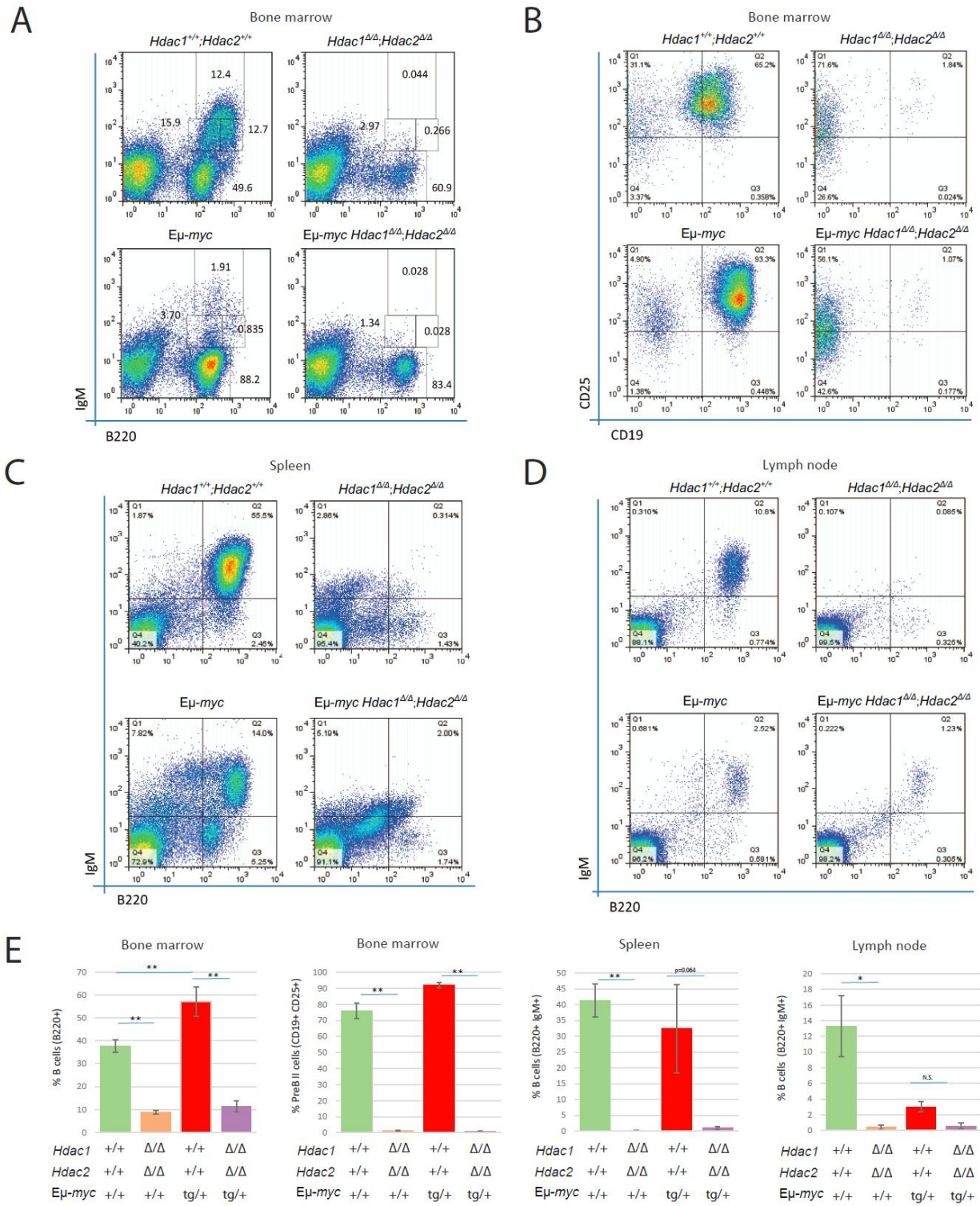
C



D

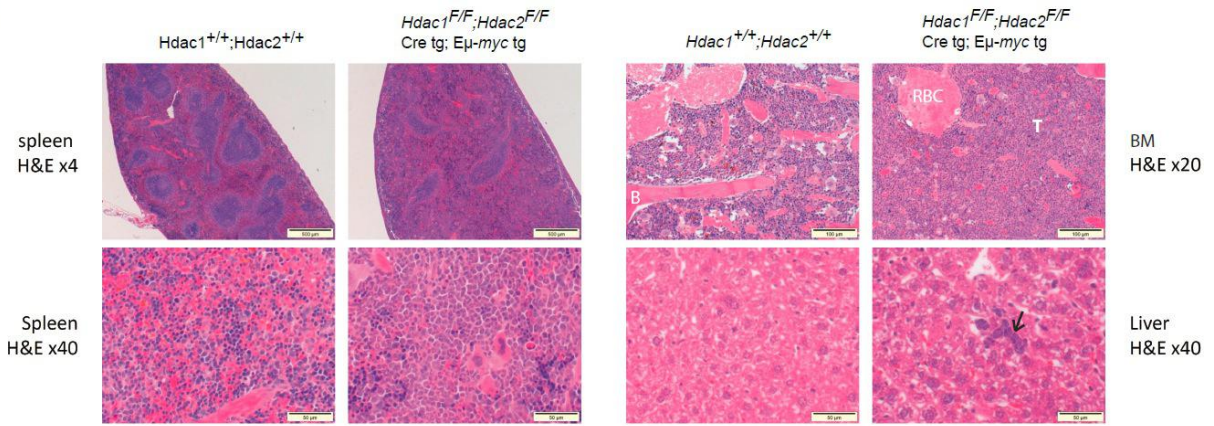


Suppl. Figure 11

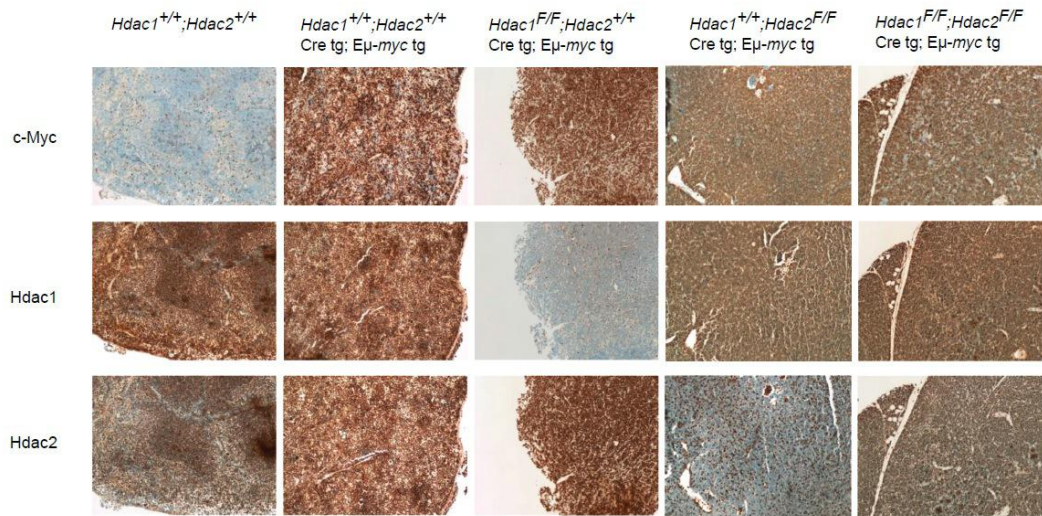


Suppl. Figure 12

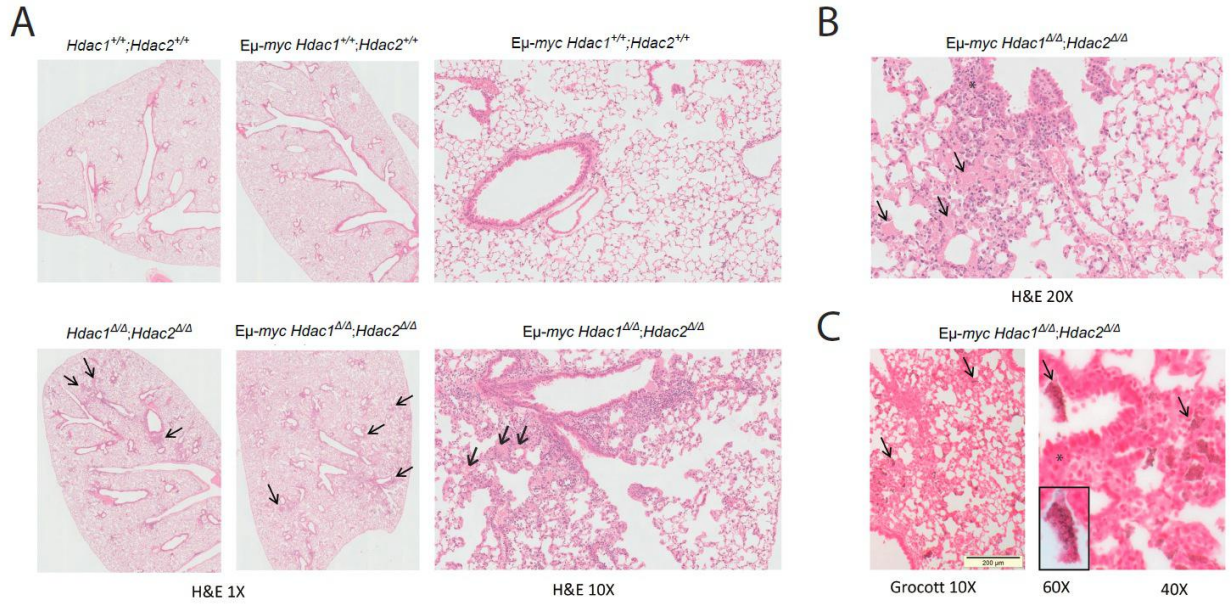
A



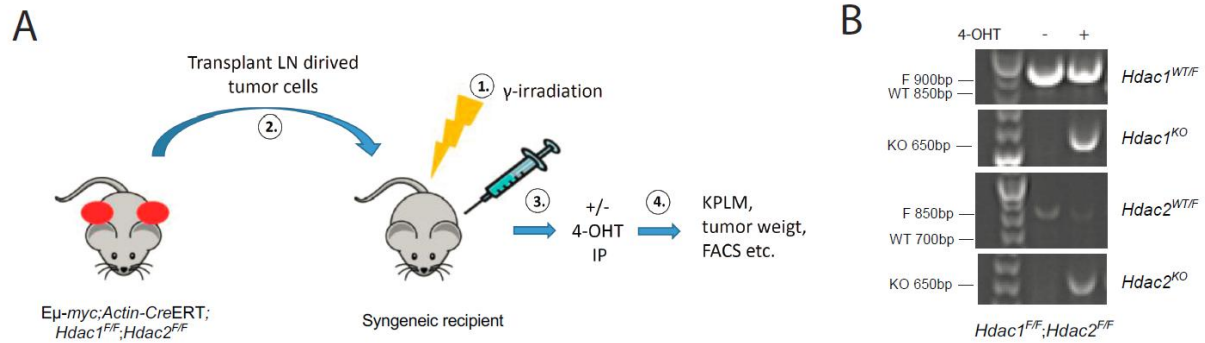
B



Suppl. Figure 13

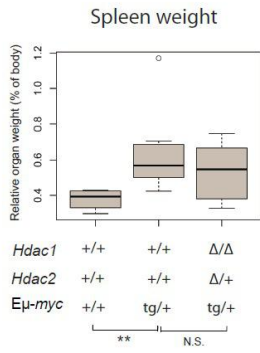


Suppl. Figure 14

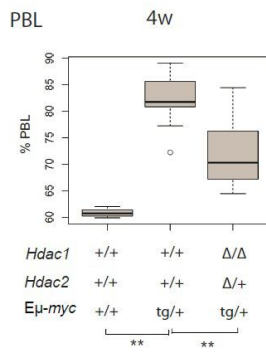


Suppl. Figure 15

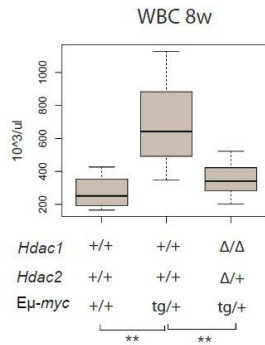
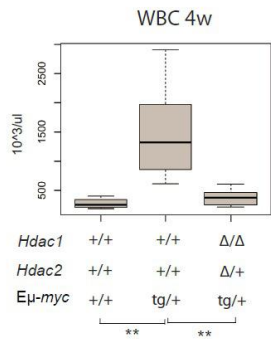
A



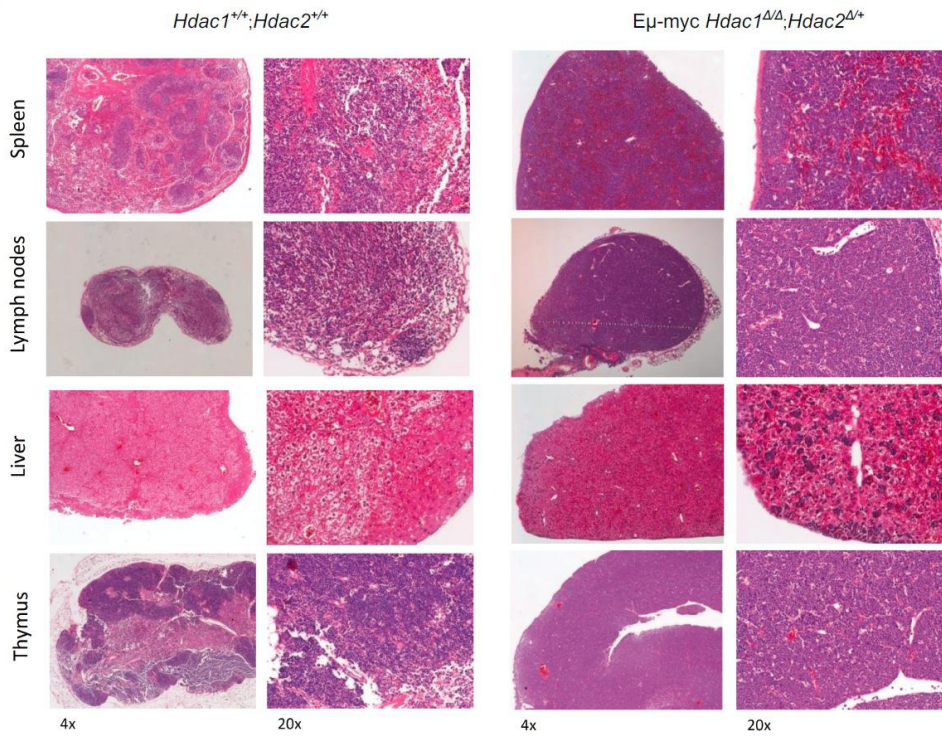
B



C

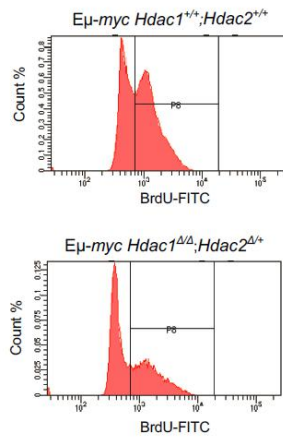


D

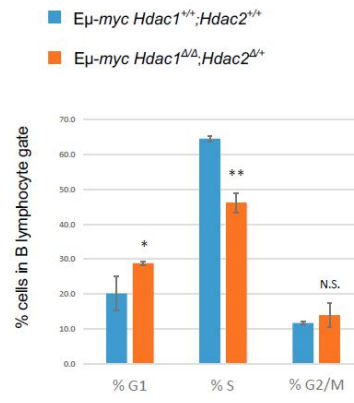


Suppl. Figure 16

A



B



Results Part 3

Results Part 3: Analysis of the functional role of Hdac1 and Hdac2 in B cell development

3.1. Results

Analysis of Hdac1^{Δ/Δ};Hdac2^{Δ/+} mice

Previous studies described that acetylation on histone lysine residues is positively correlated with gene transcription, and that histone H3 and H4 acetylation is enriched in actively transcribed euchromatin regions (Kurdistani et al., 2004; Vogelauer et al., 2000). Importantly, it was reported that Hdac1, but not Hdac2, deacetylates lysine residues on histone H3 and H4 (Dovey et al., 2010; Yamaguchi et al., 2010). This prompted us to examine the global acetylation levels on histones H3 (H3ac) and H4 (H4ac) in *Hdac1^{Δ/Δ};Hdac2^{Δ/+}* B cells. We first confirmed the genotypes by PCR (Suppl. Figure 1A). We then performed western blot analysis from *Hdac1^{Δ/Δ};Hdac2^{Δ/+}* and control *Hdac1^{+/+};Hdac2^{+/+}* splenic B cells (B220⁺; CD19⁺; CD3⁻) sorted by flow cytometry. Extracts were probed with antibodies recognizing Hdac1, Hdac2, H3Ac or H4Ac and against H3 and H4 to verify for equal protein loading. Consistent with previous reports, we observed a slight increase in global H3Ac levels, and an increase in global H4Ac levels in *Hdac1^{Δ/Δ};Hdac2^{Δ/+}* cells compared to control *Hdac1^{+/+};Hdac2^{+/+}* cells (Suppl. Figure 1B). Thus, we conclude that in our *Hdac1^{Δ/Δ};Hdac2^{Δ/+}* B cells Hdac1 and/or Hdac2 deacetylate histone H3 and H4 as expected.

Dissecting the impact of Hdac1^{Δ/Δ};Hdac2^{Δ/+} on B cell development

We previously showed that B cell development is normal in *Hdac1^{Δ/+};Hdac2^{Δ/Δ}* mice but severely impacted in *Hdac1^{Δ/Δ};Hdac2^{Δ/+}* mice and completely blocked in *Hdac1^{Δ/Δ};Hdac2^{Δ/Δ}*

mice (Pillonel *et al.*, Figure 6A). Furthermore, we observed, that $Hdac1^{A/A};Hdac2^{A/+}$, but not $Hdac1^{A/+};Hdac2^{A/A}$ mice, have higher number of pre-BI cells and a decrease in pre-BII cell numbers compared to control $Hdac1^{+/+};Hdac2^{+/+}$ mice (Pillonel *et al.*, Figure 6B). Thus, we concluded, that one allele of *Hdac1* but not *Hdac2* is sufficient to complete B cell development (Pillonel *et al.*, Figure 6). We confirmed these previous findings by repeating flow cytometry analysis with $Hdac1^{A/A};Hdac2^{A/+}$ and $Hdac1^{A/+};Hdac2^{A/A}$ mice to further determine the exact impact of Hdac1 and Hdac2 ablation on the different stages of B cell development. We confirmed that $Hdac1^{A/A};Hdac2^{+/A}$ is not sufficient to complete B cell development (Suppl. Figure 2A). We observed a significant decrease in B cell number and a massive decrease in PreBII cell number (Suppl. Figure 2B) as shown previously by Pillonel *et al.* In addition we observed a massive loss in immature B cell number (Suppl. Figure 2B). Interestingly, we also observed that $Hdac1^{A/A};Hdac2^{+/A}$ mice have more PreBI cells with high c-kit staining (Suppl. Figure 2B). This suggests that $Hdac1^{A/A};Hdac2^{+/A}$ PreBI cells remain in a less differentiated stage. Another interesting observation, was that $Hdac1^{A/A};Hdac2^{+/A}$ mice have normal amount of mature B cells in the spleen (Suppl. Figure 2B). We also observed that $Hdac1^{+/A};Hdac2^{A/A}$ mice have a normal B cell development (Suppl. Figure 2C), as previously shown by Pillonel *et al.* (Suppl. Figure 2C). These observations confirm previous observations (Pillonel *et al.*, Figure 6), that $Hdac1^{A/A};Hdac2^{+/A}$, but not $Hdac1^{+/A};Hdac2^{A/A}$ impact on B cell development. We further show that the few PreBII cells left in $Hdac1^{+/A};Hdac2^{A/A}$ mice are sufficient to eventually fill up the pool of mature B cells in the secondary lymphoid organs including the SP (Suppl. Figure 2B).

Proliferation is increased in $Hdac1^{A/A};Hdac2^{A/+}$ Pre-BI cells and decreased in Pre-BII cells

Yamaguchi et al., previously showed that ablation of both, Hdac1 and Hdac2 ($Hdac1^{A/A};Hdac2^{A/A}$) induces cells cycle arrest and apoptosis in B cells (Yamaguchi et al., 2010). These finding prompted us to test proliferation and apoptosis in $Hdac1^{A/A};Hdac2^{A/+}$ cells. We observed that $Hdac1^{A/A};Hdac2^{A/+}$ induces a massive decrease in PreBII cell number (Suppl. Figure 2B). Hence, we first investigated the impact of $Hdac1^{A/A};Hdac2^{A/+}$ on proliferation in PreBII and the preceding PreBI cell stage. To test this, we performed *in vivo* BrdU labelling of proliferating cells. We found that proliferation was slightly increased in $Hdac1^{A/A};Hdac2^{A/+}$ Pre-BI cells and decreased in Pre-BII cells (Figure 1A). Quantification of B220⁺;BrdU⁺ cells revealed a significant difference (Figure 1B). We measured the percentages of cells in the G₀/G₁-, S-, and G₂/M-phase of the cell cycle. Interestingly, we found that $Hdac1^{A/A};Hdac2^{A/+}$ PreBII cells are blocked at G₀/G₁-phase (Figure 1A). Thus, we conclude that $Hdac1^{A/A};Hdac2^{A/+}$ positively impacts on proliferation of Pre-BI and negatively impacts on proliferation of Pre-BII cells.

$Hdac1^{A/A};Hdac2^{A/+}$ Pre-BI cells have reduced apoptosis

Yamaguchi et al. reported that $Hdac1^{A/A};Hdac2^{A/A}$ PreBII cells were arrested in the cell cycle and eventually underwent apoptosis (Yamaguchi et al., 2010). The foregoing indicates that proliferation is decreased in Pre-BII cells (Figure 1). We next measured whether apoptosis is also affected in $Hdac1^{A/A};Hdac2^{A/+}$ PreBII cells. Therefore, we investigated whether apoptosis was induced in $Hdac1^{A/A};Hdac2^{A/+}$ PreBI and PreBII cells. We performed AnnexinV apoptosis assay by flow cytometry analysis. We first gated for PreBI or PreBII cell populations (Figure 2A left

panels) and measure apoptotic cells (AnnV⁺;DAPI⁻). Strikingly, we observed that *Hdac1^{Δ/Δ};Hdac2^{Δ/+}* PreBI cells underwent apoptosis at lower frequency, compared to control *Hdac1^{+/+};Hdac2^{+/+}* PreBI cells (Figure 2A, upper right panels). Quantification of these flow cytometry analysis revealed a significant decrease in apoptotic (AnnV⁺;DAPI⁻) cells (Figure 2B upper panel). In contrast, we did not detect any difference in apoptosis frequency in PreBII cells upon *Hdac1^{Δ/Δ};Hdac2^{Δ/+}* (Figure 2A, lower right panels). In summary, *Hdac1^{Δ/Δ};Hdac2^{Δ/+}* PreBI cells proliferate more (Figure 1) and undergo less frequently apoptosis (Figure 2), whereas *Hdac1^{Δ/Δ};Hdac2^{Δ/+}* PreBII cells proliferate less (Figure 1) and do undergo more frequently apoptosis (Figure 2).

Hdac1^{Δ/Δ};Hdac2^{Δ/+} Pre-BI cells have reduced intracellular IgM

We observed that *Hdac1^{Δ/Δ};Hdac2^{Δ/+}* Pre-BI cells have reduced apoptosis (Figure 2). These findings prompted us to hypothesize, that *Hdac1^{Δ/Δ};Hdac2^{Δ/+}* PreBI cells might undergo less frequently apoptosis because they might have a problem with V(D)J recombination and therefore escape the selection process for differentiating to the next B cell stage involving apoptosis. Therefore these PreBI cells might not differentiate to PreBII cells. This would explain the massive decrease in PreBII cell number we observe in *Hdac1^{Δ/Δ};Hdac2^{Δ/+}* mice (Suppl. Figure 2B). We therefore performed flow cytometry analysis of intra cellular IgM staining of *Hdac1^{Δ/Δ};Hdac2^{Δ/+}* and control *Hdac1^{+/+};Hdac2^{+/+}* PreBI cells. Our preliminary data show that *Hdac1^{Δ/Δ};Hdac2^{Δ/+}* decreased intra cellular IgM⁺ in PreBI cells (Figure 3A). Quantification revealed a decrease of intra cellular IgM⁺ PreBI cells in *Hdac1^{Δ/Δ};Hdac2^{Δ/+}* compared to *Hdac1^{+/+};Hdac2^{+/+}* mice (Figure 3B). These preliminary data suggests less IgM rearrangement in *Hdac1^{Δ/Δ};Hdac2^{Δ/+}* PreBI cells.

3.2. Figure legends

Figure 1: Proliferation is increased in *Hdac1^{Δ/Δ};Hdac2^{Δ/+}* Pre-BI cells and decreased in Pre-BII cells

Experiments were performed in 8-week-old mice. **(A)** For cell cycle analysis, mice of indicated genotype were intraperitoneally injected with 1.5mg of BrdU. 24h after BrdU injection mice were sacrificed and bone marrow cells were isolated and stained with anti-BrdU antibody for flow cytometry analysis. The percentages of cells in the G₀/G₁-, S-, and G₂/M-phase, obtained by manual gating, are indicated in the plots. Results are representative of 3 independent experiments. **(B)** BrdU-positive cells that represent cells in S-phase were quantified from (a) (n=2). Mean and standard error of BrdU-positive cells is shown.

Figure 2: *Hdac1^{Δ/Δ};Hdac2^{Δ/+}* Pre-BI cells have reduced apoptosis

Experiments were performed in 8-week-old mice. **(A)** Bone marrow cells were isolated from *Hdac1^{+/+};Hdac2^{+/+}* and *Hdac1^{Δ/Δ};Hdac2^{Δ/+}* mice and stained with Annexin V, DAPI and B cell surface markers for flow cytometry analysis. PreBI (CD19⁺, c-kit⁺) and PreBII (CD19⁺, CD25⁺) cells were gated by flow cytometry (left dot plots). AnnexinV-positive (i.e., apoptotic) cells in PreBI and PreBII lymphocytes were quantified (right panels). **(B)** Mean percentages and standard deviations of apoptotic (annexinV⁺ DAPI) cells are represented as bar plots (n=3 mice per genotype, representative from 3 independent experiments). All statistical analysis were performed with the Student unpaired 2-tailed *t* test. Significant differences in means between genotypes are indicated, **p* < 0.05; ***p* < 0.01. N.S. for not statistically significant.

Figure 3: *Hdac1*^{Δ/Δ};*Hdac2*^{Δ/+} Pre-BI cells have reduced intracellular IgM (preliminary data)

Experiments were performed in 8-week-old mice. (A) Flow cytometry analysis of *Hdac1*^{+/+};*Hdac2*^{+/+} and *Hdac1*^{Δ/Δ};*Hdac2*^{Δ/+} bone marrow cells by immunofluorescence cell surface staining with CD19 and c-kit followed by fixation, permeabilization and intra cellular IgM staining. (B) Quantification of intra IgM⁺ PreBI cells in percent are shown below (n=4 mice per genotype).

3.3. Figures

Figure 1

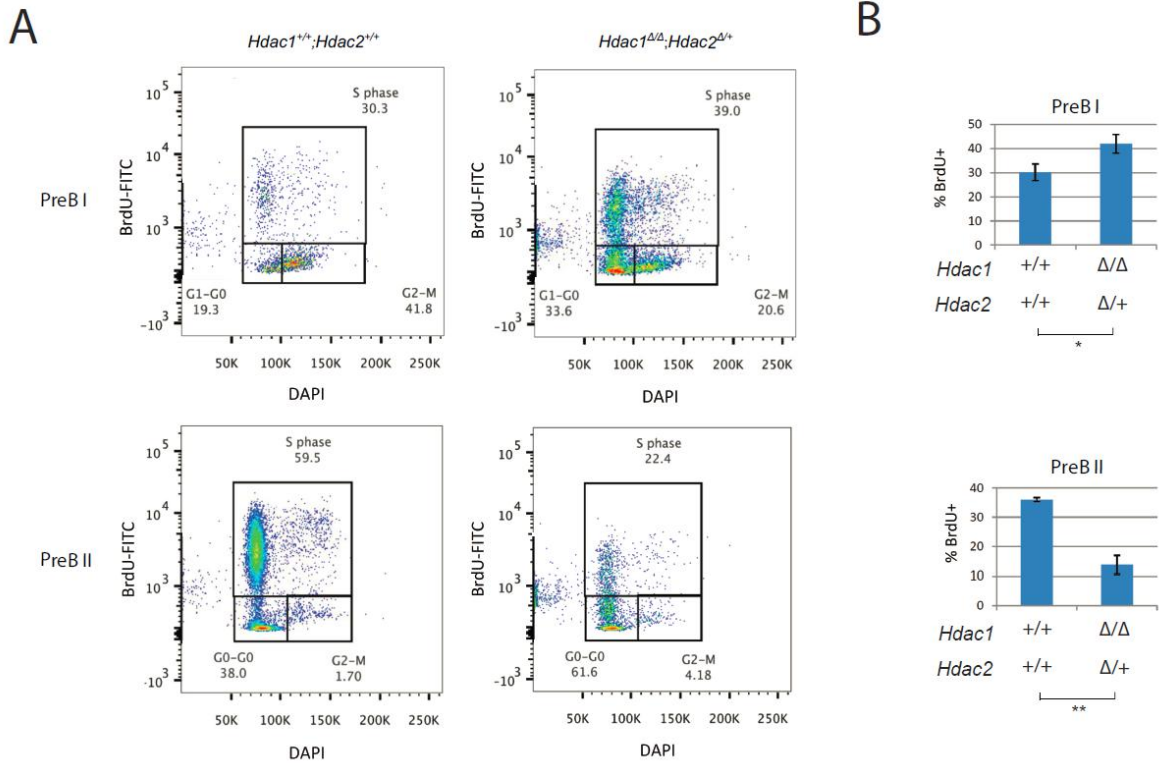
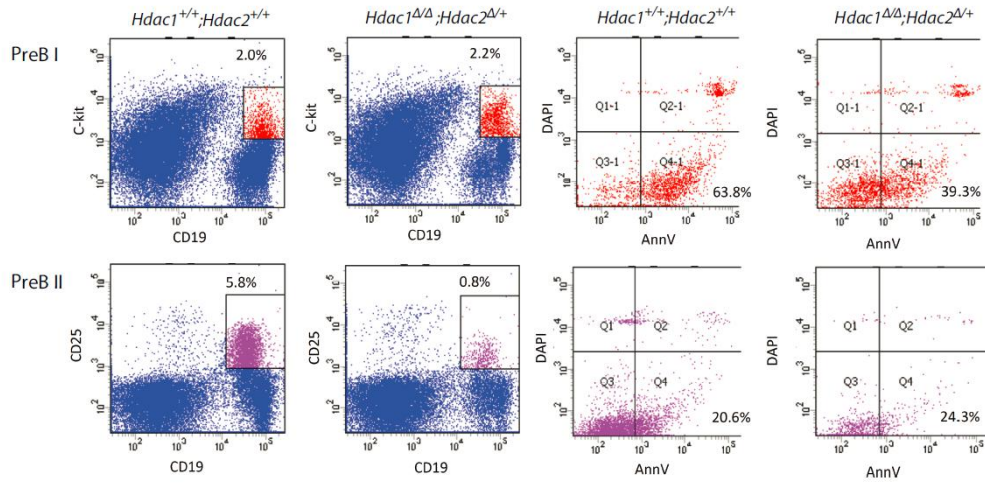


Figure 2

A



B

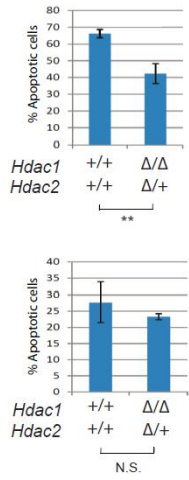
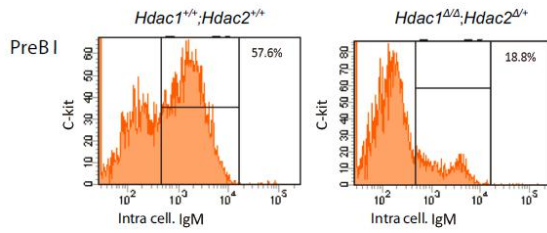
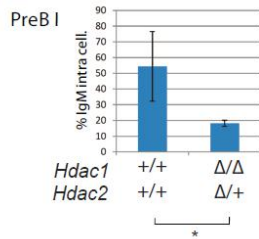


Figure 3

A



B



3.4. Supplementary figure legends

Suppl. Figure 1: Analysis of $Hdac1^{Δ/Δ};Hdac2^{Δ/+}$ mice

Experiments were performed in 8-week-old mice. **(A)** PCR genotyping from splenic B cells ($B220^+$; $CD19^+$; $CD3^-$) sorted by flow cytometry. Specific allele annotation are to the left of gel: *Hdac1* and *Hdac2* wild type (WT), floxed (FL), and knockout (KO) alleles and mb1-cre transgenes (tg). **(B)** Western blots were performed on lysates from flow cytometry sorted splenic B cells ($B220^+$; $CD19^+$; $CD3^-$) from indicated genotypes. *Hdac1*^{+/+};*Hdac2*^{+/+} and *Hdac1*^{Δ/Δ};*Hdac2*^{Δ/+} cells were analyzed for the expression of Hdac1, Hdac2, and histone H3Ac, H4Ac. H3 and H4 expression was used as loading control.

Suppl. Figure 2: Dissecting the impact of $Hdac1^{Δ/Δ};Hdac2^{Δ/+}$ on B cell development

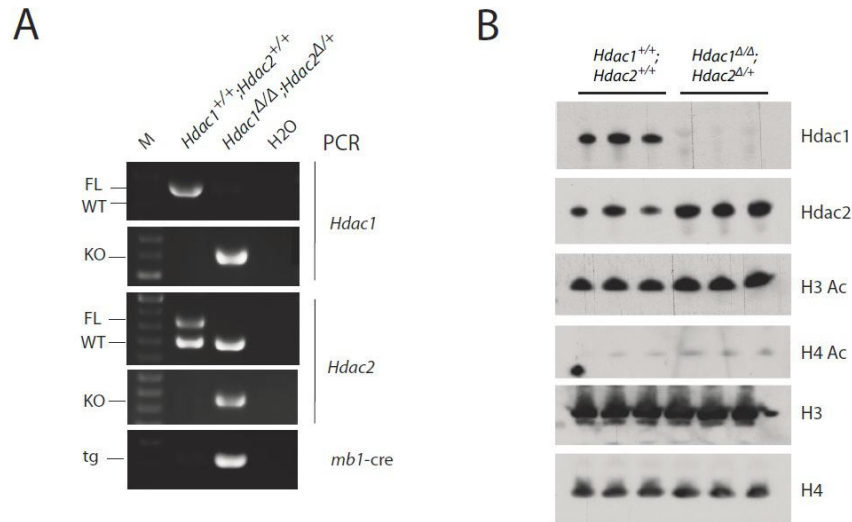
Experiments were performed in 8-week-old mice. **(A)** Representative flow cytometry dot plots of B220/IgM staining gated on total $B220^+$ lymphocytes derived from the bone marrow (BM) of *Hdac1*^{Δ/Δ};*Hdac2*^{Δ/+} and control *Hdac1*^{+/+};*Hdac2*^{+/+} mice. Gated regions in dot plots indicate the B cell subsets of interest with Pro/preB ($B220^+$; IgM^-) and ImmatureB ($B220^{low}$; IgM^+) subsets highlighted. **(B)** *Hdac1*^{Δ/Δ};*Hdac2*^{Δ/+} mice have less B cells and a huge decrease in pre-BII (and Immature B) cell number, but have normal amount of mature B cells in the spleen. Immunofluorescence staining with B cell surface marker-specific monoclonal antibodies (CD19, IgM, c-kit, and CD25) from *Hdac1*^{+/+};*Hdac2*^{+/+} and *Hdac1*^{Δ/Δ};*Hdac2*^{Δ/+} bone marrow cells followed by flow cytometry analysis. Gated regions in dot plots indicate the B cell subsets of interest with frequency in percent. Quantification of B cell numbers and B cell sub populations are shown below with SEM. The statistical analysis was performed with the Student unpaired 2-tailed *t* test. Significant differences in means between genotypes are indicated, **, $P < 0.01$. N.S.

Results

for not statistically significant. (C) *Hdac1^{+Δ};Hdac2^{Δ/Δ}* have a normal B cell development. Quantification of flow cytometry analysis from *Hdac1^{+/+};Hdac2^{+/+}* and *Hdac1^{+Δ};Hdac2^{Δ/Δ}* bone marrow B cell populations (same as (B)). N.S. for not statistically significant (Student unpaired 2-tailed *t* test).

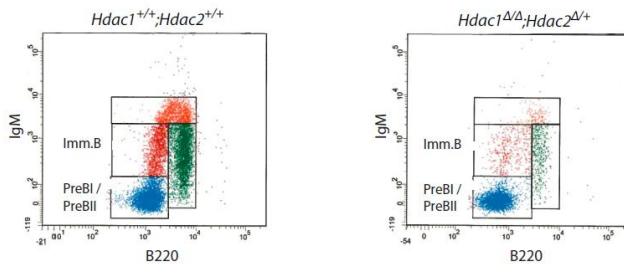
3.5. Supplementary figures

Suppl. Figure 1

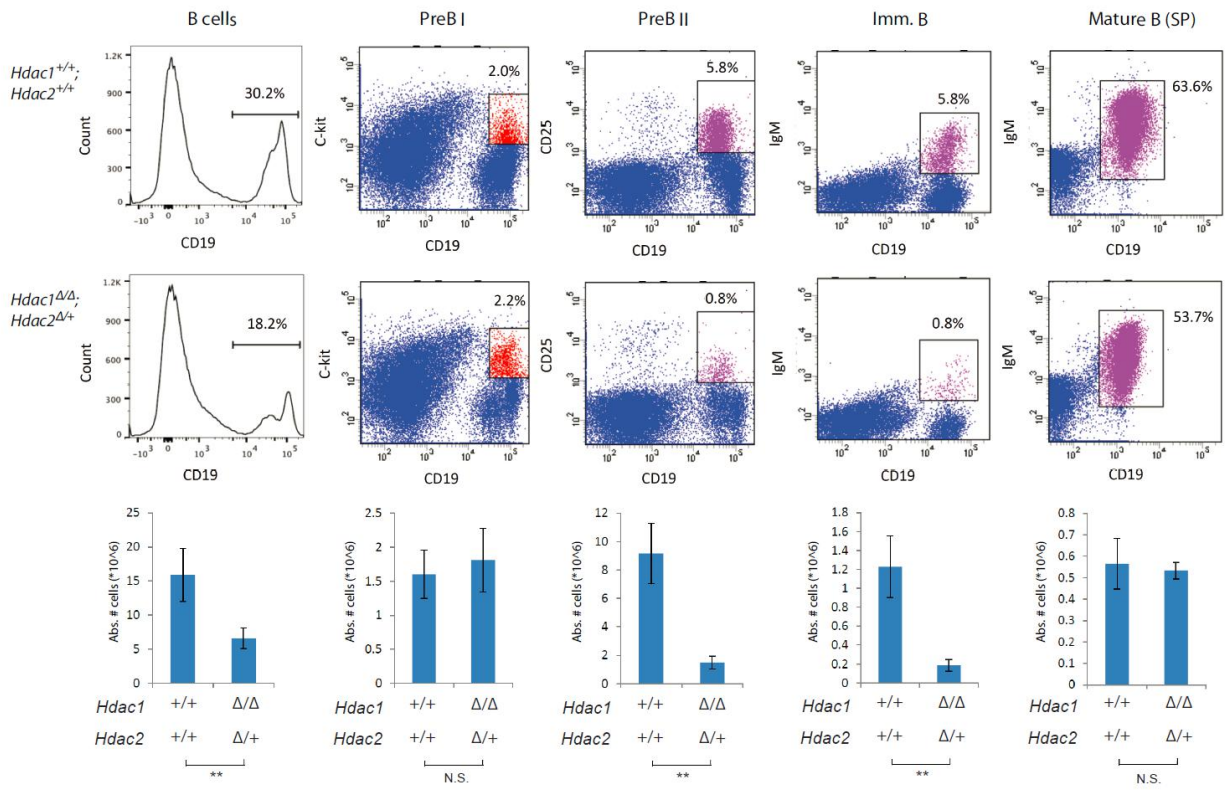


Suppl. Figure 2

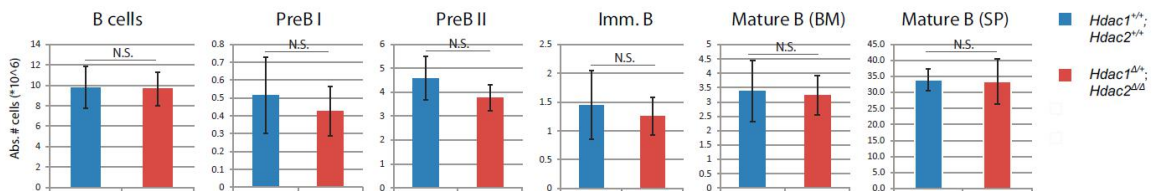
A



B



C



Results Part 4

(Hdac6 in E μ -*myc* B cell lymphoma)

Results Part 4: Dissecting the role of Hdac6 in E μ -myc B cell lymphoma

4.1. Results

High human HDAC6 expression predicts poor prognosis in DLBCL patients

We first explored the prognostic significance of human *HDAC6* gene expression with DRUGSURV, a resource for repositioning of approved and experimental drugs in oncology based on patient survival information. We examined the prediction of survival in Diffuse Large B Cell Lymphoma (DLBCL), a B cell lymphoma with *c-Myc* deregulation. We compared the survival of DLBCL patients treated with chemotherapy plus rituximab (monoclonal antibody against pan-B-cell marker CD20) according to the *HDAC6* gene expression level in DLBCL patient samples. Interestingly, we observed that high *HDAC6* expression levels predict significant poorer survival than low *HDAC6* expression levels (* $p < 0.01$) (Figure 1). This clearly demonstrates, that molecular *HDAC6* gene expression signature has a prognostic significance in patients treated with chemotherapy plus Rituximab.

Hdac6 overexpression (H6OE) accelerates lymphomagenesis whereas Hdac6 knockout in the germ line (H6KO^{GL}) may delay tumor development in E μ -myc mice

The finding that high human *HDAC6* expression predicts poor prognosis in DLBCL patients (Figure 1), prompted us to investigate the role of mouse Hdac6 in the E μ -myc mouse model of B cell lymphoma, a preclinical model with *c-Myc* deregulation. In order to test the B cell intrinsic and extrinsic effect of Hdac6 ablation, we used Hdac6 B cell specific conditional KO (H6KO^{BC}), and Hdac6 germ line knockout (H6KO^{GL}), respectively. These mice were generated in the lab by Dr. Yu Zhang (Zhang et al., 2008). In order to test the effect of Hdac6 overexpression, we used

mice overexpressing Hdac6 (H6OE), which were previously produced by Dr. Yu Zhang in our lab (unpublished). To generate these mice, the BAC clone (50M7) which contains the whole murine *Hdac6* gene (Means et al., 2000) was used for microinjection into the pronucleus of fertilized mouse oocytes to generate *Hdac6*-BAC transgenic mice, which overexpress *Hdac6* (Suppl. Figure 1A). Quantitative Western Blotting in mouse testis, revealed that *Hdac6*-BAC tg mice have increased level of Hdac6 protein and hypoacetylation of α -tubulin (Suppl. Figure 1B). To investigate the role of Hdac6 in E μ -*myc* tumorigenesis, we crossed E μ -*myc* tg mice with H6OE mice, or mice with H6KO^{BC} or H6KO^{GL} (Figure 2A, Figure 2B). We then monitored mice for tumor development over a period of 300 days by Kaplan-Meier (KPLM) analysis. Strikingly, H6OE significantly accelerated lymphomagenesis in E μ -*myc* mice (Figure 2C). H6OE E μ -*myc* mice developed tumors with a higher incidence (95% vs. 80%), shorter latency (42 days vs. 47days), and shorter mean latency (103 days vs. 141days), compared with E μ -*myc* mice (Figures 2D). Interestingly, we observed, that H6KO^{GL} may delay tumor development in E μ -*myc* mice (Figure 2C). H6KO^{GL} E μ -*myc* mice developed tumors with a lower incidence (64 % vs. 80%), later latency (96 days vs. 47 days) and later mean latency (172 days vs. 140 days) compared with E μ -*myc* (Figure 2D). However, statistical analysis revealed that the difference is not significant (p-value of 0.05504) (Figures 2D). Interestingly, we observed that H6KO^{BC} had no effect in E μ -*myc* mice (Figure 2C). H6KO^{BC} E μ -*myc* mice developed tumors with similar latency and similar incidence compared with E μ -*myc* mice (Figure 2D). This suggests that the assumed effect of H6KO^{GL} is probably a B cell extrinsic effect. In summary, we show for the first time that Hdac6 overexpression accelerates lymphomagenesis whereas Hdac6 knockout in the germ line may delay tumor development in E μ -*myc* mice.

H6OE increases, and H6KO^{GL} decreases the percentage of peripheral blood lymphocytes at early stages of Eμ-myc tumorigenesis

To determine how H6OE (and H6KO^{GL}) impact on Eμ-myc tumorigenesis, we then measured the circulating peripheral blood lymphocytes (PBL) at 4 and 10 weeks using an automated blood cell counter (Figure 3). We observed, that H6KO^{BC} had no effect on PBL at 4 and 10 weeks (Figure 3A). Interestingly, H6KO^{GL} significantly reduced the percentage of PBL at 4 weeks, but this effect was not visible later at 10 weeks (Figure 3B). In contrast, H6OE significantly increased the percentage of PBL at 4 weeks, but also had no effect at 10 weeks. Hence, we conclude, that H6KO^{GL} significantly reduced, whereas H6OE significantly increased the percentage of PBL at early but not at late stages of Eμ-myc tumorigenesis. These findings are consistent with our previously shown observations that H6OE accelerates lymphomagenesis whereas H6KO^{GL} may delay tumor development in Eμ-myc mice (Figure 2C).

We also measured the spleen (SP) weight, since Eμ-myc tg mice have an enlarged spleen (splenomegaly). Surprisingly, we found that neither H6OE nor H6KO had any significant effect on SP enlargement in Eμ-myc mice (Suppl. Figure 2A). In addition, we performed a histopathological analysis (Suppl. Figure 2B). As expected, some Eμ-myc mice displayed high grade Non-Hodgkin Lymphoma (HG-NHL) (corresponding to Burkitt's lymphoma in men), as described previously (Adams et al., 1985; Morse et al., 2002). Preliminary analysis from H6KO Eμ-myc mice, revealed that H6KO^{GL} Eμ-myc and H6KO^{BC} Eμ-myc mice had HG-NHL incidence in SP and LNs at a similar frequency compared to control Eμ-myc mice (Suppl. Figure 2B). Interestingly, histopathological analysis of old H6OE mice reveals unexpected fatty acid changes in liver (Suppl. Figure 2D). Five out of ten H6OE mice had these fatty acid changes

(Suppl. Figure 2C). We did not further investigate this phenomenon since it was not related to our research.

H6OE significantly increases tumor cell load in Eμ-myc mice

We next assessed the tumor cell load by quantifying the B220^{low} population which are characteristically highly overrepresented in Eμ-myc mice (Croxford et al., 2013). We first measured by flow cytometry the B220^{low} cells subsets in blood (BL), SP, LN, and bone marrow (BM) of 8-week-old pre-lymphoma Eμ-myc H6OE and control Eμ-myc mice. Consistently, with the results previously observed, we found that H6OE increases tumor cell load in BL, SP, LN of Eμ-myc mice (Figure 4A). Quantification of flow cytometry analysis revealed significant increase in frequency of B220^{low} cells upon H6OE in BL, SP, and LN (Figure 4B). Interestingly, B220^{low} cell numbers were not affected in the BM of H6OE mice (Figure 4B).

In addition we performed further flow cytometry analysis from BM, SP, and LN of Eμ-myc H6OE and control Eμ-myc mice. We did immunofluorescence staining with B cell surface marker-specific antibodies including B220, IgM, CD19 and CD25 to identify the different B cell populations in the BM (Suppl. Figure 3A), SP (Suppl. Figure 3B), and LN (Suppl. Figure 3C). Eμ-myc mice displayed a blast at Pro/PreB cell stage that dominates the BM (Suppl. Figure 3A), as previously reported (Sidman et al., 1993). We did not observe any effect upon H6OE in the BM by B220/IgM flow cytometry analysis (Suppl. Figure 3A). Quantifications of flow cytometry analysis in BM, SP, and LN, revealed that the average percentage of B220⁺ B lymphocytes and the average percentage of large B220⁺ cell characteristic for the Eμ-myc phenotype was similar in H6OE Eμ-myc mice compared to control Eμ-myc mice (Suppl. Figure 3D and Suppl. Figure 3E, respectively). Interestingly, and consistent with the previous observations (Figure 4), SP and LN analysis revealed that H6OE Eμ-myc had more cells which

express B220 at a low level (highlighted B220^{low} populations) (Suppl. Figure 3B and Suppl. Figure 3C, respectively). Taken together, our data show that HOE significantly increases tumor cell load in E μ -*myc* mice.

H6KO^{GL} decreases tumor cell load in E μ -*myc* mice

We showed that H6OE increases tumor cell load (B220^{low} populations) in BL, SP, and LN of E μ -*myc* mice (Figure 4), and eventually accelerates lymphomagenesis (Figure 2). We also observed that H6KO^{GL} may delay tumor development in E μ -*myc* mice (Figure 2). Hence, we hypothesize that H6KO^{GL} might also impact on B220^{low} populations in these organs. We therefore assessed the tumor cell load in 8-week-old pre-lymphoma H6KO^{GL} E μ -*myc* mice, by quantifying the B220^{low} population in BL, SP, LN, and BM (Figure 5). We observed, that H6KO^{GL} mice reduces tumor cell load in E μ -*myc* BL, SP, and LN (Figure 5A). Quantification of B220^{low} cells population in BL, SP, LN, revealed a significant decrease upon H6KO^{GL} (Figure 5B). Similar to the previous observation in H6OE mice (Figure 4), we did not observe any effect on B220^{low} cells population in the BM upon H6KO^{GL}. In addition we performed further flow cytometry analysis from BM, SP, and LN of E μ -*myc* H6OE and control E μ -*myc* mice. Consistent with our previous observations, we did not observe any effect on E μ -*myc* induced blast in the BM upon H6KO^{GL} (Suppl. Figure 4A). Consistently, quantification of large B220⁺ cell in the BM, revealed no difference between E μ -*myc* H6KO^{GL} compared to control E μ -*myc* mice (Suppl. Figure 4E). Further flow cytometry analysis of SP (Suppl. Figure 4B), and LN (Suppl. Figure 4C) did not reveal any significant impact of H6KO^{GL} on the mature B cell populations (B220⁺;IgM⁺) (Suppl. Figure 4D).

Our previous findings clearly show that ablation of Hdac6 only in B cells (H6KO^{BC}) had no impact on E μ -*myc* tumorigenesis (Figure 2). In addition, we performed flow cytometry analysis

Results

of H6KO^{BC} 8-weeks-old pre-lymphoma mice (Suppl. Figure 5). We found, that H6KO^{BC} had no impact on B220⁺ (Suppl. Figure 5A), large B220⁺ (Suppl. Figure 5B), and B220^{low} cell numbers (Suppl. Figure 5C) in E μ -*myc* mice. Taken together, our data show that H6KO^{GL}, but not H6KO^{BC}, significantly decreases tumor cell load (B220^{low} population) in the BL, SP, and LN of E μ -*myc* mice.

4.2. Figure legends

Figure 1: High human HDAC6 expression predicts poor prognosis in Diffuse Large B Cell Lymphoma (DLBCL) patients

(A) Molecular *HDAC6* gene expression signature have a prognostic significance in patients treated with chemotherapy plus Rituximab. Prediction of survival in DLBCL patients treated with chemotherapy plus rituximab (monoclonal antibody against pan-B-cell marker CD20) according to the *HDAC6* gene expression level in DLBCL patient samples: High *HDAC6* expression levels (red curve) predict significant poorer survival than low *HDAC6* expression levels (green curve) (* $p < 0.01$). Graph generated by DRUGSURV, a resource for repositioning of approved and experimental drugs in oncology based on patient survival information (www.bioprofiling.de/GEO/DRUGSURV). Gene expression Omnibus (GEO) dataset: GSE10846. 181 clinical samples from patients treated with a regimen of 4 drugs known as CHOP (cyclophosphamide, doxorubicin, vincristine, and prednisone), and 233 clinical samples from CHOP-treated patients, plus the monoclonal antibody rituximab.

Figure 2: Hdac6 overexpression (H6OE) accelerates lymphomagenesis whereas Hdac6 knockout in the germ line (H6KO^{GL}) may delay tumor development in E μ -myc mice

(A) PCR genotyping for *Hdac6* wild-type (WT), flox (FL), knockout (KO), and Bacterial Artificial Chromosome (BAC) alleles and *mb1-cre* transgene (tg). PCR was performed from CD19⁺ MACS sorted splenic B cells from 8-week-old mice with indicated genotypes: *Hdac6* KO in the germ line (H6KO^{GL}), *Hdac6* KO in B cells (H6KO^{BC}), *Hdac6* overexpression (H6OE). Specific allele annotations are to the left of the gel. Loading marker (M) is indicated. (B) Western blot analysis of protein lysates from CD19⁺ MACS sorted splenic B cells derived from

Results

8-week-old mice of indicated genotypes. Immunoblot of Hdac6 and Ac alpha tubulin. Hyperacetylated tubulin (Ac tubulin) was used as an additional readout for Hdac6 depletion. Tubulin serves as loading control. **(C)** H6OE accelerates whereas H6KO delays tumor onset in E μ -myc mice. Kaplan-Meyer (KPLM) tumor-free survival plot of 21 age-matched H6KO^{GL}, H6KO^{BC}, H6OE and control WT mice with or without E μ -myc tg. Mice were monitored over a period of 300 days for tumor onset and sacrificed when they reached termination criteria (see Material and Methods). The curves show the percentage of mice surviving without tumors at various days. The log-rank test was used to determine the level of significance between curves. **p < 0.01; N.S. for not statistically significant. **(D)** Statistical analysis from KPLM **(C)**. Incidence (%), latency and mean latency (days) of tumor induced by the E μ -myc tg in indicated genotypes.

Figure 3: H6OE increases, and H6KO^{GL} decreases the percentage of peripheral blood lymphocytes at early stages of E μ -myc tumorigenesis

Blood was analyzed in an automated blood analyzer (Sysmex XT-2000). Shown are detailed analysis of **(A)** H6KO^{BC}, **(B)** H6KO^{GL} and **(C)** H6OE animals with or without E μ -myc tg at 4 and 10 weeks (n \geq 10). Frequency (%) of Peripheral Blood Lymphocytes (PBL) is indicated. Boxplots with p-values calculated with the Wilcoxon Signed-Rank Test: *p < 0.05; **p < 0.01; N.S. for not statistically significant.

Figure 4: H6OE increases tumor cell load in E μ -myc mice

We assessed the tumor cell load by quantifying the B220^{low} population characteristic for E μ -myc phenotype. Experiments were performed in 8-week-old pre-lymphoma mice. Quantification of

Results

the proportion of malignant cells in E μ -*myc* mice expressing B220 at a low level (% of B220^{low} cells). Analysis of B220^{low} cells population in blood (BL), spleen (SP), lymph node (LN), bone marrow (BM) from E μ -*myc* Hdac6 overexpressing (H6OE) mice and control E μ -*myc* mice. **(A)** Representative flow cytometry dotplots of B220/IgM staining and representative flow cytometry histograms of B220⁺ cells, gated on total lymphocytes and then gated for B220^{low} and B220^{high} populations. Percentages in the different gates are indicated. B220^{low} populations of interest are highlighted with red gates. **(B)** H6OE increases tumor cell load in E μ -*myc* mice. Quantification of flow cytometry analysis (n=3 mice per genotype). The graphs represents the average percentage of B220^{low} cells with SEM. The statistical analysis was performed with the Student unpaired 2-tailed *t* test. Significant differences in means between genotypes are indicated, **p* < 0.05. N.S. for not statistically significant.

Figure 5: H6KO^{GL} decreases tumor cell load in E μ -*myc* mice

We assessed the tumor cell load by quantifying the B220^{low} population characteristic for the E μ -*myc* phenotype. Experiments were performed in 8-week-old pre-lymphoma mice. Quantification of the proportion of malignant cells in E μ -*myc* mice expressing B220 at a low level (% of B220^{low} cells). **(A)** H6KO^{GL} mice reduces tumor cell load in E μ -*myc* mice. Cells were derived from blood (BL), spleen (SP), lymph node (LN) and bone marrow (BM) of E μ -*myc* and E μ -*myc* H6KO^{GL} mice and analyzed by flow cytometry. Representative flow cytometry dot plots of B220/IgM staining and representative flow cytometry histograms of B220⁺ cells, gated on total lymphocytes and then gated for B220^{low} and B220^{high} populations. Percentages in the different gates are indicated. B220^{low} populations of interest are highlighted with red gates. **(B)** Quantification of B220^{low} cells population in SP, LN, BM, and BL from E μ -*myc* Hdac6 germ

Results

line KO (H6KO^{GL}) (n=3) mice compared to control E μ -*myc* animals. The graphs represents the average percentage of B220^{low} cells with SEM. The statistical analysis was performed with the Student unpaired 2-tailed *t* test. Significant differences in means between genotypes are indicated, **p* < 0.05; **, *P* < 0.01. N.S. for not statistically significant.

4.3. Figures

Figure 1

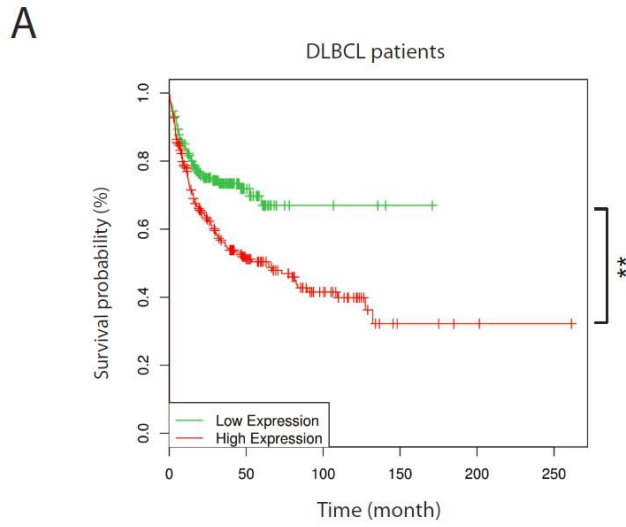


Figure 2

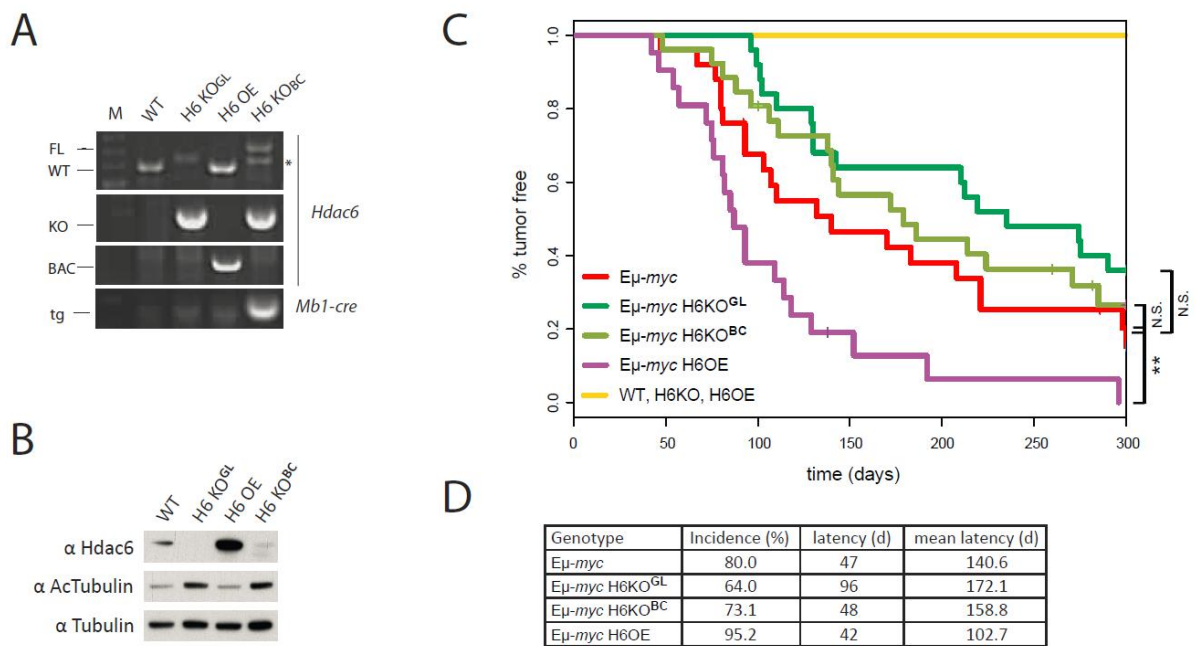


Figure 3

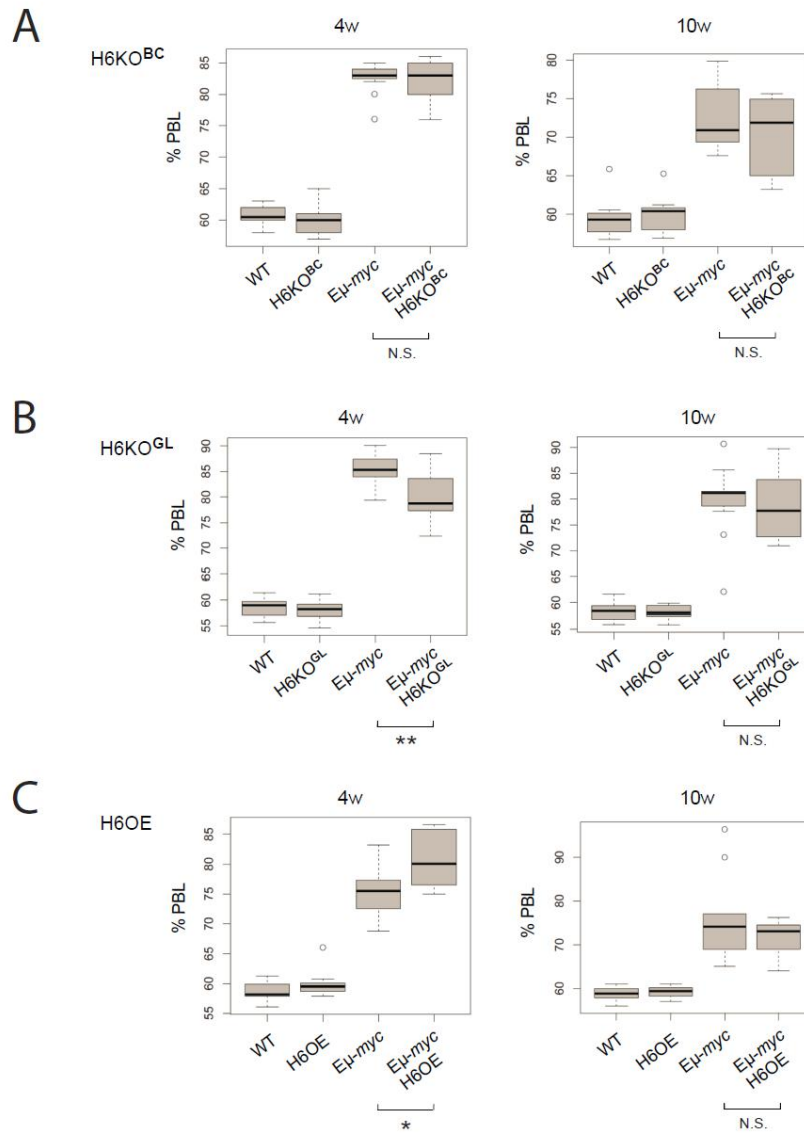


Figure 4

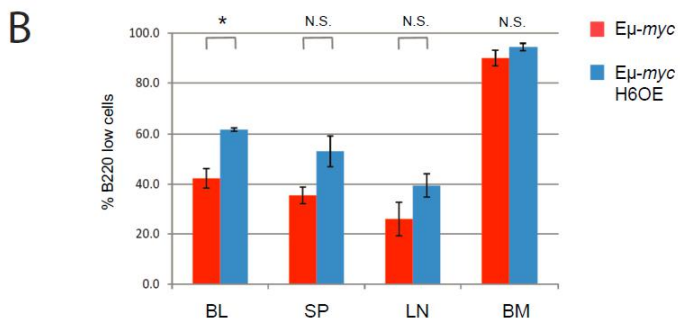
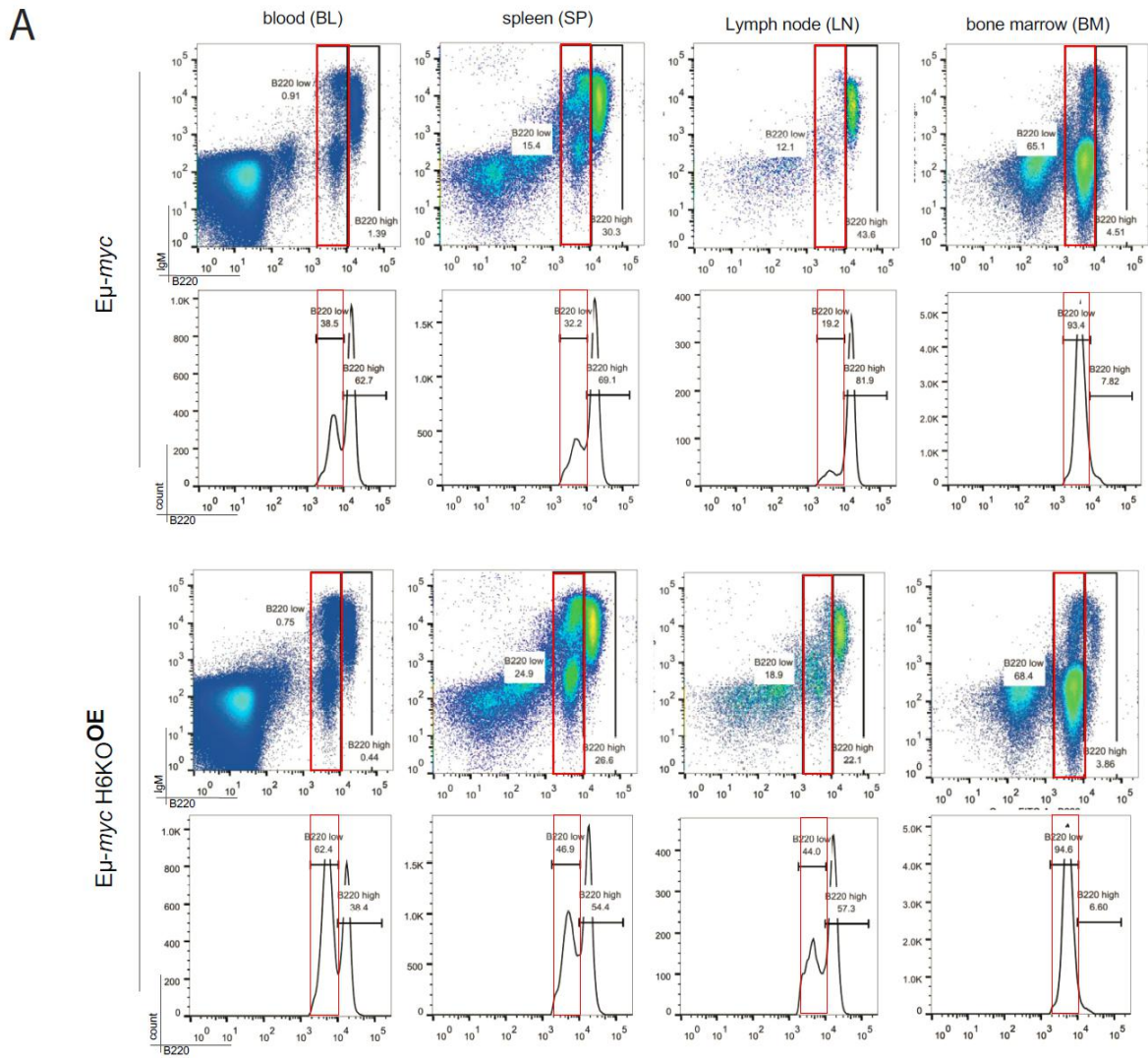
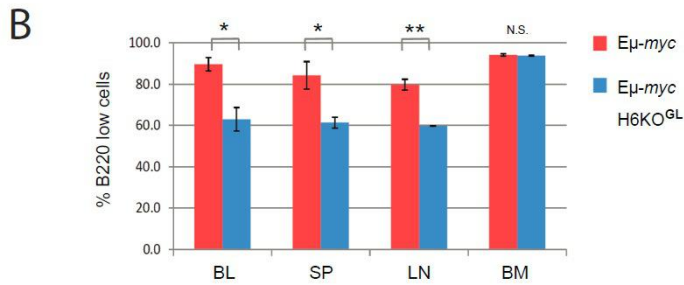
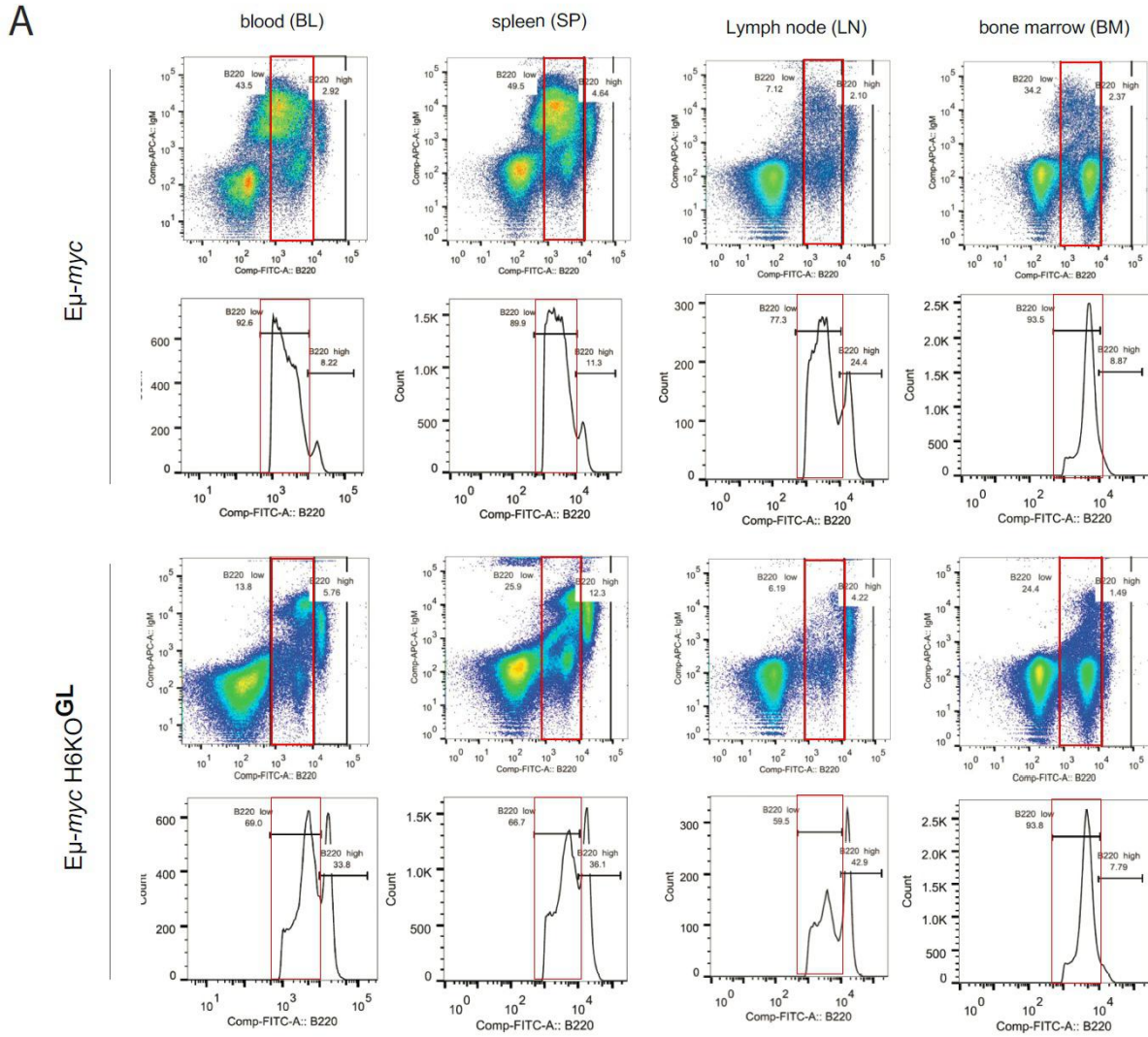


Figure 5



4.4. Supplementary figure legends

Suppl. Figure 1: Generation of *Hdac6* overexpressing (H6OE) mice

(A) Schematic illustration of the BAC chromosome containing the *Hdac6* locus. The BAC clone (50M7) which contains the whole murine *Hdac6* gene (Means et al. 2000) was used for microinjection into the pronucleus of fertilized mouse oocytes to generate *Hdac6*-BAC transgenic mice, which overexpress *Hdac6* (H6OE). The *Hdac6* gene copy number was detected in the viable and fertile founder mice by real-time PCR using a pair of specific primers which recognize the region between exon 9 and 10 of *Hdac6* (indicated with arrows). Performed previously in the lab (Yu Zhang et al., unpublished). (B) *Hdac6*-BAC mice have high levels of Hdac6 and hypoacetylation of α -tubulin. Quantitative Western Blotting (QWB) in mouse testis. Immunoblot analysis of Hdac6 expression, Ac α -tubulin, and α -tubulin as loading control. The *Hdac6*-BAC transgenic mice showed as expected, increased level of Hdac6 protein and hypoacetylation of α -tubulin. Performed previously in the lab (Yu Zhang et al., unpublished). *Hdac6*-BAC transgenic mice with 6 copies of *Hdac6* were selected for all the subsequent experiments shown in this manuscript.

Suppl. Figure 2: Histopathological analysis reveals unexpected fatty acid changes in liver of H6OE mice but no changes in spleen weight

(A) H6OE or H6KO has no significant impact on spleen enlargement (splenomegaly) in E μ -myc mice (n>10). Comparison of relative spleen weights (in % of body weight) of 8-week-old mice with indicated genotypes. Box plots with p-values generated using the Wilcoxon Signed-Rank test. Significant differences between genotypes are indicated, *p<0.05. N.S. for not statistically significant. (B) Histopathological analysis in 8-week-old mice with indicated genotypes.

Results

Pathological finding of high grade Non-Hodgkin lymphoma (HG-NHL) were scored in spleen and lymph nodes and summarized in the table (n=10). **(C)** Fatty acid changes were observed in the liver of old H6OE mice. Histopathological analysis in 8- and 40-week-old WT, Hdac6 germline knockout (H6KO^{GL}) and Hdac6 overexpressing (H6OE) mice. 50% of H6OE mice (5 out of 10) had fatty acid changes. No changes were observed in H6KO^{GL} or control WT mice (n=10). **(D)** Histopathology analysis in 40-week-old WT and H6OE mice. Representative pictures from liver sections treated with hematoxylin and eosin (H&E). Original magnification of 4X and 10X and 20X as indicated, (Nikon Eclipse E600). Pathological finding of fatty acid changes is clearly visible. Phenotype was scored in different samples and summarized in the table (C).

Suppl Figure 3: Hdac6 overexpression (H6OE) might impact on B cell populations in pre-lymphoma Eμ-myc mice

Experiments were performed in 8-week-old pre-lymphoma mice. **(A-C)** Representative flow cytometry dot plots of B220/IgM staining gated on total lymphocytes derived from the bone marrow (BM), spleen (SP) and lymph nodes (LN) cells from WT, H6OE, Eμ-myc and Eμ-myc H6OE mice. Gated regions in dot plots indicate the B cell subsets of interest with frequency in percent. **(A)** H6OE has no impact on the B cell blasts (B220⁺, IgM⁻) which dominate the BM of Eμ-myc tg mice. In contrast, H6OE in Eμ-myc mice impacts on B220 B cell population in spleen **(B)** and lymph nodes **(C)**. Some H6OE Eμ-myc mice have more cells which express B220 at a low level (highlighted B220^{low} populations). **(D-E)** Quantifications of flow cytometry analysis from mice of indicated genotypes. The bar plots represents the average percentage of B220⁺ B lymphocytes **(D)** and the average percentage of large B220⁺ cell characteristic for the Eμ-myc

phenotype (**E**). SEM are indicated (n=3 mice per genotype). The statistical analysis was performed with the Student unpaired 2-tailed *t* test. Significant differences in means between genotypes are indicated, **p* < 0.05. N.S. for not statistically significant.

Suppl. Figure 4: Hdac6 germ line knockout has no impact on B lymphocyte counts in pre-lymphoma Eμ-myc mice

All experiments were performed in 8-week-old pre-lymphoma mice. (**A-C**) H6KO^{GL} has neither an impact in WT nor in Eμ-*myc* mice in BM, SP and LN. Representative flow cytometry dot plots of B220/IgM staining gated on total lymphocytes derived from mice with indicated genotypes. Gated regions in dot plots indicate the B cell subsets of interest in percent. (**A**) H6KO^{GL} has no impact on the B cell blasts (B220⁺, IgM⁻) which dominate the BM of Eμ-*myc* tg mice. H6KO^{GL} has also no impact on the B220⁺/IgM⁺ B cell population in the SP (**B**) and LN (**C**) of WT or Eμ-*myc* mice. (**D**) Quantification of flow cytometry analysis from experiment (d-f) (n=3 mice per genotypes). The graph represents the average percentage of B220⁺ B lymphocytes with SEM. The statistical analysis was performed with the Student unpaired 2-tailed *t* test. (**E**) Representative flow cytometry histograms showing the large lymphocyte subset (FSC-H subset) in the BM of mice with indicated genotypes (left panels). The graph on the right represents the quantification of flow cytometry analysis with average percentage of large lymphocyte subsets with SEM (n=3 mice per genotype). N.S. for not statistically significant (Student unpaired 2-tailed *t* test).

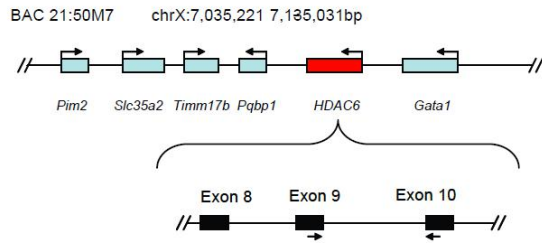
Suppl. Figure 5: Hdac6 B cell knockout has no impact on B cell populations in pre-lymphoma E μ -myc mice

All experiments were performed in 8-week-old pre-lymphoma mice (unless otherwise indicated). E μ -myc mice and Hdac6 B cell KO (H6KO^{BC}) E μ -myc mice have comparable B220⁺ and large B220⁺ and B220^{low} cell numbers. **(A-B)** Quantification of flow cytometry analysis of BM B cells from mice of indicated genotypes E μ -myc mice with a tumor are shown as control. The bar plots represents: **(A)** average percentage of B220⁺ B lymphocytes, and **(B)** average percentage of large B220⁺ cell characteristic for the E μ -myc phenotype. **(C)** Quantification of flow cytometry analysis from SP, LN, and BM. Bar plots represents average percentage of B220^{low} cells in E μ -myc and E μ -myc H6KO^{BC} mice. Experiments were performed with n=3 mice per genotype. SEM are indicated. The statistical analysis was performed with the Student unpaired 2-tailed *t* test. Significant differences in means between genotypes are indicated, **p* < 0.05. N.S. for not statistically significant.

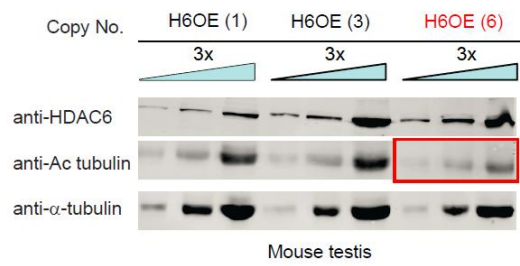
4.5. Supplementary figures

Suppl. Figure 1

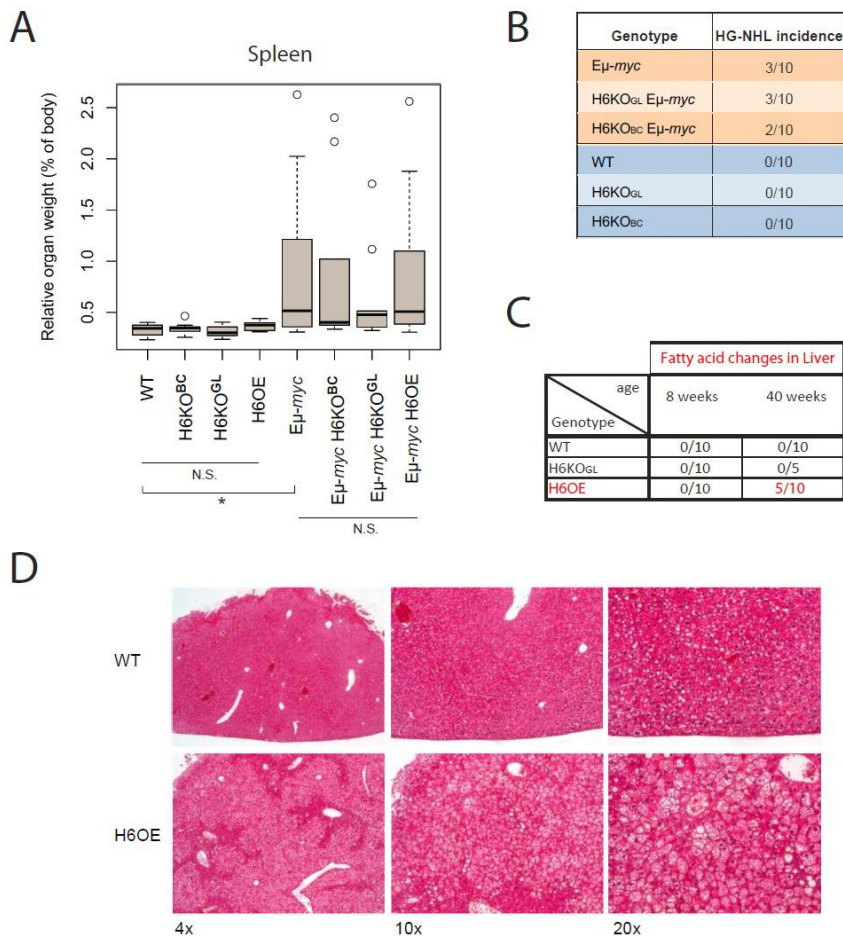
A



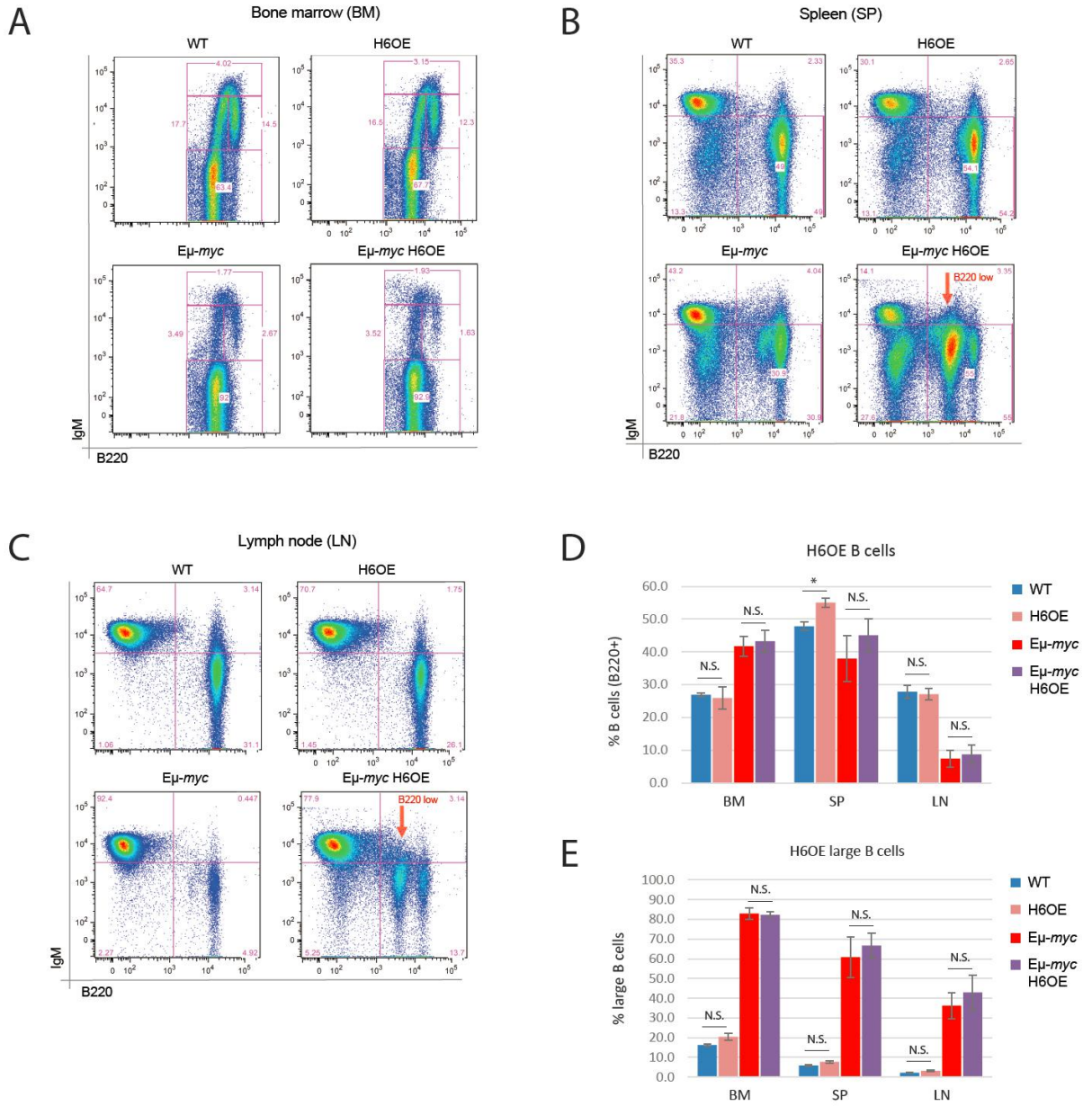
B



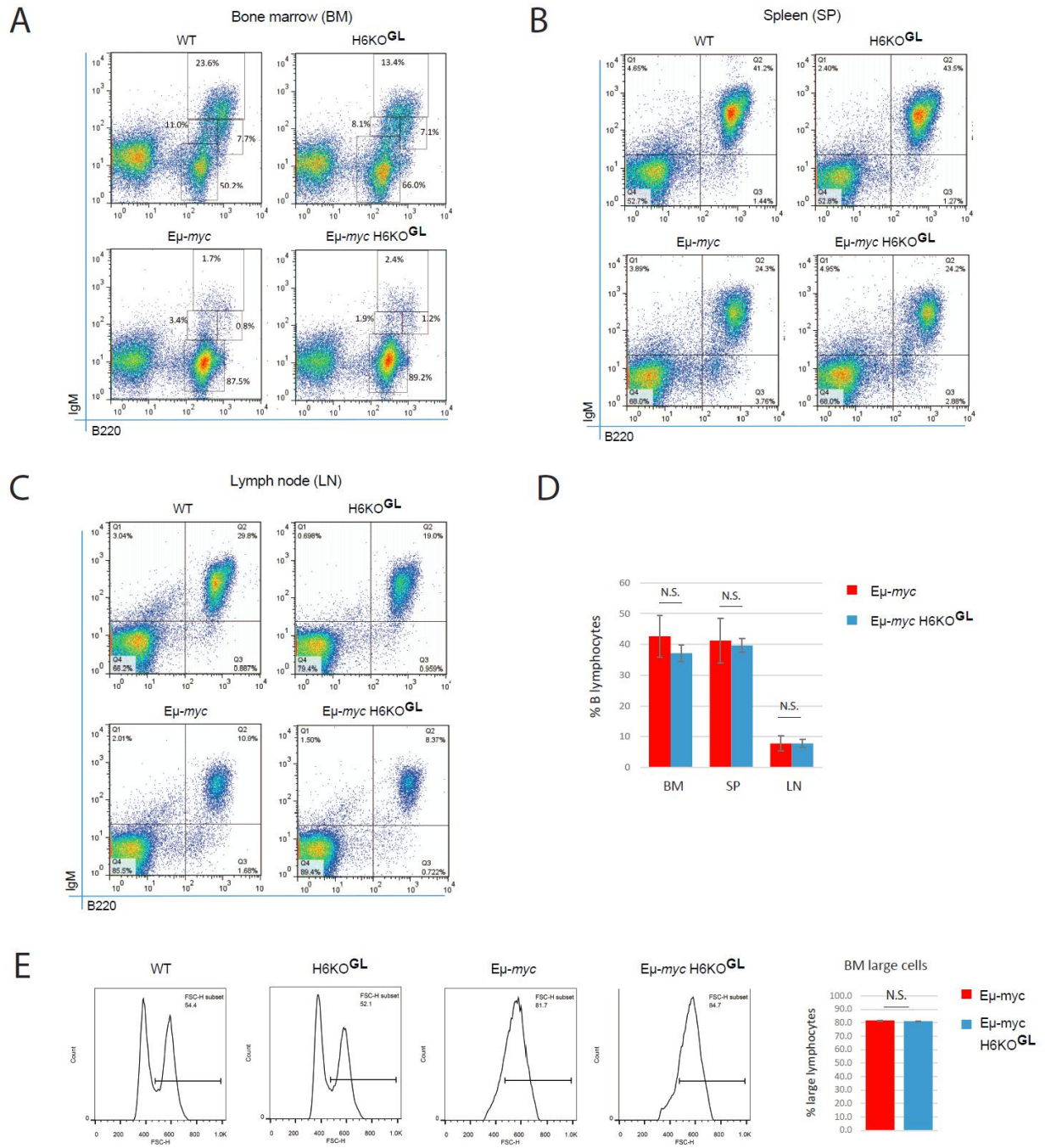
Suppl. Figure 2



Suppl. Figure 3

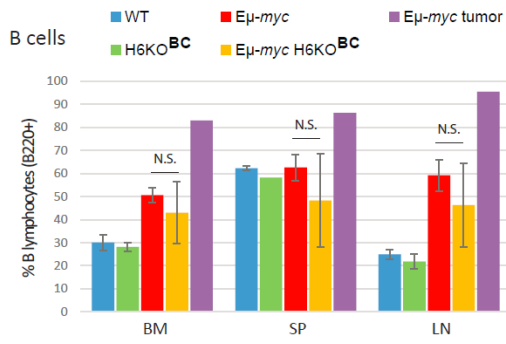


Suppl. Figure 4

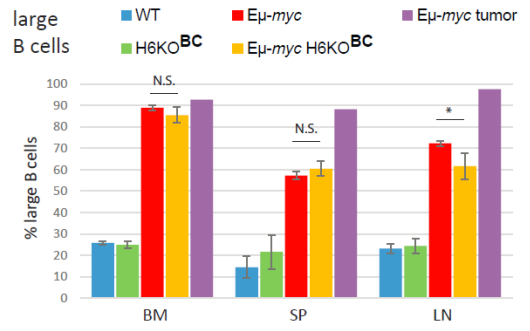


Suppl. Figure 5

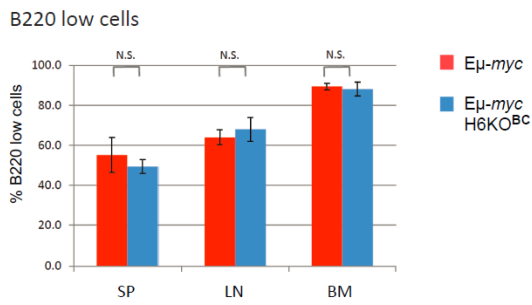
A



B



B



Discussion

Discussion

1. Hdac1 and Hdac2 in E μ -myc B cell lymphoma

In this study, using targeted conditional deletion of *Hdac1* and *Hdac2*, we investigated the functional role of these enzymes in normal B cells and the *E μ -myc* murine B cell lymphoma model. Our data reveal a predominant role of *Hdac1* in both non-malignant B cells and *E μ -myc* tg B cells. We demonstrate that *Hdac1* and *Hdac2* have a gene dose-dependent pro-oncogenic role in *E μ -myc* tumorigenesis with a predominant role of *Hdac1*. Our results highlight the tumor promoting role of Hdac1 and Hdac2, in both *E μ -myc* tumorigenesis and tumor maintenance.

Hdac1 and Hdac2 have no tumor suppressor functions in B cells

In accordance with previous studies (Yamaguchi et al., 2010), our results show that Hdac1 and Hdac2 do not have a tumor suppressor function in B lymphocytes (Figure 1). We found that ablation of *Hdac1* and/or *Hdac2* in non-malignant B cells did not lead to spontaneous tumor development, in contrast to T cells (Dovey et al., 2013; Heideman et al., 2013), and epidermal cells (Winter et al., 2013), in which *Hdac1* and *Hdac2* were reported to act as tumor suppressors. Consistently, we found that in B cells, Hdac1 and 2 do not regulate *Jdp2* (Suppl. Figure 1B), a *myc*-collaborating gene which has been reported to be regulated by Hdac1 and Hdac2 in T cells to constrain *myc*-overexpressing cells from progressing into lymphomas (Heideman et al., 2013). One plausible interpretation of this apparent discrepancy between our data and these previous studies could be a cell type specific role of Hdac1 and Hdac2.

Hdac1 and Hdac2 have pro-oncogenic roles in E μ -myc tumorigenesis

We further investigated the function of Hdac1 and Hdac2 in the *E μ -myc* murine B cell lymphoma model. In accordance with previous reports using HDACis in B lymphoid cancer models (Falkenberg and Johnstone, 2014; Haery et al., 2015; West and Johnstone, 2014), we could demonstrate that Hdac1 and Hdac2 have pro-oncogenic roles during *E μ -myc* tumorigenesis (Figure 2). Interestingly, these findings differ from previous studies using a skin tumor model (Winter et al., 2013), or acute promyelocytic leukemia (APL) (Santoro et al., 2013), in which Hdac1 (but not Hdac2) was reported to act as tumor suppressor during tumorigenesis. Interestingly, and consistent with our findings, this was not observed in another Acute Myeloid leukemia (AML) subtype close to APL (Matthews et al., 2015). Importantly, Santoro et al., reported that pharmacological inhibition of Hdacs phenocopied the effect of Hdac1 short hairpin RNA (shRNA) knockdown (KD) only in APL, but not in *E μ -myc* tumorigenesis (Santoro et al., 2013). This divergence indicates that a tumor type or oncogene-specific effects may be at play. These different findings may also be due to off targets effects of shRNA used in these studies. shRNA induce a broad variety of sequence-non-specific effects, including the deregulation of cellular microRNAs (miRNAs) levels (Olejniczak et al., 2016). Interestingly, the deregulation of miRNA expression is a common event in cancer (Volinia et al., 2006). Furthermore, miRNAs have been shown to have a direct role in lymphomagenesis (Olejniczak et al., 2016). Hence, it is tempting to speculate that off targeted miRNAs may accelerate tumor development. Thus, the contradicting phenotypes between our study and these previous studies might be explained by the following facts: First, genetic deletion is permanent, RNAi (RNA interference) knockdown is transient. Second, knockout leads to complete inactivity, RNAi is incomplete. Third, off-target effects in RNAi might be at play. Fourth, mouse backgrounds are different. Fifth, different cell

systems and cancer models were used. Furthermore, we speculate that differences between these systems is likely due to cell type/tissue-specific differences in composition of Hdac1/2 containing complexes and activities, resulting in different gene expression profiles. In agreement, it was previously observed that Hdac1 and Hdac2 have clear different target preferences (Yamaguchi et al., 2010) suggesting that they might regulate different set of genes in a cell type specific manner. The physiological activity of Hdac1 and Hdac2 enzymes is governed by incorporation into Sin3a, NuRD, CoREST and NOD1 multiprotein co-repressor complexes (Brunmeir et al., 2009; Yang and Seto, 2008). However, the molecular specificities of different isoforms of Hdac1 and 2 containing complexes are still undefined. Increasing body of evidence indicates a heterogeneity in their composition (Kelly and Cowley, 2013). Thus, it is difficult to determine which specific Hdac and/or complex is responsible for a specific effect. Importantly, some evidence suggests that the composition of these complexes might also be cell-type specific (Kelly and Cowley, 2013).

Complete Hdac1 and Hdac2 ablation ($Hdac1^{\Delta/\Delta};Hdac2^{\Delta/\Delta}$) prevents both, E μ -myc tumorigenesis and tumor maintenance

We further show that complete deletion of both *Hdac1* and *Hdac2* ($Hdac1^{\Delta/\Delta};Hdac2^{\Delta/\Delta}$) prevents E μ -myc tumorigenesis (Figure 3). Consistently, we found that $Hdac1^{\Delta/\Delta};Hdac2^{\Delta/\Delta}$ prevents E μ -myc splenomegaly, HG-NHL occurrence, reduces leukemia, and prevents the B cell blasts which dominate the BM of E μ -myc mice. These findings reveal that $Hdac1^{\Delta/\Delta};Hdac2^{\Delta/\Delta}$ prevents tumorigenesis already in the BM by preventing E μ -myc induced blast at early B cell stages. This is in agreement with our previous report in non-transformed B cells, where $Hdac1^{\Delta/\Delta};Hdac2^{\Delta/\Delta}$ induced a cell cycle block at PreBII cell stage (Yamaguchi et al., 2010). We next investigated the

direct impact of $Hdac1^{Δ/Δ};Hdac2^{Δ/Δ}$ on existing Eμ-*myc* tumor cells using an *in vivo* transplantation approach. We found that conditional ablation of *Hdac1* and *Hdac2* in tumor cells also delays tumor appearance (Figure 4). These findings show that $Hdac1^{Δ/Δ};Hdac2^{Δ/Δ}$ has a direct impact on Eμ-*myc* tg B cells. Altogether, these results demonstrate a critical pro-oncogenic role of Hdac1 and Hdac2 not only in Eμ-*myc* tumorigenesis but also in tumor progression.

Hdac1 and Hdac2 are not completely redundant; Hdac1 has a redominant role

Interestingly, we observed that single ablation of either *Hdac1* ($Hdac1^{Δ/Δ};Hdac2^{+/+}$) or *Hdac2* ($Hdac1^{+/+};Hdac2^{Δ/Δ}$) had no effect. Whereas Eμ-*myc* mice with a single allele of *Hdac2* ($Hdac1^{Δ/Δ};Hdac2^{Δ/+}$), but not with a single allele of *Hdac1* ($Hdac1^{+/Δ};Hdac2^{Δ/Δ}$), presented a delayed tumor development (Figure 2). This clearly demonstrates that Eμ-*myc* tumorigenesis is *Hdac1* and *Hdac2* gene dose-dependent, with a predominant role of *Hdac1*. Hence, a critical level of Hdac1 and Hdac2 is required for Eμ-*myc* tumorigenesis. Several other studies reported a similar dosage-dependent effect of *Hdac1* and *Hdac2* in epidermis (Winter et al., 2013), T cells (Heideman et al., 2013), neural cells (Hagelkruys et al., 2014).

Consistently, we observed that non-malignant B cell development is also *Hdac1* and *Hdac2* gene dose-dependent, with a predominant role of *Hdac1* (Figure 6). We previously showed that in a non-malignant background B cell differentiation occurs normally in absence of either Hdac1 or Hdac2, but that ablation of both, resulted in a B cell developmental block. In this study, we further investigate the individual and redundant function of Hdac1 and Hdac2 in normal B cell development, by expressing single alleles of either *Hdac1* or *Hdac2* in the absence of the respective paralog in B cells. We show that mice with a single allele of Hdac2 in B cells ($Hdac1^{Δ/Δ};Hdac2^{Δ/+}$) had significant impact on B cell development, and significant reduction in

total Hdac activity, indicating that one allele of Hdac2 is not sufficient to maintain proper B cell development (Figure 6). In contrast, mice with only one allele of Hdac1 (*Hdac1*^{+/-};*Hdac2*^{Δ/Δ}) showed no significant changes in B cell development and Hdac activity. Thus, our data indicate that a critical level of Hdac1 and Hdac2 (at least one allele of *Hdac1* or both alleles of *Hdac2*) is required for B cell development to occur normally. Interestingly, we observed that *Hdac1*^{Δ/Δ};*Hdac2*^{Δ/+} B cells had significantly reduced Hdac activity compared to *Hdac1*^{+/-};*Hdac2*^{Δ/Δ} B cells. Altogether, these data demonstrate a predominant role of Hdac1, and suggest that a critical level of Hdac activity may be required for Eμ-*myc* tumorigenesis and proper B cell development.

Here, we observe that one allele of *Hdac1*, but not *Hdac2*, can compensate for the loss of the other paralog in B cells (Figure 2 and Figure 6). Consistently, haploinsufficiency of *Hdac2* in absence of Hdac1 has also been reported in epidermal cells (Winter et al., 2013) and T cells (Dovey et al., 2013). Interestingly, the opposite effect was observed in neural cells (Hagelkruys et al., 2014): They demonstrated a predominant effect of Hdac2 in neural progenitor cell during brain development. They found that one allele of *Hdac2* but not *Hdac1* is sufficient for normal brain development in absence of its paralog. Similarly, a predominant role of Hdac2 was also observed in oocytes (Ma and Schultz, 2013). This different phenotype might be explained by cell-type-specific expression pattern of Hdac1 and Hdac2 (Hagelkruys et al., 2014; MacDonald and Roskams, 2008). Taken together, these different observations indicate that Hdac1 and Hdac2 have overlapping but specific functions during mouse development, which can differ between cell types and tissues. We therefore conclude that Hdac1 and Hdac2 have only partially redundant functions, with a predominant role of Hdac1 in B cells.

Our observations are also consistent with some previous studies reporting some enzyme specificities for Hdac1 and Hdac2. For example, Hdac1 and Hdac2 are not redundant during mouse embryogenesis, since the two paralogs cannot compensate for each other (Lagger et al., 2002; Trivedi et al., 2007; Zupkovitz et al., 2010). Interestingly, Hdac1, but not Hdac2 was shown to be essential in this process: deletion of Hdac1 impairs cell cycle and results in embryonic lethality (Lagger et al., 2002), whereas deletion of Hdac2, leads to perinatal lethality, partial embryonic lethality or partial postnatal lethality, depending on the knockout strategy (Guan et al., 2009; Montgomery et al., 2007; Reichert et al., 2012; Trivedi et al., 2007; Zimmermann et al., 2007; Zupkovitz et al., 2010). Similarly, Hdac1, but not Hdac2, has been shown to control embryonic stem cell differentiation (Dovey et al., 2010).

We observe that Hdac1 can compensate for the loss of the other paralog in B cells. We found that this compensation occurs at protein level (Figure 6E), but not at mRNA level (Suppl. Figure 1B), indicating a posttranslational compensatory mechanism as previously reported (Winter et al., 2013). Interestingly, ablation of Hdac1 resulted in massive increase in Hdac2 protein levels. However, this increase of Hdac2 upon Hdac1 KO is not sufficient to compensate for the absence of Hdac1, highlighting the predominant role of Hdac1. Interestingly, Hdac1 may act independently of Hdac2, as shown by co-immunoprecipitation experiments revealing that 40% of Hdac1 exist independently of Hdac2 (Yamaguchi et al., 2010). This may explain specific non-redundant functions of Hdac1. Consistently, several other studies reported that ablation of either Hdac1 or Hdac2 led to increased expression of the other paralog (Chen et al., 2011; Dovey et al., 2010; Jurkin et al., 2011; Lagger et al., 2002; Lagger et al., 2010; Santoro et al., 2013; Wilting et al., 2010; Yamaguchi et al., 2010; Zupkovitz et al., 2006).

Hdac1^{Δ/Δ};Hdac2^{Δ/+} impacts on proliferation and apoptosis of Eμ-myc B cells

Similar to *Hdac1^{Δ/Δ};Hdac2^{Δ/Δ}*, we found that *Hdac1^{Δ/Δ};Hdac2^{Δ/+}* impacts on Eμ-myc tumorigenesis by reducing the Eμ-myc induced blast at early preBII cell stage in the BM, resulting in reduced circulating tumor cells (Figure5). We further investigated whether the impact of *Hdac1^{Δ/Δ};Hdac2^{Δ/+}* in Eμ-myc B cells could be due to proliferation defects and/or apoptosis. Strikingly, we found that *Hdac1^{Δ/Δ};Hdac2^{Δ/+}* decreased proliferation and increased apoptosis in Eμ-myc B cells (Figure 7). These findings are consistent with earlier studies reporting that complete loss of Hdac1 and Hdac2 induces cell death in proliferating cells, including B and T cells (Dovey et al., 2013; Heideman et al., 2013; Reichert et al., 2012; Yamaguchi et al., 2010). Interestingly, combined deletion of both, Hdac1 and 2, has been shown to induce a cell cycle block only in proliferating cells, whereas their deletion in postmitotic, (resting) cells had no effect (Haberland et al., 2009a; Yamaguchi et al., 2010). Hence, this clearly shows, that dual loss of Hdac1/2 is not compatible with proliferation. Several labs including ours reported that Hdac1 and Hdac2 regulate G1-S-phase transition of the cell cycle by increasing the levels of cyclin-dependent kinase inhibitors (CKI) including p21^{WAF/CIP1}, p27^{KIP1}, and p57^{KIP2} preventing cell cycle progression in different cellular systems including primary and transformed cells (Lagger et al., 2002; Senese et al., 2007; Yamaguchi et al., 2010; Zupkovitz et al., 2010). In this study we observe that *Hdac1^{Δ/Δ};Hdac2^{Δ/+}* reduces proliferation of Eμ-myc tg B cells. Although the mechanism underlying this proliferation defect remains elusive, it is tempting to speculate that similar pathways could be activated upon loss of these enzymes in Eμ-myc tg B cells. In contrast, loss of Hdac1 was linked to enhanced proliferation in T cells (Dovey et al., 2013; Grausenburger et al., 2010; Heideman et al., 2013) and epithelial cells (Lagger et al., 2010; Winter et al., 2013). The reason for this discrepancy is still unclear, but it suggests that the

impact of Hdac1 (and Hdac2) on proliferation is dependent on the cell type and possibly on its corresponding target genes.

We observed, that *Hdac1^{Δ/Δ};Hdac2^{Δ/+}* increases apoptosis in Eμ-*myc* tg B cells. Consistently, apoptosis has been shown to be increased upon combined loss of Hdac1 and Hdac2 in many different cell types, including B cells (Yamaguchi et al., 2010), T cells (Heideman et al., 2013), fibroblasts (Haberland et al., 2009a), keratinocytes (Winter et al., 2013), and others (Hagelkruys et al., 2014; Jacob et al., 2011; Ma et al., 2012; Montgomery et al., 2007). Interestingly, Eμ-*myc* driven tumorigenesis requires inactivation of apoptosis for malignant transformation to occur (Eischen et al., 1999). Resistance to apoptosis in tumors arising in Eμ-*myc* transgenic mice is frequently acquired through spontaneous inactivation of the ARF-Mdm2-p53 tumor-suppressor pathway (Eischen et al., 1999). Interestingly, Hdac1 was shown to deacetylate p53, which is then destabilized and degraded, and thereby represses p53-dependent transcription (Ito et al., 2002; Luo et al., 2000; Tang et al., 2008). In line with this, Hdac1 and Hdac2 were shown to be the major targets for HDACi-mediated apoptosis induction (Inoue et al., 2006). Altogether, these findings demonstrate that *Hdac1^{Δ/Δ};Hdac2^{Δ/+}* reduces Eμ-*myc* induced blast in the BM and delays tumorigenesis by decreasing proliferation and inducing apoptosis.

Future medical impact

Our results provide an insight into the important pro-oncogenic roles of Hdac1 and Hdac2 in Eμ-*myc* tumorigenesis. Our study is fully consistent with the use of HDACis in clinics: Currently, four pan-HDACis, targeting classI and/or classII HDACs (Bantscheff et al., 2011), varinostat, romidepsin, belinostat, and panobinostat, are Food and Drug Administration (FDA)-approved for the following hematological malignancies: Cutaneous T cell lymphoma (CTCL), Peripheral T

cell lymphoma (PTCL) and multiple myeloma (Ghobrial et al., 2013; Rasheed et al., 2008; Richardson et al., 2013; San-Miguel et al., 2013), and several others are in clinical trials for various cancers, including B cell malignancies (Haery et al., 2015). Previous studies already demonstrated that pan-HDACis have therapeutic efficacy in E μ -myc lymphoma (Ellis et al., 2009b; Lindemann et al., 2007; Newbold et al., 2008; Newbold et al., 2013; Newbold et al., 2014). However, until recently, it was still not known whether single HDAC1 or HDAC2 isoform-selective inhibitors would impact on cell growth and/or survival. Our findings demonstrate that HDAC1 and HDAC2 can be considered as important players in E μ -myc tumorigenesis suggesting that selective HDAC1 and HDAC2 inhibitors could be effective for the treatment of BL, modeled by our preclinical E μ -myc system, and possibly other hematological malignancies including DLBCL. This provides a rationale for the development of Hdac1 and/or Hdac2 isoform-selective inhibitors. However, there are currently no available HDAC1-specific and only few HDAC2-specific inhibitors (Wagner et al., 2015), but there are several compounds capable of inhibiting both HDAC1 and HDAC2. For example, two novel HDAC1 and Hdac2 isoform selective inhibitors, RGFP233 (Matthews et al., 2015) and MRLB-223 (Newbold et al., 2013), were shown to induce apoptosis in E μ -myc lymphoma cells *in vitro* and *in vivo*, respectively. Two other Hdac1 and Hdac2 isoform specific HDACis; K560 (Choong et al., 2016) and Cpd60 (Methot et al., 2008; Schroeder et al., 2013; Stubbs et al., 2015) were recently tested in other disease models but not in E μ -myc model. Although several of these agents were shown to have an *in vitro* and/or *in vivo* therapeutic efficacy in pre-clinical models like E μ -myc, it is possible that different drugs may have different mechanistic, biological, and therapeutic activities. Furthermore, it is still unclear whether selective HDAC1 and HDAC2 inhibition might

have comparable therapeutic benefit and limit toxicity observed with these broad-spectrum inhibitors (Dawson and Kouzarides, 2012; Ononye et al., 2012).

Interestingly, we found human HDAC1 but not human HDAC2 mRNA expression is increased in some Burkitt's lymphoma (BL) and diffuse large B cell lymphoma (DLBCL) cancer cell lines and human lymphoma samples compared to other cancer cell types and other human cancer samples, respectively (Suppl. Figure 3). Hence, these data are consistent with our findings outlined above, revealing a predominant role of Hdac1. Comprehensive knowledge about the different expression profiles as well as their specific involvement in the different disease settings is crucial for future use in personalized therapies. The current aim in HDAC cancer drug discovery is to find predictive biomarkers that can predict responsiveness to HDACi therapy (Stimson and La Thangue, 2009). Further work is required to determine whether tumor cells with low HDAC activity are more responsive to HDAC inhibition. If this is the case, decreased HDAC-activity might be used as a predictive marker for HDACi sensitivity. Hence, in a clinical setting, patients having tumors with low HDAC activity level could benefit more from HDACis, whereas patients having tumors with high levels of HDAC activity would need higher doses of the inhibitor.

General conclusion - Hdac1 and Hdac2

In conclusion, our results demonstrate that Hdac1 and Hdac2 promote tumor initiation and tumor progression in E μ -myc mice by regulating proliferation and apoptosis. This is the first study showing a gene dose-dependent pro-oncogenic role of *Hdac1* and *Hdac2* in tumorigenesis.

Despite improved knowledge about the function of these Hdacs, many aspects remain unexplored. Future research will focus on identifying which Hdac isoforms are relevant in the

different cancer types. Future studies may use knockin mice with catalytically inactive Hdac1 and Hdac2 and mutant forms of Hdac1 and Hdac2 which bind only to specific co-repressor complexes. Most importantly, future research will focus on elucidating the underlying molecular mechanism, by which Hdac1 and Hdac2 regulate proliferation and apoptosis in malignant and non-malignant cells. The comprehension of these and other mechanisms will help to design selective HDACis with possibly less side effects than pan-HDACis. The predominant role of Hdac1 that we unravel in this study, raises the prospect of using selective HDAC1 inhibitor in clinics for the treatment of BL and other B cell lymphomas with Myc deregulation.

2. Hdac1 and Hdac2 in B cell development

In collaboration with R.M. Heideman, I investigated the role of Hdac1 and Hdac2 in B cell development. We could confirm our previous findings (Pillonel *et al.*, *Accepted for publication in Scientific Reports*) that Hdac1^{Δ/Δ};Hdac2^{Δ/+}, but not Hdac1^{+/-};Hdac2^{Δ/Δ} leads to severely affected B cell development with a partial developmental block at the PreBI cell stage, and significantly reduced number of PreBII (Suppl. Figure 2). In addition, we demonstrate that Hdac1^{Δ/Δ};Hdac2^{Δ/+} mice have significantly reduced immature B cells. Importantly, we also observe, that Hdac1^{Δ/Δ};Hdac2^{Δ/+} mice have normal numbers of splenic B cells (Suppl. Figure 2). This indicates that the few PreBII cells left in Hdac1^{Δ/Δ};Hdac2^{Δ/+} mice are sufficient to eventually fill up the pool of mature B cells in the secondary lymphoid organs, including SP.

We further investigated whether the observed impact of Hdac1^{Δ/Δ};Hdac2^{Δ/+} on PreBI and PreBII cells could be due to proliferation defects or apoptosis. Interestingly, we show that upon Hdac1^{Δ/Δ};Hdac2^{Δ/+}, PreBII cells proliferate less (Figure 2). These findings are fully consistent with earlier studies reporting that complete loss of Hdac1 and Hdac2 (Hdac1^{Δ/Δ};Hdac2^{Δ/Δ}) induces a cell cycle block at PreBII cell stage (Yamaguchi et al., 2010). Consistently, we observe that upon Hdac1^{Δ/Δ};Hdac2^{Δ/+}, PreBII are also arrested in G₀/G₁-phase of the cell cycle (Figure 1A). Furthermore, apoptosis has been shown to be increased upon Hdac1^{Δ/Δ};Hdac2^{Δ/Δ} in B cells (Yamaguchi et al., 2010). In contrast, our preliminary data did not show any increase in apoptosis in PreBII cells upon Hdac1^{Δ/Δ};Hdac2^{Δ/+} (Figure 2). Further experiments will be needed to confirm this.

Interestingly, we observed that in Hdac1^{Δ/Δ};Hdac2^{Δ/+} mice, PreBI cells express highly the stem cell marker c-kit, which suggests, that these PreBI cells remain probably in a less differentiated state (Suppl. Figure 2B). Consistently, we also found that Sca-1 is highly expressed at the surface

of *Hdac1^{Δ/Δ};Hdac2^{Δ/+}* PreBI cells (R.M.Heideman., data not shown). Interestingly, we observed that upon *Hdac1^{Δ/Δ};Hdac2^{Δ/+}*, PreBI cell proliferate more and undergo less frequently apoptosis (Figure 2). These findings could suggest that *Hdac1^{Δ/Δ};Hdac2^{Δ/+}* PreBI cells might undergo less frequently apoptosis because they might have a problem with V(D)J recombination, and hence, could not differentiate to PreBII cells. This would explain the massive decrease in PreBII cell number we observe in *Hdac1^{Δ/Δ};Hdac2^{Δ/+}* mice (Suppl. Figure 2B). We therefore performed flow cytometry analysis of intra cellular IgM staining. Our preliminary results demonstrate, that *Hdac1^{Δ/Δ};Hdac2^{Δ/+}* decreases intra cellular IgM⁺ in PreBI cells (Figure 3A). Our preliminary findings could suggest that less IgM rearrangement is occurring in *Hdac1^{Δ/Δ};Hdac2^{Δ/+}* PreBI cells. The IL7 receptor alpha (IL7Ra), is crucial for V(D)J rearrangement of heavy chain in PreBI cells, and light chain in PreBII cells, by (Corcoran et al., 1998; Hamel et al., 2014). Interestingly, and consistent with the findings outlined above, we also found that IL7Ra expression is slightly reduced in PreBI cells and in large PreBII cells of *Hdac1^{Δ/Δ};Hdac2^{Δ/+}* mice (R.M. Heideman, data not shown).

Our preliminary results provide an insight into the role of Hdac1 and Hdac2 in B cell development. Future research directions will focus on investigating the role of these enzymes in V(D)J recombination and IgH and IgL allelic exclusion. We hypothesize that PreBI cells cannot differentiate to PreBII because they have less intra IgM due to a problem with V(D)J recombination. Future experiments will be needed to test this hypothesis. This could be done for example by trying to rescue phenotype *in vivo* with a V(D)J knock in mouse. If our hypothesis is correct, one then could test for the recombination activation genes 1 (RAG1) and 2 (RAG2), V(D)J locus contraction by PCR or by FISH, as well as locus acetylation upon *Hdac1^{Δ/Δ};Hdac2^{Δ/+}*.

We observed that *Hdac1^{Δ/Δ};Hdac2^{Δ/+}* mice have increased H3-acetylation (Suppl. Figure 2), and normal number of B cells (R.M. Heideman, data not shown). Future research will investigate the impact of altered acetylation (upon *Hdac1^{Δ/Δ};Hdac2^{Δ/+}*) on class switch recombination (CSR) and somatic hyper mutation (SHM) in the SP. We hypothesize that in *Hdac1^{Δ/Δ};Hdac2^{Δ/+}* B cell with high H3-Ac H4-Ac, the Ig locus would be more open, and this could have an impact on CSR. To test this, one could challenge cells with IL-4 and CD40, which activates the activation induced cytidine deaminase (AID), the initiator of both CSR and SHM, and measure CSR by flow cytometry and test SHM by sequencing.

In conclusion, our result demonstrate that *Hdac1^{Δ/Δ};Hdac2^{Δ/+}* mice have abnormal early B cell development and suggests possible defects in V(D)J recombination. Despite improved knowledge about the function of Hdac1 and Hdac2, many aspects still remain unexplored. Future research will be needed to dissect the exact functional role of Hdac1 and Hdac2 in B cell development, and to characterize the underlying molecular and regulatory mechanisms. We already performed an RNA-seq analysis in PreBI cells from *Hdac1^{Δ/Δ};Hdac2^{Δ/+}* vs control *Hdac1^{+/+};Hdac2^{+/+}* mice, and found several up- and downregulated genes, and are currently validating these hits (R.M. Heideman, data not shown).

In the case that V(D)J recombination, CSR or SHM are affected in *Hdac1^{Δ/Δ};Hdac2^{Δ/+}* B cells, it would be interesting to test whether these processes are also affected during Eμ-*myc* tumorigenesis upon *Hdac1^{Δ/Δ};Hdac2^{Δ/+}*. This could help to uncover mechanisms by which *Hdac1^{Δ/Δ};Hdac2^{Δ/+}* delays Eμ-*myc* tumorigenesis (Pillonel *et al.*, *Accepted for publication in Scientific Reports*), and ultimately, will help to better understand the function of the two pro-oncogenic proteins Hdac1 and Hdac2 in B lymphoid malignancies.

3. Hdac6 in E μ -myc B cell lymphoma

In this side project, we investigated the functional role of Hdac6 in the E μ -myc murine B cell lymphoma model. We used mice with Hdac6 OE (H6OE), Hdac6 B cell specific conditional KO (H6KO^{BC}), and Hdac6 germ line knockout (H6KO^{GL}). Three main findings arise from this study. First, we show that H6OE accelerates lymphomagenesis, whereas H6KO^{GL} may delay tumor development in E μ -myc mice (Figure 2). Second, H6OE increases, and H6KO^{GL} decreases the percentage of PBL at early stages of E μ -myc tumorigenesis (Figure 3). Third, H6OE increases (Figure 4) and H6KO^{GL} decreases tumor cell load in E μ -myc mice (Figure 5). Our data show that Hdac6 plays a pro-oncogenic role during E μ -myc tumorigenesis.

We observe that high human *HDAC6* expression predicts poor prognosis in DLBCL patients (online available datasets on DRUGSURV). This observation is consistent with previous studies reporting that HDAC6 is overexpressed in several lymphoid malignancies including ALL (Bradbury et al., 2005; Moreno et al., 2010; Van Damme et al., 2012), AML (Bradbury et al., 2005), CLL (Van Damme et al., 2012; Wang et al., 2011) and CTCL (Marquard et al., 2008), and DLBCL (Marquard et al., 2009; Zhang et al., 2004). In accordance, HDAC6 was shown to have oncogenic roles in AML (Bradbury et al., 2005), and was also found to be overexpressed in advanced stage of ALL (Bradbury et al., 2005). However, HDAC6 may also play a role as tumor suppressor (Seidel et al., 2015). OE of *HDAC6* correlates with a good prognosis in DLBCL (Marquard et al., 2009), CLL (Van Damme et al., 2012) and CTCL (Marquard et al., 2008) and *HDAC6* underexpression was found to be correlated with a poor prognosis in CLL (Van Damme et al., 2012). Hence, the exact role of HDAC6 in the different cancer types remains elusive.

Interestingly, we found that only H6KO^{GL}, but not H6KO^{BC}, had an impact on tumor cell load. The cause of this difference is presently unclear. It is tempting to speculate that tumor cell

extrinsic effects in the tumor microenvironment might be at play. In this context, targeting all cell using Hdac6 isoform-selective HDACis, like tubacin, might be useful. Our data suggest that such Hdac6 specific HDACis may provide some antitumor effects, and may be effective for the treatment of hematological malignancies modeled by our preclinical *Eu-myc* system.

Further work is required to elucidate the molecular mechanism by which Hdac6 impacts on *Eμ-myc* tumorigenesis. It would be interesting to investigate the impact of HOE and H6KO on HSP90 client oncoproteins, which have been proposed to be degraded upon HDACi treatment (Bolden et al., 2006). Such proteins were shown to be involved in invasion and metastasis (Yang et al., 2008). Besides this, it would be interesting to test other pathways which could be affected in this context. Hdac6 has been shown to be implicated not only in cell motility, and EMT (Shan et al., 2008), but also in proliferation of cancer cells (Hagelkruys et al., 2011; Lee et al., 2008),

In conclusion, our findings highlight the tumor promoting role of Hdac6 in *Eμ-myc* tumorigenesis, and opens new avenues of research for the future.

Material and methods

Material and methods

Experimental mice

The *Hdac1^{F/F};Hdac2^{F/F}* conditional knockout (cKO) mice were as described in the manuscript Pillonel *et al.* (Result Part1). *Hdac6* germ line knockout (H6KO^{GL}), and *Hdac6* conditional KO mice were generated in the lab by Dr. Yu Zhang (Zhang *et al.*, 2008). *Hdac6* overexpressing (H6OE) mice were generated previously by Dr. Yu Zhang in the lab (unpublished). To generate these mice, a Bacterial Artificial Chromosome (BAC) clone (50M7) which contains the murine *Hdac6* gene (Means *et al.*, 2000) was injected into the pronucleus of fertilized mouse oocytes. Founders were screened by PCR and Southern blot. Overexpression of HDAC6 protein was confirmed by Western blot. BAC tg mice overexpressing *Hdac6* (H6OE) were crossbred with E μ -*myc* tg mice. B lymphocyte specific deletion of *Hdac6* (H6KO^{BC}) was obtained using heterozygote Mb1-cre transgenic (tg) mice (Hobeika *et al.*, 2006) in combination with *Hdac6* cKO (floxed) alleles. All these mice were interbred to heterozygote E μ -*myc* tg mice as described in the manuscript Pillonel *et al.* (Result Part1). All experiments were done with mice in pure C57BL/6 (Ly5.2⁺) genetic background (backcrossing at least 11 generations). Mice were bred and housed as described in the manuscript Pillonel *et al.* (Result Part1). All animal experiments were approved and carried out according to regulations effective in the Kanton of Basel-Stadt, Switzerland.

Genotyping PCR

Polymerase chain reaction (PCR)–based genotyping was performed on tail-derived DNA. Mice were genotyped for *Hdac1* and *Hdac2* conditional alleles, E μ -*myc* tg, Mb1-Cre tg and Actin-Cre

tg, as described in the manuscript Pillonel *et al.* (Result Part1). Genotyping for Hdac6 germline KO (H6KO^{GL}) and Hdac6 B cell specific KO (H6KO^{BC}) was determined by PCR, with primers spanning the deleted Exons of the HDAC6 gene (Zhang et al., 2008). Primers P1 (Forward; 5'-GTA CAA TGT GGC TCA CAG AA) and P45 (Reverse; 5'-CAG GCA CAG GAA TAT GAG TT) were used to detect the wild type (WT) and floxed (FL) alleles, and P1 and P42 (Reverse; 5'-CAA CTC TGC CTC TCC TGG AT) to detect the knockout (KO). For detecting the HDAC6 overexpressing BAC construct (H6OE), we used: Forward; 5'-CCG TCG ACC AAT TCT CAT GT, and Reverse; 5'-CGC AAG ATG TGG CGT GTT AC. PCRs were performed using the GoTaq Flexi DNA Polymerase Kit (Promega, Cat.M8306) and MJ Mini Thermal Cyclers (BioRad).

RNA isolation and Quantitative Real-Time PCR (RT-qPCR)

Quantitative real-time PCR (RT-qPCR) analysis was performed as described in the manuscript Pillonel *et al.* (Result Part1). The following primers were used: Hdac1 (forward; 5'-ACG GCA TTG ACG ACG AAT C; and reverse; 5'-TAA GAC CAC TGC ACT AGG CTG G); for Hdac2 (forward; 5'-CCA GAG GAT GCT GTT CAT GA; and reverse; 5'-GCT ATC CGT TTG TCT GAT GCT); Jdp2 (forward; 5'-CGC TGA CAT CCG CAA CAT TG; and reverse; 5'-CAT CTG GCT GCA GCG ACT TT).

Histopathological analysis and Immunohistochemistry (IHC)

Tumor sections from LN, SP, thymus, (lung, heart, liver) were fixed in formalin (Shandon Formal-Fixx, Thermo Scientific, Cat.9990244) for 24h. Tissues were transferred in embedding cassettes and kept in 70% ethanol for 30 min before dehydration in the medite tissue processor

(TPC15) and subsequent embedding in paraffin. Paraffin-embedded tissue were cut in 3- μ m-thick sections with an automatic microtome (Microm HM355S, Thermo Scientific). Sections were subjected to classical hematoxylin and eosin (H&E) staining. Histopathological evaluation was performed by Prof. Dr. Alexandar Tzankov, an experienced hematopathologist and head of the histopathology & autopsy at the university hospital Basel. Examinations were first performed in blind by the pathologist to determine any pathological findings, and subsequently joint reviewed with the student V.P. using a multiheaded microscope. Pathological finding of high grade Non-Hodgkin Lymphoma (HG-NHL) (corresponding to Burkitt's lymphoma in men) were scored in these organ sections according to the Bethesda proposals for classification of lymphoid neoplasms in mice (Morse et al., 2002). Histopathological evaluation of sick *Hdac1^{Δ/Δ};Hdac2^{Δ/Δ}* mice was performed in collaboration with the pathologist Dr. Annabelle Heier (NIBR, Novartis Pharma, Basel).

Immunohistochemistry experiments were performed on Ventana DiscoveryUltra instrument (Roche Diagnostics, Mannheim) with the procedure RUO Discovery Universal. CC1 (Roche Diagnostics, Mannheim) pre-treatment was used for anti-HDAC1, -HDAC2, -c-Myc and -CD45 antibodies with the following incubation times: 16, 24, 72 and 32 min respectively. Antibodies were incubated for one hour at 37°C except for anti-c-Myc and -CD45 which were incubated for 16 and 32 min respectively. In addition, a blocking step (Innovex Background Buster NB306, Innovex, 12 min incubation) was added for anti-HDAC1 and -HDAC2 antibodies. Detection of bound anti-HDAC1, -HDAC2 and -c-Myc antibodies was achieved by using anti-rabbit HQ followed by anti-HQ horseradish peroxidase (Roche Diagnostics, Mannheim) incubated for 32 min at 37°C. To detect anti-CD45 a rabbit anti-rat linker was applied for 20 min at 37°C. Finally, bound anti-p53 and anti-B220 were detected by using a secondary antibody (ImmPRESS reagent

kit peroxidase anti-rabbit Ig MP-7401, Vector) applied manually (200 microliters) and incubated for 32 min at 37°C. ChromoMap DAB kit (Roche Diagnostics, Mannheim) was used for the detection and slides were counterstained with Hematoxylin II and Bluing Reagent (Roche Diagnostics, Mannheim) for 8 min. Hdac1 and Hdac2 staining were used to confirm the genotype of the lymphoma. Scoring for p53 staining intensity in E μ -myc tumors was performed by using a wild-type spleen as a negative control.

Immunofluorescent staining, flow cytometric analysis, and cell sorting

Flow cytometry analysis was performed as described in the manuscript Pillonel *et al.* (Result Part1). Intra cellular IgM staining was performed with anti-IgM conjugated to APC (clone II/41) using the cytofix/cytoperm method according to the manufacturer's instruction (BD Biosciences). Sorting was performed on the basis of forward (FSC) and side light scatter (SSC), by exclusion of doublets and by staining with the indicated B cell subset surface markers. Absolute cell numbers of B lymphoid subpopulations were determined by counting cells excluding Trypan Blue Dye and multiplying cell numbers by the percentage of cell subsets as determined by flow cytometry.

Oncomine, Cancer Cell Line Encyclopedia and DRUGSURV database analysis

Oncomine and Cancer Cell Line Encyclopedia database analysis was performed as described in the manuscript Pillonel *et al.* (Result Part1). The free online computational tool DRUGSURV was used to examine whether there is any correlation of HDAC1, HDAC2 and HDAC6 gene expression with survival outcome in patients with cancer (<http://www.bioprofiling.de/PPISURV>) (Amelio *et al.*, 2014; Antonov *et al.*, 2014).

Additional material and methods

The following methods were performed as described in the manuscript Pillonel *et al.* (Result Part1): **KPLM analysis, E μ -myc lymphoma transplantation, blood sampling and analysis, cell preparation, B cell isolation by MACS, In vivo cell cycle analysis by BrdU incorporation, Apoptosis assay, Protein extracts and Western blot analysis, In vitro Hdac-activity assay, Affymetrix expression analysis, Statistical analysis.**

Appendix



Hematopoietic Overexpression of FOG1 Does Not Affect B-Cells but Reduces the Number of Circulating Eosinophils

Camille Du Roure^{1#a}, Aude Versavel^{1,3}, Thierry Doll², Chun Cao¹, Vincent Pillonel^{1,3}, Gabriele Matthias¹, Markus Kaller^{1#b}, Jean-François Spetz¹, Patrick Kopp¹, Hubertus Kohler¹, Matthias Müller², Patrick Matthias^{1,3*}

1 Friedrich Miescher Institute for Biomedical Research, Basel, Switzerland, **2** Novartis Institutes for Biomedical Research, Basel, Switzerland, **3** Faculty of Sciences, University of Basel, Basel, Switzerland

Abstract

We have identified expression of the gene encoding the transcriptional coactivator FOG-1 (Friend of GATA-1; *Zfp1*, *Zinc finger protein multitype 1*) in B lymphocytes. We found that FOG-1 expression is directly or indirectly dependent on the B cell-specific coactivator OBF-1 and that it is modulated during B cell development: expression is observed in early but not in late stages of B cell development. To directly test *in vivo* the role of FOG-1 in B lymphocytes, we developed a novel embryonic stem cell recombination system. For this, we combined homologous recombination with the FLP recombinase activity to rapidly generate embryonic stem cell lines carrying a Cre-inducible transgene at the *Rosa26* locus. Using this system, we successfully generated transgenic mice where FOG-1 is conditionally overexpressed in mature B-cells or in the entire hematopoietic system. While overexpression of FOG-1 in B cells did not significantly affect B cell development or function, we found that enforced expression of FOG-1 throughout all hematopoietic lineages led to a reduction in the number of circulating eosinophils, confirming and extending to mammals the known function of FOG-1 in this lineage.

Citation: Du Roure C, Versavel A, Doll T, Cao C, Pillonel V, et al. (2014) Hematopoietic Overexpression of FOG1 Does Not Affect B-Cells but Reduces the Number of Circulating Eosinophils. PLoS ONE 9(4): e92836. doi:10.1371/journal.pone.0092836

Editor: Laurent Coen, Muséum National d'Histoire Naturelle, France

Received: November 4, 2012; **Accepted:** February 26, 2014; **Published:** April 18, 2014

Copyright: © 2014 Du Roure et al. This is an open-access article distributed under the terms of the Creative Commons Attribution License, which permits unrestricted use, distribution, and reproduction in any medium, provided the original author and source are credited.

Funding: This work was funded by the Novartis Research Foundation. The funders had no role in study design, data collection and analysis, decision to publish, or preparation of the manuscript.

Competing Interests: Thierry Doll and Matthias Müller are employed by Novartis Institutes for Biomedical Research. Camille Du Roure is employed by Actelion. There are no patents, products in development or marketed products to declare. This does not alter the authors' adherence to all the PLOS ONE policies on sharing data and materials.

* E-mail: matthias@fmi.ch

#a Current address: Actelion Pharmaceuticals Ltd, Allschwil, Switzerland.

#b Current address: Institute of Pathology, Ludwig-Maximilians-University Munich, München, Germany.

Introduction

The development of specialized hematopoietic cells from self-renewing hematopoietic stem cells proceeds through a number of precursor stages with progressively restricted differentiation potential and requires a complex interplay of transcription factors and epigenetic modifiers. These regulators are responsible for orchestrating the establishment of lineage-specific gene expression patterns that underlie cellular differentiation (reviewed in [1,2]). While many factors involved in this process are already known, a complete molecular understanding is still missing. Friend of GATA-1 (FOG-1), which is encoded by the *Zfp1* (*Zinc finger protein multitype 1*) gene, was previously thought to be expressed primarily in cells of the erythroid and megakaryocytic lineages, where it is essential for differentiation [3,4]. FOG-1 is a zinc finger protein initially identified as an interacting partner of GATA factors which contributes to activation or repression of their target genes [3,5,6]. FOG-1 also interacts with the C-terminal binding protein (CtBP), mainly described as a corepressor and the nucleosome remodelling and histone deacetylase repressive (NuRD) complex and thus makes a link between transcription factors and chromatin

modifiers. FOG-1 also activates or represses gene transcription by facilitating binding of GATA factors to DNA [7], recruiting chromatin remodelling complexes [5,8], or by stabilizing tissue-specific chromatin loops [9]. FOG-1 is expressed at high level in multipotent progenitors, erythroid and megakaryocytic cells, low level in lymphoid and haematopoietic stem cells; it is absent in myeloid lineages [3]. *Zfp1*-deficient mice lack megakaryocytes and show severe defects in erythropoiesis, leading to embryonic lethality [4]. FOG-1 also plays a role in the T-lineage by repressing GATA-3-dependent induction of Th2 development [10,11]. Interestingly, overexpression of FOG-1 in avian eosinophils, which do not normally express FOG-1, reprograms these differentiated cells into multipotent cells [12], reminiscent of the reprogramming of B-cells into macrophages following ectopic expression of C/EBPalpha and C/EBPbeta [13,14]. Thus, FOG-1 is essential for specific branches of the haematopoietic system, and its inappropriate expression leads to abnormal cell differentiation.

Strikingly, we have identified relatively high FOG-1 expression in early B-lymphocytes, and low or lack of expression in late developmental stages such as mature B-cells and plasma cells. In analogy to some of the systems mentioned above, we were

intrigued by the regulated expression of FOG-1 during B cell development and hypothesized that the downregulation of FOG-1 might be a necessary step for proper differentiation and function of mature B cells. We therefore set out to test this hypothesis and for this made use of a novel transgenic mouse model strategy based on recombination mediated cassette exchange (RMCE, [15,16]) which we had designed to generate mice with conditional overexpression of any cDNA. Using this system, we generated transgenic mice in which FOG-1 expression was enforced at a physiologically relevant level in mature B-cells or in the entire hematopoietic system. We found that sustained FOG-1 expression in mature and late B cells did not affect their development or function, contrary to our hypothesis. In contrast, overexpressing FOG-1 in the whole hematopoietic system led to a reduction in the number of circulating eosinophils, confirming and extending to mammals the previously reported role of FOG-1 in repressing avian eosinophil development.

Materials and Methods

Ethics statement

Animal experimentation was carried out according to regulations effective in the canton of Basel-Stadt, Switzerland. All experimental procedures were approved by the Animal Committee of the Friedrich Miescher Institute for Biomedical Research and the Veterinary office of the Kanton Basel Stadt.

Generation of the targeting pR26-SA-FRT-Hygro^r vector

The backbone of a pre-existing targeting vector pR26-STOP-FRT-Hygro [17] was adapted to allow transcription from the endogenous *Rosa26* promoter. After removal of the unwanted sequences, the backbone vector contained two homology arms and the hygromycin B resistance gene flanked by an FRT3 and an FRTwt sites in 5' and 3', respectively. The 5' and 3' homology arms correspond to Chr6: 113 024 284–113 026 000 and to Chr6: 113 021 493–113 024 090 using the mm9 assembly on the UCSC genome browser. The integration site maps about 2 kb downstream of the insertion point obtained with the targeting vector pROSA26-1 [18]. The splice acceptor sequence (SA) of the STOP-eGFP-Rosa26TV vector (Adgene plasmid 11739) was PCR amplified and cloned upstream of the FRT3 site [19]. The STOP sequence from Adgene plasmid 11739 is based on SV40 polyA sites.

Generation of the control and FOG-1 donor vectors

The backbone of the donor vector, containing the FRT3 site, a polyA sequence and the FRTwt site, was derived from the FRT3-CAG-lox-stop-lox-Enpp1-tkNeo-FRTwt [17] vector and was further modified as follows. The loxP-Neo-STOP-loxP cassette was PCR amplified from the STOP-eGFP-Rosa26TV vector (Adgene plasmid 11739) with 5'-tagcctaggtctcgcggctcttccagtggt-3' and 3'-atgcaccggctctcgggtaccgaattgatcg-5' containing an AvrII and an AgeI site, respectively. This fragment was cloned downstream of the FRT3 site using SpeI and AgeI sites. The IRES-hCD2t fragment was obtained from the pBS-IRES-hCD2t vector (kindly provided by M. Busslinger, Vienna, [20]) and cloned downstream of the loxP-Neo-STOP-loxP cassette. The resulting control donor vector FRT3-loxP-Neo-STOP-loxP-IRES-hCD2t-FRTwt harbors a unique NotI site in between the second loxP site and the IRES sequence. The FlagFOG-1 cDNA which is encoded by the *Zfpml* gene was obtained from a pcDNA3-FlagFOG-1 vector (kindly provided by M. Crossley, Sydney) and cloned in the NotI site of the control donor vector, resulting in the 10.9 kb FOG-1 donor

vector: FRT3-loxP-Neo-STOP-loxP-FlagFOG-1-IRES-hCD2t-FRTwt.

Targeting of ES cells

The SacI-linearized targeting pR26-SA-FRT-Hygro^r vector was electroporated into 129 sv jae ES cells. Electroporated ES cells were then selected with 0.1 mg/ml hygromycin B. 480 hygromycin-resistant clones were collected, and five potentially successfully recombined clones were identified by PCR screening using the following primer pair (0F: ctactggaaagaccgcgaag, 0R: tactttctgggagttctctgc, 2 kb product).

Southern blot analysis

Verification of ES cell targeting: 10 µg of genomic DNA was analyzed by standard Southern blotting. Genomic DNA was restricted with BamHI, PstI or PvuII to confirm the 5', 3' and single integration of the targeting vector, respectively. The 5' and 3' probes were PCR amplified from genomic DNA with the following primers: 5' fwd: cgcctaaagaagaggctgtg and 5' rev: gactggagttgcagatcacg; 3' fwd: agccatctgggacctttaa and 3' rev: aaggcacagacaatccttc. The 5' probe highlighted a 5.8 kb wild-type and a 4.9 kb targeted bands. The 3' probe detected a 6.5 kb wild-type and a 7.5 kb targeted bands. The internal hygromycin probe was obtained from the targeting vector and highlighted an 8 kb band.

Verification of the RMCE targeting: 20 µg of genomic DNA was analyzed by standard Southern blotting. Genomic DNA was digested with PvuII or BglII to confirm the 5', internal and 3' single integration of the donor vector, respectively. The 5' and 3' probes were PCR amplified from genomic DNA with the following primers: 5' fwd: cgcctaaagaagaggctgtg and 5' rev: gactggagttgcagatcacg and 3' fwd: ggacaggacagtcgttgaagg and 3' rev: acaccacaatgaacagtcgcaag. The 5' probe highlighted a 5.8 kb wild-type and a 6.3 kb targeted bands. The 3' probe detected a 6.5 kb wild-type and a 6.2 kb targeted bands. The internal neomycin probe was obtained by PCR from the control donor vector using the following primers: Neo fwd: gaactctgcaagaaggc-gatagaag and Neo rev: gaacaagatggattcagcagcagg. It highlighted a 3.2 kb and a 2.4 kb bands in the control clone and FOG-1 clone, respectively in addition to a 6.3 kb targeted band detected in both clones.

Recombinase-mediated cassette exchange: FLP-mediated recombination of the control and FOG-1 donor vectors into the pre-targeted ES cells

The pre-targeted R26^{Hygro} ES cells were thawed and cultured for 2 days on feeders in ES cell culture medium without hygromycin. 0.8×10^6 cells in a 6 cm dish were then transfected with a FLP-expressing vector together with the FOG-1 donor vector (FRT3-loxP-Neo-STOP-loxP-FlagFOG-1-IRES-hCD2t-FRTwt), or the control donor vector (FRT3-loxP-Neo-STOP-loxP-IRES-hCD2t-FRTwt) using Effectene reagent according to the manufacturer's instructions. One day later, the medium was replaced by ES cell medium containing 0.2 mg/ml geneticin. Ten days later, 48 or 94 colonies were picked and single-cell suspensions made by trypsin treatment. Each colony was then plated in medium containing geneticin only or geneticin and hygromycin (0.1 mg/ml). Five days later, colonies that were geneticin resistant and hygromycin sensitive were picked and seeded in 35 mm dishes for further expansion.

Clones of interest were checked by PCR for correct insertion (see Figure S2A for a scheme of the strategy). The 5' insertion was verified by primer pair 1 (1F: 5'-aactcttcgctgtcttcc-3' and 1R: 3'-

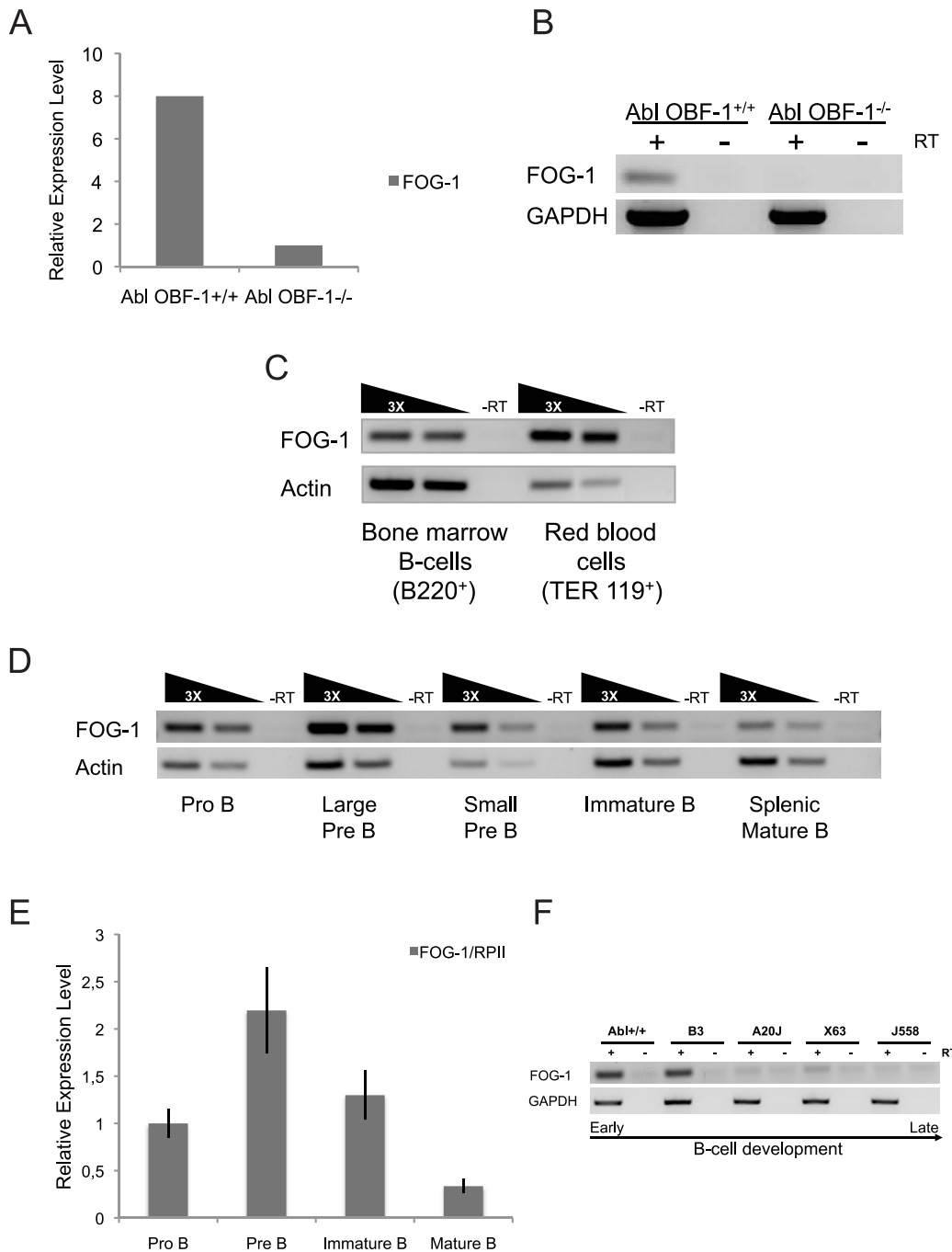


Figure 1. FOG-1 is expressed in a regulated manner during B-cell development. (A) Gene expression level of FOG-1 determined by Affymetrix microarray in wild-type or *OBF-1*^{-/-} Abl Pro-B-cells [25]. (B) Reverse transcriptase (RT)-PCR analysis of FOG-1 mRNA level in wild-type or *OBF-1*^{-/-} Abl Pro-B-cells. GAPDH mRNA amount was used as a control. +, - refer to cDNA synthesis reactions performed in the presence or absence of reverse transcriptase (RT), respectively. (C) mRNA expression level of FOG-1 in bone marrow B-cells (B220⁺) and in red blood cells (TER 119⁺) determined by semi-quantitative RT-PCR. Actin mRNA amount was used as a reference. (D) mRNA expression level of FOG-1 during B-cell development determined by semi-quantitative RT-PCR. The analysis was performed on primary Pro-B, large Pre-B, small Pre-B, immature-B and splenic mature-B cells. Actin mRNA amount was used as a reference. (E) mRNA expression level of FOG-1 measured by real-time RT-PCR during the B-cell development. The analysis was performed on primary B-cells as in (D). RNA Polymerase II mRNA was used as a reference. (F) mRNA expression level of FOG-1 in B-cell lines representing different stages of B-cell development, determined by RT-PCR. From early to late stages, the analysis was performed on the five following cell lines: wild-type Abelson (Abl^{+/+}), B3, A20J, X63 and J558. GAPDH mRNA was used as a control. doi:10.1371/journal.pone.0092836.g001

ctctgattcatcactgtgg-5') and the 3' insertion by primer pair 2 (2F: 5'-gcctcttgacgagttctctgag-3' and 2R: 3'-gaaggacggtacaccaga-gaac-5'). A primer pair 3 (3F: 5'-aactcttcgctgtcttc-3' and 3R:

3'-gacttccacacctggttc-5') and a primer pair 4 (4F: 5'-agagcttgccgtaatcatgg-3' and 4R: 3'-cgtaagggtactcgggtga-5') amplifying only products in the unrecombined allele were used as

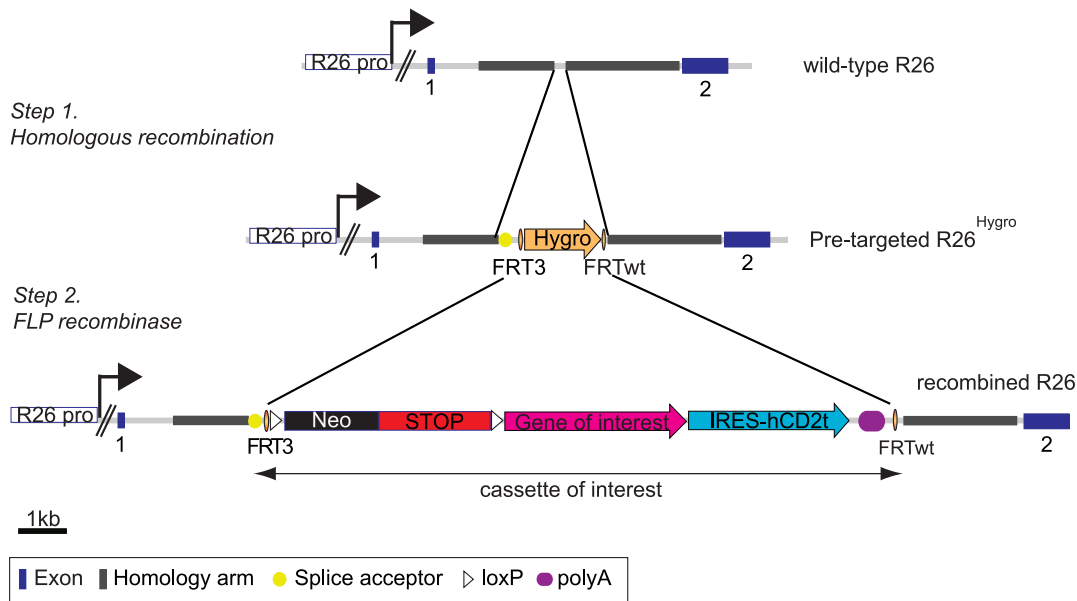


Figure 2. Strategy for the rapid generation of conditionally overexpressing ES cells. Schematic representation of the wild-type *Rosa26* (R26) locus, the pre-targeted $R26^{Hygro}$ and the recombined R26 alleles. The *Rosa26* locus was first pre-targeted by homologous recombination with a cassette containing a splice acceptor and a hygromycin B resistance gene flanked by a FRT3 site in 5' and a FRTwt site in 3' to generate the pre-targeted $R26^{Hygro}$ allele (step 1). The hygromycin B cassette is then replaced by the cassette of interest via the FRT sites using transient expression of the FLP recombinase (step 2). Our cassette of interest contains a loxP-Neo-STOP-loxP cassette for neomycin selection of ES cells and conditional expression of the transgene, and an IRES-hCD2t sequence to monitor expressing cells. Notably, Cre-mediated recombination will excise the neomycin gene from the targeted allele in the transgenic mice. Neo: neomycin resistance gene. R26 pro: promoter of the R26 gene. doi:10.1371/journal.pone.0092836.g002

negative controls. For checking the integration of the neomycin cassette by PCR, the same primers than those used for the synthesis of the internal neomycin probe and specified above were used. The integration of the hCD2t sequence was checked by PCR with the following primers: fwd: tctgaagaccgatgatcagg and rev: tcattacctcacaggtcagg. The primer pair 2' (2F': 5'-aacagatggtccagatgc-3' and 2R': 3'-agtggctcattaggaatgc-5') was used for genotyping the $R26^{FOG-1}$ mice.

Cre-expression in the recombined ES cells

10^6 $R26^{FOG-1}$ ES cells were electroporated with a Cre-expressing vector (pCAGS-nlsCre-PGK-Puro, kindly provided by D. Schübeler, Basel). Neomycin-selection was performed at a concentration of 0.2 mg/ml geneticin for 48 hrs in absence of feeders.

Mouse work

The mice were housed in groups of one to six animals at 25°C with a 12-h light-dark cycle (12 h light, 12 h dark) and were fed a standard laboratory diet containing 0.8% phosphorus and 1.1% calcium (NAFAG 890; Kliba, Basel, Switzerland). Food and water were provided *ad libitum*.

$R26^{FOG-1}$ ES cells were used to generate chimeric mice which were then crossed with C57BL/6J mice to generate transgenic animals. The $R26^{FOG-1}$ mice were subsequently crossed with different Cre-expressing mouse lines to obtain overexpression of FOG-1 in specific B cell subpopulations or throughout hematopoietic lineages. In particular, they were crossed with Cd23-Cre [20], Vav-iCre [21] or mb1-Cre mice [22] to obtain $R26^{FOG-1}$:Cd23-Cre, $R26^{FOG-1}$:Vav-iCre or $R26^{FOG-1}$:mb1-Cre mice, respectively.

Mice or targeted ES cells will be made available upon request.

Cell culture and RT-PCR analysis

Cells were cultured in a humidified tissue culture incubator set up at 5% CO_2 and 37°C. Abelson lines (OBF-1 wt or OBF-1^{-/-}), B3, A20J, X63Ag8 and J558L cell lines were cultured in RPMI 1640 completed with 10% heat-inactivated FCS, 1% penicillin-streptomycin and 4 mM L-glutamine. Total cellular RNA was extracted using RNeasy Mini Kit (Qiagen), DNaseI treated and reverse transcribed using oligo(dT) and SuperScript II RT (Invitrogen) kit according to standard procedures. Subsequent quantitative real-time PCRs were performed with the MESA GREEN qPCR MasterMix Plus for SYBR (Eurogentec) on an ABI prism 7000 instrument. The FOG-1 primers were 5'-ccaactgtgaagccatctc-3' and 3'-gatctcacccttgagcctg-5'. The primers specific for transgene-derived FOG-1 (FlagFOG-1) were 5'-atggactacaaggagcagc-3' and 5'-tccatggccttgctcttc-3'. The RNA polymerase II (RPII) primers were 5'-aggagcgcctcaatgcccagataa-3' and 5'-aggagcgcctcaatgcccagataa-3'. The GAPDH primers were 5'-TGCACCACCAACTGCTTAG-3' and 5'-TGGGAAGAGTGGGAGTTGCTG-3'. The mouse beta actin primers were: 5'-ctaagccaaccgtgaaag-3' and 5'-accagaggcctacagggaca-3'.

Western blot analysis

Proteins were separated on a 7–8% SDS-PAGE, transferred to a PROTRAN Nitrocellulose Transfer Membrane (Whatman) or to an Immobilon-P Membrane PVDF (Millipore) and immunoblotted with the appropriate primary and secondary antibodies. The following antibodies were used: anti-FOG-1 (Santa Cruz, sc-9362), anti- β -tubulin (Sigma, T4026), anti-actin (NeoMarkers, MS-1295-P1), anti-goat IgG, HRP (Abcam, ab7125), anti-mouse IgG, HRP (GE Healthcare, NA931V), anti-goat 680 and anti-mouse 680 (Molecular Probes). Signals were detected either with Amersham HyperFilm ECL (GE Healthcare) or quantified using a

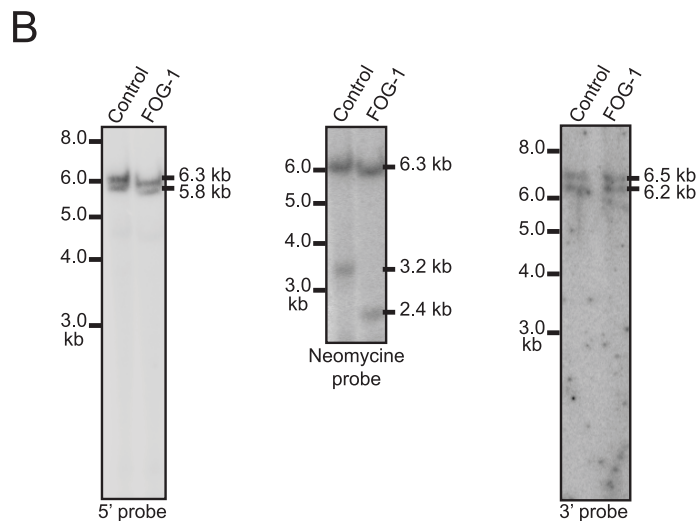
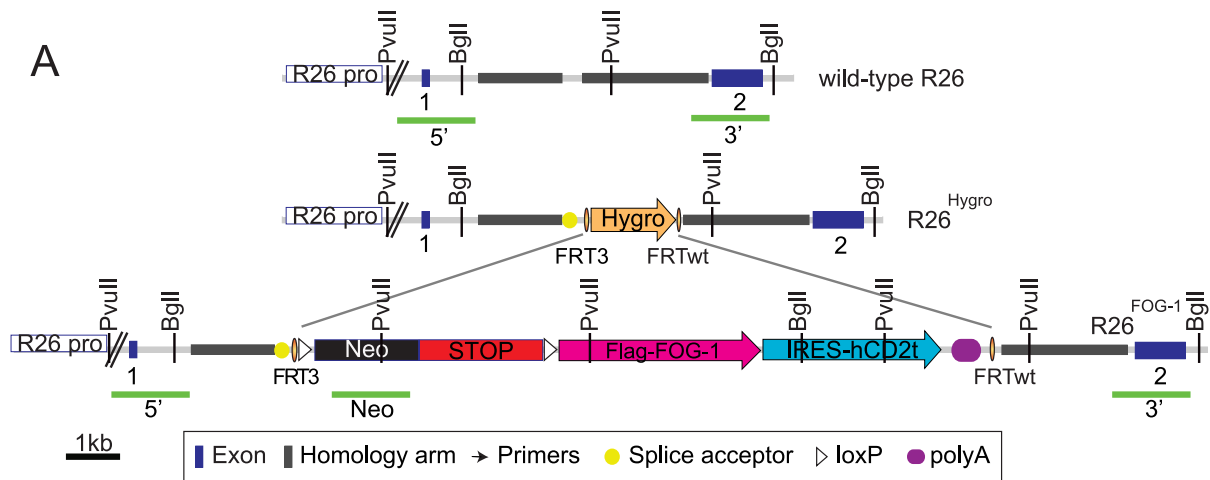


Figure 3. Correct recombination at the pre-targeted R26^{Hygro} allele by RMCE. A. Schematic representation of the wild-type R26, pre-targeted R26^{Hygro} and recombined R26^{FOG-1} alleles. In the FOG-1 cassette, the neomycin resistance gene (Neo, black) and the STOP sequence (red) are flanked by LoxP sites (white triangles) to allow conditional expression. The cDNA encoding FlagFOG-1 (pink) followed by an IRES sequence and the sequence coding for hCD2t (pale blue) were inserted downstream. A polyA signal was placed at the 3' end of the hCD2t coding sequence (blue oval). The probes (green bars) used for Southern blot analysis are shown. **B.** Correct insertion of the vectors was confirmed by Southern blotting. To test the 5' boundary, PvuII-digested ES cell genomic DNA was hybridized with the radioactively labeled 5' probe to detect the wild-type (5.8 kb) and the targeted (6.3 kb) bands (Left panel). To verify single-copy insertion, PvuII-digested DNA was hybridized with a radioactively labeled internal probe to detect the 3.2 kb or 2.4 kb targeted bands in control or FOG-1 clones, respectively, in addition to the 6.3 kb targeted band (Middle panel). To test the 3' boundary, BglII-digested DNA was hybridized with the radioactively labeled 3' probe to detect the 6.5 kb wild-type and the 6.2 kb targeted bands (Right panel).

doi:10.1371/journal.pone.0092836.g003

LI-COR Odyssey instrument and the Odyssey 2.1 software (Biosciences).

Flow cytometry analysis

Cells were stained in PBS-3%FCS for 30 min on ice with the following antibodies: anti-B220 (BD 553092), anti-CD25 (BD 553050), anti-IgM (Southern biotechnology 1140-02), anti-TER119 (BD 557915), anti-CD71 (BD 553267), anti-CD4 (BD 553729), anti-CD8 (BD 553032), and anti-hCD2t (R&D FAB 18561P). For cell sorting, the following antibody combinations were used: ProB cells, B220+, cKit+, CD25-, IgM-; large or

small Pre B, B220+, cKit-, CD25+, IgM-; immature B, B220+, IgM^{low}; splenic mature B, B220+, IgM^{high}. Cells were analyzed on a Becton Dickinson FACSCalibur or sorted on a Cytomation MoFlo instrument

Mature B-cell activation

10⁶ splenic mature B-cells purified using CD43-magnetic beads (Miltenyi Biotec) were cultured for 4 days in the presence of IL4 (10 ng/ml) and/or LPS (5 µg/ml) and/or anti-CD40 antibody (1 µg/ml; BD 553721).

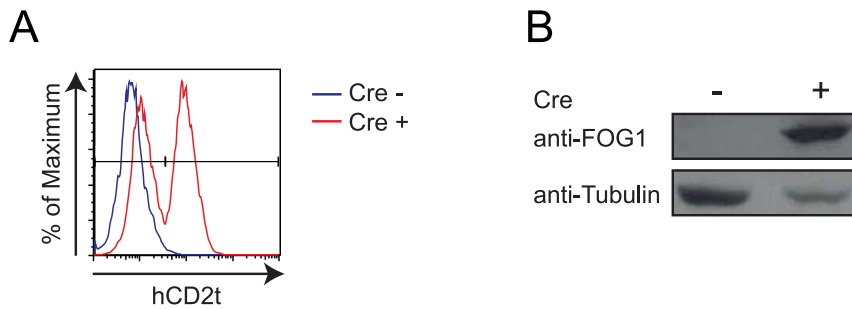


Figure 4. Cre-dependent expression of hCD2t and FOG-1 in recombined ES cells. R26^{FOG-1} ES cells were electroporated with a Cre expressing vector. Cre-induced expression of hCD2t and FOG-1 was detected by flow cytometry (A) and western blot analysis (B), respectively. doi:10.1371/journal.pone.0092836.g004

ELISA assay

IgM or IgG1 antibody titers in the mature B-cell activation cultures were determined by standard ELISA protocol.

Full blood analysis

Tail blood samples were collected in EDTA-coated tubes and analyzed with a Sysmex XT-2000iV blood analyzer.

Statistical analysis

Where appropriate, standard error of the mean is presented. Statistical significance (p value < 0.05) was determined by performing t-test analysis.

Results

Identification of FOG-1 expression in B cells

In previous studies from our laboratory microarray analysis had been used to determine expression profiles of Pre-B-cells lacking the transcriptional coactivator OBF-1 [23,24] and transgenic thymocytes overexpressing OBF-1; these experiments identified several genes that were downregulated in null cells [25] or upregulated in overexpressing cells [25,26]. Among these genes, we identified *Zfpml*, which encodes the developmental regulator FOG-1 (Fig. 1A, 1B and data not shown). *Zfpml* had also been identified as a gene consistently activated or repressed in *Ebfl* (early B-cell factor-1) gain- and loss-of-function experiments, respectively and ChIP-Seq data demonstrated that *Ebfl* binds to the promoter of *Zfpml* within 10 kb of the transcription start site [27].

In agreement with previous results [3], we detected a lower expression level of FOG-1 in total bone marrow B-cells than in red blood cells (Fig. 1C). Microarray and quantitative RT-PCR analysis demonstrated that FOG-1 was expressed from Pro-B-cell to immature B-cell stages at a relatively high level and was downregulated in mature B-cells and plasma cells. This specific expression pattern was observed in primary cells and also in cultured cell lines representative of different B-cell developmental stages (Fig. 1D, 1E and 1F).

Together these results show that FOG-1 is expressed in a regulated manner during B cell development and suggest that this factor may play a role not previously appreciated in this lineage. To examine this in greater detail, we wished to test the effect of overexpressing FOG-1 in B cells, in particular in late stages, hypothesizing that this might affect their differentiation or function. For this, we made use of a system that we had designed to generate mice overexpressing a gene of interest in a conditional manner.

Pre-targeting of the *Rosa26* locus

Our strategy has been to generate ES cells pre-targeted at the *Rosa26* (R26) locus, so that appropriate expression constructs can rapidly be inserted by recombination mediated cassette exchange (RMCE, see Figure 2). We chose to use the *Rosa26* locus, which was first described in a gene trap experiment and was shown to be expressed in the whole mouse [28]. This locus is believed to encode two non-coding transcripts and an antisense transcript of unknown function and can be used to drive the expression of any cDNA [28]. In the original gene trap experiment, the insertion of a splice acceptor and a promoter-less cDNA in intron 1 of the gene led to expression of this cDNA from the endogenous *Rosa26* promoter. For these reasons, we decided to target the *Rosa26* locus and we used 5' and 3' homology arms located in intron 1. The targeting vector containing a splice acceptor sequence to allow expression from the endogenous *Rosa26* promoter and an hygromycin B resistance gene flanked by FRT3 and FRTwt sites was linearized and introduced by electroporation into 129svjae ES cells to generate the pre-targeted R26^{Hygro} allele (Figure 2, step 1 and Figure S1A). 480 hygromycin-resistant ES cell clones were first screened by PCR using a forward primer located upstream of the 5' homology arm and a reverse primer located in the hygromycin cassette. Four clones (1–4, Figure S1B) showed the expected 2 kb band for successful homologous recombination, as compared to the aberrant product obtained for clone 5. To further confirm the correct homologous recombination, we performed Southern blot analysis using 5' and 3' probes with BamHI or PstI-digested genomic DNA blots. Clones 1–4 showed the expected 4.9 kb band for correct integration of the selection cassette in 5' (Figure S1C), as well as the 7.5 kb band for correct integration at the 3' end (Figure S1D). As a control, clone 5 only showed the wild-type bands. To ensure that a single copy was integrated in the genome, an additional Southern blot analysis was performed with a hygromycin probe and PvuII-digested genomic DNA blots. Clones 2–4 showed a single band at the expected size, whilst clone 1 showed an additional smaller band, suggesting multiple insertions of the transgene (Figure S1E). Thus, our targeting vector was successfully homologously recombined into the *Rosa26* locus to generate the pre-targeted R26^{Hygro} allele. Clone 4 was selected as our R26^{Hygro} ES cell clone for further use.

Efficient recombination of the FOG-1 cassette in the pre-targeted R26^{Hygro} locus

The combined use of the heterospecific FRT3/FRTwt sites allows replacement of a target DNA by an incoming plasmid donor cassette upon transient FLP expression [29]. Hence, any cassette of interest flanked by FRT3/FRTwt sites can readily be introduced into pre-targeted R26^{Hygro} ES cells upon transient

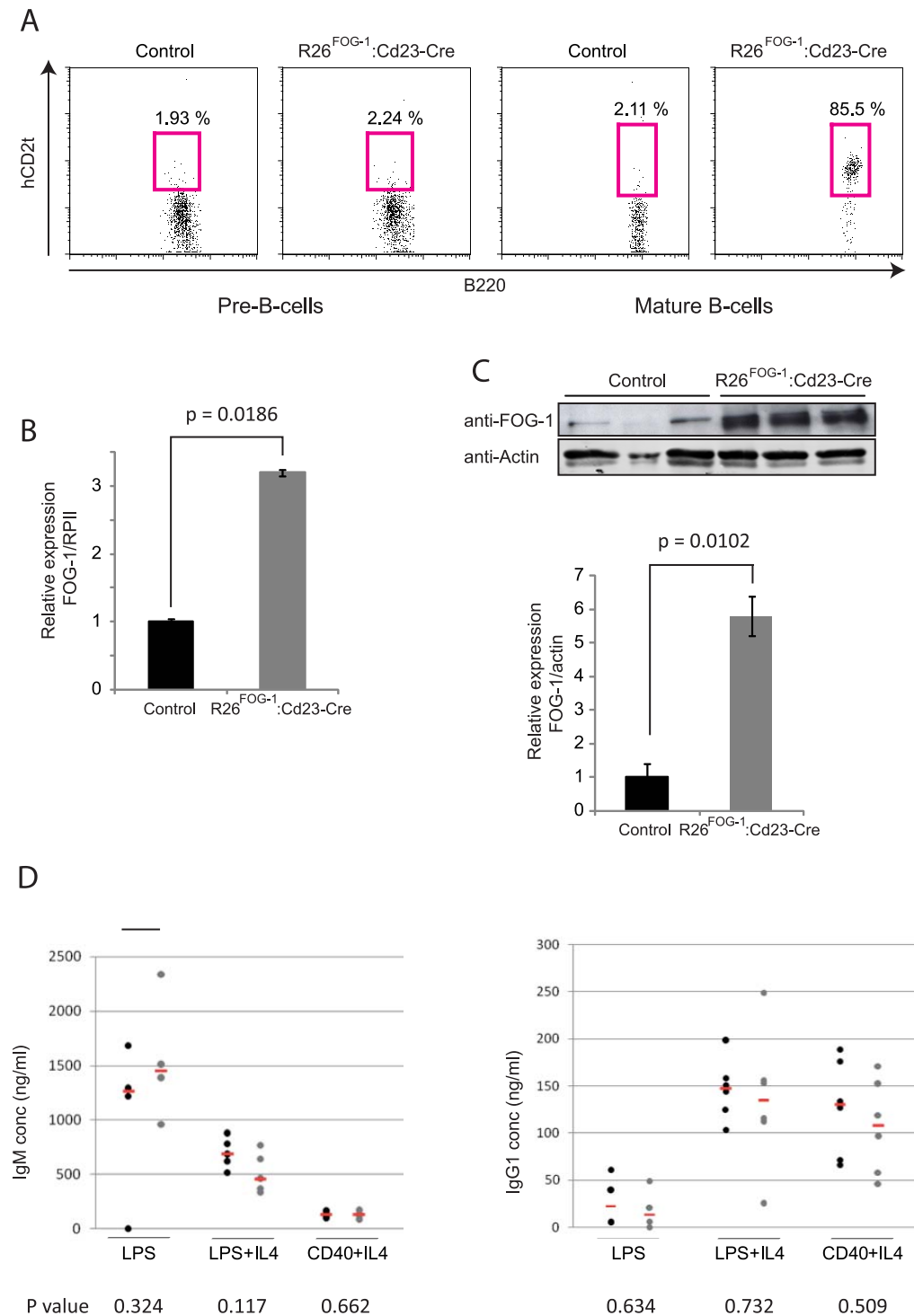


Figure 5. Overexpression of FOG-1 in mature B-cells. **A**. In R26^{FOG-1}:Cd23-Cre mice, hCD2t expression is restricted to mature B-cells. Cell surface expression of hCD2t was analyzed by flow cytometry in Pre-B-cells (B220+, CD25+) and in mature B-cells (B220+, CD25+) of control (R26^{FOG-1}) and R26^{FOG-1}:Cd23-Cre mice. Representative results of at least 3 independent experiments are shown. **B**. FOG-1 mRNA is increased 3-fold in R26^{FOG-1}:Cd23-Cre mature B-cells. RNA extracted from 3 control (R26^{FOG-1}) and 3 R26^{FOG-1}:Cd23-Cre mice was reverse transcribed and subjected to quantitative PCR to detect FOG-1 and RNA Polymerase II (RPII, for normalization) transcripts. Standard error of the mean is shown. **C**. FOG-1 protein is up-regulated ca. 6-fold in mature B-cells derived from R26^{FOG-1}:Cd23-Cre mice. FOG-1 and actin proteins were detected by western blotting in mature B-cells derived from 3 control (R26^{FOG-1}) and 3 R26^{FOG-1}:Cd23-Cre mice (upper panel). The band intensities were quantified by LiCor Odyssey scanning and normalized to expression of actin (lower panel). Standard error of the mean is shown. **D**. FOG-1-overexpressing mature B-cells respond normally to *in vitro* stimulation. Splenic resting mature B-cells isolated from 3 to 6 control (R26^{FOG-1}, black dots) or R26^{FOG-1}:Cd23-Cre mice (grey dots) were activated *in vitro* by LPS, LPS+IL4 or anti-CD40+IL4 for 4 days. Titers of IgM (left panel) or IgG1 (right panel) in the culture supernatants were determined by ELISA; means are shown (red bar) as well as the corresponding p values at the bottom. doi:10.1371/journal.pone.0092836.g005

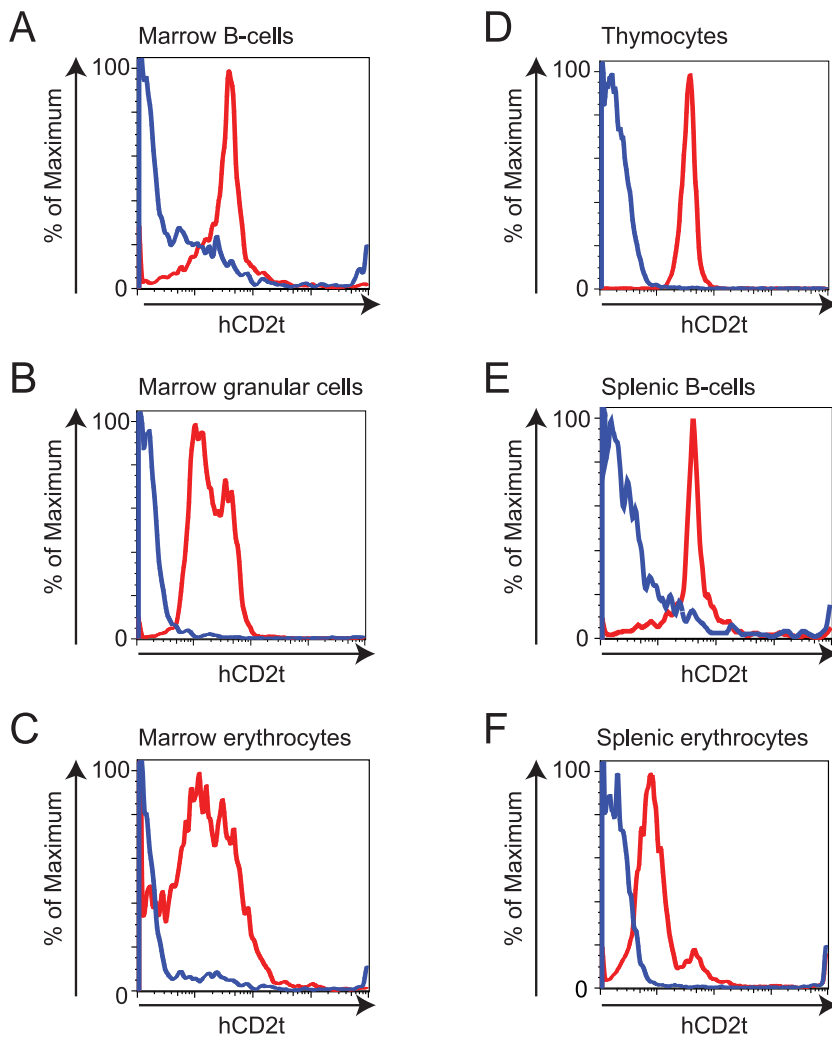


Figure 6. hCD2t is expressed in all hematopoietic cells of $R26^{FOG-1};Vav-iCre$ mice. A–F. Flow cytometry analysis of hCD2t expression in $R26^{FOG-1};Vav-iCre$ (red line) and control ($R26^{FOG-1}$, blue line) mice. **A.** Bone marrow B-lymphocytes (B220+ cells). **B.** Bone marrow granular cells (based on Forward and Side Scatters). **C.** Bone marrow erythrocytes (TER119+ cells). **D.** Thymocytes (CD4+, CD8+ cells). **E.** Splenic B-lymphocytes (B220+ cells). **F.** Splenic erythrocytes (TER119+ cells). Data for one representative animal of each genotype are shown (n = 5). doi:10.1371/journal.pone.0092836.g006

expression of the FLP recombinase (Figure 2, step 2). Inducible expression cassettes contain a loxP-Neo-STOP-loxP sequence upstream of the cDNA of interest to allow neomycin selection of the recombined clones and Cre-dependent expression of the transgene from the endogenous *Rosa26* promoter. The cassettes also contain an internal ribosome entry site (IRES) sequence derived from the Encephalomyocarditis virus placed downstream of the cDNA of interest to allow the concomitant expression of a “reporter” gene (here a truncated version of the human cell surface marker CD2, hCD2t), and selective monitoring of the recombined cells. In order to study the effect of enforced expression of FOG-1 in transgenic mice, two donor vectors were generated: (i) a control donor vector with loxP-Neo-STOP-loxP and the IRES-hCD2t sequences, but no cDNA (Figure S2A), (ii) the FOG-1 donor vector which contained a cDNA encoding Flag-tagged FOG-1 downstream of the loxP-Neo-STOP-loxP sequence and upstream of the IRES-hCD2t sequence (Figure 3A and Figure S2A).

To test the efficiency of our system, RMCE experiments were performed in $R26^{Hygro}$ ES cells: cells were transfected with either

the FOG-1 donor vector or the control donor vector, together with an expression vector encoding the FLP recombinase. The $R26^{Hygro}$ ES cells are resistant to hygromycin B and, upon successful RMCE, become sensitive to this antibiotic, while acquiring neomycin-resistance (see Figure 2). In two independent RMCE experiments, a total of 142 Neo^R colonies were picked for each vector and were tested for hygromycin B resistance, as described in the Materials and Methods section. We found that at this step 48.5% of the FOG-1 colonies and 62.5% of the control colonies were both neomycin-resistant and hygromycin-sensitive, indicative of successful RMCE. We next selected 12 $Neo^R/Hygro^S$ clones of each kind (control or FOG-1 vector) for an extensive PCR analysis which demonstrated that all the clones analyzed were properly recombined (Figure S2A–B). Successful integration of the neomycin cassette and of the hCD2t cassette in the genome of these ES cell clones was also tested and all clones were positive for these PCRs as well (Figure S2C–D). Thus, using the system described here, we efficiently recombined a large cassette of 5.0 kb or 8.0 kb at the $R26^{Hygro}$ allele of the pre-targeted ES cells to generate ES cell clones carrying the $R26^{Control}$ allele or $R26^{FOG-1}$

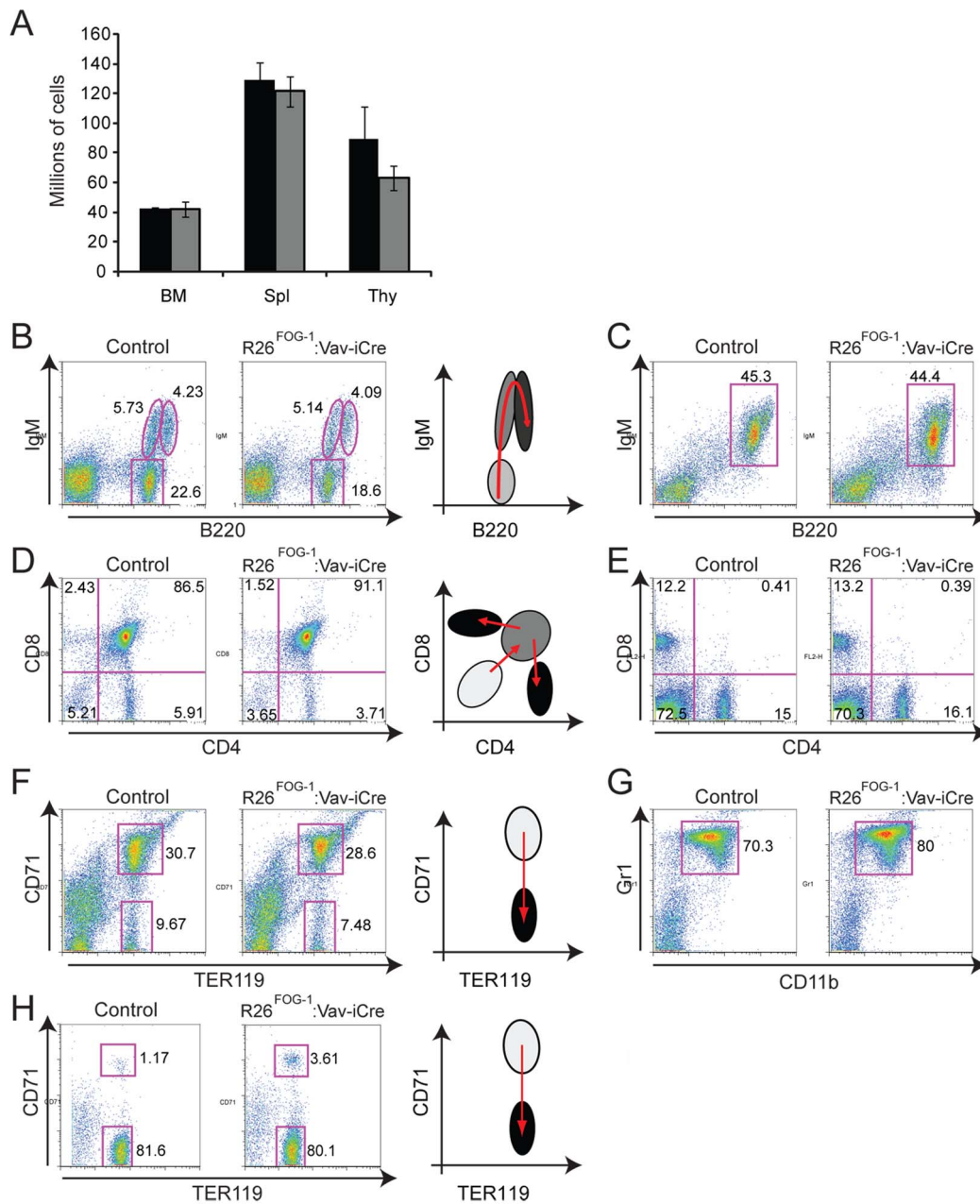


Figure 7. Normal B-cell, T-cell and granular cell populations in R26^{FOG-1}:Vav-iCre mice. **A.** Cells of the bone marrow (BM), spleen (Spl) and thymus (Thy) of R26^{FOG-1} (black bars) and R26^{FOG-1}:Vav-iCre (grey bars) mice were enumerated. Standard error of the mean is shown. **B.** Bone marrow cells were stained with anti-B220 and anti-IgM antibodies to analyze B-cell development. **C.** Splenocytes were stained with anti-B220 and anti-IgM antibodies to identify B-cells. **D.** Thymocytes were stained with anti-CD4 and anti-CD8 antibodies to analyze T-cell development. **E.** Splenocytes were stained with anti-CD4 and anti-CD8 antibodies to identify mature T-cells. **F.** Bone marrow cells were stained with anti-TER119 and anti-CD71 antibodies to analyze erythropoiesis. **G.** Bone marrow cells were stained with anti-Gr1 and anti-CD11b antibodies to identify Gr1+ CD11b+ myeloid cells. **H.** Splenocytes were stained with anti-TER119 and anti-CD71 antibodies to analyze splenic erythropoiesis. Cells were analyzed by flow cytometry in R26^{FOG-1} (control) and R26^{FOG-1}:Vav-iCre animals; data for one representative animal are shown (n = 5 for each genotype). Percentages of the populations are shown next to the gates. A diagram representing the developmental pathway of the different lineages from pale (progenitors) to dark grey (differentiated cells) is shown next to the pseudo-dotplots B, D, F and H. doi:10.1371/journal.pone.0092836.g007

allele, respectively. Based on the extensive PCR analysis presented here, 100% of the Neo^R/Hygro^S clones appear to be correctly recombined upon RMCE. We next chose one control clone and one FOG-1 clone for verifying the successful RMCE by Southern blot analysis and used genomic digests and probes allowing us to interrogate the 5' and the 3' boundaries, as well as the copy

number. This analysis also confirmed the correct recombination of the targeting vectors into the *Rosa26* locus (Figure 3A–B).

Before generating mice, we tested the Cre-inducible expression of FOG-1 and hCD2t in our recombined FOG-1 clone. To this end, a Cre-expressing vector was transiently transfected in the targeted ES cells and expression of hCD2t and FOG-1 was tested two days later by flow cytometry and western blot analysis,

respectively. As expected, the recombined R26^{FOG-1} ES cells expressed hCD2t and FOG-1 only when Cre was expressed (Figure 4A and 4B). The partial expression of hCD2t observed by flow cytometry is due to the experimental settings: here, transfected ES cells were only selected for a short period of time to avoid FOG-1-induced cell cycle arrest in ES cells [30]. As a result of this, not all ES cells were expressing Cre, leading to a heterogeneous cell population.

In conclusion, we efficiently recombined our FOG-1 donor vector in the pre-targeted R26^{Hygro} locus to generate R26^{FOG-1} ES cells and demonstrated that, upon Cre expression, both FOG-1 and hCD2t were expressed in these ES cells. We therefore used the R26^{FOG-1} ES cell clone to generate transgenic R26^{FOG-1} mice.

Enforced expression of FOG-1 does not affect B-cell differentiation or function

To investigate the potential effect of sustained level of FOG-1 in mature B-cells, we first crossed the R26^{FOG-1} mice with Cd23-Cre mice which express Cre specifically in mature B-cells [20]. Flow cytometry analysis of hCD2t expression in B-cells derived from R26^{FOG-1}:Cd23-Cre mice showed that in the early developmental stages (Pre-B-cells), no hCD2t could be detected, as expected (Figure 5A, second panel). In contrast, more than 85% of the mature B-cells derived from these animals were found to express hCD2t (Figure 5A, fourth panel). Importantly, the expression of hCD2t was never detected in control animals which carry the R26^{FOG-1} allele but do not express Cre. Next, quantitative RT-PCR and western blot analysis were performed to estimate the level of FOG-1 overexpression in mature B-cells derived from R26^{FOG-1}:Cd23-Cre animals and compared to that of R26^{FOG-1} animals. As shown in Figure 5B, FOG-1 mRNA was upregulated slightly more than three fold in the overexpressing cells, as compared to the control cells. At the protein level, the increase was even larger: careful quantification of the FOG-1 signal in relation to the expression of actin showed that the protein was upregulated about 6-fold (Figure 5C). Overall this analysis demonstrated that our system allows reliable overexpression of FOG-1 *in vivo*.

To investigate the potential biological effect of this elevated level of FOG-1 on plasma cell development, mature B-cells derived from R26^{FOG-1}:Cd23-Cre mice were activated *in vitro* with different stimuli and the antibody titers in the culture supernatants were determined by ELISA. Irrespective of the stimulus used, no difference in the level of IgM or IgG1 was observed between overexpressing and control cultures, indicating that enforced expression of FOG-1 in mature B-cells did not impair or alter their ability to differentiate into antibody-secreting cells *in vitro* (Figure 5D). In addition, we also performed immunization experiments to test whether FOG-1 overexpression in mature B cells might have an impact on the immune response *in vivo*. For this, R26^{FOG-1}:Cd23-Cre and control mice were immunized with DNP-KLH and the serum titers of antigen-specific immunoglobulins were measured by ELISA 8 and 15 days later. However, also in this case no significant difference was found (data not shown). Thus, although the expression of FOG-1 is normally downregulated during B cell development, enforcing expression of this factor at late B cell stages did not reveal any detrimental effect, contrary to our hypothesis. Finally, R26^{FOG-1} mice were also crossed with mb1-Cre mice, to induce FOG-1 overexpression from the earliest stages of B cell development onwards. However, this did not impact B cell development as examined by flow cytometric analysis (data not shown).

Reduction of eosinophil numbers upon enforced expression of FOG-1

To further analyze the consequences of an elevated level of FOG-1 in the hematopoietic system, we next crossed the R26^{FOG-1} mice with Vav-iCre mice [21] to overexpress FOG-1 in all hematopoietic lineages. Remarkably, all B-lymphocytes, myeloid cells, and erythrocytes derived from the bone marrow of R26^{FOG-1}:Vav-iCre animals expressed hCD2t (Figure 6A, 6B and 6C). Similarly, all thymocytes and splenic B-lymphocytes as well as all splenic erythrocytes expressed hCD2t (Figure 6D, 6E and 6F), thus demonstrating the usefulness of our reporter system. Expression of transgene-derived FOG-1 mRNA was analyzed by quantitative RT-PCR and showed that FlagFOG-1 mRNA is produced at a similar level in bone marrow, spleen, and thymus of R26^{FOG-1}:Vav-iCre mice (Figure S3). Altogether these data indicated that in R26^{FOG-1}:Vav-iCre animals virtually all hematopoietic cells express the transgene at a roughly similar level.

The total numbers of bone marrow cells, splenocytes, and thymocytes in overexpressing mice were comparable to the numbers obtained in control animals (Figure 7A). Using a panel of antibodies against lineage-specific surface markers we analyzed by flow cytometry the major hematopoietic cell populations. R26^{FOG-1}:Vav-iCre mice showed normal B-cell development (Figure 7B and 7C), normal T-cell development (Figure 7D and 7E), as well as a normal myeloid population (Figure 7G). Developing erythrocytes can be subdivided into early and late erythroblasts based on the expression of the cell surface markers TER119 and CD71 [31]. Using this method, we found a largely normal erythroid development, although a slight but significant increase of the early erythroblast population (CD71+ TER119+) was seen in the spleen of some ($\leq 50\%$) of the R26^{FOG-1}:Vav-iCre animals (exemplified in Figure 7H). However, no difference was observed in the bone marrow (Figure 7F). More detailed analysis will be required to understand this phenotype. Statistical analysis of the flow cytometry data showed that, except for the increase in the early splenic erythroblast population (Figure 7H), expression of FOG1 did not have any significant impact on the cell populations examined (see Figure S4). Full blood count analysis of R26^{FOG-1}:Vav-iCre females and males revealed no major difference in red blood cell count, hemoglobin content, hematocrit and platelet counts (Table 1). Similarly, no significant changes were observed in the total numbers of white blood cells, lymphocytes, monocytes, neutrophils and basophils in the blood of these mice (Table 1). In contrast, a consistent decrease in the total number of circulating eosinophils was observed for R26^{FOG-1}:Vav-iCre females and males (Table 1). A highly reproducible and significant difference of more than 3-fold was found when comparing the average numbers of circulating eosinophils in control and R26^{FOG-1}:Vav-iCre animals (Figure 8, $p = 0.00758$). To ascertain that the phenotypes observed were not due to Cre expression, which can have effects on its own in some cases [32], we also performed a flow cytometric and full blood count analysis of Vav-iCre mice in comparison with control animals lacking the Cre transgene (C57BL/6J). As can be seen in Figure S5, the flow cytometry profile of the different populations analyzed showed no difference between mice carrying the Vav-iCre transgene and control mice. Statistical analysis of the flow cytometry data demonstrated that there was indeed no significant difference between these mice (Figure S6). Furthermore, full blood count analysis also failed to show any statistically significant difference (Table S1). Finally, FOG1 mRNA expression in mature B cells was identical in C57BL/6J and Vav-iCre mice (Figure S7). Thus, the phenotypes described for the FOG1 overexpressing mice are not due to an artefact of cre expression, but are indeed FOG1-dependent.

Table 1. Full blood count of R26^{FOG-1}:Vav-iCre.

	Control				R26 ^{FOG-1} :Vav-iCre				P value
	Males	Females	Mean	Males	Females	Mean	Males	Females	
RBC (10 ⁴ /uL)	1054	1032	1132	1063	1136	1049	1063	1100	0.2981
HGB (g/L)	177	166	172	160	172	171	160	183	0.8965
HCT (10 ³ (-1)%)	534	505	516	492	525	515	492	532	0.8807
PLT (10 ³ /uL)	1124	1352	1399	1292	1241	1197	1292	1172	0.6932
WBC (10 ³ /uL)	855	901	1305	653	573	1164	653	1434	0.5698
LYMPH (10 ³ /uL)	602	657	970	485	412	858	485	1081	0.6083
MONO (10 ³ /uL)	150	130	207	75	106	185	75	230	0.6148
NEUT (10 ³ /uL)	79	83	92	82	49	85	82	107	1
BASO (10 ³ /uL)	0	0	0	0	0	0	0	0	0.6074
EO (10 ³ /uL)	24	31	36	11	6	34	11	16	0.007589

Blood samples from 4 control (R26^{FOG-1}) and 4 R26^{FOG-1}:Vav-iCre mice were examined with a mouse blood analyzer. Individual values are shown, as well as the corresponding averages (highlighted in bold) and the p values of the comparison between the 4 control and 4 FOG-1 expressing mice, determined by using Student's two-tailed t-test. Note the highly significant reduction of circulating eosinophils in FOG-1 overexpressing animals (highlighted in **italics**). RBC: red blood cells; HGB: hemoglobin; HCT: hematocrit; PLT: platelets; WBC: white blood cells; LYMPH: lymphocytes; MONO: monocytes; NEUT: neutrophils; BASO: basophils; EO: eosinophils. doi:10.1371/journal.pone.0092836.t001

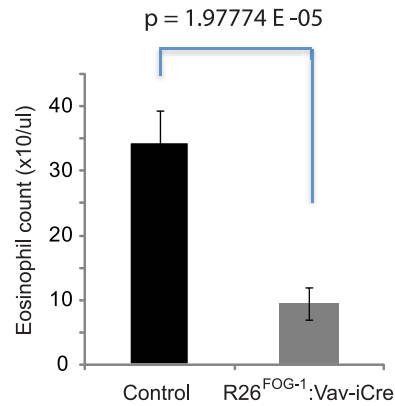


Figure 8. Altered eosinophil numbers in R26^{FOG-1}:Vav-iCre mice. Reduction of circulating eosinophils. The numbers of eosinophils obtained in full blood count analysis of 8 control (R26^{FOG-1}) and 8 R26^{FOG-1}:Vav-iCre including those presented in Table 1 mice were averaged. Standard error of the mean is shown. doi:10.1371/journal.pone.0092836.g008

Discussion

We have shown here that FOG-1 expression is regulated during B cell development, being high in early stages (e.g. pre-B cells) and low or absent in late stages such as mature B cells and plasma cells. Based on these observations, we hypothesized that this downregulation is important for effective B cell development and that artificially maintaining FOG-1 expression at late stages might have an impact on normal B cell development or function. However, we did not observe any major phenotypes when FOG-1 was selectively overexpressed in mature B-cells. Flow cytometric analysis of the major B cell populations failed to reveal alterations in R26^{FOG-1}:Cd23-Cre mice, demonstrating no obvious developmental impact. Furthermore, *in vivo* immune response to a T cell-dependent antigen or antibody secretion following *in vitro* stimulation were also not affected, thus suggesting that B cell function was not impaired. In addition, mice overexpressing FOG-1 from the pre-B cell stage onwards also did not show any remarkable phenotype. Nevertheless, it remains possible that FOG-1 affects a B cell subset that was not examined here and additional experiments will be required to determine this. Furthermore, since B cells do not express GATA factors (our unpublished data), other B cell ancillary factors must be postulated for a role for FOG-1 in these and potentially other cells (Versavel et al., in preparation).

In contrast, R26^{FOG-1}:Vav-iCre mice with enforced expression of FOG-1 in the entire hematopoietic system showed two main phenotypes. First, consistent with the known role of FOG-1 in red blood cell development [4,6,33,34], we observed a moderately altered erythropoiesis in the spleen of some ($\leq 50\%$) R26^{FOG-1}:Vav-iCre animals. The reason for the partial penetrance of this phenotype is unclear and additional work will be required. Second, we found a striking and highly significant reduction of the total number of circulating eosinophils. This is of great interest, since a previous study concluded that FOG-1 is a repressor of the eosinophil lineage in avian cells [12]. Our results, therefore, extend this finding to mammals. In the future, the R26^{FOG-1}:Vav-iCre mice will be analyzed further to draw a more complete view of FOG-1 functions in hematopoiesis.

The Recombinase-Mediated Cassette Exchange technology relies on the exquisite selectivity of recombinases such as cre or flp and has been developed to facilitate the generation of

transgenic ES cell lines [29,35] [35–41] [15,16]. To allow inducible or lineage-specific expression, the RMCE technology has been combined with tetracycline-inducible systems [42–44], or with the Cre recombinase activity [45,46]. Recent studies made use of a pre-targeted locus to generate shRNA-expressing mice [47,48] and Hitz *et al.* combined the C31 integrase-mediated recombination at a pre-targeted locus with Cre-dependent expression to establish shRNA-expressing mice [49]. Other systems that allow RMCE into pre-modified ES cells [50,51] or in human ES cells pre-targeted at the *HPRT* locus [52] have also been developed.

To alter the expression pattern of FOG-1 *in vivo*, we developed a novel and rapid transgenic system that is also based on the RMCE technology and that allows rapid insertion of expression cassettes into the Rosa 26 locus. In this system, expression of the transgene from the endogenous *Rosa26* promoter is dependent on Cre recombinase-mediated excision of a STOP sequence, allowing cell- or temporal-specific control of expression. A hCD2t cDNA is also included as a reporter to track transgene-expressing cells *in vitro* and *in vivo*.

Our strategy is broadly similar to the one described by Hitz and colleagues, where C31 integrase-mediated recombination is used instead of FLP-mediated recombination to insert a transgene at a modified *Rosa26* locus and where the loxP/Cre system is used for conditional expression of shRNAs [49]; the RMCE efficiency of the two systems is also comparable. A particularly useful feature of our system is the concomitant expression of a “marker” gene, hCD2t, together with our transgene (i.e. FOG-1); this allows to monitor Cre-recombined cells *ex vivo* or *in vivo*. This is especially useful in situations where Cre expression, and therefore transgene expression, is only partial or mosaic and leads to a mixture of recombined and non-recombined cells; having a marker gene such as hCD2t then allows to selectively examine –and potentially isolate– the transgene-expressing cells. Expression of hCD2t can conveniently be detected by flow cytometry and is therefore particularly well suited for analyses in the hematopoietic system. Furthermore, since the antibodies recognizing hCD2t are species-specific, expression of the endogenous mouse protein (e.g. by T cells) does not interfere. Finally, hCD2t can also be detected by immunohistochemistry, further extending the range of cells that can be selectively examined.

Using this system we generated mice with moderate overexpression of FOG-1 either in mature B cells (R26^{FOG-1}:Cd23-Cre mice), throughout B cell development (R26^{FOG-1}:mb1-Cre), or in all hematopoietic lineages (R26^{FOG-1}:Vav-iCre mice). Remarkably, flow cytometry analysis of bone marrows and spleens derived from R26^{FOG-1}:Vav-iCre mice revealed that all hematopoietic cells expressed hCD2t. In contrast and as expected, in R26^{FOG-1}:Cd23-Cre mice, where Cre starts being expressed just before the mature B-cell stage, hCD2t was only detected in mature B-cells. Importantly, cells derived from control R26^{FOG-1} mice lacking Cre expression did not express any hCD2t. These results demonstrate that conditional expression of a transgene using our system is tightly regulated and underscore the utility of having a marker gene.

We found that the *Rosa26* promoter drives moderate FOG-1 expression in the hematopoietic system. Interestingly, this expression level was sufficient to marginally alter splenic erythropoiesis and to significantly reduce the number of circulating eosinophils in R26^{FOG-1}:Vav-iCre mice, demonstrating its physiological relevance. Such moderate expression level is an advantage to unravel the roles of proteins in physiologic and pathologic situations, as it avoids aberrant phenotypes that may be partly caused by too strong overexpression. Since targeted *Rosa26* homozygous mice are viable and appear normal, the expression level of the transgene

could be doubled by generating R26^{FOG-1}/R26^{FOG-1} homozygous mice [18] or by inserting additional regulatory elements in the expression cassette. Following this idea, Tchorz *et al.* generated a modified RMCE-compatible *Rosa26* locus for the expression of transgenes and characterized several promoters with different strengths [17].

In conclusion, despite our finding that the expression of FOG-1 is tightly regulated throughout B-cell differentiation and is dependent on the B-cell specific coactivator OBF1, we could not demonstrate a role for FOG-1 in B-cell differentiation or function. However, we could confirm the finding that FOG-1 is a negative regulator of eosinophil development and extend it to mammals. Further work will be required to better understand this important function of FOG-1 in the mouse.

Supporting Information

Figure S1 Pre-targeting of ES cells with the pR26-SA-FRT-Hygro^R vector. **A.** Schematic representation of the wild-type and pre-targeted R26^{Hygro} alleles. The splice acceptor (yellow dot) and the hygromycin B resistance cassette (Hygro, orange) flanked by FRT sites were inserted using the homology arms (thick grey) between exons 1 and 2 (blue). The PCR primers (0F, 0R; arrows) as well as the restriction sites and probes (green bars) used for Southern blotting are shown. For clarity, only the relevant PstI sites are shown. **B.** PCR screening of the putative R26^{Hygro} ES cell clones. Clones 1–4 are positive, clone 5 shows an aberrant product. **C–E.** Correct insertion of the transgene confirmed by Southern blotting. Clone 5 was included as a negative control. To test the 5′ insertion, BamHI-digested ES cell genomic DNA was hybridized with the radioactively labeled 5′ probe to detect the wild-type (WT, 5.8 kb) and the targeted (Targ, 4.9 kb) bands (**C**). To test the 3′ insertion, PstI-digested DNA was hybridized with the radioactively labeled 3′ probe to detect the 6.5 kb WT and the 7.5 kb targeted bands (**D**). To verify single-copy insertion, PvuII-digested DNA was hybridized with a radioactively labeled internal probe to detect the 8 kb targeted band (arrow). Note that clone 1 shows an aberrant extra band, indicating multiple insertions in this clone (**E**). (EPS)

Figure S2 Efficiency of RMCE at the pre-targeted R26^{Hygro} allele. **A.** Schematic representation of the different alleles, from top to bottom: wild-type R26 locus, R26^{Hygro}, R26^{Control} and R26^{FOG-1}. The different primer pairs used for PCR analysis of the ES clones are depicted by arrows. **B.** PCR analysis of Neo^R/Hygro^S ES cell clones for testing RMCE recombination at the 5′ (FRT3) and at the 3′ (FRTwt) sites. Lanes 1–12: control clones, cells derived from RMCE with the control donor vector; lanes 1′–12′: FOG-1 clones, cells derived from RMCE with the FOG-1 donor vector; + Ctl, positive control. From top to bottom: PCR screening with primer pairs 1F/1R and 3F/3R at the 5′ end junction of the recombined cassette. PCR screening with primer pairs 2F/2R and 4F/4R at the 3′ end junction of the recombined cassette. Appropriate positive controls were chosen for each PCR set up. Note that on the presented gel control clone 9 shows a faint band with primer pair 3F/3R. Upon reanalysis of the DNA it was however found to be positive only with primers 1F/1R, as would be expected from a correctly recombined clone. **C.** PCR analysis of Neo^R/Hygro^S ES cell clones for presence of the Neomycin resistance gene; -Ctl, negative control. **D.** PCR analysis of Neo^R/Hygro^S ES cell clones for presence of the human CD2t gene. Lanes labeling as in (B) above. As shown, all clones analyzed are positive for both the Neomycin and the hCD2t gene. (EPS)

Figure S3 Expression of transgene-derived FOG-1 in R26FOG-1:Vav-iCre animals. Total RNA from bone marrow (BM), spleen (Spl), and thymus (Thy) of 3 R26^{FOG-1}:Vav-iCre animals was extracted, reverse transcribed and subjected to quantitative PCR to specifically detect transgene-derived FlagFOG-1 mRNA. Values are relative to RNA Polymerase II (RPII) expression. Standard error of the mean is shown. FlagFOG-1/RPII relative expression in bone marrow was arbitrarily set to 1. (EPS)

Figure S4 Statistical analysis of the flow cytometry data. The flow cytometric data of R26^{FOG-1} (blue bars) and R26^{FOG-1}:Vav-iCre (red bars) animals (including the mice presented in Figure 7) were used for statistical analysis applying Student's two-tailed t-test. **A.** Bone marrow B-cells. **B.** Bone marrow myeloid cells. **C.** Bone marrow erythroid cells. **D.** Splenic B-cells. **E.** Splenic mature T-cells. **F.** Splenic erythropoiesis. **G.** Thymocytes. (EPS)

Figure S5 Normal B-cell and granular cell populations in Vav-iCre mice. **A.** Cells of the bone marrow (BM), spleen (Spl) and thymus (Thy) of control (C57BL/6J, blue bars) and Vav-iCre (red bars) mice were enumerated. Standard error of the mean is shown. **B.** Bone marrow cells were stained with anti-B220 and anti-IgM antibodies to analyze B-cell development. **C.** Splenocytes were stained with anti-B220 and anti-IgM antibodies to identify B-cells. **D.** Bone marrow cells were stained with anti-TER119 and anti-CD71 antibodies to analyze erythropoiesis. **E.** Bone marrow cells were stained with anti-Gr1 and anti-CD11b antibodies to identify Gr1+ CD11b+ myeloid cells. **F.** Splenocytes were stained with anti-TER119 and anti-CD71 antibodies to analyze splenic erythropoiesis. Cells were analyzed by flow cytometry; data for one representative animal are shown (n=4 for each genotype). Percentages of the populations are shown next to the gates. The statistical analysis (two-tailed Student's t-test) of the data is presented. (EPS)

Figure S6 Statistical analysis of the flow cytometry data in Vav-iCre mice. The flow cytometric data presented in Figure S5 of

control (C57BL/6, blue bars) and Vav-iCre animals (red bars) were used for statistical analysis applying Student's two-tailed t-test. **A.** Bone marrow B-cells. **B.** Bone marrow erythroid cells. **C.** Bone marrow myeloid cells. **D.** Splenic B-cells. **E.** Splenic erythropoiesis. (EPS)

Figure S7 Unchanged FOG1 expression in Vav-iCre mice. RNA from mature B cells from C57BL/6J (WT) or Vav-iCre mice (n=4 per genotype) was used to measure FOG1 mRNA expression by RT-qPCR. Statistical analysis was done using Student's two-tailed t-test. (EPS)

Table S1 Blood samples from 4 control (C57BL/6J) and 4 Vav-iCre mice were examined with a mouse blood analyzer. Individual values are shown, as well as the corresponding averages (in red) and the p values of the comparison between the 4 control and 4 Cre expressing mice. Note the absence of significant variation. RBC: red blood cells; HGB: hemoglobin; HCT: hematocrit; PLT: platelets; WBC: white blood cells; LYMPH: lymphocytes; MONO: monocytes; NEUT: neutrophils; BASO: basophils; EO: eosinophils. (DOCX)

Acknowledgments

We thank M. Busslinger for providing the Cd23-Cre mice and the pBS-IRES-hCD2t vector, M. Crossley for providing the pcDNA3-FlagFOG-1 vector, D. Kioussis for providing the Vav-iCre mice and M. Stadler for help with statistical analysis. We also thank N. Reichert, F. Brellier, A. G. Rolink, R. G. Clerc and F. Cubizolles for useful discussions and critical reading of the manuscript.

Author Contributions

Conceived and designed the experiments: CDR MK AV MM PM. Performed the experiments: CDR AV MK CC GM VP TD HK PK JFS MM PM. Analyzed the data: CDR AV MM CC VP GM MM PM. Contributed reagents/materials/analysis tools: MM. Wrote the paper: CDR PM AV.

References

- Matthias P, Rolink AG (2005) Transcriptional networks in developing and mature B cells. *Nature reviews Immunology* 5: 497–508.
- Orkin SH, Zon LI (2008) Hematopoiesis: an evolving paradigm for stem cell biology. *Cell* 132: 631–644.
- Cantor AB, Orkin SH (2005) Coregulation of GATA factors by the Friend of GATA (FOG) family of multitype zinc finger proteins. *Seminars in cell & developmental biology* 16: 117–128.
- Tsang AP, Fujiwara Y, Hom DB, Orkin SH (1998) Failure of megakaryopoiesis and arrested erythropoiesis in mice lacking the GATA-1 transcriptional cofactor FOG. *Genes Dev* 12: 1176–1188.
- Fox AH, Liew C, Holmes M, Kowalski K, Mackay J, et al. (1999) Transcriptional cofactors of the FOG family interact with GATA proteins by means of multiple zinc fingers. *The EMBO journal* 18: 2812–2822.
- Tsang AP, Visvader JE, Turner CA, Fujiwara Y, Yu C, et al. (1997) FOG, a multitype zinc finger protein, acts as a cofactor for transcription factor GATA-1 in erythroid and megakaryocytic differentiation. *Cell* 90: 109–119.
- Pal S, Cantor AB, Johnson KD, Moran TB, Boyer ME, et al. (2004) Coregulator-dependent facilitation of chromatin occupancy by GATA-1. *Proceedings of the National Academy of Sciences of the United States of America* 101: 980–985.
- Hong W, Nakazawa M, Chen YY, Kori R, Vakoc CR, et al. (2005) FOG-1 recruits the NuRD repressor complex to mediate transcriptional repression by GATA-1. *The EMBO journal* 24: 2367–2378.
- Vakoc CR, Letting DL, Gheldof N, Sawado T, Bender MA, et al. (2005) Proximity among distant regulatory elements at the beta-globin locus requires GATA-1 and FOG-1. *Molecular cell* 17: 453–462.
- Kurata H, Lee HJ, McClanahan T, Coffman RL, O'Garra A, et al. (2002) Friend of GATA is expressed in naive Th cells and functions as a repressor of GATA-3-mediated Th2 cell development. *J Immunol* 168: 4538–4545.
- Zhou M, Ouyang W, Gong Q, Katz SG, White JM, et al. (2001) Friend of GATA-1 represses GATA-3-dependent activity in CD4+ T cells. *J Exp Med* 194: 1461–1471.
- Querfurth E, Schuster M, Kulesa H, Crispino JD, Doderlein G, et al. (2000) Antagonism between C/EBPbeta and FOG in eosinophil lineage commitment of multipotent hematopoietic progenitors. *Genes Dev* 14: 2515–2525.
- Rapino F, Robles EF, Richter-Larrea JA, Kallin EM, Martínez-Climent JA, et al. (2013) C/EBPalpha induces highly efficient macrophage transdifferentiation of B lymphoma and leukemia cell lines and impairs their tumorigenicity. *Cell reports* 3: 1153–1163.
- Xie H, Ye M, Feng R, Graf T (2004) Stepwise reprogramming of B cells into macrophages. *Cell* 117: 663–676.
- Brandt CS, Dymecki SM (2004) Talking about a revolution: The impact of site-specific recombinases on genetic analyses in mice. *Dev Cell* 6: 7–28.
- Schnutgen F, Stewart AF, von Melchner H, Anastassiadis K (2006) Engineering embryonic stem cells with recombinase systems. *Methods Enzymol* 420: 100–136.
- Tchorj JS, Suply T, Ksiazek I, Giachino C, Cloetta D, et al. (2012) A modified RMCE-compatible Rosa26 locus for the expression of transgenes from exogenous promoters. *PLoS one* 7: e30011.
- Soriano P (1999) Generalized lacZ expression with the ROSA26 Cre reporter strain. *Nat Genet* 21: 70–71.
- Sasaki Y, Derudder E, Hobeika E, Pelanda R, Reth M, et al. (2006) Canonical NF-kappaB activity, dispensable for B cell development, replaces BAFF-receptor signals and promotes B cell proliferation upon activation. *Immunity* 24: 729–739.
- Kwon K, Hutter C, Sun Q, Bilic I, Cobaleda C, et al. (2008) Instructive role of the transcription factor E2A in early B lymphopoiesis and germinal center B cell development. *Immunity* 28: 751–762.

21. de Boer J, Williams A, Skavdis G, Harker N, Coles M, et al. (2003) Transgenic mice with hematopoietic and lymphoid specific expression of Cre. *Eur J Immunol* 33: 314–325.
22. Hobeika E, Thiemann S, Storch B, Jumaa H, Nielsen PJ, et al. (2006) Testing gene function early in the B cell lineage in mb1-cre mice. *Proc Natl Acad Sci U S A* 103: 13789–13794.
23. Schubart DB, Rolink A, Kosco-Vilbois MH, Botteri F, Matthias P (1996) B-cell-specific coactivator OBF-1/OCA-B/Obf1 required for immune response and germinal centre formation. *Nature* 383: 538–542.
24. Strubin M, Newell JW, Matthias P (1995) OBF-1, a novel B cell-specific coactivator that stimulates immunoglobulin promoter activity through association with octamer-binding proteins. *Cell* 80: 497–506.
25. Bartholdy B, Du Roure C, Bordon A, Emslie D, Corcoran LM, et al. (2006) The Ets factor Spi-B is a direct critical target of the coactivator OBF-1. *Proceedings of the National Academy of Sciences of the United States of America* 103: 11665–11670.
26. Bordon A, Bosco N, Du Roure C, Bartholdy B, Kohler H, et al. (2008) Enforced expression of the transcriptional coactivator OBF1 impairs B cell differentiation at the earliest stage of development. *PLoS one* 3: e4007.
27. Treiber T, Mandel EM, Pott S, Gyory I, Firner S, et al. (2010) Early B cell factor 1 regulates B cell gene networks by activation, repression, and transcription-independent poising of chromatin. *Immunity* 32: 714–725.
28. Zambrowicz BP, Imamoto A, Fiering S, Herzenberg LA, Kerr WG, et al. (1997) Disruption of overlapping transcripts in the ROSA beta geo 26 gene trap strain leads to widespread expression of beta-galactosidase in mouse embryos and hematopoietic cells. *Proc Natl Acad Sci U S A* 94: 3789–3794.
29. Schlake T, Bode J (1994) Use of mutated FLP recognition target (FRT) sites for the exchange of expression cassettes at defined chromosomal loci. *Biochemistry* 33: 12746–12751.
30. Tanaka M, Zheng J, Kitajima K, Kita K, Yoshikawa H, et al. (2004) Differentiation status dependent function of FOG-1. *Genes Cells* 9: 1213–1226.
31. Du Roure C, Takacs K, Maxwell PH, Roberts I, Dazzi F, et al. (2006) Correction of severe anaemia using immuno-regulated gene therapy is achieved by restoring the early erythroblast compartment. *Br J Haematol* 132: 608–614.
32. Schmidt-Supprian M, Rajewsky K (2007) Vagaries of conditional gene targeting. *Nat Immunol* 8: 665–668.
33. Harju-Baker S, Costa FC, Fedosyuk H, Neades R, Peterson KR (2008) Silencing of Agamma-globin gene expression during adult definitive erythropoiesis mediated by GATA-1-FOG-1-Mi2 complex binding at the –566 GATA site. *Mol Cell Biol* 28: 3101–3113.
34. Katz SG, Cantor AB, Orkin SH (2002) Interaction between FOG-1 and the corepressor C-terminal binding protein is dispensable for normal erythropoiesis in vivo. *Mol Cell Biol* 22: 3121–3128.
35. Sauer B, Henderson N (1990) Targeted insertion of exogenous DNA into the eukaryotic genome by the Cre recombinase. *New Biol* 2: 441–449.
36. Dymecki SM (1996) FLP recombinase promotes site-specific DNA recombination in embryonic stem cells and transgenic mice. *Proc Natl Acad Sci U S A* 93: 6191–6196.
37. Dymecki SM, Tomaszewicz H (1998) Using FLP-recombinase to characterize expansion of Wnt1-expressing neural progenitors in the mouse. *Dev Biol* 201: 57–65.
38. O’Gorman S, Fox DT, Wahl GM (1991) Recombinase-mediated gene activation and site-specific integration in mammalian cells. *Science* 251: 1351–1355.
39. Rodriguez CI, Buchholz F, Galloway J, Sequerra R, Kasper J, et al. (2000) High-efficiency deleter mice show that FLP is an alternative to Cre-loxP. *Nat Genet* 25: 139–140.
40. Seibler J, Bode J (1997) Double-reciprocal crossover mediated by FLP-recombinase: a concept and an assay. *Biochemistry* 36: 1740–1747.
41. Soukharev S, Miller JL, Sauer B (1999) Segmental genomic replacement in embryonic stem cells by double lox targeting. *Nucleic Acids Res* 27: e21.
42. Beard C, Hochedlinger K, Plath K, Wutz A, Jaenisch R (2006) Efficient method to generate single-copy transgenic mice by site-specific integration in embryonic stem cells. *Genesis* 44: 23–28.
43. Masui S, Shimamoto D, Toyooka Y, Yagi R, Takahashi K, et al. (2005) An efficient system to establish multiple embryonic stem cell lines carrying an inducible expression unit. *Nucleic Acids Res* 33: e43.
44. Wutz A, Rasmussen TP, Jaenisch R (2002) Chromosomal silencing and localization are mediated by different domains of Xist RNA. *Nat Genet* 30: 167–174.
45. Hohenstein P, Slight J, Ozdemir DD, Burn SF, Berry R, et al. (2008) High-efficiency Rosa26 knock-in vector construction for Cre-regulated overexpression and RNAi. *Pathogenetics* 1: 3.
46. Nyabi O, Naessens M, Haigh K, Gembaraska A, Goossens S, et al. (2009) Efficient mouse transgenesis using Gateway-compatible ROSA26 locus targeting vectors and F1 hybrid ES cells. *Nucleic Acids Res* 37: e55.
47. Seibler J, Kuter-Luks B, Kern H, Streu S, Plum L, et al. (2005) Single copy shRNA configuration for ubiquitous gene knockdown in mice. *Nucleic Acids Res* 33: e67.
48. Seibler J, Kleinriders A, Kuter-Luks B, Nichaves S, Bruning JC, et al. (2007) Reversible gene knockdown in mice using a tight, inducible shRNA expression system. *Nucleic Acids Res* 35: e54.
49. Hitz C, Wurst W, Kuhn R (2007) Conditional brain-specific knockdown of MAPK using Cre/loxP regulated RNA interference. *Nucleic Acids Res* 35: e90.
50. Schebelle L, Wolf C, Stribl C, Javaheri T, Schnutgen F, et al. (2010) Efficient conditional and promoter-specific in vivo expression of cDNAs of choice by taking advantage of recombinase-mediated cassette exchange using FLEX gene traps. *Nucleic acids research* 38: e106.
51. Sandhu U, Cebula M, Behme S, Riemer P, Wodarczyk C, et al. (2011) Strict control of transgene expression in a mouse model for sensitive biological applications based on RMCE compatible ES cells. *Nucleic acids research* 39: e1.
52. Sakurai K, Shimoji M, Tahimic CG, Aiba K, Kawase E, et al. (2010) Efficient integration of transgenes into a defined locus in human embryonic stem cells. *Nucleic acids research* 38: e96.

Manuscript in preparation: HDAC1 and 2 repress lineage inappropriate expression of *Flt3* and *Ptprf* in B cells via Pax5 and Grg4

Nina Reichert¹, Teppei Yamaguchi², **Vincent Pillonel**¹, Karen Cornille³, Chun Cao¹ & Patrick Matthias^{1#}

¹*Friedrich Miescher Institute for Biomedical Research, Novartis Research Foundation, PO Box 2543, Maulbeerstrasse 66, 4058 Basel, Switzerland.* ²*University of California, Berkeley, Department of Molecular & Cell Biology, 16 Barker Hall # 3204, Berkeley, CA 94720-3204, USA.* ³ *Department of Biomedicine of the University of Basel, Basel, Switzerland.* [#]*To whom correspondence should be addressed (email: patrick.matthias@fmi.ch).*

Abstract

We showed previously that B cell development strictly requires the presence of either HDAC1 or 2, as ablation of both proteins leads to a strong developmental block at the pre-BII cell stage. Using microarrays, we identified novel putative HDAC target genes in the remaining early pre-BI cells. In particular, two interesting target genes have been analyzed: *Flt3* (fms-like tyrosine kinase 3), which is critical for early hematopoietic differentiation and *Ptprf* (protein tyrosine phosphatase, receptor type, F), which encodes a T cell lineage-specific phosphatase. Both genes are strongly expressed in HDAC double-deficient cells, and the failure to down-regulate these genes in multipotent progenitors has been reported to impair B cell development. We found that in committed B cells, the transcription factor Pax5, in addition to recruiting the Groucho family member Grg4, also co-recruits HDAC1 and 2, thereby leading to hypoacetylation and repression of the *Flt3* and *Ptprf* promoters. Thus, HDAC1 and 2 play a critical role in B cell differentiation by promoting cell cycle progression at the pre-BII stage and by repressing important developmental regulators antagonistic of the B cell lineage at the pre-BI stage.

Bibliography

Bibliography

Adams, H., Fritzsche, F.R., Dirnhofer, S., Kristiansen, G., and Tzankov, A. (2010). Class I histone deacetylases 1, 2 and 3 are highly expressed in classical Hodgkin's lymphoma. Expert opinion on therapeutic targets *14*, 577-584.

Adams, J.M., and Cory, S. (2007). The Bcl-2 apoptotic switch in cancer development and therapy. *Oncogene* *26*, 1324-1337.

Adams, J.M., Harris, A.W., Pinkert, C.A., Corcoran, L.M., Alexander, W.S., Cory, S., Palmiter, R.D., and Brinster, R.L. (1985). The c-myc oncogene driven by immunoglobulin enhancers induces lymphoid malignancy in transgenic mice. *Nature* *318*, 533-538.

Aka, J.A., Kim, G.W., and Yang, X.J. (2011). K-acetylation and its enzymes: overview and new developments. *Handbook of experimental pharmacology* *206*, 1-12.

Albihn, A., Johnsen, J.I., and Henriksson, M.A. (2010). MYC in oncogenesis and as a target for cancer therapies. *Advances in cancer research* *107*, 163-224.

Aldana-Masangkay, G.I., and Sakamoto, K.M. (2011). The role of HDAC6 in cancer. *Journal of biomedicine & biotechnology* *2011*, 875824.

Allfrey, V.G., Faulkner, R., and Mirsky, A.E. (1964). Acetylation and methylation of histones and their possible role in the regulation of RNA synthesis. *Proceedings of the National Academy of Sciences of the United States of America* *51*, 786-794.

Amelio, I., Gostev, M., Knight, R.A., Willis, A.E., Melino, G., and Antonov, A.V. (2014). DRUGSURV: a resource for repositioning of approved and experimental drugs in oncology based on patient survival information. *Cell death & disease* *5*, e1051.

Antonov, A.V., Krestyaninova, M., Knight, R.A., Rodchenkov, I., Melino, G., and Barlev, N.A. (2014). PPISURV: a novel bioinformatics tool for uncovering the hidden role of specific genes in cancer survival outcome. *Oncogene* *33*, 1621-1628.

Atsumi, A., Tomita, A., Kiyoi, H., and Naoe, T. (2006). Histone deacetylase 3 (HDAC3) is recruited to target promoters by PML-RARalpha as a component of the N-CoR co-repressor complex to repress transcription in vivo. *Biochemical and biophysical research communications* *345*, 1471-1480.

Attema, J.L., Papathanasiou, P., Forsberg, E.C., Xu, J., Smale, S.T., and Weissman, I.L. (2007). Epigenetic characterization of hematopoietic stem cell differentiation using miniChIP and bisulfite sequencing analysis. *Proceedings of the National Academy of Sciences of the United States of America* *104*, 12371-12376.

- Baeriswyl, V., and Christofori, G. (2009). The angiogenic switch in carcinogenesis. *Seminars in cancer biology* 19, 329-337.
- Balasubramanian, S., Verner, E., and Buggy, J.J. (2009). Isoform-specific histone deacetylase inhibitors: the next step? *Cancer letters* 280, 211-221.
- Bali, P., Pranpat, M., Bradner, J., Balasis, M., Fiskus, W., Guo, F., Rocha, K., Kumaraswamy, S., Boyapalle, S., Atadja, P., *et al.* (2005). Inhibition of histone deacetylase 6 acetylates and disrupts the chaperone function of heat shock protein 90: a novel basis for antileukemia activity of histone deacetylase inhibitors. *The Journal of biological chemistry* 280, 26729-26734.
- Banerjee, I., Miyake, Y., Nobs, S.P., Schneider, C., Horvath, P., Kopf, M., Matthias, P., Helenius, A., and Yamauchi, Y. (2014). Influenza A virus uses the aggresome processing machinery for host cell entry. *Science (New York, N.Y.)* 346, 473-477.
- Bannister, A.J., and Kouzarides, T. (2011). Regulation of chromatin by histone modifications. *Cell research* 21, 381-395.
- Bantscheff, M., Hopf, C., Savitski, M.M., Dittmann, A., Grandi, P., Michon, A.-M., Schlegl, J., Abraham, Y., Becher, I., Bergamini, G., *et al.* (2011). Chemoproteomics profiling of HDAC inhibitors reveals selective targeting of HDAC complexes. *Nat Biotech* 29, 255-265.
- Batty, N., Malouf, G.G., and Issa, J.P. (2009). Histone deacetylase inhibitors as anti-neoplastic agents. *Cancer letters* 280, 192-200.
- Berger, S.L. (2007). The complex language of chromatin regulation during transcription. *Nature* 447, 407-412.
- Bergers, G., and Benjamin, L.E. (2003). Tumorigenesis and the angiogenic switch. *Nature reviews. Cancer* 3, 401-410.
- Bernard, S., and Eilers, M. (2006). Control of cell proliferation and growth by Myc proteins. *Results and problems in cell differentiation* 42, 329-342.
- Bernstein, B.E., Meissner, A., and Lander, E.S. (2007). The mammalian epigenome. *Cell* 128, 669-681.
- Bernstein, B.E., Tong, J.K., and Schreiber, S.L. (2000). Genomewide studies of histone deacetylase function in yeast. *Proceedings of the National Academy of Sciences of the United States of America* 97, 13708-13713.
- Berx, G., and van Roy, F. (2009). Involvement of members of the cadherin superfamily in cancer. *Cold Spring Harbor perspectives in biology* 1, a003129.
- Beumer, J.H., and Tawbi, H. (2010). Role of histone deacetylases and their inhibitors in cancer biology and treatment. *Current clinical pharmacology* 5, 196-208.

Bibliography

- Bhaskara, S., Knutson, S.K., Jiang, G., Chandrasekharan, M.B., Wilson, A.J., Zheng, S., Yenamandra, A., Locke, K., Yuan, J.L., Bonine-Summers, A.R., *et al.* (2010). Hdac3 is essential for the maintenance of chromatin structure and genome stability. *Cancer cell* 18, 436-447.
- Bolden, J.E., Peart, M.J., and Johnstone, R.W. (2006). Anticancer activities of histone deacetylase inhibitors. *Nat Rev Drug Discov* 5, 769-784.
- Boyault, C., Gilquin, B., Zhang, Y., Rybin, V., Garman, E., Meyer-Klaucke, W., Matthias, P., Muller, C.W., and Khochbin, S. (2006). HDAC6-p97/VCP controlled polyubiquitin chain turnover. *The EMBO journal* 25, 3357-3366.
- Boyault, C., Sadoul, K., Pabion, M., and Khochbin, S. (2007). HDAC6, at the crossroads between cytoskeleton and cell signaling by acetylation and ubiquitination. *Oncogene* 26, 5468-5476.
- Bradbury, C.A., Khanim, F.L., Hayden, R., Bunce, C.M., White, D.A., Drayson, M.T., Craddock, C., and Turner, B.M. (2005). Histone deacetylases in acute myeloid leukaemia show a distinctive pattern of expression that changes selectively in response to deacetylase inhibitors. *Leukemia* 19, 1751-1759.
- Bradner, J.E., West, N., Grachan, M.L., Greenberg, E.F., Haggarty, S.J., Warnow, T., and Mazitschek, R. (2010). Chemical phylogenetics of histone deacetylases. *Nature chemical biology* 6, 238-243.
- Brownell, J.E., Zhou, J., Ranalli, T., Kobayashi, R., Edmondson, D.G., Roth, S.Y., and Allis, C.D. (1996). Tetrahymena histone acetyltransferase A: a homolog to yeast Gcn5p linking histone acetylation to gene activation. *Cell* 84, 843-851.
- Brunmeir, R., Lagger, S., and Seiser, C. (2009). Histone deacetylase HDAC1/HDAC2-controlled embryonic development and cell differentiation. *The International journal of developmental biology* 53, 275-289.
- Buchwald, M., Kramer, O.H., and Heinzl, T. (2009). HDACi--targets beyond chromatin. *Cancer letters* 280, 160-167.
- Bui, T.V., and Mendell, J.T. (2010). Myc: Maestro of MicroRNAs. *Genes & cancer* 1, 568-575.
- Busslinger, M. (2004). Transcriptional control of early B cell development. *Annual review of immunology* 22, 55-79.
- Butler, K.V., Kalin, J., Brochier, C., Vistoli, G., Langley, B., and Kozikowski, A.P. (2010). Rational design and simple chemistry yield a superior, neuroprotective HDAC6 inhibitor, tubastatin A. *Journal of the American Chemical Society* 132, 10842-10846.

- Cai, Q., Medeiros, L.J., Xu, X., and Young, K.H. (2015). MYC-driven aggressive B-cell lymphomas: biology, entity, differential diagnosis and clinical management. *Oncotarget* 6, 38591-38616.
- Campo, E., Swerdlow, S.H., Harris, N.L., Pileri, S., Stein, H., and Jaffe, E.S. (2011). The 2008 WHO classification of lymphoid neoplasms and beyond: evolving concepts and practical applications. *Blood* 117, 5019-5032.
- Carapeti, M., Aguiar, R.C., Goldman, J.M., and Cross, N.C. (1998). A novel fusion between MOZ and the nuclear receptor coactivator TIF2 in acute myeloid leukemia. *Blood* 91, 3127-3133.
- Carmeliet, P. (2005). VEGF as a key mediator of angiogenesis in cancer. *Oncology* 69 Suppl 3, 4-10.
- Champagne, N., Pelletier, N., and Yang, X.J. (2001). The monocytic leukemia zinc finger protein MOZ is a histone acetyltransferase. *Oncogene* 20, 404-409.
- Chang, T.C., Yu, D., Lee, Y.S., Wentzel, E.A., Arking, D.E., West, K.M., Dang, C.V., Thomas-Tikhonenko, A., and Mendell, J.T. (2008). Widespread microRNA repression by Myc contributes to tumorigenesis. *Nature genetics* 40, 43-50.
- Chen, P.B., Hung, J.H., Hickman, T.L., Coles, A.H., Carey, J.F., Weng, Z., Chu, F., and Fazio, T.G. (2013). Hdac6 regulates Tip60-p400 function in stem cells. *eLife* 2, e01557.
- Chen, Y., Wang, H., Yoon, S.O., Xu, X., Hottiger, M.O., Svaren, J., Nave, K.A., Kim, H.A., Olson, E.N., and Lu, Q.R. (2011). HDAC-mediated deacetylation of NF-kappaB is critical for Schwann cell myelination. *Nature neuroscience* 14, 437-441.
- Chiu, B.C., and Hou, N. (2015). Epidemiology and etiology of non-hodgkin lymphoma. *Cancer treatment and research* 165, 1-25.
- Choong, C.J., Sasaki, T., Hayakawa, H., Yasuda, T., Baba, K., Hirata, Y., Uesato, S., and Mochizuki, H. (2016). A novel histone deacetylase 1 and 2 isoform-specific inhibitor alleviates experimental Parkinson's disease. *Neurobiology of aging* 37, 103-116.
- Chou, C.W., and Chen, C.C. (2008). HDAC inhibition upregulates the expression of angiostatic ADAMTS1. *FEBS letters* 582, 4059-4065.
- Choudhary, C., Kumar, C., Gnad, F., Nielsen, M.L., Rehman, M., Walther, T.C., Olsen, J.V., and Mann, M. (2009). Lysine acetylation targets protein complexes and co-regulates major cellular functions. *Science (New York, N.Y.)* 325, 834-840.
- Choukrallah, M.A., Song, S., Rolink, A.G., Burger, L., and Matthias, P. (2015). Enhancer repertoires are reshaped independently of early priming and heterochromatin dynamics during B cell differentiation. *Nature communications* 6, 8324.

Chowdhury, D., and Sen, R. (2001). Stepwise activation of the immunoglobulin mu heavy chain gene locus. *The EMBO journal* *20*, 6394-6403.

Cobaleda, C., and Busslinger, M. (2008). Developmental plasticity of lymphocytes. *Current opinion in immunology* *20*, 139-148.

Conacci-Sorrell, M., McFerrin, L., and Eisenman, R.N. (2014). An overview of MYC and its interactome. *Cold Spring Harbor perspectives in medicine* *4*, a014357.

Corcoran, A.E., Riddell, A., Krooshoop, D., and Venkitaraman, A.R. (1998). Impaired immunoglobulin gene rearrangement in mice lacking the IL-7 receptor. *Nature* *391*, 904-907.

Croxford, J.L., Tang, M.L., Pan, M.F., Huang, C.W., Kamran, N., Phua, C.M., Chng, W.J., Ng, S.B., Raulet, D.H., and Gasser, S. (2013). ATM-dependent spontaneous regression of early Emu-myc-induced murine B-cell leukemia depends on natural killer and T cells. *Blood* *121*, 2512-2521.

Dang, C.V. (2012). MYC on the path to cancer. *Cell* *149*, 22-35.

Dang, C.V. (2014). Gene regulation: fine-tuned amplification in cells. *Nature* *511*, 417-418.

Dang, C.V., O'Donnell K, A., and Juopperi, T. (2005). The great MYC escape in tumorigenesis. *Cancer cell* *8*, 177-178.

Dawson, M.A., and Kouzarides, T. (2012). Cancer epigenetics: from mechanism to therapy. *Cell* *150*, 12-27.

de Ruijter, A.J., van Gennip, A.H., Caron, H.N., Kemp, S., and van Kuilenburg, A.B. (2003). Histone deacetylases (HDACs): characterization of the classical HDAC family. *The Biochemical journal* *370*, 737-749.

Delmore, J.E., Issa, G.C., Lemieux, M.E., Rahl, P.B., Shi, J., Jacobs, H.M., Kastiris, E., Gilpatrick, T., Paranal, R.M., Qi, J., *et al.* (2011). BET bromodomain inhibition as a therapeutic strategy to target c-Myc. *Cell* *146*, 904-917.

Dhanak, D., and Jackson, P. (2014). Development and classes of epigenetic drugs for cancer. *Biochemical and biophysical research communications* *455*, 58-69.

Dovey, O.M., Foster, C.T., Conte, N., Edwards, S.A., Edwards, J.M., Singh, R., Vassiliou, G., Bradley, A., and Cowley, S.M. (2013). Histone deacetylase 1 and 2 are essential for normal T-cell development and genomic stability in mice. *Blood* *121*, 1335-1344.

Dovey, O.M., Foster, C.T., and Cowley, S.M. (2010). Histone deacetylase 1 (HDAC1), but not HDAC2, controls embryonic stem cell differentiation. *Proceedings of the National Academy of Sciences of the United States of America* *107*, 8242-8247.

- Du Roure, C., Versavel, A., Doll, T., Cao, C., Pillonel, V., Matthias, G., Kaller, M., Spetz, J.F., Kopp, P., Kohler, H., *et al.* (2014). Hematopoietic overexpression of FOG1 does not affect B-cells but reduces the number of circulating eosinophils. *PLoS one* 9, e92836.
- Eilers, M., and Eisenman, R.N. (2008). Myc's broad reach. *Genes & development* 22, 2755-2766.
- Eischen, C.M., Weber, J.D., Roussel, M.F., Sherr, C.J., and Cleveland, J.L. (1999). Disruption of the ARF-Mdm2-p53 tumor suppressor pathway in Myc-induced lymphomagenesis. *Genes & development* 13, 2658-2669.
- Ellis, L., Atadja, P.W., and Johnstone, R.W. (2009a). Epigenetics in cancer: targeting chromatin modifications. *Molecular cancer therapeutics* 8, 1409-1420.
- Ellis, L., Bots, M., Lindemann, R.K., Bolden, J.E., Newbold, A., Cluse, L.A., Scott, C.L., Strasser, A., Atadja, P., Lowe, S.W., and Johnstone, R.W. (2009b). The histone deacetylase inhibitors LAQ824 and LBH589 do not require death receptor signaling or a functional apoptosome to mediate tumor cell death or therapeutic efficacy. *Blood* 114, 380-393.
- Ellis, L., Hammers, H., and Pili, R. (2009c). Targeting tumor angiogenesis with histone deacetylase inhibitors. *Cancer letters* 280, 145-153.
- Esteller, M. (2006). The necessity of a human epigenome project. *Carcinogenesis* 27, 1121-1125.
- Esteller, M. (2008). Epigenetics in cancer. *The New England journal of medicine* 358, 1148-1159.
- Evan, G., and Littlewood, T. (1998). A matter of life and cell death. *Science (New York, N.Y.)* 281, 1317-1322.
- Falkenberg, K.J., and Johnstone, R.W. (2014). Histone deacetylases and their inhibitors in cancer, neurological diseases and immune disorders. *Nat Rev Drug Discov* 13, 673-691.
- Friedmann, D.R., and Marmorstein, R. (2013). Structure and mechanism of non-histone protein acetyltransferase enzymes. *The FEBS journal* 280, 5570-5581.
- Furumai, R., Matsuyama, A., Kobashi, N., Lee, K.H., Nishiyama, M., Nakajima, H., Tanaka, A., Komatsu, Y., Nishino, N., Yoshida, M., and Horinouchi, S. (2002). FK228 (depsipeptide) as a natural prodrug that inhibits class I histone deacetylases. *Cancer research* 62, 4916-4921.
- Gao, L., Cueto, M.A., Asselbergs, F., and Atadja, P. (2002). Cloning and functional characterization of HDAC11, a novel member of the human histone deacetylase family. *The Journal of biological chemistry* 277, 25748-25755.

Gao, Y.S., Hubbert, C.C., Lu, J., Lee, Y.S., Lee, J.Y., and Yao, T.P. (2007). Histone deacetylase 6 regulates growth factor-induced actin remodeling and endocytosis. *Molecular and cellular biology* 27, 8637-8647.

Gershey, E.L., Vidali, G., and Allfrey, V.G. (1968). Chemical studies of histone acetylation. The occurrence of epsilon-N-acetyllysine in the f2a1 histone. *The Journal of biological chemistry* 243, 5018-5022.

Ghobrial, I.M., Campigotto, F., Murphy, T.J., Boswell, E.N., Banwait, R., Azab, F., Chuma, S., Kunsman, J., Donovan, A., Masood, F., *et al.* (2013). Results of a phase 2 trial of the single-agent histone deacetylase inhibitor panobinostat in patients with relapsed/refractory Waldenstrom macroglobulinemia. *Blood* 121, 1296-1303.

Girdwood, D., Bumpass, D., Vaughan, O.A., Thain, A., Anderson, L.A., Snowden, A.W., Garcia-Wilson, E., Perkins, N.D., and Hay, R.T. (2003). P300 transcriptional repression is mediated by SUMO modification. *Molecular cell* 11, 1043-1054.

Glaser, K.B., Li, J., Staver, M.J., Wei, R.Q., Albert, D.H., and Davidsen, S.K. (2003). Role of class I and class II histone deacetylases in carcinoma cells using siRNA. *Biochemical and biophysical research communications* 310, 529-536.

Gloghini, A., Buglio, D., Khaskhely, N.M., Georgakis, G., Orłowski, R.Z., Neelapu, S.S., Carbone, A., and Younes, A. (2009). Expression of histone deacetylases in lymphoma: implication for the development of selective inhibitors. *British journal of haematology* 147, 515-525.

Glozak, M.A., Sengupta, N., Zhang, X., and Seto, E. (2005). Acetylation and deacetylation of non-histone proteins. *Gene* 363, 15-23.

Grausenburger, R., Bilic, I., Boucheron, N., Zupkovitz, G., El-Housseiny, L., Tschismarov, R., Zhang, Y., Rembold, M., Gaisberger, M., Hartl, A., *et al.* (2010). Conditional deletion of histone deacetylase 1 in T cells leads to enhanced airway inflammation and increased Th2 cytokine production. *Journal of immunology* 185, 3489-3497.

Gregoret, I.V., Lee, Y.M., and Goodson, H.V. (2004). Molecular evolution of the histone deacetylase family: functional implications of phylogenetic analysis. *Journal of molecular biology* 338, 17-31.

Groves, F.D., Linet, M.S., Travis, L.B., and Devesa, S.S. (2000). Cancer surveillance series: non-Hodgkin's lymphoma incidence by histologic subtype in the United States from 1978 through 1995. *Journal of the National Cancer Institute* 92, 1240-1251.

Grozinger, C.M., and Schreiber, S.L. (2002). Deacetylase enzymes: biological functions and the use of small-molecule inhibitors. *Chemistry & biology* 9, 3-16.

Gruhn, B., Naumann, T., Gruner, D., Walther, M., Wittig, S., Becker, S., Beck, J.F., and Sonnemann, J. (2013). The expression of histone deacetylase 4 is associated with prednisone poor-response in childhood acute lymphoblastic leukemia. *Leukemia research* 37, 1200-1207.

Guan, J.S., Haggarty, S.J., Giacometti, E., Dannenberg, J.H., Joseph, N., Gao, J., Nieland, T.J., Zhou, Y., Wang, X., Mazitschek, R., *et al.* (2009). HDAC2 negatively regulates memory formation and synaptic plasticity. *Nature* 459, 55-60.

Guccione, E., Martinato, F., Finocchiaro, G., Luzi, L., Tizzoni, L., Dall' Olio, V., Zardo, G., Nervi, C., Bernard, L., and Amati, B. (2006). Myc-binding-site recognition in the human genome is determined by chromatin context. *Nature cell biology* 8, 764-770.

Gui, C.Y., Ngo, L., Xu, W.S., Richon, V.M., and Marks, P.A. (2004). Histone deacetylase (HDAC) inhibitor activation of p21WAF1 involves changes in promoter-associated proteins, including HDAC1. *Proceedings of the National Academy of Sciences of the United States of America* 101, 1241-1246.

Haberland, M., Carrer, M., Mokalled, M.H., Montgomery, R.L., and Olson, E.N. (2010). Redundant control of adipogenesis by histone deacetylases 1 and 2. *The Journal of biological chemistry* 285, 14663-14670.

Haberland, M., Johnson, A., Mokalled, M.H., Montgomery, R.L., and Olson, E.N. (2009a). Genetic dissection of histone deacetylase requirement in tumor cells. *Proceedings of the National Academy of Sciences of the United States of America* 106, 7751-7755.

Haberland, M., Montgomery, R.L., and Olson, E.N. (2009b). The many roles of histone deacetylases in development and physiology: implications for disease and therapy. *Nature reviews. Genetics* 10, 32-42.

Haery, L., Thompson, R.C., and Gilmore, T.D. (2015). Histone acetyltransferases and histone deacetylases in B- and T-cell development, physiology and malignancy. *Genes & cancer* 6, 184-213.

Hagelkruys, A., Lagger, S., Krahmer, J., Leopoldi, A., Artaker, M., Pusch, O., Zezula, J., Weissmann, S., Xie, Y., Schofer, C., *et al.* (2014). A single allele of Hdac2 but not Hdac1 is sufficient for normal mouse brain development in the absence of its paralog. *Development (Cambridge, England)* 141, 604-616.

Hagelkruys, A., Sawicka, A., Rennmayr, M., and Seiser, C. (2011). The biology of HDAC in cancer: the nuclear and epigenetic components. *Handbook of experimental pharmacology* 206, 13-37.

Hamel, K.M., Mandal, M., Karki, S., and Clark, M.R. (2014). Balancing Proliferation with Igkappa Recombination during B-lymphopoiesis. *Frontiers in immunology* 5, 139.

Bibliography

Hanahan, D., and Folkman, J. (1996). Patterns and emerging mechanisms of the angiogenic switch during tumorigenesis. *Cell* *86*, 353-364.

Hanahan, D., and Weinberg, R.A. (2000). The hallmarks of cancer. *Cell* *100*, 57-70.

Hanahan, D., and Weinberg, R.A. (2011). Hallmarks of cancer: the next generation. *Cell* *144*, 646-674.

Harris, A.W., Pinkert, C.A., Crawford, M., Langdon, W.Y., Brinster, R.L., and Adams, J.M. (1988). The E mu-myc transgenic mouse. A model for high-incidence spontaneous lymphoma and leukemia of early B cells. *The Journal of experimental medicine* *167*, 353-371.

Harris, C.C. (1996). p53 tumor suppressor gene: from the basic research laboratory to the clinic--an abridged historical perspective. *Carcinogenesis* *17*, 1187-1198.

Heideman, M.R., Wilting, R.H., Yanover, E., Velds, A., de Jong, J., Kerkhoven, R.M., Jacobs, H., Wessels, L.F., and Dannenberg, J.H. (2013). Dosage-dependent tumor suppression by histone deacetylases 1 and 2 through regulation of c-Myc collaborating genes and p53 function. *Blood* *121*, 2038-2050.

Hobeika, E., Thiemann, S., Storch, B., Jumaa, H., Nielsen, P.J., Pelanda, R., and Reth, M. (2006). Testing gene function early in the B cell lineage in mb1-cre mice. *Proceedings of the National Academy of Sciences of the United States of America* *103*, 13789-13794.

Hubbert, C., Guardiola, A., Shao, R., Kawaguchi, Y., Ito, A., Nixon, A., Yoshida, M., Wang, X.F., and Yao, T.P. (2002). HDAC6 is a microtubule-associated deacetylase. *Nature* *417*, 455-458.

Igarashi, H., Gregory, S.C., Yokota, T., Sakaguchi, N., and Kincade, P.W. (2002). Transcription from the RAG1 locus marks the earliest lymphocyte progenitors in bone marrow. *Immunity* *17*, 117-130.

Ikawa, T. (2014). Genetic and epigenetic control of early lymphocyte development. *Current topics in microbiology and immunology* *381*, 1-20.

Inche, A.G., and La Thangue, N.B. (2006). Chromatin control and cancer-drug discovery: realizing the promise. *Drug discovery today* *11*, 97-109.

Inoue, S., Mai, A., Dyer, M.J., and Cohen, G.M. (2006). Inhibition of histone deacetylase class I but not class II is critical for the sensitization of leukemic cells to tumor necrosis factor-related apoptosis-inducing ligand-induced apoptosis. *Cancer research* *66*, 6785-6792.

Itazaki, H., Nagashima, K., Sugita, K., Yoshida, H., Kawamura, Y., Yasuda, Y., Matsumoto, K., Ishii, K., Uotani, N., Nakai, H., and et al. (1990). Isolation and structural elucidation of new cyclotetrapeptides, trapoxins A and B, having detransformation activities as antitumor agents. *The Journal of antibiotics* *43*, 1524-1532.

Ito, A., Kawaguchi, Y., Lai, C.H., Kovacs, J.J., Higashimoto, Y., Appella, E., and Yao, T.P. (2002). MDM2-HDAC1-mediated deacetylation of p53 is required for its degradation. *The EMBO journal* 21, 6236-6245.

Jacob, C., Christen, C.N., Pereira, J.A., Somandin, C., Baggiolini, A., Lotscher, P., Ozcelik, M., Tricaud, N., Meijer, D., Yamaguchi, T., *et al.* (2011). HDAC1 and HDAC2 control the transcriptional program of myelination and the survival of Schwann cells. *Nature neuroscience* 14, 429-436.

Jenuwein, T., and Allis, C.D. (2001). Translating the histone code. *Science (New York, N.Y.)* 293, 1074-1080.

Johnson, K., Angelin-Duclos, C., Park, S., and Calame, K.L. (2003). Changes in histone acetylation are associated with differences in accessibility of V(H) gene segments to V-DJ recombination during B-cell ontogeny and development. *Molecular and cellular biology* 23, 2438-2450.

Johnstone, R.W. (2002). Histone-deacetylase inhibitors: novel drugs for the treatment of cancer. *Nat Rev Drug Discov* 1, 287-299.

Johnstone, R.W., and Licht, J.D. (2003). Histone deacetylase inhibitors in cancer therapy: is transcription the primary target? *Cancer cell* 4, 13-18.

Junttila, M.R., and Evan, G.I. (2009). p53--a Jack of all trades but master of none. *Nature reviews. Cancer* 9, 821-829.

Jurkin, J., Zupkovitz, G., Lagger, S., Grausenburger, R., Hagelkruys, A., Kenner, L., and Seiser, C. (2011). Distinct and redundant functions of histone deacetylases HDAC1 and HDAC2 in proliferation and tumorigenesis. *Cell cycle (Georgetown, Tex.)* 10, 406-412.

Ke, Q., and Costa, M. (2006). Hypoxia-inducible factor-1 (HIF-1). *Molecular pharmacology* 70, 1469-1480.

Kelly, R.D., and Cowley, S.M. (2013). The physiological roles of histone deacetylase (HDAC) 1 and 2: complex co-stars with multiple leading parts. *Biochemical Society transactions* 41, 741-749.

Khan, N., Jeffers, M., Kumar, S., Hackett, C., Boldog, F., Khramtsov, N., Qian, X., Mills, E., Berghs, S.C., Carey, N., *et al.* (2008). Determination of the class and isoform selectivity of small-molecule histone deacetylase inhibitors. *The Biochemical journal* 409, 581-589.

Kidder, B.L., and Palmer, S. (2012). HDAC1 regulates pluripotency and lineage specific transcriptional networks in embryonic and trophoblast stem cells. *Nucleic acids research* 40, 2925-2939.

- Kim, M.S., Kwon, H.J., Lee, Y.M., Baek, J.H., Jang, J.E., Lee, S.W., Moon, E.J., Kim, H.S., Lee, S.K., Chung, H.Y., *et al.* (2001). Histone deacetylases induce angiogenesis by negative regulation of tumor suppressor genes. *Nature medicine* 7, 437-443.
- Kim, S.C., Sprung, R., Chen, Y., Xu, Y., Ball, H., Pei, J., Cheng, T., Kho, Y., Xiao, H., Xiao, L., *et al.* (2006). Substrate and functional diversity of lysine acetylation revealed by a proteomics survey. *Molecular cell* 23, 607-618.
- Kim, S.H., Jeong, J.W., Park, J.A., Lee, J.W., Seo, J.H., Jung, B.K., Bae, M.K., and Kim, K.W. (2007). Regulation of the HIF-1 α stability by histone deacetylases. *Oncology reports* 17, 647-651.
- Kioussis, D., and Georgopoulos, K. (2007). Epigenetic flexibility underlying lineage choices in the adaptive immune system. *Science (New York, N.Y.)* 317, 620-622.
- Klapproth, K., and Wirth, T. (2010). Advances in the understanding of MYC-induced lymphomagenesis. *British journal of haematology* 149, 484-497.
- Kondo, M., Weissman, I.L., and Akashi, K. (1997). Identification of clonogenic common lymphoid progenitors in mouse bone marrow. *Cell* 91, 661-672.
- Kouzarides, T. (2000). Acetylation: a regulatory modification to rival phosphorylation? *The EMBO journal* 19, 1176-1179.
- Kouzarides, T. (2007). Chromatin modifications and their function. *Cell* 128, 693-705.
- Kovacs, J.J., Murphy, P.J., Gaillard, S., Zhao, X., Wu, J.T., Nicchitta, C.V., Yoshida, M., Toft, D.O., Pratt, W.B., and Yao, T.P. (2005). HDAC6 regulates Hsp90 acetylation and chaperone-dependent activation of glucocorticoid receptor. *Molecular cell* 18, 601-607.
- Krebs, J.E., Fry, C.J., Samuels, M.L., and Peterson, C.L. (2000). Global role for chromatin remodeling enzymes in mitotic gene expression. *Cell* 102, 587-598.
- Kurdistani, S.K., Robyr, D., Tavazoie, S., and Grunstein, M. (2002). Genome-wide binding map of the histone deacetylase Rpd3 in yeast. *Nature genetics* 31, 248-254.
- Kurdistani, S.K., Tavazoie, S., and Grunstein, M. (2004). Mapping global histone acetylation patterns to gene expression. *Cell* 117, 721-733.
- Kurland, J.F., and Tansey, W.P. (2008). Myc-mediated transcriptional repression by recruitment of histone deacetylase. *Cancer research* 68, 3624-3629.
- Lagger, G., O'Carroll, D., Rembold, M., Khier, H., Tischler, J., Weitzer, G., Schuettengruber, B., Hauser, C., Brunmeir, R., Jenuwein, T., and Seiser, C. (2002). Essential function of histone deacetylase 1 in proliferation control and CDK inhibitor repression. *The EMBO journal* 21, 2672-2681.

Lagger, S., Meunier, D., Mikula, M., Brunmeir, R., Schleder, M., Artaker, M., Pusch, O., Egger, G., Hagelkruys, A., Mikulits, W., *et al.* (2010). Crucial function of histone deacetylase 1 for differentiation of teratomas in mice and humans. *The EMBO journal* 29, 3992-4007.

Lai, A.Y., and Kondo, M. (2008). T and B lymphocyte differentiation from hematopoietic stem cell. *Seminars in immunology* 20, 207-212.

Langdon, W.Y., Harris, A.W., Cory, S., and Adams, J.M. (1986). The c-myc oncogene perturbs B lymphocyte development in E-mu-myc transgenic mice. *Cell* 47, 11-18.

LeBoeuf, M., Terrell, A., Trivedi, S., Sinha, S., Epstein, J.A., Olson, E.N., Morrisey, E.E., and Millar, S.E. (2010). Hdac1 and Hdac2 act redundantly to control p63 and p53 functions in epidermal progenitor cells. *Developmental cell* 19, 807-818.

Lee, J.Y., Koga, H., Kawaguchi, Y., Tang, W., Wong, E., Gao, Y.S., Pandey, U.B., Kaushik, S., Tresse, E., Lu, J., *et al.* (2010). HDAC6 controls autophagosome maturation essential for ubiquitin-selective quality-control autophagy. *The EMBO journal* 29, 969-980.

Lee, Y.S., Lim, K.H., Guo, X., Kawaguchi, Y., Gao, Y., Barrientos, T., Ordentlich, P., Wang, X.F., Counter, C.M., and Yao, T.P. (2008). The cytoplasmic deacetylase HDAC6 is required for efficient oncogenic tumorigenesis. *Cancer research* 68, 7561-7569.

Levens, D. (2013). Cellular MYC economics: Balancing MYC function with MYC expression. *Cold Spring Harbor perspectives in medicine* 3.

Li, B., Carey, M., and Workman, J.L. (2007). The role of chromatin during transcription. *Cell* 128, 707-719.

Li, G., Zan, H., Xu, Z., and Casali, P. (2013). Epigenetics of the antibody response. *Trends in immunology* 34, 460-470.

Liang, J., Prouty, L., Williams, B.J., Dayton, M.A., and Blanchard, K.L. (1998). Acute mixed lineage leukemia with an inv(8)(p11q13) resulting in fusion of the genes for MOZ and TIF2. *Blood* 92, 2118-2122.

Lin, C.Y., Loven, J., Rahl, P.B., Paranal, R.M., Burge, C.B., Bradner, J.E., Lee, T.I., and Young, R.A. (2012). Transcriptional amplification in tumor cells with elevated c-Myc. *Cell* 151, 56-67.

Lindemann, R.K., Newbold, A., Whitecross, K.F., Cluse, L.A., Frew, A.J., Ellis, L., Williams, S., Wiegmanns, A.P., Dear, A.E., Scott, C.L., *et al.* (2007). Analysis of the apoptotic and therapeutic activities of histone deacetylase inhibitors by using a mouse model of B cell lymphoma. *Proceedings of the National Academy of Sciences of the United States of America* 104, 8071-8076.

Lopez-Granados, E. (2011). Epigenetic control of lymphocyte differentiation. *Advances in experimental medicine and biology* 711, 26-35.

- Lowe, S.W., Cepero, E., and Evan, G. (2004). Intrinsic tumour suppression. *Nature* 432, 307-315.
- Luo, J., Su, F., Chen, D., Shiloh, A., and Gu, W. (2000). Deacetylation of p53 modulates its effect on cell growth and apoptosis. *Nature* 408, 377-381.
- Luscher, B., and Vervoorts, J. (2012). Regulation of gene transcription by the oncoprotein MYC. *Gene* 494, 145-160.
- Ma, P., Pan, H., Montgomery, R.L., Olson, E.N., and Schultz, R.M. (2012). Compensatory functions of histone deacetylase 1 (HDAC1) and HDAC2 regulate transcription and apoptosis during mouse oocyte development. *Proceedings of the National Academy of Sciences of the United States of America* 109, E481-489.
- Ma, P., and Schultz, R.M. (2013). Histone deacetylase 2 (HDAC2) regulates chromosome segregation and kinetochore function via H4K16 deacetylation during oocyte maturation in mouse. *PLoS genetics* 9, e1003377.
- MacDonald, J.L., and Roskams, A.J. (2008). Histone deacetylases 1 and 2 are expressed at distinct stages of neuro-glial development. *Developmental dynamics : an official publication of the American Association of Anatomists* 237, 2256-2267.
- Maes, J., Maleszewska, M., Guillemin, C., Pflumio, F., Six, E., Andre-Schmutz, I., Cavazzana-Calvo, M., Charron, D., Francastel, C., and Goodhardt, M. (2008). Lymphoid-affiliated genes are associated with active histone modifications in human hematopoietic stem cells. *Blood* 112, 2722-2729.
- Mai, A., and Altucci, L. (2009). Epi-drugs to fight cancer: from chemistry to cancer treatment, the road ahead. *The international journal of biochemistry & cell biology* 41, 199-213.
- Mandel, E.M., and Grosschedl, R. (2010). Transcription control of early B cell differentiation. *Current opinion in immunology* 22, 161-167.
- Marino-Ramirez, L., Kann, M.G., Shoemaker, B.A., and Landsman, D. (2005). Histone structure and nucleosome stability. *Expert review of proteomics* 2, 719-729.
- Marks, P.A. (2010). The clinical development of histone deacetylase inhibitors as targeted anticancer drugs. *Expert opinion on investigational drugs* 19, 1049-1066.
- Marquard, L., Gjerdrum, L.M., Christensen, I.J., Jensen, P.B., Sehested, M., and Ralfkiaer, E. (2008). Prognostic significance of the therapeutic targets histone deacetylase 1, 2, 6 and acetylated histone H4 in cutaneous T-cell lymphoma. *Histopathology* 53, 267-277.
- Marquard, L., Poulsen, C.B., Gjerdrum, L.M., de Nully Brown, P., Christensen, I.J., Jensen, P.B., Sehested, M., Johansen, P., and Ralfkiaer, E. (2009). Histone deacetylase 1, 2, 6 and acetylated histone H4 in B- and T-cell lymphomas. *Histopathology* 54, 688-698.

- Matthews, G.M., Mehdipour, P., Cluse, L.A., Falkenberg, K.J., Wang, E., Roth, M., Santoro, F., Vidacs, E., Stanley, K., House, C.M., *et al.* (2015). Functional-genetic dissection of HDAC dependencies in mouse lymphoid and myeloid malignancies. *Blood* *126*, 2392-2403.
- Matthias, P., and Rolink, A.G. (2005). Transcriptional networks in developing and mature B cells. *Nature reviews. Immunology* *5*, 497-508.
- Matthias, P., Yoshida, M., and Khochbin, S. (2008). HDAC6 a new cellular stress surveillance factor. *Cell cycle (Georgetown, Tex.)* *7*, 7-10.
- McMurry, M.T., and Krangel, M.S. (2000). A role for histone acetylation in the developmental regulation of VDJ recombination. *Science (New York, N.Y.)* *287*, 495-498.
- Means, G.D., Toy, D.Y., Baum, P.R., and Derry, J.M. (2000). A transcript map of a 2-Mb BAC contig in the proximal portion of the mouse X chromosome and regional mapping of the scurfy mutation. *Genomics* *65*, 213-223.
- Medina, K.L., Garrett, K.P., Thompson, L.F., Rossi, M.I., Payne, K.J., and Kincade, P.W. (2001). Identification of very early lymphoid precursors in bone marrow and their regulation by estrogen. *Nature immunology* *2*, 718-724.
- Mercurio, C., Minucci, S., and Pelicci, P.G. (2010). Histone deacetylases and epigenetic therapies of hematological malignancies. *Pharmacological research* *62*, 18-34.
- Mertz, J.A., Conery, A.R., Bryant, B.M., Sandy, P., Balasubramanian, S., Mele, D.A., Bergeron, L., and Sims, R.J., 3rd (2011). Targeting MYC dependence in cancer by inhibiting BET bromodomains. *Proceedings of the National Academy of Sciences of the United States of America* *108*, 16669-16674.
- Methot, J.L., Chakravarty, P.K., Chenard, M., Close, J., Cruz, J.C., Dahlberg, W.K., Fleming, J., Hamblett, C.L., Hamill, J.E., Harrington, P., *et al.* (2008). Exploration of the internal cavity of histone deacetylase (HDAC) with selective HDAC1/HDAC2 inhibitors (SHI-1:2). *Bioorganic & medicinal chemistry letters* *18*, 973-978.
- Meyer, N., and Penn, L.Z. (2008). Reflecting on 25 years with MYC. *Nature reviews. Cancer* *8*, 976-990.
- Miller, K.M., Tjeertes, J.V., Coates, J., Legube, G., Polo, S.E., Britton, S., and Jackson, S.P. (2010). Human HDAC1 and HDAC2 function in the DNA-damage response to promote DNA nonhomologous end-joining. *Nature structural & molecular biology* *17*, 1144-1151.
- Min, J., Landry, J., Sternglanz, R., and Xu, R.M. (2001). Crystal structure of a SIR2 homolog-NAD complex. *Cell* *105*, 269-279.

Montgomery, R.L., Davis, C.A., Potthoff, M.J., Haberland, M., Fielitz, J., Qi, X., Hill, J.A., Richardson, J.A., and Olson, E.N. (2007). Histone deacetylases 1 and 2 redundantly regulate cardiac morphogenesis, growth, and contractility. *Genes & development* *21*, 1790-1802.

Montgomery, R.L., Hsieh, J., Barbosa, A.C., Richardson, J.A., and Olson, E.N. (2009). Histone deacetylases 1 and 2 control the progression of neural precursors to neurons during brain development. *Proceedings of the National Academy of Sciences of the United States of America* *106*, 7876-7881.

Moradei, O., Vaisburg, A., and Martell, R.E. (2008). Histone deacetylase inhibitors in cancer therapy: new compounds and clinical update of benzamide-type agents. *Current topics in medicinal chemistry* *8*, 841-858.

Moreno, D.A., Scrideli, C.A., Cortez, M.A., de Paula Queiroz, R., Valera, E.T., da Silva Silveira, V., Yunes, J.A., Brandalise, S.R., and Tone, L.G. (2010). Differential expression of HDAC3, HDAC7 and HDAC9 is associated with prognosis and survival in childhood acute lymphoblastic leukaemia. *British journal of haematology* *150*, 665-673.

Morrison, S.J., Wandycz, A.M., Hemmati, H.D., Wright, D.E., and Weissman, I.L. (1997). Identification of a lineage of multipotent hematopoietic progenitors. *Development (Cambridge, England)* *124*, 1929-1939.

Morse, H.C., 3rd, Anver, M.R., Fredrickson, T.N., Haines, D.C., Harris, A.W., Harris, N.L., Jaffe, E.S., Kogan, S.C., MacLennan, I.C., Pattengale, P.K., and Ward, J.M. (2002). Bethesda proposals for classification of lymphoid neoplasms in mice. *Blood* *100*, 246-258.

Morshead, K.B., Ciccone, D.N., Taverna, S.D., Allis, C.D., and Oettinger, M.A. (2003). Antigen receptor loci poised for V(D)J rearrangement are broadly associated with BRG1 and flanked by peaks of histone H3 dimethylated at lysine 4. *Proceedings of the National Academy of Sciences of the United States of America* *100*, 11577-11582.

Mostoslavsky, R., Kirillov, A., Ji, Y.H., Goldmit, M., Holzmann, M., Wirth, T., Cedar, H., and Bergman, Y. (1999). Demethylation and the establishment of kappa allelic exclusion. *Cold Spring Harbor symposia on quantitative biology* *64*, 197-206.

Mottamal, M., Zheng, S., Huang, T.L., and Wang, G. (2015). Histone deacetylase inhibitors in clinical studies as templates for new anticancer agents. *Molecules (Basel, Switzerland)* *20*, 3898-3941.

Mottet, D., Pirotte, S., Lamour, V., Hagedorn, M., Javerzat, S., Bikfalvi, A., Bellahcene, A., Verdin, E., and Castronovo, V. (2009). HDAC4 represses p21(WAF1/Cip1) expression in human cancer cells through a Sp1-dependent, p53-independent mechanism. *Oncogene* *28*, 243-256.

Mujtaba, S., Zeng, L., and Zhou, M.M. (2007). Structure and acetyl-lysine recognition of the bromodomain. *Oncogene* *26*, 5521-5527.

Nemazee, D., and Weigert, M. (2000). Revising B cell receptors. *The Journal of experimental medicine* *191*, 1813-1817.

Nesbit, C.E., Tersak, J.M., and Prochownik, E.V. (1999). MYC oncogenes and human neoplastic disease. *Oncogene* *18*, 3004-3016.

Newbold, A., Lindemann, R.K., Cluse, L.A., Whitecross, K.F., Dear, A.E., and Johnstone, R.W. (2008). Characterisation of the novel apoptotic and therapeutic activities of the histone deacetylase inhibitor romidepsin. *Molecular cancer therapeutics* *7*, 1066-1079.

Newbold, A., Matthews, G.M., Bots, M., Cluse, L.A., Clarke, C.J., Banks, K.M., Cullinane, C., Bolden, J.E., Christiansen, A.J., Dickins, R.A., *et al.* (2013). Molecular and biologic analysis of histone deacetylase inhibitors with diverse specificities. *Molecular cancer therapeutics* *12*, 2709-2721.

Newbold, A., Salmon, J.M., Martin, B.P., Stanley, K., and Johnstone, R.W. (2014). The role of p21(waf1/cip1) and p27(Kip1) in HDACi-mediated tumor cell death and cell cycle arrest in the Emu-myc model of B-cell lymphoma. *Oncogene* *33*, 5415-5423.

Nie, Z., Hu, G., Wei, G., Cui, K., Yamane, A., Resch, W., Wang, R., Green, D.R., Tessarollo, L., Casellas, R., *et al.* (2012). c-Myc is a universal amplifier of expressed genes in lymphocytes and embryonic stem cells. *Cell* *151*, 68-79.

Norris, K.L., Lee, J.Y., and Yao, T.P. (2009). Acetylation goes global: the emergence of acetylation biology. *Science signaling* *2*, pe76.

Nutt, S.L., and Kee, B.L. (2007). The transcriptional regulation of B cell lineage commitment. *Immunity* *26*, 715-725.

Ocker, M., and Schneider-Stock, R. (2007). Histone deacetylase inhibitors: signalling towards p21cip1/waf1. *The international journal of biochemistry & cell biology* *39*, 1367-1374.

Olejniczak, M., Urbanek, M.O., Jaworska, E., Witucki, L., Szczesniak, M.W., Makalowska, I., and Krzyzosiak, W.J. (2016). Sequence-non-specific effects generated by various types of RNA interference triggers. *Biochimica et biophysica acta* *1859*, 306-314.

Olzscha, H., Sheikh, S., and La Thangue, N.B. (2015). Deacetylation of chromatin and gene expression regulation: a new target for epigenetic therapy. *Critical reviews in oncogenesis* *20*, 1-17.

Ononye, S.N., van Heyst, M., Falcone, E.M., Anderson, A.C., and Wright, D.L. (2012). Toward isozyme-selective inhibitors of histone deacetylase as therapeutic agents for the treatment of cancer. *Pharmaceutical patent analyst* *1*, 207-221.

Ott, G., Rosenwald, A., and Campo, E. (2013). Understanding MYC-driven aggressive B-cell lymphomas: pathogenesis and classification. *Blood* *122*, 3884-3891.

Bibliography

- Paoluzzi, L., Scotto, L., Marchi, E., Zain, J., Seshan, V.E., and O'Connor, O.A. (2010). Romidepsin and belinostat synergize the antineoplastic effect of bortezomib in mantle cell lymphoma. *Clinical cancer research : an official journal of the American Association for Cancer Research* 16, 554-565.
- Parra, M. (2009). Epigenetic events during B lymphocyte development. *Epigenetics* 4, 462-468.
- Pasqualucci, L., Bereshchenko, O., Niu, H., Klein, U., Basso, K., Guglielmino, R., Cattoretti, G., and Dalla-Favera, R. (2003). Molecular pathogenesis of non-Hodgkin's lymphoma: the role of Bcl-6. *Leukemia & lymphoma* 44 Suppl 3, S5-12.
- Pasqualucci, L., Dominguez-Sola, D., Chiarenza, A., Fabbri, G., Grunn, A., Trifonov, V., Kasper, L.H., Lerach, S., Tang, H., Ma, J., *et al.* (2011). Inactivating mutations of acetyltransferase genes in B-cell lymphoma. *Nature* 471, 189-195.
- Peart, M.J., Tainton, K.M., Ruefli, A.A., Dear, A.E., Sedelies, K.A., O'Reilly, L.A., Waterhouse, N.J., Trapani, J.A., and Johnstone, R.W. (2003). Novel mechanisms of apoptosis induced by histone deacetylase inhibitors. *Cancer research* 63, 4460-4471.
- Peinado, H., Olmeda, D., and Cano, A. (2007). Snail, Zeb and bHLH factors in tumour progression: an alliance against the epithelial phenotype? *Nature reviews. Cancer* 7, 415-428.
- Pelengaris, S., Khan, M., and Evan, G. (2002). c-MYC: more than just a matter of life and death. *Nature reviews. Cancer* 2, 764-776.
- Peng, L., and Seto, E. (2011). Deacetylation of nonhistone proteins by HDACs and the implications in cancer. *Handbook of experimental pharmacology* 206, 39-56.
- Polyak, K., and Weinberg, R.A. (2009). Transitions between epithelial and mesenchymal states: acquisition of malignant and stem cell traits. *Nature reviews. Cancer* 9, 265-273.
- Portela, A., and Esteller, M. (2010). Epigenetic modifications and human disease. *Nature biotechnology* 28, 1057-1068.
- Qian, D.Z., Kachhap, S.K., Collis, S.J., Verheul, H.M., Carducci, M.A., Atadja, P., and Pili, R. (2006). Class II histone deacetylases are associated with VHL-independent regulation of hypoxia-inducible factor 1 alpha. *Cancer research* 66, 8814-8821.
- Raica, M., Cimpean, A.M., and Ribatti, D. (2009). Angiogenesis in pre-malignant conditions. *European journal of cancer (Oxford, England : 1990)* 45, 1924-1934.
- Rasheed, W., Bishton, M., Johnstone, R.W., and Prince, H.M. (2008). Histone deacetylase inhibitors in lymphoma and solid malignancies. *Expert review of anticancer therapy* 8, 413-432.

Reichert, N., Choukrallah, M.A., and Matthias, P. (2012). Multiple roles of class I HDACs in proliferation, differentiation, and development. *Cellular and molecular life sciences : CMLS* 69, 2173-2187.

Richardson, P.G., Schlossman, R.L., Alsina, M., Weber, D.M., Coutre, S.E., Gasparetto, C., Mukhopadhyay, S., Ondovik, M.S., Khan, M., Paley, C.S., and Lonial, S. (2013). PANORAMA 2: panobinostat in combination with bortezomib and dexamethasone in patients with relapsed and bortezomib-refractory myeloma. *Blood* 122, 2331-2337.

Richon, V.M., Garcia-Vargas, J., and Hardwick, J.S. (2009). Development of vorinostat: current applications and future perspectives for cancer therapy. *Cancer letters* 280, 201-210.

Richon, V.M., Sandhoff, T.W., Rifkind, R.A., and Marks, P.A. (2000). Histone deacetylase inhibitor selectively induces p21WAF1 expression and gene-associated histone acetylation. *Proceedings of the National Academy of Sciences of the United States of America* 97, 10014-10019.

Robert, T., Vanoli, F., Chiolo, I., Shubassi, G., Bernstein, K.A., Rothstein, R., Botrugno, O.A., Parazzoli, D., Oldani, A., Minucci, S., and Foiani, M. (2011). HDACs link the DNA damage response, processing of double-strand breaks and autophagy. *Nature* 471, 74-79.

Rodriguez-Paredes, M., and Esteller, M. (2011). Cancer epigenetics reaches mainstream oncology. *Nature medicine* 17, 330-339.

Sabo, A., Kress, T.R., Pelizzola, M., de Pretis, S., Gorski, M.M., Tesi, A., Morelli, M.J., Bora, P., Doni, M., Verrecchia, A., *et al.* (2014). Selective transcriptional regulation by Myc in cellular growth control and lymphomagenesis. *Nature* 511, 488-492.

Sambucetti, L.C., Fischer, D.D., Zabudoff, S., Kwon, P.O., Chamberlin, H., Trogani, N., Xu, H., and Cohen, D. (1999). Histone deacetylase inhibition selectively alters the activity and expression of cell cycle proteins leading to specific chromatin acetylation and antiproliferative effects. *The Journal of biological chemistry* 274, 34940-34947.

San-Miguel, J.F., Richardson, P.G., Gunther, A., Sezer, O., Siegel, D., Blade, J., LeBlanc, R., Sutherland, H., Sopala, M., Mishra, K.K., *et al.* (2013). Phase Ib study of panobinostat and bortezomib in relapsed or relapsed and refractory multiple myeloma. *Journal of clinical oncology : official journal of the American Society of Clinical Oncology* 31, 3696-3703.

Sandor, V., Senderowicz, A., Mertins, S., Sackett, D., Sausville, E., Blagosklonny, M.V., and Bates, S.E. (2000). P21-dependent G1 arrest with downregulation of cyclin D1 and upregulation of cyclin E by the histone deacetylase inhibitor FR901228. *British journal of cancer* 83, 817-825.

Santoro, F., Botrugno, O.A., Dal Zuffo, R., Pallavicini, I., Matthews, G.M., Cluse, L., Barozzi, I., Senese, S., Fornasari, L., Moretti, S., *et al.* (2013). A dual role for Hdac1: oncosuppressor in tumorigenesis, oncogene in tumor maintenance. *Blood* 121, 3459-3468.

Schatz, D.G., and Ji, Y. (2011). Recombination centres and the orchestration of V(D)J recombination. *Nature reviews. Immunology* *11*, 251-263.

Schmitt, C.A., Rosenthal, C.T., and Lowe, S.W. (2000). Genetic analysis of chemoresistance in primary murine lymphomas. *Nature medicine* *6*, 1029-1035.

Schroeder, F.A., Lewis, M.C., Fass, D.M., Wagner, F.F., Zhang, Y.L., Hennig, K.M., Gale, J., Zhao, W.N., Reis, S., Barker, D.D., *et al.* (2013). A selective HDAC 1/2 inhibitor modulates chromatin and gene expression in brain and alters mouse behavior in two mood-related tests. *PloS one* *8*, e71323.

Seidel, C., Florean, C., Schnekenburger, M., Dicato, M., and Diederich, M. (2012). Chromatin-modifying agents in anti-cancer therapy. *Biochimie* *94*, 2264-2279.

Seidel, C., Schnekenburger, M., Dicato, M., and Diederich, M. (2015). Histone deacetylase 6 in health and disease. *Epigenomics* *7*, 103-118.

Senese, S., Zaragoza, K., Minardi, S., Muradore, I., Ronzoni, S., Passafaro, A., Bernard, L., Draetta, G.F., Alcalay, M., Seiser, C., and Chiocca, S. (2007). Role for histone deacetylase 1 in human tumor cell proliferation. *Molecular and cellular biology* *27*, 4784-4795.

Shan, B., Yao, T.P., Nguyen, H.T., Zhuo, Y., Levy, D.R., Klingsberg, R.C., Tao, H., Palmer, M.L., Holder, K.N., and Lasky, J.A. (2008). Requirement of HDAC6 for transforming growth factor-beta1-induced epithelial-mesenchymal transition. *The Journal of biological chemistry* *283*, 21065-21073.

Shankland, K.R., Armitage, J.O., and Hancock, B.W. (2012). Non-Hodgkin lymphoma. *Lancet* *380*, 848-857.

Shao, W., Growney, J.D., Feng, Y., O'Connor, G., Pu, M., Zhu, W., Yao, Y.M., Kwon, P., Fawell, S., and Atadja, P. (2010). Activity of deacetylase inhibitor panobinostat (LBH589) in cutaneous T-cell lymphoma models: Defining molecular mechanisms of resistance. *International journal of cancer. Journal international du cancer* *127*, 2199-2208.

Sharma, S., Kelly, T.K., and Jones, P.A. (2010). Epigenetics in cancer. *Carcinogenesis* *31*, 27-36.

Sidman, C.L., Shaffer, D.J., Jacobsen, K., Vargas, S.R., and Osmond, D.G. (1993). Cell populations during tumorigenesis in Eu-myc transgenic mice. *Leukemia* *7*, 887-895.

Siegel, R.L., Miller, K.D., and Jemal, A. (2015). Cancer statistics, 2015. *CA: a cancer journal for clinicians* *65*, 5-29.

Simms-Waldrip, T., Rodriguez-Gonzalez, A., Lin, T., Ikeda, A.K., Fu, C., and Sakamoto, K.M. (2008). The aggresome pathway as a target for therapy in hematologic malignancies. *Molecular genetics and metabolism* *94*, 283-286.

Bibliography

- Simoes-Pires, C., Zwick, V., Nurisso, A., Schenker, E., Carrupt, P.A., and Cuendet, M. (2013). HDAC6 as a target for neurodegenerative diseases: what makes it different from the other HDACs? *Molecular neurodegeneration* 8, 7.
- Slingerland, M., Guchelaar, H.J., and Gelderblom, H. (2014). Histone deacetylase inhibitors: an overview of the clinical studies in solid tumors. *Anti-cancer drugs* 25, 140-149.
- Smith, B.C., Hallows, W.C., and Denu, J.M. (2008). Mechanisms and molecular probes of sirtuins. *Chemistry & biology* 15, 1002-1013.
- Spangrude, G.J., Heimfeld, S., and Weissman, I.L. (1988). Purification and characterization of mouse hematopoietic stem cells. *Science (New York, N.Y.)* 241, 58-62.
- Stimson, L., and La Thangue, N.B. (2009). Biomarkers for predicting clinical responses to HDAC inhibitors. *Cancer letters* 280, 177-183.
- Strahl, B.D., and Allis, C.D. (2000). The language of covalent histone modifications. *Nature* 403, 41-45.
- Stubbs, M.C., Kim, W., Bariteau, M., Davis, T., Vempati, S., Minehart, J., Witkin, M., Qi, J., Krivtsov, A.V., Bradner, J.E., *et al.* (2015). Selective Inhibition of HDAC1 and HDAC2 as a Potential Therapeutic Option for B-ALL. *Clinical cancer research : an official journal of the American Association for Cancer Research* 21, 2348-2358.
- Su, I.H., and Tarakhovskiy, A. (2005). Epigenetic control of B cell differentiation. *Seminars in immunology* 17, 167-172.
- Subramanian, C., Jarzembowski, J.A., Opipari, A.W., Jr., Castle, V.P., and Kwok, R.P. (2011). HDAC6 deacetylates Ku70 and regulates Ku70-Bax binding in neuroblastoma. *Neoplasia (New York, N.Y.)* 13, 726-734.
- Tang, Y., Zhao, W., Chen, Y., Zhao, Y., and Gu, W. (2008). Acetylation is indispensable for p53 activation. *Cell* 133, 612-626.
- Taunton, J., Hassig, C.A., and Schreiber, S.L. (1996). A mammalian histone deacetylase related to the yeast transcriptional regulator Rpd3p. *Science (New York, N.Y.)* 272, 408-411.
- Thiery, J.P., Acloque, H., Huang, R.Y., and Nieto, M.A. (2009). Epithelial-mesenchymal transitions in development and disease. *Cell* 139, 871-890.
- Torchia, J., Rose, D.W., Inostroza, J., Kamei, Y., Westin, S., Glass, C.K., and Rosenfeld, M.G. (1997). The transcriptional co-activator p/CIP binds CBP and mediates nuclear-receptor function. *Nature* 387, 677-684.

Trivedi, C.M., Luo, Y., Yin, Z., Zhang, M., Zhu, W., Wang, T., Floss, T., Goettlicher, M., Noppinger, P.R., Wurst, W., *et al.* (2007). Hdac2 regulates the cardiac hypertrophic response by modulating Gsk3 beta activity. *Nature medicine* *13*, 324-331.

Valenzuela-Fernandez, A., Alvarez, S., Gordon-Alonso, M., Barrero, M., Ursa, A., Cabrero, J.R., Fernandez, G., Naranjo-Suarez, S., Yanez-Mo, M., Serrador, J.M., *et al.* (2005). Histone deacetylase 6 regulates human immunodeficiency virus type 1 infection. *Molecular biology of the cell* *16*, 5445-5454.

Van Damme, M., Crompton, E., Meuleman, N., Mineur, P., Bron, D., Lagneaux, L., and Stamatopoulos, B. (2012). HDAC isoenzyme expression is deregulated in chronic lymphocytic leukemia B-cells and has a complex prognostic significance. *Epigenetics* *7*, 1403-1412.

Van Dang, C., and McMahon, S.B. (2010). Emerging Concepts in the Analysis of Transcriptional Targets of the MYC Oncoprotein: Are the Targets Targetable? *Genes & cancer* *1*, 560-567.

Verdin, E., and Ott, M. (2015). 50 years of protein acetylation: from gene regulation to epigenetics, metabolism and beyond. *Nature reviews. Molecular cell biology* *16*, 258-264.

Vita, M., and Henriksson, M. (2006). The Myc oncoprotein as a therapeutic target for human cancer. *Seminars in cancer biology* *16*, 318-330.

Vogelauer, M., Wu, J., Suka, N., and Grunstein, M. (2000). Global histone acetylation and deacetylation in yeast. *Nature* *408*, 495-498.

Volinia, S., Calin, G.A., Liu, C.G., Ambs, S., Cimmino, A., Petrocca, F., Visone, R., Iorio, M., Roldo, C., Ferracin, M., *et al.* (2006). A microRNA expression signature of human solid tumors defines cancer gene targets. *Proceedings of the National Academy of Sciences of the United States of America* *103*, 2257-2261.

von Burstin, J., Eser, S., Paul, M.C., Seidler, B., Brandl, M., Messer, M., von Werder, A., Schmidt, A., Mages, J., Pagel, P., *et al.* (2009). E-cadherin regulates metastasis of pancreatic cancer in vivo and is suppressed by a SNAIL/HDAC1/HDAC2 repressor complex. *Gastroenterology* *137*, 361-371, 371.e361-365.

Waddington, C.H. (1942). The epigenotype. *Endeavour* *1*, 18-20.

Wagner, F.F., Zhang, Y.L., Fass, D.M., Joseph, N., Gale, J.P., Weiwer, M., McCarren, P., Fisher, S.L., Kaya, T., Zhao, W.N., *et al.* (2015). Kinetically Selective Inhibitors of Histone Deacetylase 2 (HDAC2) as Cognition Enhancers. *Chemical science (Royal Society of Chemistry : 2010)* *6*, 804-815.

Walz, S., Lorenzin, F., Morton, J., Wiese, K.E., von Eyss, B., Herold, S., Rycak, L., Dumay-Odelot, H., Karim, S., Bartkuhn, M., *et al.* (2014). Activation and repression by oncogenic MYC shape tumour-specific gene expression profiles. *Nature* *511*, 483-487.

Wang, G.G., Allis, C.D., and Chi, P. (2007). Chromatin remodeling and cancer, Part I: Covalent histone modifications. *Trends in molecular medicine* 13, 363-372.

Wang, J.C., Kafeel, M.I., Avezbakiyev, B., Chen, C., Sun, Y., Rathnasabapathy, C., Kalavar, M., He, Z., Burton, J., and Lichter, S. (2011). Histone deacetylase in chronic lymphocytic leukemia. *Oncology* 81, 325-329.

Wang, Z., Zang, C., Cui, K., Schones, D.E., Barski, A., Peng, W., and Zhao, K. (2009). Genome-wide mapping of HATs and HDACs reveals distinct functions in active and inactive genes. *Cell* 138, 1019-1031.

Waterborg, J.H. (2002). Dynamics of histone acetylation in vivo. A function for acetylation turnover? *Biochemistry and cell biology = Biochimie et biologie cellulaire* 80, 363-378.

Weinberg, M.S., Hart, J.R., and Vogt, P.K. (2015). A brave new MYC-amplified world. *Aging* 7, 459-460.

West, A.C., and Johnstone, R.W. (2014). New and emerging HDAC inhibitors for cancer treatment. *The Journal of clinical investigation* 124, 30-39.

Wilson, A.J., Byun, D.S., Nasser, S., Murray, L.B., Ayyanar, K., Arango, D., Figueroa, M., Melnick, A., Kao, G.D., Augenlicht, L.H., and Mariadason, J.M. (2008). HDAC4 promotes growth of colon cancer cells via repression of p21. *Molecular biology of the cell* 19, 4062-4075.

Wilson, A.J., Byun, D.S., Popova, N., Murray, L.B., L'Italien, K., Sowa, Y., Arango, D., Velcich, A., Augenlicht, L.H., and Mariadason, J.M. (2006). Histone deacetylase 3 (HDAC3) and other class I HDACs regulate colon cell maturation and p21 expression and are deregulated in human colon cancer. *The Journal of biological chemistry* 281, 13548-13558.

Wilting, R.H., Yanover, E., Heideman, M.R., Jacobs, H., Horner, J., van der Torre, J., DePinho, R.A., and Dannenberg, J.H. (2010). Overlapping functions of Hdac1 and Hdac2 in cell cycle regulation and haematopoiesis. *The EMBO journal* 29, 2586-2597.

Winter, M., Moser, M.A., Meunier, D., Fischer, C., Machat, G., Mattes, K., Lichtenberger, B.M., Brunmeir, R., Weissmann, S., Murko, C., *et al.* (2013). Divergent roles of HDAC1 and HDAC2 in the regulation of epidermal development and tumorigenesis. *The EMBO journal* 32, 3176-3191.

Witt, O., Deubzer, H.E., Milde, T., and Oehme, I. (2009). HDAC family: What are the cancer relevant targets? *Cancer letters* 277, 8-21.

Xu, W.S., Parmigiani, R.B., and Marks, P.A. (2007). Histone deacetylase inhibitors: molecular mechanisms of action. *Oncogene* 26, 5541-5552.

- Yamaguchi, T., Cubizolles, F., Zhang, Y., Reichert, N., Kohler, H., Seiser, C., and Matthias, P. (2010). Histone deacetylases 1 and 2 act in concert to promote the G1-to-S progression. *Genes & development* 24, 455-469.
- Yang, X.J., and Gregoire, S. (2005). Class II histone deacetylases: from sequence to function, regulation, and clinical implication. *Molecular and cellular biology* 25, 2873-2884.
- Yang, X.J., and Seto, E. (2007). HATs and HDACs: from structure, function and regulation to novel strategies for therapy and prevention. *Oncogene* 26, 5310-5318.
- Yang, X.J., and Seto, E. (2008). The Rpd3/Hda1 family of lysine deacetylases: from bacteria and yeast to mice and men. *Nature reviews. Molecular cell biology* 9, 206-218.
- Yang, Y., Rao, R., Shen, J., Tang, Y., Fiskus, W., Nechtman, J., Atadja, P., and Bhalla, K. (2008). Role of acetylation and extracellular location of heat shock protein 90alpha in tumor cell invasion. *Cancer research* 68, 4833-4842.
- Yoshida, M., and Beppu, T. (1988). Reversible arrest of proliferation of rat 3Y1 fibroblasts in both the G1 and G2 phases by trichostatin A. *Experimental cell research* 177, 122-131.
- Zain, J., and O'Connor, O.A. (2010). Targeting histone deacetylases in the treatment of B- and T-cell malignancies. *Investigational new drugs* 28 *Suppl 1*, S58-78.
- Zain, J., Rotter, A., Weiss, L., Forman, S., and Kirschbaum, M.H. (2007). Valproic acid monotherapy leads to CR in a patient with refractory diffuse large B cell lymphoma. *Leukemia & lymphoma* 48, 1216-1218.
- Zan, H., and Casali, P. (2015). Epigenetics of Peripheral B-Cell Differentiation and the Antibody Response. *Frontiers in immunology* 6, 631.
- Zeng, L., Zhang, Q., Li, S., Plotnikov, A.N., Walsh, M.J., and Zhou, M.M. (2010). Mechanism and regulation of acetylated histone binding by the tandem PHD finger of DPF3b. *Nature* 466, 258-262.
- Zhang, X., Chen, X., Lin, J., Lwin, T., Wright, G., Moscinski, L.C., Dalton, W.S., Seto, E., Wright, K., Sotomayor, E., and Tao, J. (2012). Myc represses miR-15a/miR-16-1 expression through recruitment of HDAC3 in mantle cell and other non-Hodgkin B-cell lymphomas. *Oncogene* 31, 3002-3008.
- Zhang, X., Yuan, Z., Zhang, Y., Yong, S., Salas-Burgos, A., Koomen, J., Olashaw, N., Parsons, J.T., Yang, X.J., Dent, S.R., *et al.* (2007). HDAC6 modulates cell motility by altering the acetylation level of cortactin. *Molecular cell* 27, 197-213.
- Zhang, Y., Kwon, S., Yamaguchi, T., Cubizolles, F., Rousseaux, S., Kneissel, M., Cao, C., Li, N., Cheng, H.L., Chua, K., *et al.* (2008). Mice lacking histone deacetylase 6 have

hyperacetylated tubulin but are viable and develop normally. *Molecular and cellular biology* 28, 1688-1701.

Zhang, Y., Ng, H.H., Erdjument-Bromage, H., Tempst, P., Bird, A., and Reinberg, D. (1999). Analysis of the NuRD subunits reveals a histone deacetylase core complex and a connection with DNA methylation. *Genes & development* 13, 1924-1935.

Zhang, Y., Zhang, M., Dong, H., Yong, S., Li, X., Olashaw, N., Kruk, P.A., Cheng, J.Q., Bai, W., Chen, J., *et al.* (2009). Deacetylation of cortactin by SIRT1 promotes cell migration. *Oncogene* 28, 445-460.

Zhang, Z., Yamashita, H., Toyama, T., Sugiura, H., Omoto, Y., Ando, Y., Mita, K., Hamaguchi, M., Hayashi, S., and Iwase, H. (2004). HDAC6 expression is correlated with better survival in breast cancer. *Clinical cancer research : an official journal of the American Association for Cancer Research* 10, 6962-6968.

Zhao, S., Xu, W., Jiang, W., Yu, W., Lin, Y., Zhang, T., Yao, J., Zhou, L., Zeng, Y., Li, H., *et al.* (2010). Regulation of cellular metabolism by protein lysine acetylation. *Science (New York, N.Y.)* 327, 1000-1004.

Zimmermann, S., Kiefer, F., Prudenziati, M., Spiller, C., Hansen, J., Floss, T., Wurst, W., Minucci, S., and Gottlicher, M. (2007). Reduced body size and decreased intestinal tumor rates in HDAC2-mutant mice. *Cancer research* 67, 9047-9054.

Zou, X., Lin, Y., Rudchenko, S., and Calame, K. (1997). Positive and negative regulation of c-Myc transcription. *Current topics in microbiology and immunology* 224, 57-66.

Zupkovitz, G., Grausenburger, R., Brunmeir, R., Senese, S., Tischler, J., Jurkin, J., Rembold, M., Meunier, D., Egger, G., Lagger, S., *et al.* (2010). The cyclin-dependent kinase inhibitor p21 is a crucial target for histone deacetylase 1 as a regulator of cellular proliferation. *Molecular and cellular biology* 30, 1171-1181.

Zupkovitz, G., Tischler, J., Posch, M., Sadzak, I., Ramsauer, K., Egger, G., Grausenburger, R., Schweifer, N., Chiocca, S., Decker, T., and Seiser, C. (2006). Negative and positive regulation of gene expression by mouse histone deacetylase 1. *Molecular and cellular biology* 26, 7913-7928.

Acknowledgements

Acknowledgements

First and foremost, I would like to acknowledge my thesis supervisor Patrick Matthias for giving me the opportunity to perform my thesis in his lab. I thank him for trusting me during the entire time of my thesis and for his support to enable this work to be published. He granted me substantial freedom of action, which brought me to work independently. During these intense 4.5 years in his lab, one of the most stimulating periods of my life, I considerably grew up scientifically and gained in maturity.

I would like to thank my thesis committee members, Nancy E. Hynes and Jürg Schwaller for their help and scientific advices, not only during our committee meetings, but also during the entire course of my thesis. They have always been there to talk to, and have given great inputs for the projects.

I cannot forget to thank Alexandar Tzankov, who performed the histopathological analysis, and always was there to help and provide useful suggestions.

I want to thank all my current and former lab colleagues who gave me suggestions and helped me during my thesis: Special thanks to Chun Cao, who kindly helped me maintaining and genotyping mice. Special thanks to Nina Reichert and Teppei Yamaguchi, two former lab members, who designed and performed some experiments at the inception of the project. I thank Richard M. Heideman, for his scientific support and our collaboration. I want to thank Roger G. Clerc for proofreading of the publication manuscript, scientific discussions and for his support over the last years. I thank Amin M. Choukrallah, for critical and helpful review of my publication manuscript, and for his continuous availability in addressing scientific discussion/questions. Thanks also to the present lab members, Gabriele Matthias, Makoto Saito, Longlong Wang, Shuang Song, and Patricia Nigg, as well as the former members, Yasuyuki

Acknowledgements

Miyake, Karen Cornille and Oliver Truee, for their support during my thesis. I also would like to thank all other former lab members, who I could not mention because of space limitation.

Thanks to the FMI PhD program who gave me this unique experience of perusing a PhD thesis in a highly competitive and stimulating international environment. I wish to acknowledge the following FMI facility members, who contributed by their remarkable technical support to the accomplishment of this work: I thank for help Hubertus Kohler for FACS sort; Karina Drumm for animal facility; Jean-Francois Spetz for embryo freezing, Sandrine Bichet for IHC, Tim Roloff for microarray; and Michael Stadler for statistical analysis. Thanks also to Annabelle Heier from NIBR, Novartis Pharma, Basel for some histopathological analysis.

I want to thank all friends from the FMI, the Biozentrum and the Department of Biomedicine of the University of Basel for the great time we shared together. And last but not least, I would like to thank my family for their constant support during all these years.

Curriculum Vitae

Vincent Pillonel

Curriculum Vitae

PERSONAL

Name: Vincent Pillonel
 Date of Birth: July 08, 1986
 Nationality: Swiss
 Current Address: Holeestrasse 95,
 4054 Basel, Switzerland
 Tel: +41 78 679 39 32
 E-mail: vincent.pillonel@fmi.ch



Ph.D. student in cell biology completing thesis. Experience in conducting and performing research in the fields of cancer and epigenetics. Flexible, proactive, creative with excellent interpersonal and communication skills, working highly independent.

EDUCATION

- 2012-2016 **Ph.D. thesis**, Friedrich Miescher Institute for Biomedical Research (FMI), Basel, Switzerland.
- 2007-2012 **Bachelor and Master thesis in Molecular Biology**, Biozentrum, Universität Basel, Switzerland.
- 2003-2006 **High school**: core area biology & chemistry, Gymnasium Muttenz, Switzerland.

RELEVANT WORK EXPERIENCE

- **PhD thesis project (2012-2016)** in Prof. Patrick Matthias lab (FMI), Basel: "Dissecting the role of histone deacetylase Hdac1, 2 and 6 in E μ -myc driven B cell lymphoma."
- **Master thesis project (2011-2012)** in Prof. Michael Hall's lab (Biozentrum, Universität Basel), department of biochemistry. Project: "TORC2-Ribosome Association in *Saccharomyces cerevisiae*".
- **Bachelor of Science laboratory block courses (2010)**. Good laboratory practice from one year lab work during block courses: Biochemistry, Biophysics & Structural Biology, Microbiology & Immunology, Cell & Neurobiology.
- **High school "Matura Arbeit" (2006)** in the lab of Dr. Daniel Schlatter, F. Hoffmann-La Roche Basel, entitled "Klonierung und Expression des Human-Cathepsin G Gens in *E. coli*."

SCIENTIFIC PUBLICATIONS

- **Vincent Pillonel**, Nina Reichert, Chun Cao, Alexander Tzankov, Patrick Matthias (2016). Histone Deacetylase (HDAC) 1 plays a predominant role in E μ -myc driven B cell lymphoma. *Accepted for publication in Sci Rep*.
- Du Roure, C., Versavel, A., Doll, T., Cao, C., **Pillonel, V.**, Matthias, G., *et al.* (2014). Hematopoietic overexpression of FOG1 does not affect B-cells but reduces the number of circulating eosinophils. *PLoS one* 9, e92836.

LANGUAGES

French: Native speaker; **German**: Native speaker (bilingual); **English**: Fluently written and spoken; **Spanish**: good speaking and writing skills.

HOBBIES

Reading, learning new languages (Russian, Chinese, Italian), cycling, playing piano and chess.

REFERENCES

Prof. Dr. Patrick Matthias,

Position: Group leader at Friedrich Miescher
Institute for Biomedical Research (FMI)
Department of Epigenetics,
Relation: PhD Thesis Advisor
Contact: patrick.matthias@fmi.ch
+41 61 69 76661

Prof. Dr. Roger G. Clerc,

Position: Visiting Scientist at Friedrich Miescher
Institute for Biomedical Research (FMI)
Department of Epigenetics,
Relation: Career mentor & scientific advisor
Contact: roger.clerc@fmi.ch
+41 61 69 61733